Versatile phosphorus ligands : synthesis, coordination chemistry and catalysis

Versatile Phosphorus Ligands

Synthesis, Coordination Chemistry and Catalysis

Versatile Phosphorus Ligands

Synthesis, Coordination Chemistry and Catalysis

PROEFSCHRIFT

ter verkrijging van de graad van doctor aan de Technische Universiteit Eindhoven, op gezag van de Rector Magnificus, prof.dr. R.A. van Santen, voor een commissie aangewezen door het College voor Promoties in het openbaar te verdedigen op maandag 27 oktober 2003 om 16.00 uur

door

Jarl Ivar van der Vlugt

geboren te Schiedam

Dit proefschrift is goedgekeurd door de promotoren:

prof.dr. D. Vogt
en
prof.dr. D.J. Cole-Hamilton

CIP-DATA LIBRARY TECHNISCHE UNIVERSITEIT EINDHOVEN

Vlugt, Jarl Ivar van der

Versatile phosphorus ligands : synthesis, coordination chemistry and catalysis / by Jarl Ivar van der Vlugt. – Eindhoven : Technische Universiteit Eindhoven, 2003.
Proefschrift. – ISBN 90-386-2675-4
NUR 913
Subject headings: rhodium catalyzed hydroformylation / phosphorus ligands / coordination chemistry / silsesquioxanes / transition metal complexes

Omslag: Origineel ontwerp van wijlen Paul Snoek en Rikkes Voss.
Huidige vormgeving door Jarl Ivar van der Vlugt en Jan Willem Luiten.
Een verantwoorde uitleg voor dit ontwerp kan worden gevonden door creativiteit en dichterlijke vrijheid te koppelen aan een nadere bestudering van de inhoud van dit proefschrift.
Druk: *Universiteitsdrukkerij*, Technische Universiteit Eindhoven.

The research described in this thesis was financially supported by the National Research School Combination – Catalysis (NRSC-Catalysis).

‘Uiteindelijk is het niets anders dan: leuk gezegd, mooi gedaan, goed gevonden.’

Youp van ‘t Hek

‘Life is just chemicals.
A drop here, a drip there.
Everything’s changed.’

Terry Pratchett

‘Ik zweer bij de schoonheid van het nutteloze
en zie het nutteloze van de schoonheid in.’

Paul Snoek

‘De zon is mijn oudste vriend en hij weet het. De zon is immers een vader.
Mijn moeder is de moeder van een alchemist, met gouden schouders.
Mijn ouders zijn mijn beste werk, ik heb ze lief, ik draag ze op
en in mijn handen, breekbaar als een koppel witte duiven.’

(vrij naar) Paul Snoek

Summary

Phosphorus containing compounds are among the most widely used ligands in homogeneous catalysis employing transition metal complexes. Undoubtedly this is due to the enormous variety that can be achieved in the design of such compounds. Amidst all reactions performed by means of homogenous catalysis, the hydroformylation, *i.e.* the conversion of a C-C double bond to an aldehyde moiety by reaction with synthesis gas, is often considered a true success story, both with respect to the application of homogeneous catalysis in an industrial process as well as for underlining the importance of ligand design as a key factor of control over the outcome of the catalytic reaction.

The classification used to distinguish phosphorus ligands as far as the oxidation state of the phosphorus atom is concerned, *i.e.* phosphines, phosphinites, phosphonites and phosphites, is appropriate for a rough subdivision, although recent developments include the incorporation of non carbon or oxygen substituted compounds, *viz.* by employing nitrogen or silicon.

A thorough understanding of the factors governing a) the properties of the ligands synthesized and b) the outcome of catalytic reactions in which such compounds are applied is essential for clever design and synthesis of next generations of phosphorus containing ligands. This understanding can be achieved by *i*) characterization of the bare ligand system, *ii*) unraveling the coordination of such species towards desired transition metals, and *iii*) studying the catalytic system incorporating such ligands. Various tools are available, ranging from chemical reactivity tests, molecular modelling, X-ray crystallography to *in situ* spectroscopic techniques, such as NMR and IR.

The work described in this dissertation is aimed at the development (*i.e.* design and synthesis) of novel classes of phosphorus ligands, thereby *i*) providing a modular synthetic approach by employing backbone scaffolds that have so far remained untouched but which are intrinsically promising, for instance from an economic point of view, *ii*) triggering academic curiosity by combination of two areas of expertise that may lead to exciting transition metal chemistry, and/or *iii*) giving insight into the potential of compounds with specific phosphorus moieties in homogeneous catalysis, and to apply these new compounds in the rhodium catalyzed hydroformylation. To date, many different types of ligands have been employed in this sort of reactions, allowing for good comparison and thus (fair) judgement of the newly applied systems and their respective added values.

In **Chapter one**, the literature dealing with the design of ligands, applied in the hydroformylation of alkenes and related reactions, is reviewed. The four main classes of phosphorus ligands, are considered. Besides this topic special attention is given to the coordination chemistry

reported for both phosphinites and phosphonites. The main conclusions that can be derived from this survey are *i*) that phosphines are still and by far the most studied of all phosphorus ligands, with the focus nowadays on the development of chiral ligands for asymmetric catalysis, *ii*) that new phosphites and their transition metal complexes continue to create opportunities for application in the Rh catalyzed hydroformylation, although the synthetic limitation –the ligand backbone needs to have an hydroxyl-functionality - can not be disregarded, *iii*) that there is renewed interest in the chemistry of phosphinites and *iv*) that the coordination chemistry of especially phosphonites (and to a lesser extent phosphinites as well) with transition metals in general is hardly explored to date.

Chapter two is dedicated to the 'neglected' class of phosphonite ligands and sterically constrained diphosphonites are considered as specific representatives thereof. The coordination chemistry of some typical examples from this new class of ligands is described, resulting in the characterization of seven molecular structures of Pd, Pt and Rh complexes with diphosphonites. Subtle structural differences in the ligands are shown to have great impact on the coordination mode of the ligand to the various metals. Rh catalysts comprised of these diphosphonite ligands are tested in the hydroformylation of 1-octene and 2-butene. For both substrates high activities and selectivities are obtained, showing for the first time the successful application of diphosphonite ligands in such reactions. In case of 2-butene, selective conversion to *n*-pentanal is possible in up to 66% under the chosen reaction conditions. NMR and IR spectroscopic techniques are used to gain insight in the catalytic resting state of the rhodium complexes present under catalytic conditions. Predominant formation of complexes with the diphosphonite ligand coordinated in an equatorial-equatorial fashion is observed.

Based on the results obtained with achiral diphosphonites in the rhodium catalyzed hydroformylation in the previous chapter, **Chapter three** describes the use of a chiral diphosphonite with a xanthene backbone and binaphthyl units on the P atoms. The coordination of this ligand with Pd, Pt and Rh is examined, which results in the characterization of the molecular structures for both the *cis*-Pd and the *cis*-Pt complex. In both cases an unprecedented structural motif, with a dihedral angle between the metal plane and the ligand plane of around 112-115°, is found. Furthermore, the Rh complex is applied in the asymmetric hydroformylation of styrene. Low enantioselectivities, with a maximum of 33% ee at 100 °C, are obtained. A positive dependency of the ee on the reaction temperature is found. In the rhodium catalyzed asymmetric hydrogenation of methyl (*Z*)-2-acetamido-cinnamate low activities but promising ee's of up to 54% are found.

Chapter four involves a study into the applicability of Bisphenol A and derivatives thereof as backbones, since this could lead to a modular class of easy accessible and low-cost phosphorus ligands. As a first approach four diphosphine ligands with the general name BPphos are synthesized. Also one compound based on a terphenyl skeleton, Terphos, is prepared via a slightly modified synthetic procedure. The ligands can be obtained in good yields in three reaction steps and are fully characterized, including molecular structures for four of the compounds. To assess the potential for homogeneous catalysis of the novel ligands, the complexation of one illustrative member of the BPphos family with Pd, Pt and Rh is studied. The resulting molecular structures can be described as face-to-face dimers. Applying the Terphos compound a monomeric *cis*-Pt complex is obtained, with the diphosphine ligand acting as a chelating bidentate ligand. As a first example for the application of these ligands in homogeneous catalysis, the rhodium catalyzed hydroformylation of 1-octene is studied. High activities of up to 3500 h^{-1} are obtained with low regioselectivities for the linear aldehyde.

Silsesquioxanes are explored as novel backbones for the synthesis of mono- and bidentate compounds in **Chapter five**. From the incompletely condensed silsesquioxane disilanol several monophosphites as well as a diphosphinite and a diphosphite compound are synthesized. Alternatively, a completely condensed silsesquioxane monosilanol is converted to a monophosphinite and a monophosphite. The electron-withdrawing character of such silsesquioxane frameworks is addressed by DFT calculations on model compounds as well as by complexation studies. The molecular structures of corresponding Pd, Pt, Mo and Rh complexes with both bidentate ligands are described for the diphosphinite ligand, whereby the *cis*-coordination is highly favoured. For the analogous diphosphite ligand, characterization of the molecular structures for the Pd, Mo and Rh complexes shows that various modes of coordination are possible with this more sterically constrained ligand. By applying a catalyst comprising either one of the series of monodentate phosphites in the rhodium catalyzed hydroformylation of 1-octene, high activities are obtained compared to the results with the bidentate phosphite.

Samenvatting

Verbindingen die fosfor functionaliteiten bevatten, behoren tot de meest gebruikte in het onderzoeksgebied van de homogene katalyse met behulp van overgangsmetaal komplexen, ongetwijfeld deels vanwege de enorme diversiteit die kan worden bereikt in het ontwerp van dergelijke verbindingen. Van alle homogeen gekatalyseerde reacties wordt de hydroformylering, dat wil zeggen de omzetting van een C-C dubbele binding naar een aldehyde door reactie met synthese-gas, vaak gezien als een echt succesverhaal, niet alleen wat betreft de toepassing van de homogene katalyse in een industrieel proces, maar ook voor het onderstrepen van het belang van een doeltreffend ontwerp van fosfor liganden als sleutel voor de controle over de uitkomsten van de katalyse.

De klassificeringen die worden gebruikt om fosforliganden te onderscheiden wat betreft het substitutiepatroon op het fosfor atoom, namelijk fosfines, fosfinieten, fosfonieten en fosfieten, zijn geschikt voor een eerste onderverdeling, alhoewel recente ontwikkeling ondermeer de introductie van atomen anders dan koolstof en zuurstof laat zien, bijvoorbeeld door gebruik te maken van stikstof of silicium.

Een gedegen begrip van de factoren die a) de eigenschappen van de gesynthetiseerde liganden en b) de resultaten van katalytische reacties die afhankelijk zijn van dergelijke systemen bepalen, is noodzakelijk voor een doordacht ontwerp en synthese van de volgende generaties fosfor liganden. Dit begrip kan worden verkregen door i) karakterizatie van het naakte ligand systeem, ii) het ontrafelen van de coordinatie van dergelijke species aan gewenste overgangsmetalen en iii) het bestuderen van het katalytische systeem, de liganden inbegrepen. Verscheidene gereedschappen zijn hiervoor beschikbaar, variërend van proeven om de chemische reactiviteit te testen, moleculaire modellering, röntgendiffractie tot *in situ* spectroscopische technieken.

Het werk beschreven in dit proefschrift is gericht op de ontwikkeling (zowel het ontwerp als de synthese) van nieuwe fosfor gefunctionaliseerde liganden, waardoor *i*) een synthetisch modulaire benadering mogelijk wordt door gebruik te maken van basisstructuren die tot op heden niet zijn beschouwd hoewel ze in zichzelf veelbelovend zijn, bijvoorbeeld vanuit economisch oogpunt, *ii*) de academische nieuwsgierigheid geprikkeld wordt omdat twee deelgebieden worden gecombineerd, waardoor mogelijk nieuwe overgangsmetaalchemie kan worden verkend en/of *iii*) inzicht wordt gegeven in het potentieel van specifieke fosfor gefunctionaliseerde verbindingen voor de homogene katalyse, en de toepassing van deze nieuwe verbindingen in de rhodium gekatalyseerde hydroformylering. Tot op heden zijn zeer veel verschillende typen fosfor liganden toegepast in dit

type reactie, waardoor een goede vergelijking en een objectieve beoordeling van de waarde van de nieuwe systemen en hun toegevoegde waarde mogelijk wordt.

In **Hoofdstuk één** wordt de literatuur die zich richt op het ontwerp van liganden die worden toegepast in de hydroformylering van alkenen en gerelateerde reacties besproken. De vier hoofdklassen van fosfor liganden worden behandeld. Naast dit onderwerp zal speciale aandacht worden besteed aan de coordinatiechemie van zowel fosfinieten als fosfonieten. De algemene conclusies die kunnen worden getrokken uit dit literatuuronderzoek zijn *i*) dat fosfines nog steeds veruit de meest bestudeerde van alle fosfor liganden zijn, waarbij de nadruk tegenwoordig ligt op het ontwikkelen van chirale liganden voor asymmetrische katalyse, *ii*) dat de introductie van nieuwe fosfieten en hun overgangsmetaalcomplexen nieuwe mogelijkheden creëert voor de succesvolle toepassing in de rhodium gekatalyseerde hydroformylering, hoewel de synthetische beperking – er dient een hydroxyl functionaliteit in de basisstructuur van het ligand aanwezig te zijn – niet mag worden onderschat, *iii*) dat er hernieuwde interesse is voor de chemie van fosfinieten en *iv*) dat de coordinatiechemie van met name de klasse van fosfoniet-liganden (en in mindere mate van de fosfinieten) met overgangsmetalen tot op heden nauwelijks aandacht heeft gekregen in de literatuur.

Hoofdstuk twee richt zich op sterisch gehinderde difosfonieten als specifieke vertegenwoordigers van deze 'verwaarloosde' klasse van fosfor bevattende liganden. De coordinatiechemie van een aantal typerende exemplaren uit deze ligand familie is bestudeerd, wat geresulteerd heeft in de karakterisatie van zeven moleculaire structuren voor Pd, Pt en Rh complexen met difosfonieten. Subtiele structurele verschillen in de liganden blijken grote invloed te hebben op de coordinatie-mode van het ligand in de diverse metaalcomplexen. Rh katalysatoren gebaseerd op deze liganden zijn getest in de hydroformylering van 1-octeen en 2-buteen. Voor beide substraten zijn hoge activiteiten en selectiviteiten verkregen, waarmee voor de eerste keer de succesvolle toepassing van difosfoniet liganden in dergelijke reacties is aangetoond. 2-Buteen kan tot 66% selectiviteit worden omgezet tot *n*-pentanal onder niet-geoptimaliseerde reactie-condities. NMR en IR spectroscopische technieken zijn gebruikt om inzicht te verkrijgen in de katalytische rust-toestand van de rhodium complexen onder de katalytische condities. Hierdoor is aangetoond dat de vorming van een complex waarin het difosfoniet ligand coordineert in een bis-equatoriale positie overheerst.

Gebaseerd op de resultaten verkregen in de rhodium gekatalyseerde hydrofomylering door de toepassing van achirale difosfonieten uit het vorige hoofdstuk, beschrijft **Hoofdstuk drie** het gebruik van een chiraal difosfoniet ligand met een xantheen basistructuur en binaphthyl eenheden op de fosfor atomen. De coordinatie van dit ligand met Pd, Pt and Rh is onderzocht, resulterend in de

karakterizatie van de moleculaire structuren van het *cis*-Pd en het *cis*-Pt complex. In beide gevallen wordt een ongekend structuur-motief, gekenmerkt door een dihedrale hoek tussen het metaal vlak en het ligand vlak van ongeveer 112-115°, gevonden. Verder is het overeenkomstige Rh complex toegepast in de asymmetrische hydroformylering van styreen. Lage enantioselectiviteiten (ee), met een maximum van 33% ee bij 100 °C, zijn verkregen. Er bestaat een positieve correlatie van de ee met de reactie-temperatuur. In de rhodium gekatalyseerde asymmetrische hydrogenering van methyl (*Z*)-2-acetamido-cinnamaat zijn lage activiteiten verkregen, terwijl de gevonden enantioselectiviteiten tot 54% ee bemoedigend zijn.

Hoofdstuk vier behelst een studie naar de toepasbaarheid van Bisphenol A en derivaten als basisstructuur, aangezien dit zou kunnen leiden tot een modulaire, makkelijk toegankelijke en goedkope klasse fosfor liganden. Als eerste aanzet zijn vier difosfine liganden, met de algemene naam BPphos, gesynthetiseerd. Tevens is een verbinding, gebaseerd op een terphenyl skelet, Terphos, op soortgelijke wijze verkregen. De liganden zijn toegankelijk in goede opbrengsten via een drie-staps synthese en ze zijn volledig gekarakteriseerd, inclusief de moleculaire structuren voor vier van de vijf verbindingen. Om het potentieel voor toepassing in homogeen gekatalyseerde reacties van dit nieuwe type liganden vast te stellen, zijn de complexen van een illustratief lid van de BPphos familie met Pd, Pt en Rh bestudeerd. De verkregen moleculaire structuren kunnen worden beschreven als dimeren. Met de Terphos verbinding is een monomeer *cis*-Pt complex verkregen, waarin het diphosphine ligand opereert als chelerend bidentaat ligand. Als eerste voorbeeld voor de toepassing van deze liganden in homogene katalyse is de rhodium gekatalyseerde hydroformylering van 1-octeen bestudeerd. Hoge activiteiten tot 3500 h^{-1} zijn gevonden, terwijl de regioselectiviteiten voor de lineaire aldehyde relatief laag zijn.

Silsesquioxanen zijn onderzocht als nieuwe basisstructuren voor de synthese van mono- and bidentaat fosfor liganden in **Hoofdstuk vijf**. Vanuit de onvolledig gecondenseerde silsesquioxaan disilanol zijn verscheidene monofosfieten alsmede een difosfiniet en een difosfiet verbinding gesynthetiseerd. Daarnaast is een kompleet gecondenseerd silsesquioxaan monosilanol omgezet in een monofosfiniet en een monofosfiet. Het electronenzuigende karakter van dergelijke silsesquioxaan verbindingen kan met behulp van DFT berekeningen in combinatie met complexatie studies worden aangetoond. Voor de bidentaat liganden zijn de moleculaire structuren van de Pd, Mo and Rh complexen beschreven, waarbij het difosfiniet ligand de *cis*-coordinatie prefereert. Voor het analoge difosfiet zijn diverse coordinatiemodes gevonden. In de rhodium gekatalyseerde hydroformylering van 1-octeen worden hoge activiteiten verkregen, met name met de monofosfieten.

Graphical Abstract

Chapter 2: *Coordination Chemistry of Sterically Constrained Diphosphonites*
Selective Hydroformylation of Terminal and Internal Alkenes

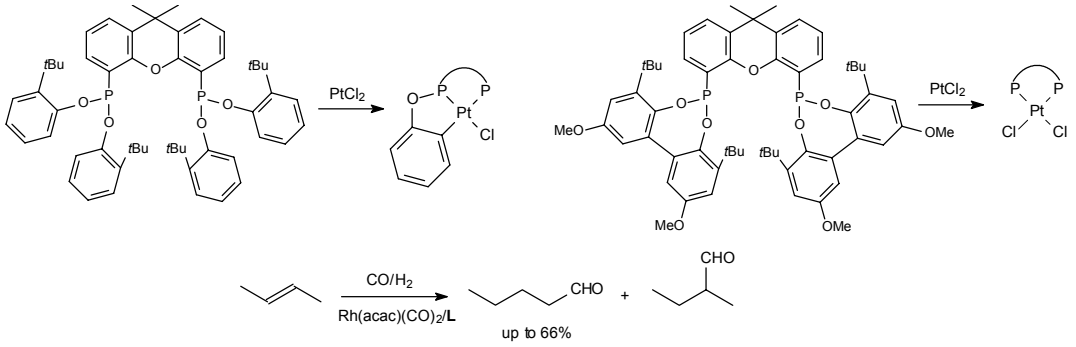

Chapter 3: *Rhodium Mediated Asymmetric Catalysis Using a Chiral Diphosphonite*

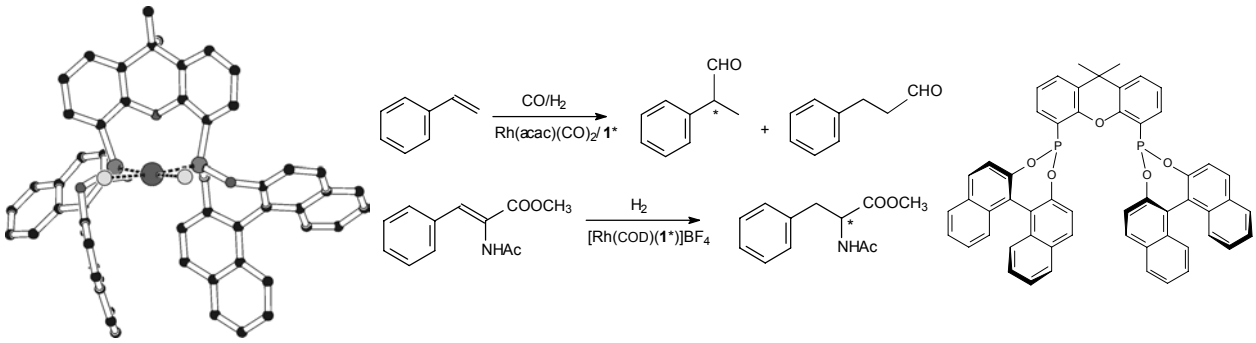

Chapter 4: *A New Class of Diphosphine Ligands Derived from Bisphenol A*

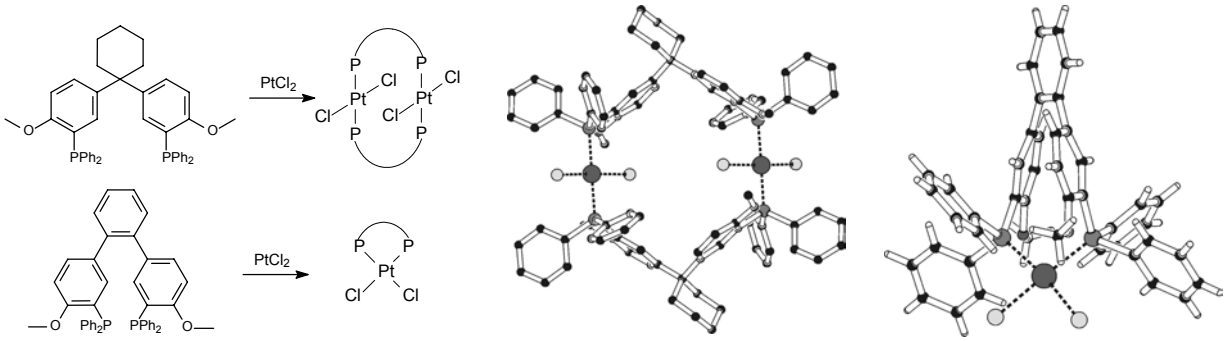

Chapter 5: *Novel Silsesquioxane Based Phosphorus Containing Ligands*

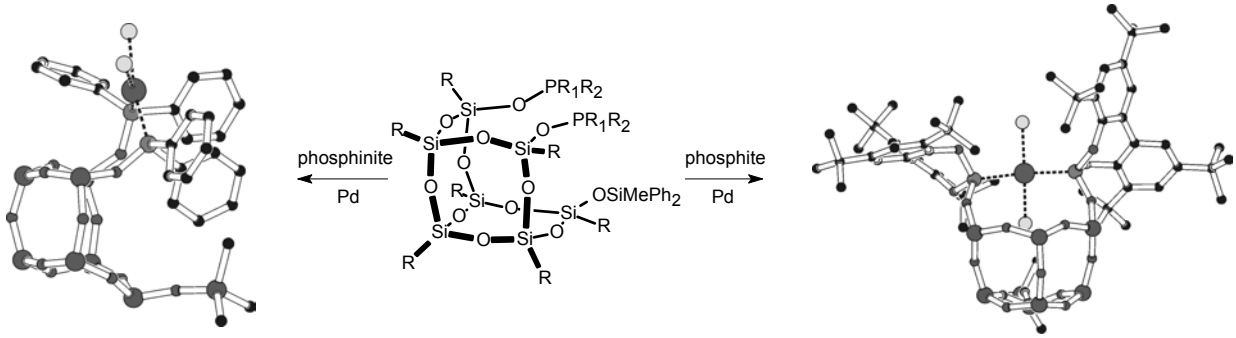

Contents

1

Phosphines, Phosphinites, Phosphonites and Phosphites in Rhodium Catalyzed Hydroformylation

Coordination Chemistry of Phosphinites and Phosphonites

Abstract *The rhodium catalyzed hydroformylation of alkenes is introduced by means of historic and recent developments in the field, especially with addressing advances in ligand design. The main classes of phosphorus ligands employed, viz. phosphines, phosphites, phosphinites and phosphonites, are discussed. Compared to the extensive research published on both the transition metal complexes with phosphines and phosphites as well as on their applications in homogeneous catalysis, the related classes of phosphinites and especially phosphonites have been hitherto largely neglected. Recent developments reported by academic groups as well as by industrial parties are directed to overcome this lack of knowledge. The results obtained thus far are promising and show the potential for new applications with these types of ligands. This chapter serves as an introduction for the chemistry described in Chapters 2-5 of this thesis and includes the aim and scope of the research.*

1.1 History of Hydroformylation

Discovered by accident by Otto Roelen in 1938 during his investigations about the origin of oxygenated products occurring in cobalt catalyzed Fischer-Tropsch reactions,[1] hydroformylation, or formally the addition of a formyl group to an alkene to yield an aldehyde, has grown to become one of the largest homogeneous catalytic process today, next to the carbonylation of methanol and the oxidation of *p*-xylene. The world-wide annual oxo capacity reached 6.6 x 10^6 tons in 1995, and shot up to 9.2 x 10^6 tons in 1998.[2,3] Most of these aldehydes and their hydrogenated alcohols are converted into plasticizers for the polymer industry. In addition there are also many applications as detergents, surfactants or other chemical intermediates, underlining the important role of hydroformylation in industrial chemistry.

Roelen observed that ethylene was converted to propanal by reaction with H_2 and CO in the presence of a Co catalyst, and that at higher pressures diethyl ketone was formed. Based on this result and further experiments Heck and Breslow proposed a mechanism that is now accepted as the general mechanism for cobalt (and rhodium) catalyzed hydroformylation.[4] While until the early 1970´s cobalt catalysts completely dominated industrial hydroformylation, a radical change came with the introduction of rhodium catalysts. The first investigations on rhodium catalyzed hydroformylation were based on simple unmodified precursors,[5] but they already showed that the rhodium-based catalysts were far more active than cobalt catalysts. Yet, the formation of rhodium hydrides required high pressures of hydrogen.[6] Fundamental work by Evans, Osborn and Wilkinson[7] however showed that rhodium complexes with PPh_3 (triphenylphosphine or TPP) allowed the reaction to proceed at much lower pressures, thus offering the prospect of a cheap industrial application. The synthesis and spectroscopic characterization of the formed rhodium-hydride species with the ligand triphenylphosphine gave further hints about the mechanism and lead to the tremendous variety of modified Rh catalysts known today incorporating phosphorus ligands.[8,9]

Another challenge besides high reaction rates, chemo- and regioselectivity under moderate conditions, was the separation of catalyst and products formed in the reaction mixture. In 1984 the Ruhrchemie/Rhône-Poulenc (RCH-RP) process, based on the water soluble rhodium complex of meta-trisulfonated triphenylphosphine (TPPTS), was developed. Here the concept of biphasic catalysis, first introduced in Shell's SHOP process,[10a,b] which is based on two organic phases, was applied to hydroformylation, with the modification that an aqueous and an organic phase are used.[2,10c] The aldehydes formed are more soluble in the organic phase and thus are easily separated from the catalyst in the water phase in a continuous process. Unreacted alkenes are separated from the products and recycled.

The desired linear aldehydes are in most cases only intermediates and they will be processed to obtain various products. Alcohols, especially long-chain alcohols, used in detergents, can be made from linear higher alkenes. Diols such as 1,4-butanediol, a key intermediate in the petrochemical industry, can be obtained via Rh catalyzed hydroformylation of allylic alcohol. After the hydroformylation of propene, aldol-condensation leads to 2-ethyl-1-hexanol, a major plasticizer alcohol.[2,3]

1.2 Mechanism of Hydroformylation

A key issue in the hydroformylation process is the control of regioselectivity, i.e. the ratio between linear and branched aldehyde produced. Furthermore, other side reactions like hydrogenation to produce alcohols or isomerization leading to internal and less reactive alkenes should normally also be suppressed.

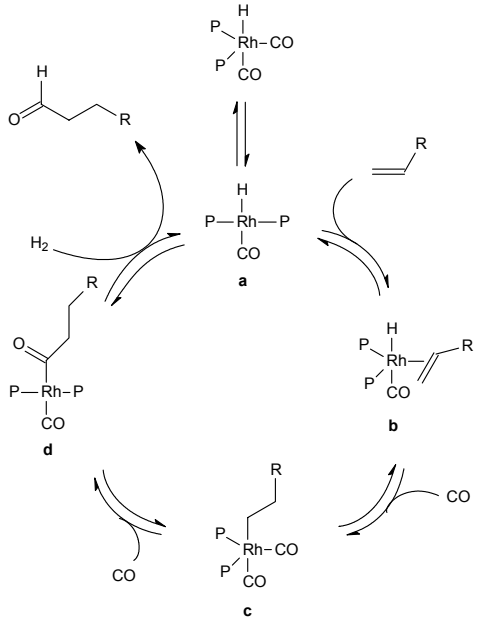

Scheme 1.1: *Catalytic cycle of the Rh catalyzed hydroformylation as a modification of the scheme proposed for cobalt based catalysts.*[4]

The mechanism (Scheme 1.1) starts with the dissociation of one carbon monoxide ligand and formation of the hydride complex $Rh(H)(CO)(P)_2$ (**a**), after which coordination of the alkene leads to complex (**b**). Formation of the alkyl complex (**c**) proceeds via migratory insertion. Subsequent insertion of a CO ligand results in the formation of the $Rh(CO)(P)_2$(acyl) complex (**d**). Reaction with hydrogen then gives the desired aldehyde under regeneration of the unsaturated $Rh(H)(CO)(PPh_3)_2$ complex to close the catalytic cycle. Side-reactions are the formation of the undesired branched

aldehyde or β-hydride elimination, leading to isomerization. In case P is PPh_3, the linearity of the aldehyde product generally increases with higher concentrations of the ligand combined with lower partial pressures of carbon monoxide. An explanation for this behaviour is probably the steric congestion around the rhodium center, which increases with the number of coordinated TPP ligands. In a more sterically hindered complex the formation of the linear alkyl chain is favoured relative to the branched alkyl chain.

Structural information on the catalytic resting state but also on the various intermediates in the catalytic cycle would add to the understanding of important ligand features that steer the selectivity towards linear or branched products. Several groups have reported major contributions on the spectroscopic and crystallographic characterization of the species present in solution during catalysis. Ibers published X-ray structures for both $[Rh(H)(CO)(PPh_3)_3]$ and $[Rh(H)(CO)_2(PPh_3)_2]$[11] while Brown and Kent published NMR spectroscopic data for these species.[12] Eisenberg succeeded in mimicking individual steps in the catalytic cycle, using $[Ir(Et)(CO)_2(dppe)]$ (dppe = (diphenylphosphino)ethane).[13] So far no structural characterization of intermediates such as (**a**) or (**b**) has been reported.

Recently, a lot of attention has been given to the hydroformylation of internal alkenes because of their potential as alternative feedstock in industry and synthetic organic chemistry (see *Chapter* 2). To selectively obtain the linear aldehyde, isomerization of the internal double bond to the terminal position needs to precede the hydroformylation to the linear aldehyde. Novel ligands have been synthesized, as discussed in forthcoming paragraphs, but this specific reaction is still a relatively unexplored field for the rhodium systems.

1.3 Ligand Characteristics

Ligand effects can have a dramatic influence on the reaction parameters (rate, regioselectivity) and on the amount of side-products. Therefore, extensive studies have been carried out on their steric and electronic properties. Related to steric influence, Tolman introduced his concept of a *cone angle* θ[14] to indicate the approximate amount of space that the ligand consumes around the metal. It is defined by the cone, originating from a metal center at 2.28 Å from the phosphorus atom, that confines all atoms of the substituents on that phosphorus, based on van der Waals radii (Figure 1.1). If an X-ray structure of the specific ligand is not available, this parameter can be determined via modelling of the corresponding M-L fragment and then minimizing its energy. For bidentate ligands like diphosphines Casey and Whiteker developed the concept of the natural *bite angle* β_n as an additional characteristic.[15]

Figure 1.1: *Illustration of the cone angle θ (left) and the bite angle β_n (right) in a rhodium complex.*

The steric properties of the ligand however intertwine with its electronic character. In the case of phosphorus ligands the combination of σ-donation and π-acceptor character is therefore crucial. Strohmeier showed that phosphorus ligands could be ranked in an electronic series based on CO stretching frequencies.[16] Tolman expanded this work based on the carbonyl complex $Ni(CO)_3L$ for different ligands L. His *electronic parameter* χ is defined as the shift of the symmetric CO stretch frequency of this complex referenced to $[Ni(CO)_3(P(t\text{-}Bu)_3)]$ caused by the different bond strengths between metal and CO ligands.[17] Today these parameters are known for many ligands.[18]

Figure 1.2: *Effect on CO bonding for weak (left) and strong (right) back-donation towards phosphorus ligand.*

Phosphites are generally better π-acceptors than phosphines and therefore have great potential in hydroformylation catalysis. This is due to their suitable antibonding orbitals with π-symmetry. These orbitals play the role of a strong π-acceptor on phosphorus and therefore are competing with the coordinated CO ligands for the electron back-donation. As a result the metal-CO bonds are activated for CO dissociation and reaction rates are increased (Figure 1.2).

1.4 A Closer Look at Phosphines

This class of ligands was the first to be extensively studied in rhodium catalyzed hydroformylation. The complex $Rh(H)(CO)(PPh_3)_3$ was first reported by Vaska[19] in 1963, while Wilkinson and co-workers described its use for hydroformylation a few years later. Its chemistry has been reviewed many times.[20,21] For decades, bidentate phosphines have been the subject of research, which is still continued to date. DIOP (**1**), first applied by Kagan[22] in 1971 in the rhodium catalyzed hydrogenation, was studied together with $Rh(H)(CO)(PPh_3)_3$ in the hydroformylation of 1-alkenes by Consiglio. He reported linear to branched ratios (l/b) of 13 at 25 °C and 1 bar of synthesis gas.[23] Later,

Hughes and Unruh (Celanese) in 1981 used DIOP together with the more common dppe – (diphenylphosphino)ethane - and dppp - (diphenylphosphino)propane - in the rhodium catalyzed hydroformylation.[24a] Unruh also developed dppf – (diphenylphosphino)ferrocene – (**2**) and various derivatives and found good selectivities with $Rh(acac)(CO)_2$, giving l/b ratios of up to 11.[24b,25] In 1987 Devon and co-workers from Texas Eastman published work with a new diphosphine ligand, BISBI (**3**),[26] which was found to have a natural bite angle β_n of 124° in the Rh complex by X-ray crystallography.[27] The catalytic system containing this wide bite angle ligand gave very high regioselectivities for linear aldehydes with l/b ratios of 24 compared to 0.8 with dppp or 4.0 with DIOP.[26] These results were obtained at entirely different conditions as used by Consiglio, namely 16 bar of synthesis gas and temperatures around 100 °C. By further modifications on the ligand structure, *viz.* different substituents on the P-atoms, and under optimized reaction conditions, l/b ratios as high as 288 could be reached.[26b] One could however question the significance of such an 'improvement' in the l/b value, not only in terms of GC-accuracy but also regarding the very small incremental difference in selectivity with an l/b ratio of *e.g.* 100.

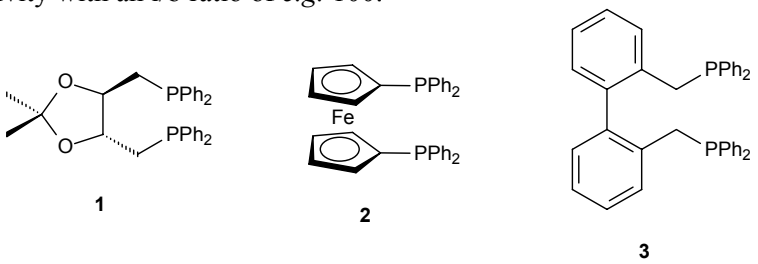

Figure 1.3: *Structures of DIOP (**1**), dppf (**2**) and BISBI (**3**) (with binaphthyl backbone: NAPHOS).*

More recently, Xantphos (**4**) and closely related ligands of this family have been applied in various transition metal catalyzed reactions such as hydroformylation[28a-f] and hydrocyanation.[28g,h] Ligands with the type of structure of (**5**) also showed activity for the conversion of internal alkenes to terminal aldehyde.[28b,c] Similar observations were reported recently by Beller,[29] using the already known ligand NAPHOS (2,2'-bis(diphenylphosphino)methyl-1,1'-binaphthyl), a structural derivative of BISBI.[30]

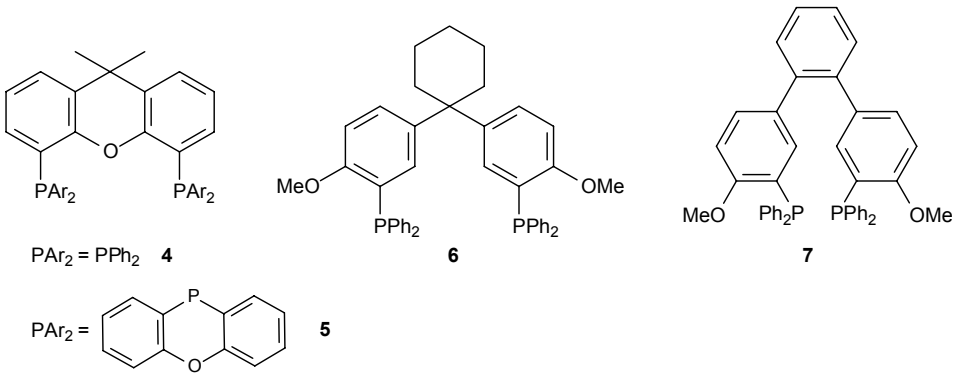

Figure 1.4: *Illustration of Xantphos derivatives (**4, 5**), BPphos (**6**) and Terphos (**7**).*

New developments in the area of (di)phosphine ligand design are governed by the quest for new chiral ligands for applications in asymmetric catalysis,[31-34] by the search for *trans*-spanning ligands[35-38] or by the modular design of new classes of ligands. Concerning this last topic, promising results have been obtained by introducing Bisphenol A derived structures as novel backbones, leading to BPphos ligands[39a-c] (**6**) and Terphos (**7**) (Figure 1.4).[39b,d]

Although not belonging to the class of PR_3 phosphines (R being any carbon linked substituent), much is to be expected from the relatively new approach to use pyrrole as a substituent on the phosphorus atoms instead of *e.g.* aryl groups. Little is known about the influence of the different electronic character of such ligands in catalysis. Since the stability of these compounds towards oxidation is most likely higher and new families of pyrrole substituted phosphines have already been reported.[40-44] Also the introduction of various amines as substituents on the phosphorus atoms is likely to find its applications. One of the most successful examples so far is based on a bis(diazaphospholidine) ligand that has been applied in the asymmetric hydroformylation of vinylacetate and induced to up to 89% ee.[45] The more exotic monodentate ligand subclasses of phospholes,[46] phospanorbornadienes[47] and phosphabenzenes[48] have not found widespread acceptance yet, but given their behaviour in Rh catalysts in *e.g.* the hydroformylation of styrene (all are at least four times as active as TPP) and their electronic properties, more applications can be foreseen despite their cumbersome syntheses.

A very elegant methodology that might initiate more activity into the design of phosphine (and related) ligands is the approach published very recently by Breit.[49] By a careful choice of components, he was able to show that monodentate phosphines with both donor and acceptor units present in the 'backbone' 2-pyridone could self-assemble into the dimeric species by hydrogen-bonding interactions. This interaction is made possible by the tautomerization of 2-pyridone to 2-hydroxypyridine, as illustrated in Figure 1.5. This ultimately yielded a self-assembled diphosphine-system (DPPon) that acted as a bidentate ligand in a *cis*-platinum complex (Figure 1.5, right).

Furthermore, excellent results were obtained for the hydroformylation of various alkenes for both activity and regioselectivity.

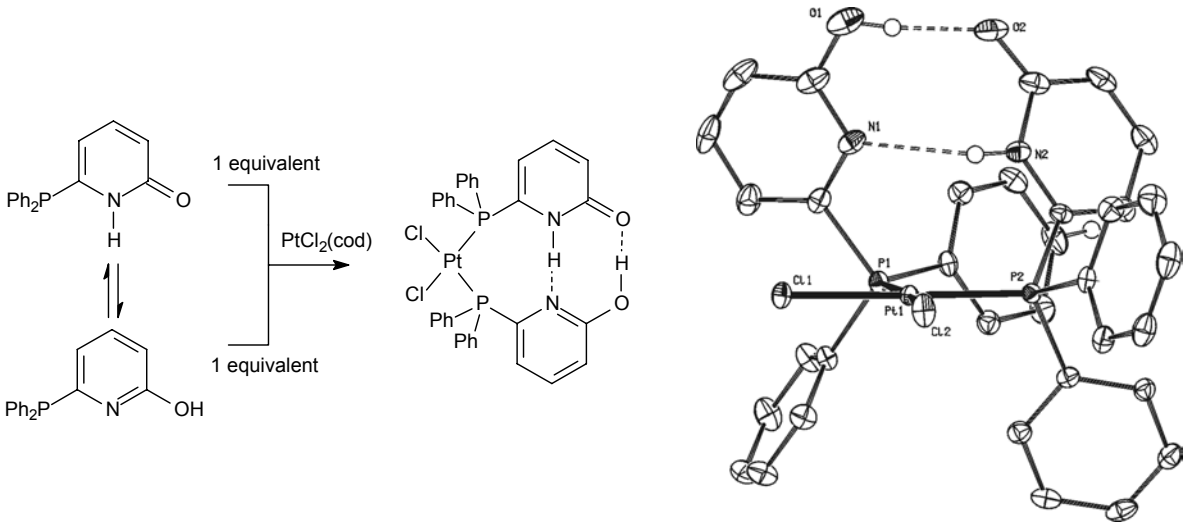

Figure 1.5: *Schematic representation of the methodology published by Breit (left) and the corresponding* cis-*[PtCl$_2$(DPPon)$_2$] complex, showing the hydrogen bonding motif.*[49]

1.5 Phosphites In Extrema

The first examples for phosphite ligands in rhodium catalyzed hydroformylation of 1-alkenes were reported by Pruett and Smith[50] from Union Carbide. Advantages of ligands from this class are their, in general, easy synthesis and the low sensitivity towards oxidation. On the other hand, phosphites are more sensitive to side reactions such as hydrolysis, alcoholysis, C-O cleavage and the Arbuzov reaction.[51]

Recent developments in the area of phosphite based chemistry start from either of three approaches: the synthesis of chiral ligands, the development of bulky monophosphites or the design of specific diphosphites. In asymmetric catalysis, the renowned ligand BINAPHOS, a phosphine-phosphite with a binaphthyl backbone, developed in 1991 by Takaya, marked a breakthrough for the Rh catalyzed hydroformylation of vinyl arenes giving enantioselectivities of up to 96%.[52] The other major contribution came from Babin and Whiteker at Union Carbide, applying chiral (2*R*, 4*R*)-pentane-2,4-diol as backbone for bulky diphosphite ligands, leading to ee's of up to 90%.[53] Shortly before, the first Pt-systems with diphosphites had appeared which showed similar high ee's.[54] The asymmetric hydroformylation will not be discussed in further details, the reader is referred to literature for more information.[55,56]

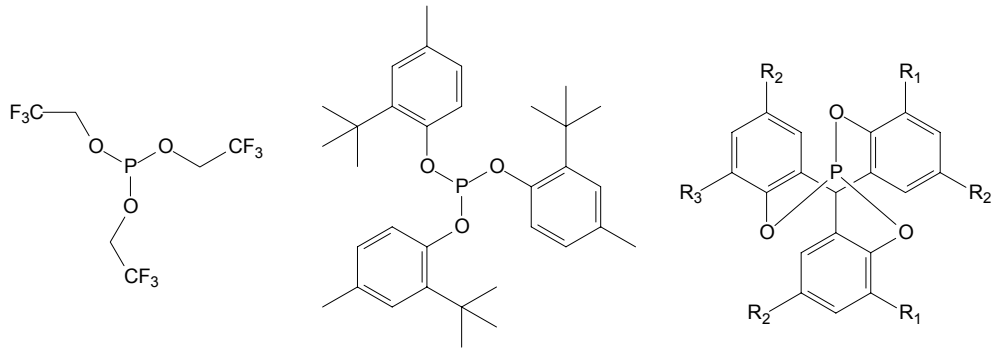

8 **9** **10**

Figure 1.6: *Monophosphite ligands: (**8**) van Leeuwen, 1983; (**9**) van Leeuwen, 1983/1995; (**10**) Dinger, 2001.*

Most of the recent work on the Rh catalyzed hydroformylation of terminal alkenes, using sterically constrained monophosphites, started with work carried out at Shell in the 70's/80's and the early 90's by van Leeuwen, showing that monoligated Rh complexes, especially when the ligand carried electron-withdrawing groups, (**8**), gave very nice catalytic results.[57] This was later followed by a detailed study using tris(2-*tert*-butyl-4-methylphenyl)phosphite as bulky ligand (**9**).[58] Recent work by Dinger *et al.* on C_3-symmetric monophosphites based on tris(3,5-dialkyl-2-hydroxyphenyl)methane (**10**), including the structural characterization of the monoligated complex [Rh(acac)(CO)(L)] seems promising, however no catalytic results have been published yet.[59] The groups of Pringle[60] and van Leeuwen[61a] have independently reported on the use of calix[4]arene based monophosphites, which yield highly active yet rather unselective catalysts.

Bryant and co-workers from Union Carbide reported on diphosphites based on 2,2-dihydroxy-1,1'-biphenyl backbones and similar substituents on the phosphorus atoms in the late 80's (**11**). These sterically constrained ('bulky') diphosphites were shown to give highly active and selective Rh catalysts for the hydroformylation of 1-octene (and styrene) with l/b ratios up to 48.[62] Also with the internal alkene 2-butene as substrate, impressive results were obtained, with low activities but linear to branched ratios of 2.8. More recent work by Börner focussed on internal octenes, with similar bulky bidentate phosphites, yet employing new oxaphosphepin moieties (**12**).[63] Starting with a mixture of *n*-octenes, the selectivity for 1-nonanal reached up to 69%.

The calix[4]arene backbone has also found use for the synthesis of diphosphites, as described by Parlevliet *et al.*[61b] and Schmutzler and Börner.[64] In the latter case, the results for the hydroformylation of 1-octene showed very poor regioselectivities with a maximum *n*:iso of 2.58.

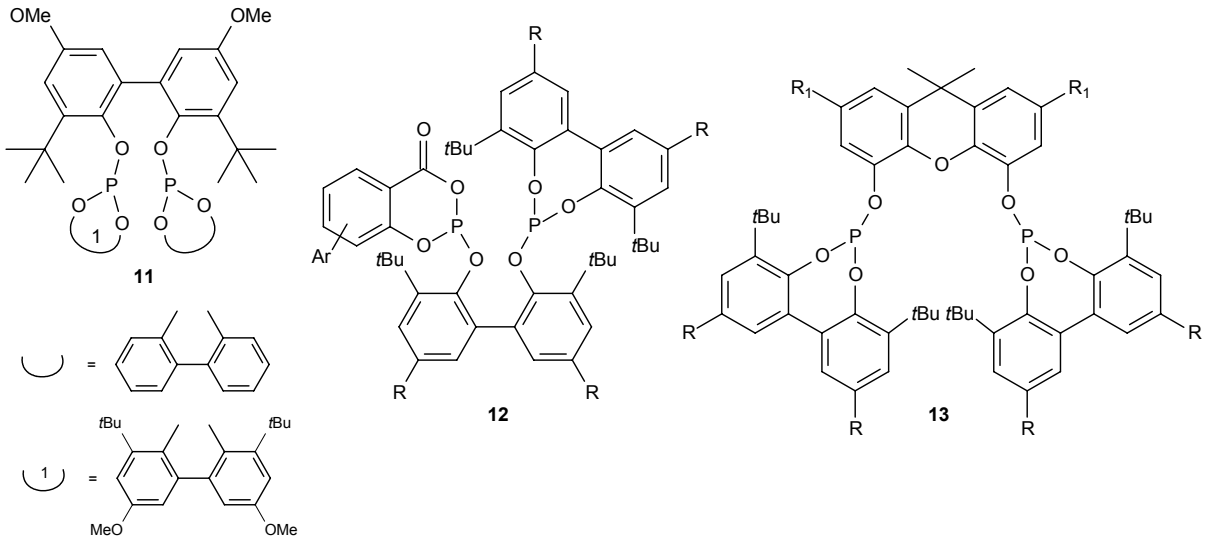

Figure 1.7: *The diphosphite systems developed by Bryant (**11**), Börner (**12**) and Vogt (**13**).*

Vogt *et al.*[65] and based on this work, van Leeuwen[66] as well, have been active in the modification of the well-known xanthene backbone (*vide supra)* to yield a functional compound with two hydroxyl groups. This diphenol derivative of xanthene was obtained after tedious synthetic work and then used as a starting material for the synthesis of bulky diphosphites (generic structure (**13**) in Figure 1.7).

The use of silsesquioxanes as versatile backbones, amongst others for the synthesis of phosphite ligands, has only recently been pioneered and explored (see *Chapter* 5). The disilanol moiety present in the framework of $(c\text{-}C_5H_9)_7Si_7O_9(OSiMePh_2)(OH)_2$ is used as a building block for the synthesis of both monophosphites[67a] and diphosphites. Also completely condensed silsesquioxanes with one peripheral silanol functionality have been applied as starting material for the synthesis of monophosphites.[67b] Much attention is paid lately to the development of so-called phosphoramidites ($(RO)_2P(NR^1R^2)$) and their application in especially the asymmetric hydrogenation of several classes of substrates.[68] Surprisingly, so far no reports have appeared on their application in the (asymmetric) hydroformylation.

1.6 Phosphinites Rediscovered

Besides the two major categories of phosphines and phosphites, the third class that has attracted attention in the past decades is that of the phosphinites. Most significant is the family generally referred to as aminophosphine-phosphinite (AMPP) ligands (**14**), as indicated in a recent review.[69a] These chiral compounds have been applied in the Rh catalyzed asymmetric

hydroformylation of styrene and vinyl acetate, as shown by the work of Mortreux[69b-e] and Vogt.[70] The latter group introduced P-stereogenic groups in combination with a chiral backbone, yielding ee's up to 77%. Furthermore, this subclass of ligands has been applied in the $Pt/SnCl_2$ catalyzed hydroformylation.[71] Also the asymmetric hydrogenation has been studied, amongst others by Chan.[72,73] Alper has developed chiral aminophosphinites derived from ephedrine.[74]

Ligands of the pincer type ('*PCP* ligands') often employ phosphinite moieties in the side-arms of these tridentate ligands, as in 1,3-bis(diphenylphosphinito)benzene. Their rich coordination chemistry is recently reviewed,[75] and will not be discussed here because of the inherent chemical incompatibility with truly mono-or diphosphinite compounds.

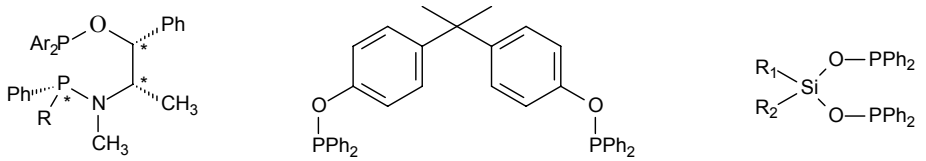

14 **15** **16**

Figure 1.8: *Several types of phosphinite compounds: Family of AMPP ligands (**14**), a Bisphenol A derived diphosphinite by Faraone (**15**) and the silyl diphosphinite moiety (**16**).*

Recent developments have mainly been in the use of chiral diphosphinites in the asymmetric hydrocyanation[76] and hydrogenation, as evidenced by the work of RajanBabu,[77] Chan,[78] Zhang,[79] Jiang[80] and Oehme.[81] Hauptman *et al*. have recently reported on the application of chiral tetrahydrothiophene based bis(phosphinite) ligands in the asymmetric hydrogenation, yet these compounds coordinate in a (P,S)-fashion forming dinuclear species, as was shown by a crystallographic study.[82] Yamamoto has developed both phosphine and phosphinite ligands derived from bicyclo[2.2.2]heptane, which are in principle available as optically pure compounds. However, in the asymmetric hydroformylation of styrene no ee was detected.[83] Kollár *et al*. have prepared and used tetraphosphinites in both the $Pt/SnCl_2$ and the Rh catalyzed hydroformylation of styrene, showing the usual high chemo- and regioselectivity.[84] Faraone has developed bis(phosphinite) ligands based on Bisphenol A as the backbone (**15**) and tested them in the rhodium catalyzed hydroformylation of 1-octene. These ligands acted as monodentate ligands in several transition metal complexes.[85] Deshpande *et al.* have studied the interaction of mixtures of terminal alkenes (*e.g.* 1-decene and 4-phenyl-1-butene) with a monophosphinite functionalized cyclodextrin, to determine if host-guest interactions, by preferential inclusion of one substrate from the mixture, would lead to any effect on the results in the Rh catalyzed hydroformylation.[86] Although some indications were noted during the experiments, no decisive conclusions could be drawn from this study. Kostas has reported

on a flexible diphosphinite with an *N*-phenyldiethylamino-unit as linker. The corresponding Rh catalyst showed normal activities in the hydroformylation of styrene.[87]

1.6.1 Coordination Chemistry of Phosphinites

Strikingly, relatively few reports have appeared on the structural characterization of transition metal complexes of *e.g.* Rh, Pd and Pt with (di)phosphinite ligands, in contrast to the numerous publications on metal complexes with phosphines and phosphites.

Rhodium. Nolan has synthesized a monophosphinite ligand with a fluorous tail. Besides the use of this ligand in Rh catalyzed hydrogenation in fluorous phase, the molecular structure of *trans*-$RhCl(CO)(L)_2$ was described.[88] Burrows and co-workers have elucidated the structure of a dinuclear rhodium complex with the ligand $(pyr)_2POP(pyr)_2$ (pyr = pyrrole).[89] Kempe has been quite active in this field of research, which has resulted in several rhodium complexes with 1,2-dioxobenzene derived ligands.[90]

Palladium and Platinum. Faraone has published on the face-to-face dimeric structures of Pd and Pt with phosphinites derived from Bisphenol A backbones, characterized by X-ray crystallography.[85b] Floriani has made calix[4]arenes with four phosphinite moieties on the upper rim of the structure. These ligands were shown to act as bidentate ligands with palladium and platinum precursors.[91] Faidherbe *et al.* on the other hand made monophosphinites based on the same backbone.[92] Maitlis communicated the preparation of a Pd complex with monodentate phosphinites derived from cholesterol.[93] Kraatz has used amino-acids, other than proline, for the synthesis of monophosphinites and their palladium and platinum complexes.[94] The group of Bergamini has documented an interesting reverse methodology for the preparation of chiral vicinal diphosphinites and their Pd and Pt metal complexes. The synthesis starts with the formation of $MCl_2(PPh_2Cl)_2$, which is subsequently reacted with the desired diol to yield the diphosphinite.[95] This procedure is a modification of the template approach described by Pringle of the preparation of a diphenylsilyldiphosphinite-based *cis*-Pt complex, starting from *cis*-$[PtCl_2(PPh_2OH)_2]$ and $SiCl_2Ph_2$.[96] Other groups have used the same ligand skeleton (**16**) to prepare Mo and Cr complexes.[97,98a] Keim has applied a related Pd complex in the copolymerization of ethylene and CO, but the catalyst rapidly decomposed under those reaction conditions.[98b]

As an extension of this work on silyl based phosphinites, silsesquioxanes were employed as backbone for the synthesis of a novel diphosphinite (**17**) (see *Chapter* 5).[99] The corresponding Pd, Pt, Mo and Rh-complexes were characterized by X-ray crystallography.

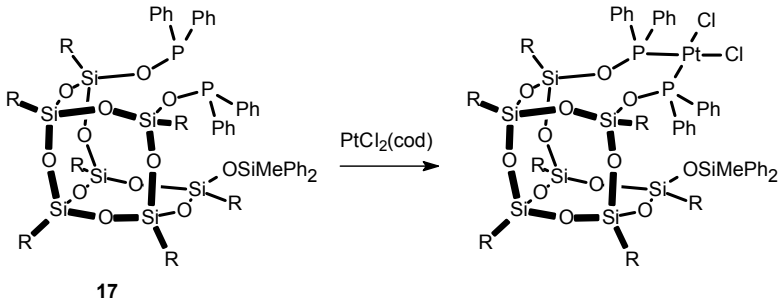

17

Figure 1.9: *Schematic representation of the silsesquioxane based diphosphinite (**17**) and the corresponding complex* cis-*[$PtCl_2$(**17**)]*.

Wendt isolated both the dimeric and the monomeric form of a platinum complex containing 1,3-bis(di-*iso*propylphosphinito)cyclohexane and reported on their respective molecular structures.[100] Recently, Balakrishna synthesized a diphosphinite with a bis(2-hydroxy-1-naphthyl)methane backbone and described various transition metal complexes thereof.[101] This research is linked with the extensive work carried out with the diphosphinite BINAPO, (2,2'-bis(diphenylphosphinito)-1,1'-binaphthyl), first reported in 1977 by Grubbs,[102] and closely related compounds that have been used in catalysis as well as in coordination chemistry.[103]

1.7 Powerful Phosphonites

By far the most overlooked and neglected class of phosphorus containing ligands, regarding both the coordination chemistry with transition metals as well as the applicability of such complexes in homogeneous catalysis, phosphonites have only recently received some attention in the literature. This includes the patent literature, which is dominated at the moment by BASF. Activities are ongoing in both the hydrocyanation[104] as well as the hydroformylation of alkenes.[105] Co-workers from Du Pont de Nemours have claimed a series of ferrocene based ligands and their application in processes regarding the hydroformylation of especially butadiene.[106] This work with ferrocene as a backbone for phosphonite ligands appears to be similar to the work of Shum *et al*. at Ciba Geigy.[107]

Other groups have published recently on the application of (di)phosphonites in homogeneous catalysis. Promising results have been obtained by Vogt and co-workers in the asymmetric hydrocyanation of styrene, applying XantBino (**18**),[108] the Cu catalyzed diethylzinc addition[109a,110a] and the conjugate addition of arylboronic acids using ligands such as (**19**).[109b] This work is

complementary to research on the Rh catalyzed asymmetric hydrogenation, also by Reetz,[109c] Claver and Pringle[110b,c] and by Zanotti-Gerosa at Chirotech, who employed ligand (**20**) based on the chiral paracyclophane backbone.[111] Also monodentate chiral phosphonites have been applied by Reetz[109d] and Scharf,[112] using a TADDOL derived ligand also employed by Seebach.[113] Tillack and co-workers reported on Ni systems with chiral phosphonites for the reaction of cyclopentene with phenylisocyanate.[114] This work included a monophosphonite with a binaphthyl backbone and a phenyl substituent on the phosphorus atom, already reported in 1994 by Tani.[115]

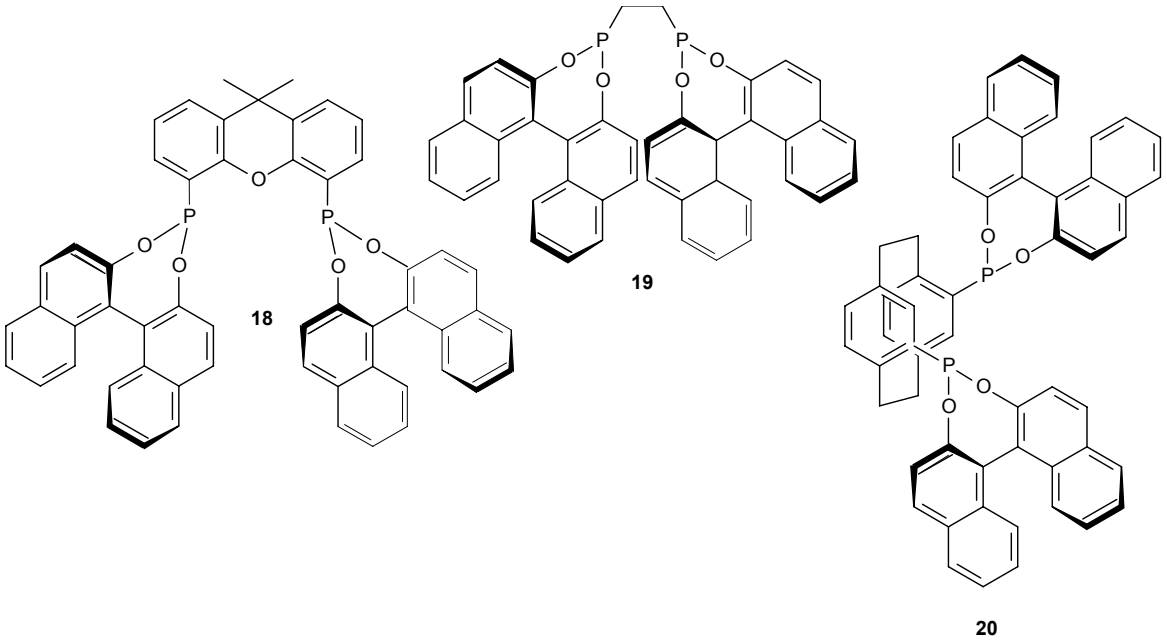

Figure 1.10: *Illustration of the structures of XantBino (**18**),[108] the diphosphonite analogue of dppe (**19**) by Reetz[109c] and the paracyclophane based system (**20**).*[111]

Furthermore, significant achievements have been made in the preparation of mixed ligand systems, which have one phosphonite moiety and contain either a phosphine group[116] or a phosphite,[117] yet little catalytic tests have been performed with these systems. For the hydroformylation of alkenes Börner, in a cooperation with Oxeno Olefin, has reported on the application of monodentate phosphonites.[118] The two ligand systems applied – either with an oxaphosphorine moiety or the non-cyclic derivative thereof - can generally be depicted as compounds (**21**) and (**22**), respectively. In the hydroformylation of 1-octene low regioselectivities are obtained, although the systems showed high activities. More intriguing are the results with a mixture of *n*-octenes, showing high activities and encouraging regioselectivities, with up to 48% of *n*-nonanal. The same structural motif as found in (**21**) was used by Schmutzler and Börner, when they investigated the use of a calix[4]arene-based diphosphonite (for analogous phosphites, *vide supra*) in the

hydroformylation of 1-octene.[64a] However, the regioselectivity obtained (*n*:iso ≤ 1.73) did not point to bidentate character of the ligand during catalysis. The latest contribution came from Vogt and co-workers applying xanthene based sterically constrained diphosphonites, such as *e.g.* ligand structure (**23**). Besides the substrate 1-octene, for which an *n*:iso ratio of up to 9 was obtained, also 2-butene was tested in the Rh catalyzed hydroformylation. Unprecedented regioselectivities of up to 62% *n*-pentanal were achieved at 140 °C.[119]

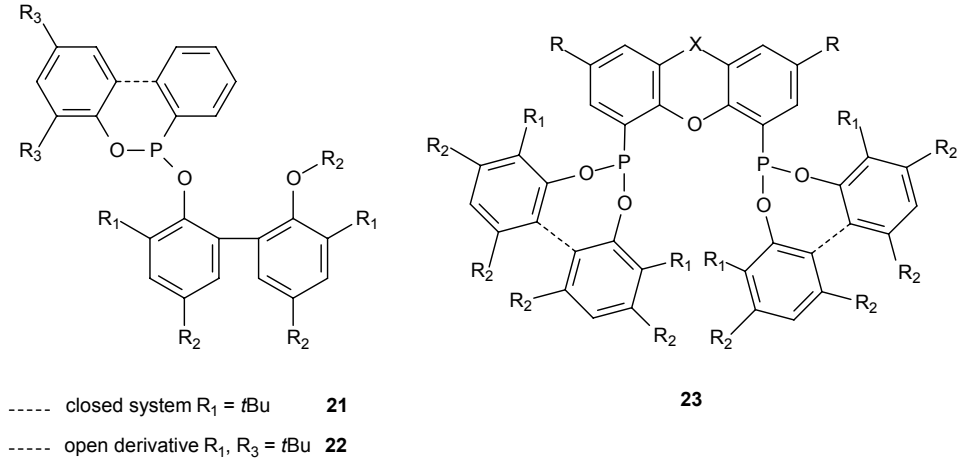

Figure 1.11: *General structures of the monophosphonites (**21**) and (**22**) applied by Börner*[118] *and the xanthene based diphosphonites (**23**) described by Vogt.*[119]

1.7.1 Coordination Chemistry of Phosphonites

As for the coordination chemistry and especially the characterization by X-ray crystallography of diphosphonite transition metal complexes, little has been done to date. The Ciba-Geigy group[107a] has published the first $Rh^{(I)}$ complex with a diphosphonite ligand, as recent as *2002*! This surprising result is based on a survey in the Cambridge Crystallographic Database, thereby disregarding the family of phosphoramidites. Nifant'ev *et al.* have reported the first synthesis of a $[Rh(CO)(L)]^{+}Cl^{-}$ complex, with a ferrocene based diphosphonite. They also reported the molecular structure for the Ag complex with this ligand.[120]

Rhodium. Work performed in the late 70's and 80's on so-called aminophosphoranes – cyclic phosphonites with an additional coordinating amino-functionality, can be considered as early research on monophosphonite transition metal complexes.[121] Already in 1990, Puddephatt showed the formation of a face-to-face dinuclear Rh complex with the ligand $(PhO)_2PCH_2P(OPh)_2$.[122a] A true monodentate $Rh^{(III)}$ phosphonite complex, $Rh(Cp)Cl_2PPh(OPh)_2$, has been structurally characterized by Atherton.[123]

Platinum. Atherton *et al.* also included [$PtCl_2(PEt_3)L$] complexes (L is a highly fluorinated monophosphonite).[123] The phosphonite ligand showed a coupling constant $J_{Pt\text{-}P}$ of around 5200 Hz. In their comparison of monodentate and bidentate chiral phosphonites, Claver and Pringle included two X-ray structures of Pt complexes, one with a monodentate ligand with a biphenanthryl backbone, the other with a biphenanthryl derivative of (**19**).[110b] Squires *et al.* described the chemistry of various bis(dialkoxyphosphino)ethane ligands and their platinum complexes,[124] complementary to the extensive work by Dahlenburg *et al.* on cyclopentane based diphosphonites, their Pt complexes, and on the activity of such complexes in the $Pt/SnCl_2$ catalyzed hydroformylation of styrene.[125] For *cis*-coordinated platinum-diphosphonite complexes, the coupling constant $J_{Pt\text{-}P}$ was found to be around 4700 Hz. Besides the rhodium dimer (*vide supra*), Puddephatt also described the *cis,cis*-(Pt_2Cl_4) dimer with a modified version of the same ligand bearing ethoxy substituents.[122b] Later, a specific calix[4]resorcinarene was modified with four phosphonite moieties on the upper rim and the Au, Cu and Pt complexes of this compound were studied by Puddephatt.[126] Closely related to this work is the supramolecular chemistry carried out with a tetra(thiophosphonato) cavitand and its Ag complex, as reported by Dutasta.[127]

Palladium. There is little data on Pd-complexes with (di)phosphonite ligands. Very recently Schmutzler described a *cis*-$PdCl_2$(PP) complex, PP being 1,8-[bis(dimethoxy)phosphino]naphthalene, as the first example of a palladium-diphosphonite complex.[128] Braunstein and co-workers have created novel compounds that consist of two oxazoline moieties, linked by a phosphonite unit, and which are shown to coordinate as tridentate ligands to Pd.[129] Agbossou had already established two Pd complexes with cyclic aminomonophosphonites.[130] The group of Faraone has worked on modified quinoline ligands with phosphonite functionalities. The analogous Pd complex confirmed the chelate character of this P,N-ligand.[131]

Kubas and co-workers succeeded in elucidating the first Fe complex containing a diphosphonite ligand.[132] Some ruthenium complexes have been studied, but so far without any structural characterization of the complexes formed.[133] Carballo *et al.* managed to obtain crystallographic confirmation for several Re compounds containing simple monophosphonites,[134] while Bravo *et al.* used the same ligand systems to study the corresponding Mn complexes.[135]

1.8 Aim and Scope of this Thesis

This thesis is aimed at the exploration of all four major classes of phosphorus containing ligands, to develop strategies to synthesize new families of suitable ligands and to apply them in the rhodium catalyzed hydroformylation of higher alkenes. Besides the catalytic studies, emphasis will be put on the coordination chemistry of the various ligand systems. This combination of organometallic chemistry with catalysis will prove powerful and sometimes vital for a clear understanding and explanation of the results obtained.

Chapter 2 is dedicated to the coordination chemistry and catalysis with ligands belonging to the class of diphosphonites. In particular achiral xanthene derived and sterically constrained compounds are studied. Molecular structures of their palladium, platinum and rhodium complexes are described. These ligands are able to adopt various coordination modes, depending on the conditions and the transition metal. The exciting results obtained in the hydroformylation of 1-octene and 2-butene are discussed, supported by spectroscopic investigations.

In **Chapter 3** the results obtained with a chiral xanthene derived diphosphonite XantBino in the rhodium catalyzed asymmetric hydroformylation of styrene and the rhodium catalyzed asymmetric hydrogenation of methyl (*Z*)-2-acetamido-cinnamate are described. Palladium and platinum complexes of this ligand are characterized, including molecular structures. Hydroformylation results obtained are discussed in terms of the effect of temperature and pressure on the enantioselectivity.

Chapter 4 includes work on new easy accessible diphosphine ligands based on commercially available Bisphenol A type of backbones. The synthesis is described for in total five ligands, including molecular structures for four compounds. A crystallographic study of the Pd, Pt and Rh complexes with one illustrative example of the new family of ligands as well as results obtained in the Rh catalyzed hydroformylation are disclosed. This work will open up a new route to a potentially interesting class of modular phosphorus ligands with various options for further modification, partly due to a wide range of available backbones.

The development of novel silsesquioxane based phosphorus containing ligands is reported in **Chapter 5**. For the first time several well-defined monophosphites, a diphosphite as well as a diphosphinite compound based on this structural skeleton are synthesized and characterized. Various crystal structures incorporating either palladium, platinum, molybdenum or rhodium are discussed with respect to the coordination behaviour of the ligands. The results of the rhodium catalyzed hydroformylation of 1-octene applying these ligands are reported. Both the electron-withdrawing character of the silsesquioxane framework as well as the steric bulk of the phosphorus moiety are shown to have significant effects on the catalyst performance.

1.9 References

1 O. Roelen, *Ger. Pat.* 849548, **1938**.

2 H.-W. Bohnen and B. Cornils, *Adv. Catal.*, **2002**, *47*, 1.

3 P. Arnoldy, in *Rhodium Catalyzed Hydroformylation*; P.W.N.M. van Leeuwen, C. Claver, Ed.; Kluwer, Amsterdam, **2001**, 203.

4 R.F. Heck and D.S. Breslow, *J. Am. Chem. Soc.*, **1961**, *83*, 4023.

5 *Organometallic Chemistry of Transition Elements*; F. P. Pruchnik, Ed.; Plenum Press, New York, **1990**.

6 J.L. Vidal and W.E. Walker, *Inorg. Chem.*, **1981***, 20*, 249.

7 a) D. Evans, J. A. Osborn and G. Wilkinson, *J. Chem. Soc. A*, **1968**, 3133; b) D. Evans, G. Yagupky and G. Wilkinson, *J. Chem. Soc. A*, **1968**, 2660; c) C.K. Brown and G. Wilkinson, *J. Chem. Soc. A*, **1970**, 2753.

8 C. P. Casey, E.L. Paulsen, E.W. Beuttenmueller, B.R. Proft, B.A. Matter and D.R. Powell, *J. Am. Chem. Soc.*, **1999**, *121*, 63.

9 L.A. van der Veen, P. C. J. Kamer and P. W. N. M. Van Leeuwen, *Organometallics*, **1999**, *18*, 4765.

10 a) D. Vogt, in *Applied Homogeneous Catalysis with Organometallic Compounds*; B. Cornils, W.A. Herrmann, Ed.; Wiley VCH, Weinheim, **2002**, vol 1, 240; b) D. Vogt, in *Aqueous-Phase Organometallic Catalysis*; B. Cornils and W. A. Hermann, Ed.; Wiley-VCH, Weinheim **1998**, 541; c) B. Cornils and E.G. Kuntz, in *Aqueous-Phase Organometallic Catalysis*; B. Cornils and W. A. Hermann, Ed.; Wiley-VCH, Weinheim **1998**, 271.

11 S.J. LaPlaca and J.A. Ibers, *J. Am. Chem. Soc.*, **1963**, *85*, 3501.

12 a) J.M. Brown, L.R. Canning, A.G. Kent and P.J. Sidebottom, *J. Chem. Soc., Chem. Commun.*, **1982**, 721; b) J.M. Brown and A.G. Kent, *J. Chem. Soc., Perkin Trans. 2*, **1987**, 1597.

13 P.P. Deutsch and R. Eisenberg, *Organometallics*, **1990**, *9*, 709.

14 C.A. Tolman, *Chem. Rev.*, **1977**, *77*, 313.

15 C. P. Casey and G. T. Whiteker, *Isr. J. Chem.*, **1990**, *30*, 299.

16 W. Strohmeier and F. J. Müller, *Chem. Ber.*, **1967**, *100*, 2812.

17 C.A. Tolman, *J. Am. Chem. Soc.*, **1970**, *92*, 2953.

18 P. B. Dias, M. De Piedade and J. A. M. Simoes, *Coord. Chem. Rev.* **1994**, *135/136*, 737.

19 S. S. Bath and L. Vaska, *J. Am. Chem. Soc.*, **1963**, *85*, 3500.

20 F. H. Jardine, *Polyhedron*, **1982**, *1*, 569.

21 A. M. Trzreciak and J. J. Ziolkowski, *Coord. Chem. Rev.*, **1999**, *190-2*, 883.

22 J. C. Poulin, T. P. Dang and H. B. Kagan, *J. Organometal. Chem.*, **1975**, *84*, 87.

23 G. Consiglio, C. Botteghi, C. Salomon and P. Pino, *Angew. Chem.*, **1973**, *85*, 665.

24 a) O. R. Hughes and J. D. Unruh, *J. Mol. Cat.* **1981**, *12*, 71; b) J.D. Unruh and J.R. Christenson, *J. Mol. Cat.*, **1982**, *14*, 19.

25 U. Nettekoven, P.C.J. Kamer. M. Widhalm and P.W.N.M. van Leeuwen, *Organometallics*, **2000**, *19*, 4596.

26 a) T.J. Devon, H.W. Philips, T.A. Puckette, J.L. Stavinoha and J.J. Vanderbilt (to Texas Eastman) U.S. Pat. 4,694,109, **1987** [*Chem. Abstr.*, **1988**, *108*, 7890]; b) T.J. Devon, H.W. Philips, T.A. Puckette, J.L. Stavinoha and J.J. Vanderbilt (to Texas Eastman) U.S. Pat. 5,332,846, **1994** [*Chem. Abstr.*, **1994**, *121*, 280879].

27 C.P. Casey, G.T. Whiteker, M.G. Melville, L.M. Petrovich, J.A. Gavney Jr. and D.R. Powell, *J. Am. Chem. Soc.*, **1992**, *114*, 5535.

28 a) Z. Freixa and P.W.N.M. van Leeuwen, *J. Chem. Soc., Dalton Trans.*, **2003**, 1890; b) P.C.J. Kamer, J.N.H. Reek and P.W.N.M. van Leeuwen, *Acc. Chem. Res.*, **2001**, *34*, 895; c) P.W.N.M. van Leeuwen, P.C.J. Kamer, J.N.H. Reek and P. Dierkes, *Chem. Rev.*, **2000**, *100*, 2741; d) R.P.J. Bronger, S.M. Silva, P.C.J. Kamer and P.W.N.M. van Leeuwen, *Chem. Commun.*, **2002**, 3044; e) L.A. van der Veen, P.C.J. Kamer and P.W.N.M. van Leeuwen, *Organometallics*, **1999**, *18*, 4765; f) M. Kranenburg, Y.E.M. van der Burgt, P.C.J. Kamer, P.W.N.M. van Leeuwen, K. Goubitz and J. Fraanje, *Organometallics*, **1995**, *14*, 3081; g) W. Goertz, W. Keim, D. Vogt, U. Englert, M.D.K. Boele, L.A. van der Veen, P.C.J. Kamer and P.W.N.M. van Leeuwen, *J. Chem. Soc., Dalton Trans.*, **1998**, 2981; h) W. Goertz, P.C.J. Kamer, P.W.N.M. van Leeuwen and D. Vogt, *Chem. Commun.*, **1997**, 1521.

29 H. Klein, R. Jackstell, K.D. Wiese, C. Borgmann and M. Beller, *Angew. Chem. Int. Ed.*, **2001**, *40*, 3408.

30 a) K. Tamao, H. Yamamoto, H. Matsumoto, N. Miyake, T. Hayashi and M. Kumada, *Tetrahedron Lett.*, **1977**, *16*, 1389; b) W.A. Herrmann, R. Schmid, C.W. Kohlpaintner and T. Priermeier, *Organometallics*, **1995**, *14*, 1961.

31 a) J.K. Stille, H. Su, P. Brechot, G. Parrinello and L.S. Hegedus, *Organometallics*, **1991**, *10*, 1183; b) I. Ojima, T. Kogure and N. Yoda, *J. Org. Chem.*, **1980**, *45*, 4728; c) I. Ojima, T. Kogure and N. Yoda, *Chem. Lett*, **1979**, 495; d) K. Achiwa, *J. Am. Chem. Soc.*, **1976**, *98*, 8265.

32 H.-H. Xie, L.-X. Wang, Y. Fu, S.-F. Zhu, B.-M. Fan, H.-F. Duan and Q.-L. Zhou, *J. Am. Chem. Soc.*, **2003**, *125*, 4404.

33 S.J. Lu, S.D. Li and A.L. Wang, *Catal. Today*, **2000**, *63*, 531.

34 a) W. Tang and X. Zhang, *Chem. Rev.*, **2003**, *103*, 3029; b) W. Tang and X. Zhang, *Angew. Chem. Int. Ed.*, **2002**, *41*, 1612. The ligand 'Tangphos' officially represents a bidentate phosphole derivative.

35 C.A. Bessel, P. Aggarwal, A.C. Marschilok and K.J. Takeuchi, *Chem. Rev.*, **2001**, *101*, 1031.

36 Z. Freixa, M.S. Beentjes, G.D. Batema, C.B. Dieleman, G.P.F. van Strijdonck, J.N.H. Reek, P.C.J. Kamer, J. Fraanje, K. Goubitz and P.W.N.M. van Leeuwen, *Angew. Chem. Int. Ed.*, **2003**, *42*, 1284.

37 a) M. Sawamura, H. Hamashima, M. Sugawara, R. Kuwano and Y. Ito, *Organometallics*, **1995**, *14*, 4549; b) M. Sawamura, H. Hamashima and Y. Ito, *Tetrahedron: Asymmetry*, **1991**, *2*, 593.

38 H. Kawano, Y. Nishimura and M. Onishi, *J. Chem. Soc., Dalton Trans.*, **2003**, 1808.

39 a) W. Ahlers, R. Paciello, D. Vogt and J.I. van der Vlugt, (to BASF AG) U.S. Pat. 111,517, **2002** [*Chem. Abstr.*, **2002**, *137*, 169060]; b) J.I. van der Vlugt, J.M. Bonet, A.M. Mills, A.L. Spek and D. Vogt, *Tetrahedron Lett.*, **2003**, *44*, 4389; c) J.I. van der Vlugt, M.M.P. Grutters, A.M. Mills, H. Kooijman, A.L. Spek and D. Vogt, *Eur. J. Inorg. Chem.*, **2003**, *accepted*; d) J.I. van der Vlugt, R. van Duren, C. Müller, A. Meetsma and D. Vogt, *manuscript in preparation*; e) See *Chapter* **4** of this thesis.

40 W. Ahlers, R. Paciello, D. Vogt and P. Hofmann (to BASF AG) WO 02/83695, **2002** [*Chem. Abstr.*, **2002**, *137*, 311033].

41 T.S. Barnard and M.R. Mason, *Organometallics*, **2001**, *20*, 206.

42 S.C. van der Slot, J. Duran, J. Luten, P.C.J. Kamer and P.W.N.M. van Leeuwen, *Organometallics,* **2001**, *21*, 3873.

43 R. Jackstell, H. Klein, M. Beller, K.D. Wiese and D. Rottger, *Eur. J. Org. Chem.*, **2001**, 3871.

44 K.G. Moloy and J.L. Petersen, *J. Am. Chem. Soc.*, **1995**, *117*, 7696.

45 S.W. Breeden and M. Wills, *J. Org. Chem.*, **1999**, *64*, 9735.

46 T. Hayashi, M. Tanaka and I. Ogata, *J. Mol. Cat.*, **1979**, *53*, 1.

47 a) D. Neibecker and R. Reau, *J. Mol. Cat.*, **1989**, *57*, 153; b) D. Neibecker and R. Reau, *Angew. Chem. Int. Ed.*, **1989**, *28*, 500; c) D. Neibecker and R. Reau, *J. Mol. Cat.*, **1989**, *53*, 219; d) C. Bergounhou, D. Neibecker and R. Reau, *J. Chem. Soc., Chem. Commun.*, **1988**, 1370.

48 a) B. Breit, R. Winde, T. Mackewitz, R. Paciello and K. Harms, *Chem. Eur. J.*, **2001**, *7*, 3106; b) B. Breit, R. Winde and K. Harms, *J. Chem. Soc., Perkin Trans. 1*, **1997**, 2681; c) B. Breit, *J. Chem. Soc., Chem. Commun.*, **1996**, 2071.

49 B. Breit and W. Seiche, *J. Am. Chem. Soc.*, **2003**, *125*, 6608.

50 a) R. L. Pruett and J. A. Smith; *J. Org. Chem.*, **1969**, *34*, 327; b) R.L. Pruett and J.A. Smith (to Union Carbide) S. Afr. Pat. 6,804,937, **1968** [*Chem. Abstr.*, **1969**, *71*, 90819].

51 A. K. Bhattacharya and G. Thyagarajan; *Chem. Rev.*, **1981**, *81*, 415-430.

52 a) N. Sakai, S. Mano, K. Nozaki and H. Takaya, *J. Am. Chem. Soc.*, **1993**, *115*, 7033; b) K. Nozaki, N. Sakai, T. Nanno, T. Higashijima, S. Mano, T. Horiuchi and H. Takaya,. *J. Am. Chem. Soc.*, **1997**, *119*, 4413.

53 J.E. Babin and G.T. Whiteker (to Union Carbide) WO 93/03830, **1992**.

54 S. Cserépi-Szüca and J. Bakos, *Chem. Commun.*, **1997**, 635.

55 For recent reviews on asymmetric hydroformylation see: a) B. Breit and W. Seiche, *Synthesis*, **2001**, 1; b) F. Agbossou, J.-F. Carpentier and A. Mortreux, *Chem. Rev.*, **1995**, *95*, 2485.

56 a) Y. Jiang, S. Xue, Z. Li, J. Deng, A. Mi and A.S.C. Chan, *Tetrahydron: Asymmetry*, **1998**, *9*, 3185; b) Y. Jiang, S. Xue, K. Yu, Z. Li, J. Deng, A. Mi and A.S.C. Chan, *J. Organomet. Chem.*, **1999**, *586*, 159; c) Z. Freixa and J.C. Bayon, *J. Chem. Soc., Dalton Trans.*, **2001**, 1293; d) A. Suárez, M.A. Méndez-Rojas and A. Pizzano, *Organometallics*, **2002**, *21*, 4611. The ligands described herein are actually phosphine-phosphite compounds and as such analogues of BINAPHOS; e) R. Kadyrov, D. Heller and R. Selke, *Tetrahedron: Asymmetry*, **1998**, *9*, 329; f) M. Diéguez, O. Pàmies, A. Ruiz, S. Castillón and C. Claver, *Chem. Commun.*, **2000**, 1607; g) O. Pamies, G. Net, A. Ruiz and C. Claver, *Tetrahedron: Asymmetry*, **2000**, *11*, 1097; h) M. Diéguez, O. Pàmies, G. Net, A. Ruiz and C. Claver, *Tetrahedron:*

Asymmetry, **2001**, *12*, 651; j) M. Diéguez, O. Pàmies, A. Ruiz, S. Castillón and C. Claver, *Chem. Eur. J.*, **2001**, *7*, 3086.

57 a) P.W.N.M. van Leeuwen and C.F. Roobeek, *J. Organomet. Chem.*, **1983**, *258*, 343; b) c) T. Jongsma, G. Challa and P.W.N.M. van Leeuwen, *J. Organomet. Chem.*, **1991**, *421*, 121.

58 a) A. van Rooij, E.N. Orij, P.C.J. Kamer and P.W.N.M. van Leeuwen, *Organometallics*, **1995**, *14*, 34; b) A. van Rooij, P.C.J. Kamer, P.W.N.M. van Leeuwen, K. Goubitz, J. Fraanje, N. Veldman and A.L. Spek, *Organometallics*, **1996**, *15*, 835.

59 M.B. Dinger and M.J. Scott, *Inorg. Chem.*, **2001**, *40*, 856.

60 a) C.J. Cobley, D.D. Ellis, A.G. Orpen and P.G. Pringle, *J. Chem. Soc., Dalton Trans.*, **2000**, 1109; b) C.J. Cobley, D.D. Ellis, A.G. Orpen and P.G. Pringle, *J. Chem. Soc., Dalton Trans.*, **2000**, 1101.

61 a) F.J. Parlevliet, C. Kiener, J. Fraanje, K. Goubitz, M. Lutz, A.L. Spek, P.C.J. Kamer and P.W.N.M. van Leeuwen, *J. Chem. Soc., Dalton Trans.*, **2000**, 1113; b) F.J. Parlevliet, M.A. Zuideveld, C. Kiener, H. Kooijman, A.L. Spek, P.C.J. Kamer and P.W.N.M. van Leeuwen, *Organometallics*, **1999**, *18*, 3394.

62 a) E. Billig, A.G. Abatjoglou and D.R. Bryant (to Union Carbide) U.S. Pat. 4,769,498, **1988** [*Chem. Abstr.*, **1989**, *111*, 117287]; b) E. Billig, A.G. Abatjoglou and D.R. Bryant (to Union Carbide) U.S. Pat. 4,668,651; Eur. Pat. 213,639, **1987** [*Chem. Abstr*., **1987**, *107*, 7392]; c) E. Billig, A.G. Abatjoglou, D.R. Bryant, R.E. Murray and J.M. Maher (to Union Carbide) U.S. Pat. 4,599,206, **1986** [*Chem. Abstr*., **1988**, *109*, 233177].

63 D. Selent, D. Hess, K.-D. Wiese, D. Röttinger, C. Kunze and A. Börner, *Angew. Chem. Int. Ed.*, **2001**, *40*, 1696.

64 a) C. Kunze, D. Selent, I. Neda, M. Freytag, P.G. Jones, R. Schmutzler, W. Baumann and A. Börner, *Z. Anorg. Allg. Chem.*, **2002**, *628*, 779; b) C. Kunze, D. Selent, I. Neda, R. Schmutzler, A. Spannenberg and A. Börner, *Heteroatom Chem.*, **2001**, *12*, 577.

65 a) A.C. Hewat, *PhD. Thesis*, RWTH Aachen, **2000**.; b) see ref. 40.

66 C.B. Dieleman, P.C.J. Kamer, J.N.H. Reek and P.W.N.M. van Leeuwen, *Helv. Chim. Acta*, **2001**, *84*, 3269.

67 a) J.I. van der Vlugt, M.M.P. Grutters, J. Ackerstaff, R.W.J.M. Hanssen, H.C.L. Abbenhuis and D. Vogt, *Tetrahedron Lett.*, *accepted*; b) J.I. van der Vlugt, T. Dijkstra, R. van Duren, H. Kooijman, A.L. Spek, R. Duchateau and D. Vogt, *manuscript in preparation*; c) See *Chapter* **5** of this thesis.

68 For a recent review on mixed P-O/N ligands, see: J. Ansell and M. Wills, *Chem. Soc. Rev.*, **2002**, *31*, 259.

69 a) F. Agbossou-Niedercorn and I. Suisse, *Coord. Chem. Rev.*, **2003**, *242*, 145; b) F. Agbossou, J.-F. Carpentier, F. Hapiot, I. Suisse and A. Mortreux, *Coord. Chem. Rev.*, **1998**, *178-180*, 1615. c) S. Naïli, A. Mortreux and F. Agbossou, *Tetrahedron: Asymmetry*, **1998**, *9*, 3421; d) A. Roucoux, L. Thieffry, J.-F. Carpentier, M. Devocelle, C. Méliet, F. Agbossou and A. Mortreux, *Organometallics*, **1996**, *15*, 2440; e) Y. Pottier, A. Mortreux and F. Petit, *J. Organomet. Chem.*, **1989**, *370*, 333.

70 R. Ewalds, E.B. Eggeling, A.C. Hewat, P.C.J. Kamer, P.W.N.M. van Leeuwen and D. Vogt, *Chem. Eur. J.*, **2000**, *6*, 1496.

71 a) S. Naïli, J.-F. Carpentier, F. Agbossou, A. Mortreux, G.Nowogrocki and J.-P. Wignacourt, *New J. Chem.*, **1997**, *21*, 919; b) S. Naïli, J.-F. Carpentier, F. Agbossou, A. Mortreux, G. Nowogrocki and J.-P. Wignacourt, *Organometallics*, **1995**, *14*, 401.

72 a) R. Lou, A. Mi, Y. Jiang, Y. Qin, Z. Li, F. Fu and A.S.C. Chan and Y. Wong, *Tetrahedron*, **2000**, *56*, 5857; b) X. Li, R. Lou, C.-H. Yeung, A.S.C. Chan and W.K. Wong, *Tetrahedron: Asymmetry*, **2000**, *11*, 2077.

73 D. Heller, R. Kadyrov, M. Michalik, T. Freier, U. Schmidt and H.W. Krause, *Tetrahedron: Asymmetry*, **1996**, *7*, 3025.

74 V.F. Kuznetsov, G.A. Facey, G.P.A. Yap and H. Alper, *Organometallics*, **1999**, *18*, 4706.

75 M.E. van der Boom and D. Milstein, *Chem. Rev.*, **2003**, *103*, 1759.

76 T.V. RajanBabu and A.L. Casalnuovo, *J. Am. Chem. Soc.*, **1992**, *114*, 6265.

77 a) T.V. RajanBabu, B. Radetich, K.K. You, T.A. Ayers, A.L. Casalnuovo and J.C. Calabrese, *J. Org. Chem.*, **1999**, *64*, 3429; b) T.V. RajanBabu, T.A. Ayers, G.A. Halliday, K.K. You and J.C. Calabrese, *J. Org. Chem.*, **1997**, *62*, 6012; c) T.V. RajanBabu and T.A. Ayers, *Tetrahedron Lett.*, **1994**, *35*, 4295.

78 a) A.S.C. Chan, W. Hu, C.-C. Pai, C.-P. Lau, Y. Jiang, A. Mi, M. Yan, J. Sun, R. Lou and J. Deng, *J. Am. Chem. Soc.*, **1997**, *119*, 9570; b) W. Hu, M. Yan, C.-P. Lau, S.M. Yang, A.S.C. Chan, Y. Jiang and A. Mi, *Tetrahedron Lett.*, **1999**, *40*, 973.

79 G. Zhu and X. Zhang, *J. Org. Chem.*, **1998**, *63*, 3133.

80 A.. Zhang and B. Jiang, *Tetrahedron Lett.*, **2001**, *42*, 1761.

81 R. Selke, M. Schwarze, H. Baudisch, I. Grassert, M. Michalik, G. Oehme, N. Stoll and B. Costisella, *J. Mol. Cat. A: Chem.*, **1993**, *84*, 223.

82 E. Hauptman, R. Shapiro and W. Marshall, *Organometallics*, **1998**, *17*, 4976.

83 K. Yamamoto, S. Momose, M. Funahashi, S. Ebata, H. Ohmura, H. Komatsu and M. Miyazawa, *Chem. Lett.*, **1994**, 189.

84 Z. Csók, G. Szalontai, G. Czira and L. Kollár, *J. Organomet. Chem.*, **1998**, *570*, 23.

85 a) C.G. Arena, D. Drago and F. Faraone, *J. Mol. Cat A: Chem.*, **1999**, *144*, 379; b) C.G. Arena, D. Drommi, F. Faraone, C. Graiff and A. Tiripicchio, *Eur. J. Inorg. Chem.*, **2001**, 247.

86 R. M. Deshpande, A. Fukuoka and M. Ichikawa, *Chem. Lett.*, **1999**, *28*, 13.

87 I.D. Kostas, *J. Organomet. Chem.*, **2001**, *626*, 221.

88 C.M. Haar, J. Huang, S.P. Nolan and J.L. Petersen, *Organometallics*, **1998**, *17*, 5018.

89 A.D. Burrows, M.F. Mahon, M.T. Palmer and M. Varrone, *Inorg. Chem.*, **2002**, *41*, 1695.

90 a) R. Kempe, M. Schwarze and R. Selke, *Z. Kristallogr.*, **1995**, *210*, 555; b) R. Kempe, A. Spannenberg, and D. Heller, *Z. Kristallogr.*, **1998**, *213*, 631; c) R. Kempe, A. Spannenberg, D. Heller, R. Kadyrov and V. Fehring, *Z. Kristallogr.*, **2001**, *216*, 157.

91 M. Stolmàr, C. Floriani, A. Chiesi-Villa and C. Rizzoli, *Inorg. Chem.*, **1997**, *36*, 1694.

92 P. Faidherbe, C. Wieser, D. Matt, A. Harriman, A. De Cian and J. Fischer, *Eur. J. Inorg. Chem.*, **1998**, 451.

93 P. Berdagué, J. Courtieu, H. Adams, N.A. Bailey and P.M. Maitlis, *J. Chem. Soc., Chem. Commun.*, **1994**, 1589.

94 P.W. Galka and H.-B. Kraatz, *J. Organomet. Chem.*, **2003**, *674*, 24.

95 P. Bergamini, V. Bertolasi, M. Cattabriga, V. Ferretti, U. Loprieno, N. Mantovani and L. Marvelli, *Eur. J. Inorg. Chem.*, **2003**, 918.

96 J.K. Hogg, S.L. James, A.G. Orpen and P.G. Pringle, *J. Organomet. Chem.*, **1994**, *480*, C1.

97 G.M. Gray, F.P. Fish, D.K. Srivastava, A. Varshney, M.J. van der Woerd and S.E. Ealick, *J. Organomet. Chem.*, **1990**, *385*, 49.

98 a) H. Voelker, S Freitag, U. Pieper and H.W. Roesky, *Z. Anorg. Allg. Chem.* **1995**, *621*, 694; b) W. Keim and H. Maas, *J. Organomet. Chem.*, **1996**, *514*, 271.

99 a) J.I. van der Vlugt, M. Fioroni, J. Ackerstaff, R.W.J.M. Hanssen, A.M. Mills, A.L. Spek, A. Meetsma, H.C.L. Abbenhuis and D. Vogt, *Organometallics*, *accepted*; b) See *Chapter* **5** of this thesis.

100 S. Sjövall, C. Andersson and O.F. Wendt, *Inorg. Chim. Acta*, **2001**, *325*, 182.

101 M.S. Balakrishna, R. Panda and J.T. Mague, *J. Chem. Soc., Dalton Trans.*, **2002**, 4617.

102 R. Grubbs and R.A. DeVries, *Tetrahedron Lett.*, **1977**, 1879.

103 a) F.-Y. Zhang, W.H. Kwok and A.S.C. Chan, *Tetrahedron: Asymmetry*, **2001**, *12*, 2337; b) Y.-G. Zhou and X. Zhang, *Chem. Commun.*, **2002**, 1124; c) M. Mori, T. Nishimata and Y. Nagasawa and Y. Sato, *Adv. Synth. Catal.*, **2001**, *343*, 34; d) B.M. Trost and D.J. Murphy, *Organometallics*, **1985**, *4*, 1143.

104 M. Bartsch, R. Baumann, D.P. Kunsmann-Keitel, G. Haderlein, T. Jungkamp, M. Altmayer, W. Siegel and F. Molnar (to BASF AG) WO 03/033509, **2003** [*Chem. Abstr.*, **2003**, *138*, 321395]; b) M. Bartsch, R. Baumann, D.P. Kunsmann-Keitel, G. Haderlein, T. Jungkamp, M. Altmayer, W. Siegel and F. Molnar (to BASF AG) DE 10,150,286, **2003** [*Chem. Abstr.*, **2003**, *138*, 304408]; c) M. Bartsch, R. Baumann, D.P. Kunsmann-Keitel, G. Haderlein, T. Jungkamp, M. Altmayer and W. Siegel (to BASF AG) DE 10,136,488, **2003** [*Chem. Abstr.*, **2003**, *138*, 137726]; d) M. Bartsch, R. Baumann, D.P. Kunsmann-Keitel, G. Haderlein, D. Vogt and A. Hewat (to BASF AG) DE 10150286, **2003** [*Chem. Abstr.*, **2002**, *136*, 264838]; e) J. Fischer, W. Siegel, D.P. Keitel and L. Siggel (to BASF AG) DE 19,825,212, **1999** [*Chem. Abstr.*, **1999**, *132*, 37251]; f) H. Maas, R. Paciello, M. Röper, J. Fischer and W. Siegel (to BASF AG) WO 99/46044, **1999** [*Chem. Abstr.*, **1999**, *131*, 230267].

105 a) W. Ahlers, D. Wiebelhaus, R. Paciello, M. Bartsch, R. Baumann, D. Vogt and A. Hewat (to BASF AG) WO 02/22261, **2002** [*Chem. Abstr.*, **2002**, *136*, 249380]; b) W. Ahlers, M. Röper, P. Hofmann, D.C.M. Warth and R. Paciello (to BASF AG) WO 01/058589, **2001** [*Chem. Abstr.*, **2001**, *135*, 168206].

106 a) E.E. Bunel (to Du Pont de Nemours) U.S. Pat. 6,437,192, **2002** [*Chem. Abstr.*, **2002**, *137*, 169652]; b) E.E. Bunel and KE. Schwiebert (to Du Pont de Nemours) U.S. Pat. 6,362,354, **2002** [*Chem. Abstr.*, **2002**, *136*, 263268].

107 a) S.P. Shum, S.D. Pastor and G. Rihs, *Inorg. Chem.*, **2002**, *41*, 127; b) S.D. Pastor and S.P. Shum (to Ciba Geigy) U.S. Pat. 5,817,850, **1998** [*Chem. Abstr.*, **1999**, *129*, 290222].

108 W. Goertz, P.C.J. Kamer, P.W.N.M. van Leeuwen and D. Vogt, *Chem. Eur. J.*, **2001**, *7*, 1614.

109 a) M.T. Reetz, A. Gosberg and D. Moulin, *Tetrahedron Lett.*, **2002**, *43*, 1189; b) M.T. Reetz, D. Moulin and A. Gosberg, *Org. Lett.*, **2001**, *3*, 4083; c) M.T. Reetz, A. Gosberg, R. Goddard and S.-H. Kyung, *Chem. Commun.*, **1998**, 2077; d) M.T. Reetz and T. Sell, *Tetrahedron Lett.*, **2000**, *41*, 6333.

110 a) A. Martorell, R. Naasz, B.L. Feringa and P.G. Pringle, *Tetrahedron: Asymmetry*, **2001**, *12*, 2497; b) C. Claver, E. Fernandez, A. Gillon, K. Heslop, D.J. Hyett, A. Martorell, A.G. Orpen and P.G. Pringle, *Chem. Commun.*, **2000**, 961; c) A. Martorell, C. Claver and E. Fernandez, *Inorg. Chem. Commun.*, **2000**, *3*, 132.

111 A. Zanotti-Gerosa, C. Malan and D. Herzberg, *Org. Lett.*, **2001**, *3*, 3687.

112 D. Haag, J. Runsink and H.-D. Scharf, *Organometallics*, **1998**, *17*, 398.

113 J. Sakaki, W.B. Schweizer and D. Seebach, *Helv. Chim. Acta*, **1993**, *76*, 2654.

114 A. Tillack, R. Selke, Ch. Fischer, D. Bilda and K. Kortus, *J. Organomet. Chem.*, **1996**, *518*, 79.

115 K. Tani, P. Yamagada and K. Nagada, *Acta Cryst.*, **1994**, *C50*, 1274.

116 a) K.W. Kottsieper, U. Kühner and O. Stelzer, *Tetrahedron: Asymmetry*, **2001**, *12*, 1159; b) M. Laly, R. Broussier and B. Gautheron, *Tetrahedron Lett.*, **2000**, *41*, 1183; c) M.T. Reetz and A. Gosberg, *Tetrahedron: Asymmetry*, **1999**, *10*, 2129; T.L. Schull and D.A. Knight, *Tetrahedron: Asymmetry*, **1999**, *10*, 207.

117 M.T. Reetz and M. Pastó, *Tetrahedron Lett.*, **2000**, *41*, 3315.

118 D. Selent, K.-D. Wiese, D. Röttger and A. Börner, *Angew. Chem. Int. Ed.*, **2000**, *39*, 1639.

119 a) J.I. van der Vlugt, R. Sablong, P.C.M.M. Magusin and D. Vogt, *Angew. Chem. Int. Ed.*, submitted; b) See *Chapter* **2** of this thesis.

120 I.É. Nifant'ev, L.F. Manzhukova, M.Y. Antipin, Y.T. Struchkov and E.É. Nifant'ev, *Russ. J. Gen. Chem.*, **1995**, *65*, 682.

121 a) J. Wachter, F. Jeanneaux, G. Le Borgne and J.G. Riess, *Organometallics*, **1984**, *3*, 1034; b) D. Bondoux, B.F. Mentzen and I. Tkatchenko, *Inorg. Chem.*, **1981**, *20*, 839; c) C. Pradat, J.G. Riess, D. Bondoux, B.F. Mentzen, I. Tkatchenko and D. Houalla, *J. Am. Chem. Soc.*, **1979**, *101*, 2234; d) D. Bondoux, I. Tkatchenko, D. Houalla, R. Wolf, C. Pradat, J.G. Riess and B.F. Mentzen, *Chem. Commun.*, **1978**, 1022.

122 a) R. Kumar, R.J. Puddephatt and F.R. Fronczek, *Inorg. Chem.*, **1990**, *29*, 4850; b) L. Manojlović-Muir, I.R. Jobe, B.J. Maya and R.J. Puddephatt, *J. Chem. Soc., Dalton Trans.*, **1987**, 2117.

123 M.J. Atherton, J. Fawcett, A.P. Hill, J.H. Holloway, E.G. Hope, D.R. Russell, G.C. Saunders and R.M.J. Stead, *J. Chem. Soc., Dalton Trans.*, **1997**, 1137.

124 M.E. Squires, D.J. Sardella and L.B. Kool, *Organometallics*, **1994**, *13*, 2970.

125 a) L. Dahlenburg and S. Mertel, *J. Organomet. Chem.*, **2001**, *630*, 221; b) L. Dahlenburg, C. Becker, J. Höck and S. Mertel, *J. Organomet. Chem.*, **1998**, *564*, 155.

126 a) W. Xu, J.J. Vittal and R.J. Puddephatt, *Inorg. Chem.*, **1997**, *36*, 86; b) W. Xu, J.P. Rourke, J.J. Vittal and R.J. Puddephatt, *Inorg. Chem.*, **1995**, *34*, 323.

127 B. Bibal, B. Tinant, J.-P. Declercq and J.-P. Dutasta, *Chem. Commun.*, **2002**, 432.

128 A. Karaçar, M. Freytag, P.G. Jones, R. Bartsch and R. Schmutlzer, *Z. Anorg. Allg. Chem.*, **2001**, *627*, 1571.

129 P. Braunstein, F. Naud, A. Dedieu, M.-M. Rohmer, A. DeCian and S.J. Rettig, *Organometallics*, **2001**, *20*, 2966.

130 a) S. Agbossou, M.C. Bonnet, F. Dahan and I. Tkatchenko, *Acta Cryst.*, **1989**, *C45*, 1149; M.C. Bonnet, S. Agbossou, I. Tkatchenko, R. Faure and H. Loiseleur, *Acta Cryst.*, **1987**, *C43*, 445.

131 G. Franciò, D. Drommi, C. Graiff, F. Faraone and A. Tiripicchio, *Inorg. Chim. Acta*, **2002**, *338*, 59.

132 X. Fang, B.L. Scott, J.G. Watkin and G.J. Kubas, *Organometallics*, **2001**, *20*, 2413.

133 B. Steinmetz, M. Hagel and W.A. Schenk, *Z. Naturforsch*, **1999**, *B54*, 1265.

134 R. Carballo, A. Castiñeiras, S. García-Fontán, P. Losada-González, U. Abram and E.M. Vázquez-López, *Polyhedron*, **2001**, *20*, 2371.

135 J. Bravo, J. Castro, S. García-Fontán, E.M. Lamas and P. Rodríguez-Seoane, *Z. Anorg. Allg. Chem.*, **2003**, *629*, 297.

2

Coordination Chemistry of Sterically Constrained Diphosphonites

Selective Hydroformylation of Terminal and Internal Alkenes

Abstract *Two representative structures, compounds **1** and **6**, from a class of recently developed diphosphonite ligands based on xanthene and phenoxathiin backbones are studied with respect to their coordination to palladium, platinum and rhodium. Subtle variation of the steric bulk of the ligands leads to significant differences in coordination behaviour. The resulting complexes **9-15** are studied by NMR spectroscopy as well as by X-ray crystallography. The molecular structures obtained reveal the hitherto unexplored coordination chemistry with diphosphonite ligands. The electronic properties of these diphosphonite ligands are studied via the NMR-coupling constants of the ^{195}Pt satellites of [$PtCl_2$(ligand)] complexes and via the IR-frequencies for the CO stretch vibration (ν_{CO}) in [RhCl(CO)(ligand)] complexes. In the rhodium catalyzed hydroformylation of 1-octene, catalysts containing these novel ligands show high activities, combined with good regioselectivities to the desired linear aldehyde, with l/b ratios of up to 9. With the industrially important substrate 2-butene, isomerization precedes the hydroformylation of the resulting 1-butene, with selectivities for* n-*pentanal of up to 62%. High pressure NMR and IR spectroscopic measurements are performed under typical reaction conditions. In the catalytic resting state Rh(H)$(CO)_2$(ligand), the ligands are predominantly coordinated in the equatorial-equatorial (**ee**) mode.*

2.1 Introduction

Homogeneous catalysis remains a field in which academic research is flourishing, while the number of industrial applications is still limited.[1,2] A wide range of specific applications have been targeted in the design and synthesis of sophisticated phosphorus containing ligands. This search has led to the discovery of a number of new classes of ligands in the past decades.[3] Most of these ligands either bear diphosphines[4-7] or diphosphites[8-10] as the chelating group. Besides those, monophosphines and monophosphites have been reported extensively.[11] On the contrary, very few examples on diphosphonites have appeared in literature to date. The group of Reetz,[12] Zanotti-Gerosa *et al.*[13] and also Pringle and co-workers[14] have published on the catalytic activity of various (chiral) diphosphonites based on known backbones. Claver[15] Haag *et al.*[16] as well as the Reetz group[17] have published on the synthesis and use of monophosphonites.

The rhodium catalyzed hydroformylation of alkenes is one of the best-known examples of homogeneous catalysis performed on a large industrial scale. One of the systems to emerge during the last years for various C-C coupling reactions is a class of ligands based on the xanthene backbone, for which the synthesis was first described by the group of Haenel,[18] and almost simultaneously by the van Leeuwen group, who also applied these novel ligands in catalysis.[19] The proposed strength of these compounds is their rigid backbone which limits the possible coordination modes, and maybe the influence of the oxygen atom in the xanthene skeleton, but this is still under debate.

The plasticizer alcohol 2-ethylhexanol is one of the major products based on *n*-butanal, produced from propene. Environmental concern as well as economic reasons spur the search for alternate feedstock and products. From an economical point of view, internal alkenes or mixtures such as Raffinate-II from cracking facilities,[20a] consisting of *n*-butane and the *n*-butenes, are interesting substrates. Another source of a range of short and medium chain-length internal alkenes is the SHOP process.[20b] This requires however, at least formally, the consecutive double bond isomerization towards the chain-end followed by selective hydroformylation of the terminal alkene. Unfortunately the fast reacting terminal alkene is only present in less than a few percent in the thermodynamic equilibrium mixture. The ultimate catalyst needed for this reaction therefore has to combine a very high isomerization activity with a high preference for terminal alkenes and a high regioselectivity for the linear aldehyde in the hydroformylation step.

The highly active and selective Rh based hydroformylation catalysts unfortunately possess only low isomerization rates, leaving this field to the classic Co systems, which on the other hand suffer from unwanted parallel and side-reactions leading to the hydrogenation of starting material and

the aldehyde product. Recently, Rh systems able to convert internal alkenes to desired linear products have been published.[21-24]

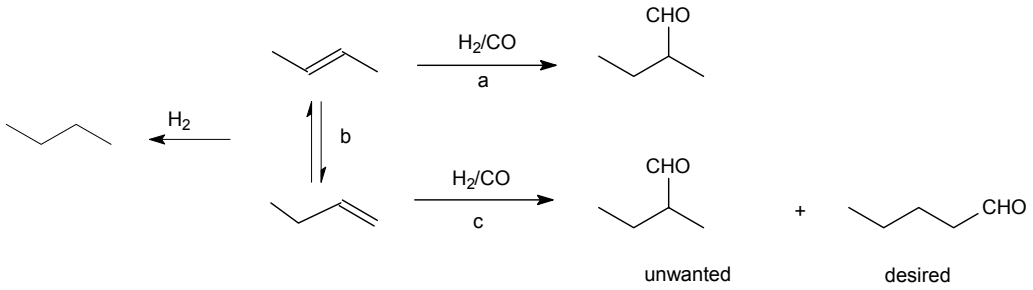

Scheme 2.1: *Hydroformylation of 2-butene: a) direct hydroformylation to branched aldehyde; b) isomerization to 1-butene; c) hydroformylation to both linear and branched aldehyde.*

In hydroformylation, the ligand can greatly effect the regioselectivity and the catalyst activity. For bidentate ligands one defined property is the bite angle, first described by Casey *et al.*[25] The same group made a study on the influence of this bite angle on the regioselectivity in the hydroformylation.[7] They found that angles of around 120° increased the selectivity to linear products. In case of a trigonal bipyramidal complex, such as $Rh(H)(CO)_2(P)_2$, which is the catalytic resting state in the hydroformylation, both donor atoms can be coordinated in an equatorial position (**ee**) or one in an equatorial and the other in an apical position (**ea**). The **ee** coordination seems to be highly favourable for a good regioselectivity to the linear product. The steric bulk of the ligand is known to have a big influence on the regioselectivity of the corresponding catalyst, and on the deactivation of the catalytic species by inhibiting bis-chelates.

So far, *di*phosphonites have not been considered for the hydroformylation of alkenes, with the exception of a paper by Schmutzler and Börner, using a calix[4]arene based ligand. Poor regioselectivities of below 2 were reported however.[26] Besides this, very little is known about the coordination chemistry of diphosphonites with various transition metals. Recently a new class of sterically constrained diphosphonites has been developed with xanthene derived backbones via a straightforward synthetic procedure.[27] These ligands were successfully applied in the nickel catalyzed isomerization of unsaturated nitriles. This chapter will describe the versatile coordination chemistry of these diphosphonite compounds (Figure 2.1) with various transition metals. Furthermore, the application of these ligands in the rhodium catalyzed hydroformylation of both 1-octene and 2-butene will be discussed.

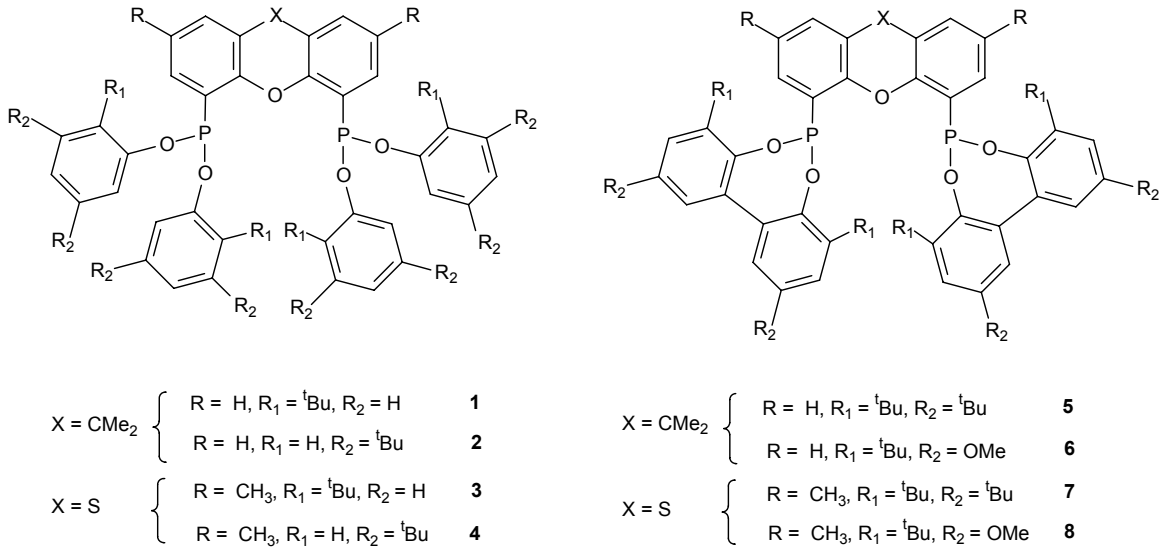

Figure 2.1: *Schematic structures of novel diphosphonites **1-8**.*

2.2 Synthesis

Starting from the commercially available 9,9-dimethylxanthene or 2,7-dimethylphenoxathiin as a backbone and the appropriate (bis)phenols, compounds **1-8** have been prepared (Scheme 2.2). First the bis(diethylamido)phosphonito derivative of the corresponding backbone is synthesized via a well-known procedure.[27c] Subsequently, reaction with the desired phenolic compound yields the diphosphonite compound in good yield. Tetrazole is used as a protonation agent to force the reaction to completion.

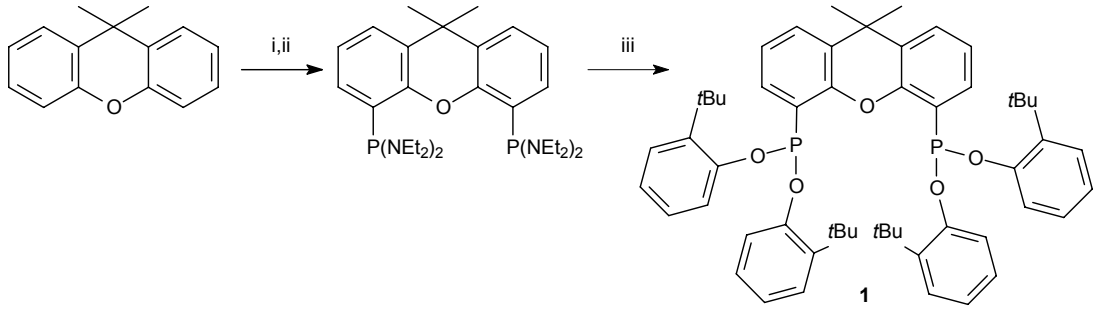

Scheme 2.2: *Synthetic route to diphosphonite ligand **1**: i)* n-*BuLi, TMEDA, Et_2O, -40 ºC, 16 h; ii) $ClP(NEt_2)_2$, pentane, -60 ºC, 16 h; iii) 2-tert-butylphenol (6 eq.), diglyme, tetrazole, Δ, 3 days.*

Single crystals, suitable for X-ray analysis, were obtained for compound **1** by recrystallization from hot acetonitrile. Contrary to the structures reported for Xantphos derivatives[19] no π-stacking of

the aromatic rings is found in the molecular structure of **1** (Figure 2.2). Most likely the steric bulk of the *tert*-butyl substituents prevents such a spatial orientation. Instead the phenol groups are bent in an *anti*-parallel fashion. Table 2.1 contains selected data on bond lengths and angles.

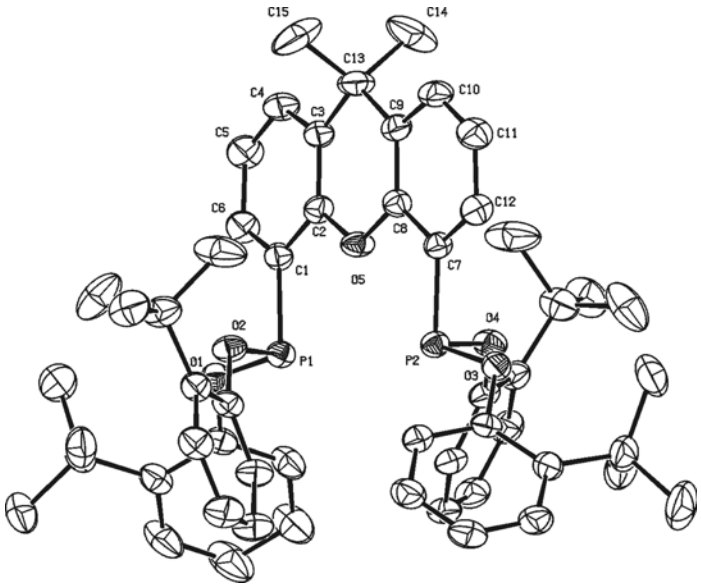

Figure 2.2: *ORTEP representation of compound **1**. Displacement ellipsoids are drawn at the 50% probability level. All hydrogen atoms and solvent molecules are omitted for clarity.*

The P_1-P_2 distance is 4.1298(8) Å, slightly larger than the distance for a xanthene based diphosphine,[19] while the phosphorus-oxygen bonds are in the order of 1.65 Å, comparable to bond lengths in known phosphite crystal structures. The xanthene backbone is only slightly bent with a dihedral angle of 173.3°, which is in accordance with the absence of any stacking of the aromatic rings due to steric congestion.[28] The ligand has approximate C_2 symmetry, with the main deviation arising from the different tilt angles of the terminal phenyl rings of the phosphonite moieties. Table 2.11 in the Experimental Section contains further crystallographic details.

From an unsuccessful reaction between **1** and $Mo(CO)_4(piperidine)_2$ another molecular structure for this compound was obtained (Figure 2.3), which turned out to be polymorph **1A** of the above described structure of **1** (see Table 2.11 for details). Since there are only minute deviations from the values enlisted in Table 2.1, no further details will be disclosed on the bond lengths and angles. However, in this specific case, the xanthene backbone was tilted to a dihedral angle of 144°. This leads to an intramolecular P_1-P_2 distance of 3.9261(5) Å. This discrepancy is believed to originate solely from features of the solid state, while in solution the flat backbone is most likely the energetically favoured conformation.

Table 2.1: *Selected bond lengths, distances and angles for compound **1**.*

Bond lengths (Å)					
P_1-O_1	1.6570(13)	P_1-O_2	1.6512(16)	P_2-O_3	1.6502(14)
P_2-O_4	1.6495(16)	P_1-C_1	1.8252(17)	P_2-C_7	1.8292(17)
O_5-C_2	1.381(2)	O_5-C_8	1.378(2)	P_1-P_2	4.1298(8)
Angles (°)					
O_1-P_1-O_2	99.18(7)	O_3-P_2-O_4	98.10(7)	O_1-P_1-C_1	95.89(7)
O_2-P_1-C_1	95.22(8)	O_3-P_2-C_7	97.05(7)	O_4-P_2-C_7	94.60(8)
C_2-O_5-C_8	119.32(12)	C_3-C_{13}-C_9	110.34(15)		

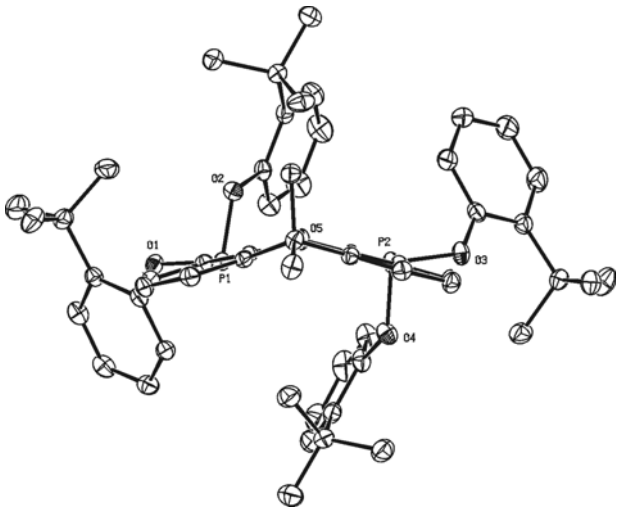

Figure 2.3: *ORTEP representation of the polymorph **1A**, top view. Displacement ellipsoids are drawn at the 50% probability level. All hydrogen atoms and solvent molecules are omitted for clarity.*

To estimate the stability of the new ligands against oxidation and related decomposition processes, compound **1** was allowed to react with an excess of selenium for over five days at 90 °C in toluene. No conversion to the corresponding selenide was observed, indicative of a high stability of the ligand.

2.3 Coordination Chemistry

The coordination behaviour of compounds **1** and **6** with Pd, Pt and Rh was studied. Ligand **1** bears 2-*tert*-butylphenol groups, while the phosphonite units of ligand **6** are derived from 2,2'dihydroxy-3,3'-di(*tert*-butyl)-5,5'-dimethoxy-1,1'-biphenyl. Main research objective was to study whether a difference in coordination mode would be noticeable, changing from palladium via platinum to rhodium, on variation of the steric bulk of the ligands.

2.3.1 Palladium

To date, only four papers have appeared on the X-ray structure determination of palladium phosphonite species. Schmutzler has reported on the preparation of 1,8-bis[(dimethoxy)phosphino]naphthalene (***I***) and its corresponding Pd complex, yielding the first diphosphonite based palladium complex to be structurally characterized.[29] Agbossou *et al.* have characterized a *cis*-dichloropalladium(dioxazaphosphocine) complex as well as a Pd-allyl complex employing the same ligand (***II***).[30] Braunstein and co-workers synthesized monophosphonite-bis-oxazoline compounds (***III***) that acted as tridentate ligands in Pd complexes.[31]

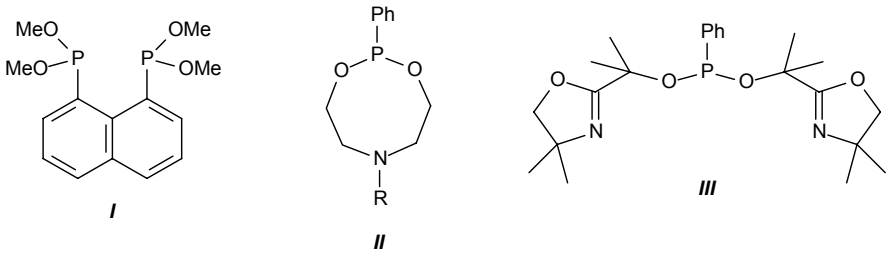

I ***II*** ***III***

Figure 2.4: *Schematic representations of ligands **I-III**, for which molecular structures of the corresponding Pd -complexes have been reported in literature.*

^{31}P NMR and ^{1}H NMR measurements were performed to understand the behaviour of ligands **1** and **6** towards palladium precursors. The reaction of ligand **1** with $PdCl_2$(cod) as the metal source was slow at room temperature, with a conversion of only 40% overnight. When the same reaction was carried out at 60 °C, one singlet was observed at δ = 109.7 ppm in the ^{31}P NMR spectrum. Attempts to crystallize the complex thus formed failed. In order to be able to determine whether the ligand coordinated in a *cis* or *trans*-fashion, $PdCl(CH_3)$(cod) was used as precursor instead.

Also in this case, the complexation reaction was very slow at room temperature, but proceeded readily at 60 °C. For the compound thus obtained one singlet was found at δ = 123.1 ppm in the ^{31}P NMR spectrum, while the ^{1}H NMR spectrum, depicted in Figure 2.5, showed a clear triplet at δ = 0.80 ppm for the methyl ligand. Both findings indicate that the desired complex $PdCl(CH_3)$(**1**) is formed, with a preferred *trans*-coordination of the ligand.

The methyl groups in the xanthene backbone and the *tert*-butyl groups on the phenol rings of the phosphonite moieties appear as two sets of singlets in the same ^{1}H NMR spectrum, indicating that they are chemically inequivalent. This will be due to the bending of the xanthene backbone.[32]

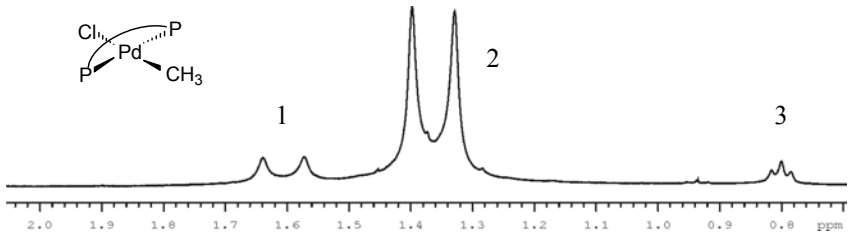

Figure 2.5: *^{1}H NMR of the complex PdCl(CH_3)(**1**) showing both CH_3-groups of the xanthene backbone (1), the* tert*-butyl groups of the phenolic units (2) and the triplet of the methyl ligand (3).*

Single crystals, suitable for X-ray analysis, were obtained, albeit in low yield, by slow diffusion of CH_3CN into a CH_2Cl_2 solution of this compound PdCl(CH_3)(**1**). The molecular structure of the resulting complex **9** is depicted in Figure 2.6. Table 2.2 contains data on selected bond lengths and angles.

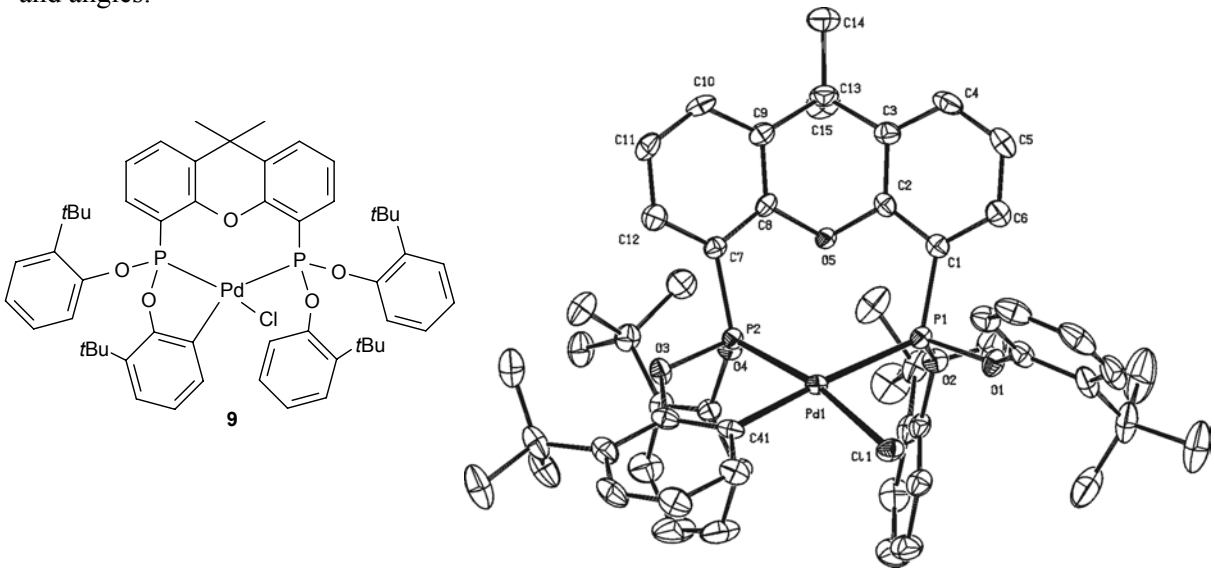

Figure 2.6: *ORTEP representation of complex **9**, [PdCl{κ^3(C-P-P)**1**}]. Displacement ellipsoids are drawn at the 50% probability level. All hydrogen atoms are omitted for clarity.*

Unexpectedly, the structure determined by X-ray diffraction does not correspond to the expected compound PdCl(CH_3)(**1**) but rather appears to be that of an *ortho*-metallated species, with the chlorine atom still coordinated to the palladium. The CH_3 group has been replaced by a phenolate group, originating from one phosphonite moiety, leading to the complex [PdCl{κ^3(*C-P-P)***1**}]. The spectroscopic data presented for the original product from the reaction of PdCl(CH_3)(cod) and **1** (*vide supra*), however, do not fit with the structure of this complex.

The formation of the *ortho*-metallated species might proceed via slow activation of the Pd-CH_3 bond in the crystallization solvent mixture, which would lead to the formation of methane (this has not actually been detected). To confirm this, the conversion of the initial complex PdCl(CH_3)(**1**)

into complex **9** in $CDCl_3$ was followed in time. After 1 week, two doublets were present in the ^{31}P NMR spectrum as a minor species (~10%). This observation suggests the slow formation of the *ortho*-metallated product to occur during crystallization as well. However, the precise mechanism is still uncertain.

The geometry around the palladium atom of complex **9** is distorted square planar, with the two phosphorus atoms coordinating in a *cis*-fashion to the palladium center. The bite angle of the ligand in this conformation, P_1-Pd-P_2, is found to be only 103.91(3)°, while the Cl-Pd-C_{41} angle is 91.11(7)°. The two Pd-P bond lengths differ significantly since Pd-P_1 is 2.4416(8) Å while Pd-P_2 is 2.2131(7) Å. This is due to the phenolate *trans* to P_1, leading to elongation of the bond length of Pd-P_1. The carbon-palladium bond length Pd-C_{41} is 2.073(3) Å, which agrees well with other (*ortho*-metallated) Pd-aryl complexes described in literature.[33,34] Remarkably, the metal atom is positioned relatively far outside of the ligand plane, creating a dihedral angle between the P_1-O_5-P_2 plane and the Cl_1-Pd-C_{41} plane of 155°. Alternatively, the dihedral angle between the plane P_1-P_2-C_1 and the plane Cl_1-Pd-C_{41} is found to be 115.6°. Figure 2.7 contains a fragment of complex **9** showing the side view on the metal core.

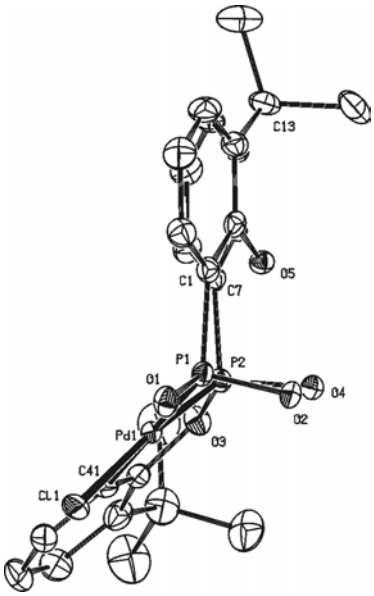

Figure 2.7: *Side view on the metallacycle of complex* ***9*** *showing the existence of a large dihedral angle between the P_1-Pd-P_2 plane and the C_1-P_1-P_2 plane.*

The dihedral angle of the aromatic rings in the backbone is 100.34°, meaning a large deformation from the situation in the free ligand in order to accompany this atypical conformation. The constrained *cis*-position of the two phosphorus atoms is also reflected in a decreased

intramolecular P-P distance from 4.1298(8) Å in the uncoordinated ligand **1** to 3.6685(11) Å in complex **9**.

Table 2.2: *Selected bond lengths, distances and angles for complex **9**,* cis-*[PdCl{κ³(C-P-P)**1**}]*.

Bond lengths (Å)					
$Pd-P_1$	2.4416(8)	$Pd-P_2$	2.2131(7)	Pd-Cl	2.3416(7)
$Pd-C_{41}$	2.073(3)	P_1-O_1	1.6208(19)	P_1-O_2	1.6119(17)
P_1-C_1	1.826(3)	P_2-O_3	1.6126(18)	P_2-O_4	1.6106(17)
P_2-C_7	1.809(2)	O_5-C_2	1.387(3)	O_5-C_8	1.395(3)
$Pd-O_1$	3.5308(16)	P_1-P_2	3.6685(11)		
Angles (°)					
Cl_1-Pd-C_{41}	91.11(7)	P_1-Pd-P_2	103.91(3)	$Cl-Pd-P_1$	85.93(2)
Cl_1-Pd-P_2	169.06(3)	P_1-Pd-C_{41}	176.82(7)	P_2-Pd-C_{41}	78.94(7)
$O_1-P_1-O_2$	97.54(9)	$O_3-P_2-O_4$	101.82(9)	$Pd-P_1-O_1$	117.08(7)
$Pd-P_1-O_2$	114.94(8)	$Pd-P_2-O_3$	108.79(7)	$Pd-P_2-O_4$	121.02(7)
$Pd-P_1-C_1$	123.85(8)	$Pd-P_2-C_7$	121.84(8)	$C_2-O_5-C_8$	112.49(17)
$C_3-C_{13}-C_9$	106.1(2)	$O_1-P_1-C_1$	100.61(11)	$O_2-P_1-C_1$	98.22(10)
$O_3-P_2-C_7$	102.67(10)	$O_4-P_2-C_7$	97.68(9)		

For the product of the *in situ* NMR reaction between ligand **2**, which is structurally related to **1** (except that 3,5-di(*tert*-butyl)phenolate groups are present in this case), and $PdCl_2(cod)$ a singlet was found at δ = 101.7 ppm in the ^{31}P NMR spectrum. The reaction already went to completion after overnight stirring at room temperature. Upon changing to $PdCl(CH_3)(cod)$ as a metal source a mixture of complexes was initially observed. Besides a singlet at δ = 122.1 ppm for the *trans*-complex also two doublets were found at δ = 128.1 ppm and δ = 120.5 ppm. Both doublets of this AB system showed a coupling constant $J_{P\text{-}P}$ of 51.4 Hz. These signals are attributed to the *cis*-complex, whereby two chemically inequivalent phosphorus atoms are present in the complex, one *trans* to the chlorine and one *trans* to the methyl ligand. Following the reaction in time, 60 minutes after addition the two products appeared in a 45:55 *cis*:*trans* ratio, while overnight there was a near quantitative conversion to the *trans*-product. The *trans*-coordination mode therefore is thought to be thermodynamically more stable while the *cis*-complex is the initial product. The signal for the protons of the methyl ligand was obscured by the other aliphatic signals during the *in situ* measurements of the reaction.

With ligand **6**, no unwanted side-reaction to any *ortho*-palladated complex can occur, since *tert*-butyl groups occupy all ortho-positions of the phenolic moieties. The reaction with $PdCl_2(cod)$ proceeded smoothly at room temperature during overnight stirring. A singlet was found at δ = 136.5

ppm in the ^{31}P NMR spectrum. This chemical shift indicates a *trans*-coordination of the diphosphonite ligand, since the chemical shift difference $\Delta\delta$ of ~30 ppm compared to uncoordinated ligand **6** is in the same range as that seen with ligand **1** and **2**.

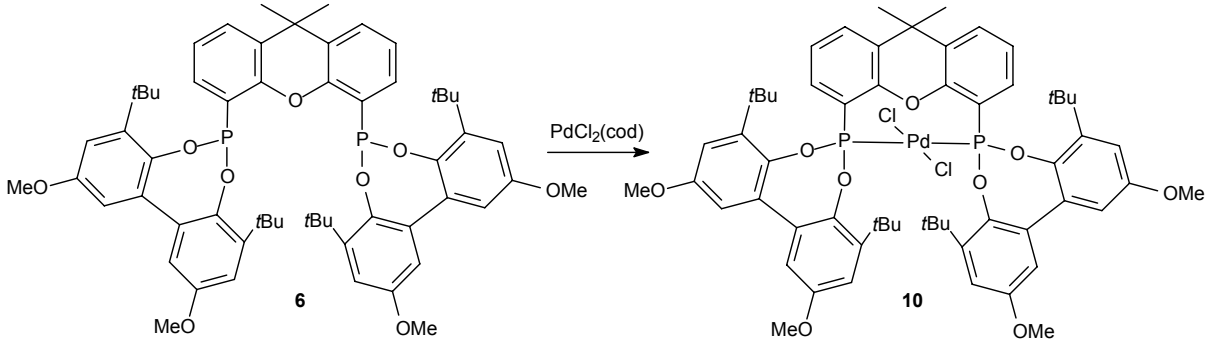

Scheme 2.3: *Reaction of ligand **6** with $PdCl_2$(cod) to yield complex **10,*** trans-*[$PdCl_2$(**6**)]*.

In the ^{1}H NMR spectrum, two singlets are present for the methoxy units as well as for the *tert*-butyl groups, due to chemical inequivalency. Single crystals, suitable for a crystallographic study, could be grown by slow diffusion of acetonitrile into a CH_2Cl_2 solution of this compound. The resulting molecular structure for complex **10** is presented in Figure 2.8, while Table 2.3 contains selected bond lengths and angles.

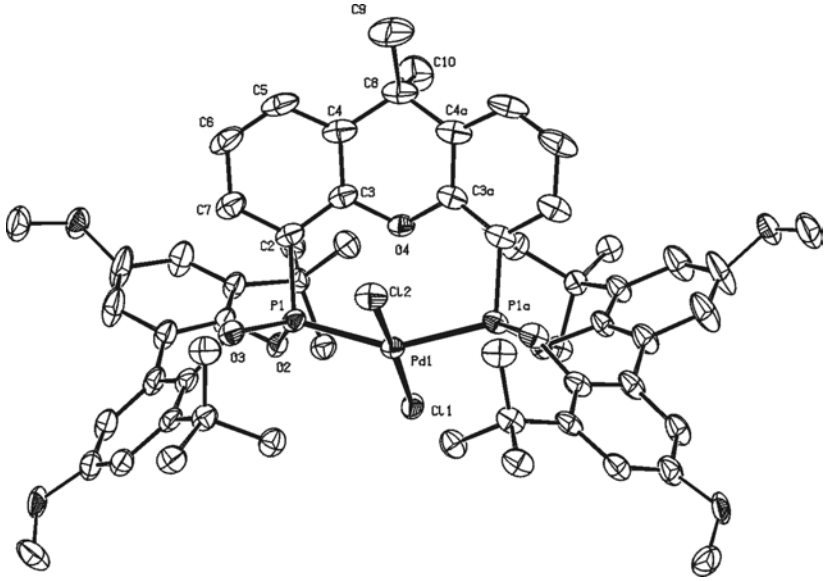

Figure 2.8: *ORTEP representation of complex **10**,* trans-*[$PdCl_2$(**6**)]. Displacement ellipsoids are drawn at the 50% probability level. All hydrogen atoms are omitted for clarity.*

Ligand **6** indeed coordinated in a *trans*-fashion to the palladium atom in complex **10**. The geometry around the palladium atom is distorted square planar. The P_1-Pd-P_2 angle is only 150.12(3)°,

while the Cl_1-Pd-Cl_2 angle is nearly straight at 174.79(4)°. The backbone deformation is only moderate compared to complex **9**, with a dihedral angle between the two aromatic planes of 155.8°. The molecule possesses a plane of symmetry. The Pd-P bond length is 2.2767(6) Å, which is in the same range as the distances found in the work of Agbossou[30] and slightly larger than found in complex **9**. However, due to the *trans*-effect, the Pd-Cl bond is slightly shortened to 2.30 Å on average, while the Pd-P bond is slightly elongated in comparison with these two *cis*-complexes and the work by Schmutzler.[29] The palladium-chloride bond lengths are close to the values found in palladium-(di)phosphite based structures.[35,36]

The *trans*-coordination in square planar palladium complexes with xanthene-based diphosphine ligands has been reported before, both by van Leeuwen[37] and independently by Buchwald.[38] In both cases, bite angles of around 150° were found in the solid state structures with Pd-$O_{backbone}$ distances of around 2.6 Å, which might point to a weak bonding interaction, and consequently to a square pyramidal coordination around the palladium atom.[39a] Normal palladium-ether bonds are in the order of 2.04-2.15 Å.[39] In complex **10**, the distortion from square planarity is evident from the various angles described. The Pd-O_4 intramolecular distance is 2.694(2) Å, which is at least 20% larger than covalent Pd-O(ether) bond lengths. From the solid state structure alone no decisive conclusions can be drawn on the precise nature of this interaction. The situation in complex **10** is distinctly different from the cationic complexes described by Zuideveld *et al.*, where a true bonding interaction is observed (Pd-O bond length of 2.1537(14) Å).[37]

Table 2.3: *Selected bond lengths, distances and angles for complex **10**,* trans-*[$PdCl_2$(**6**)]*.

Bond lengths (Å)					
Pd-P_1	2.2767(6)	Pd-Cl_1	2.2823(8)	Pd-Cl_2	2.3262(10)
P_1-O_2	1.6048(18)	P_1-O_3	1.6114(19)	P_1-C_2	1.823(2)
Pd-O_4	2.694(2)	P_1-P_2	4.3995(9)		
Angles (°)					
P_1-Pd-P_{1a}	150.12(3)	Cl_1-Pd-Cl_2	174.79(4)	Cl_1-Pd-P_1	93.78(2)
Cl_2-Pd-P_1	87.53(2)	Pd-P_1-O_2	113.34(7)	Pd-P_1-O_3	124.30(7)
Pd-P_1-C_2	107.21(9)	O_2-P_1-O_3	104.80(9)	O_2-P_1-C_2	108.42(11)
O_3-P_1-C_2	96.86(11)	C_3-O_4-C_{3a}	118.4(2)	C_4-C_8-C_{4a}	109.5(3)

2.3.2 Platinum

When $PtCl_2$(cod) was employed in the complexation studies, a remarkable difference in reactivity was found for ligand **1** and ligands **2** and **6**. By way of an *in situ* NMR reaction, it was

found that ligand **2** coordinated to platinum without any difficulty and at room temperature. In the ^{31}P NMR spectrum a singlet was present at δ = 72.5 ppm flanked by ^{195}Pt satellites, and a coupling constant $J_{Pt\text{-}P}$ of 5078 Hz. This value found for *cis*-[$PtCl_2$(**2**)] fits with the observed trend in literature for *cis*-$PtCl_2(P)_2$ complexes regarding the coupling constants $J_{Pt\text{-}P}$, going from diphosphites (J ~ 5800 Hz),[40] diphosphinites (J ~ 4200 Hz)[41,42] to diphosphines (J ~ 3500 Hz).[43] The observed spectrum is therefore assigned to originate from a *cis*-platinum-diphosphonite complex. This is also in agreement with unpublished results from our group on platinum complexes with chiral diphosphonites, leading to coupling constants $J_{Pt\text{-}P}$ of 5200 Hz.[44]

To date, only six papers, dealing specifically with platinum *di*phosphonite complexes, have appeared in the literature. Two reports are based on diphosphonites with 1,2-substituted cyclopentyl backbones, giving typical coupling constants of J~ 4700 Hz,[45] while a third paper deals with various other alkyl-derived backbones and with one alkyl ligand instead of a chlorine.[46] Due to these differences, those results are not really comparable with the present work. Claver and Pringle have jointly published both a mono- and a diphosphonite platinum complex.[15] No spectroscopic data for these complexes in solution was provided. Puddephatt and coworkers have reported on a dimeric species, using diethoxyphosphonitomethane as the ligand.[47] The groups of Schmutzler and Börner have prepared a new calix[4]arene based diphosphonite, starting from 6-chloro-dibenzo-1-oxa-$\sigma^3\lambda^3$-phosphorine as the P-building block. They have also reported the related Pt complex, for which the ^{31}P NMR spectrum showed two doublets (due to stereogenic P atoms) and coupling constants $J_{Pt\text{-}P}$ of around 5060 Hz.[26]

Contrary, the reaction between $PtCl_2$(cod) and ligand **1** only proceeded at elevated reaction temperatures of around 70 °C. The ^{31}P NMR spectrum showed two broad singlets at δ = 118.9 ppm and δ = 128.0 ppm. Both peaks were flanked by ^{195}Pt satellites, and respective coupling constants $J_{Pt\text{-}P}$ of 5270 Hz and $J_{Pt\text{-}P}$ of 2517 Hz. The broad signals indicate fluxional behaviour or a dynamic exchange of ligands. It is plausible that one particular species is present, most likely involving a *cis*-coordination of both phosphorus atoms, each with a different ligand in the *trans* position. The two different values found for the coupling constants (^1J ~ 5000 Hz versus ^2J ~ 2500 Hz) are similar as found in *cis*-$PtCl(CH_3)(P)_2$ complexes, first described by Pidcock[48] and later by Cobley *et al.*, for both phosphines and phosphites.[43] For the compound obtained, single crystals could be grown by slow diffusion of CH_3CN into a CH_2Cl_2 solution. The crystallographic study revealed the molecular structure of complex **11**, as depicted in Figure 2.9. For this structure, selected bond lengths and angles are listed in Table 2.4.

The structure is that of an *ortho*-metallated species, again. One chlorine atom is still coordinated to the platinum atom, together with a phenolate group from the phosphonite moiety, so the structure is isomorphous to complex **9**. The existence of two different substituents on the platinum atom, next to the P-P ligand, also explains the complex ^{31}P NMR spectrum. The broad singlets are probably due to rapid exchange of the phosphorus atoms. The difference in coupling constants arises from the fact that one phosphorus is *trans* to the chlorine (J_{Pt-P} = 5240 Hz), while the other phosphorus atom is *trans* to a 'carbon' (J_{Pt-P} = 2517 Hz).

To the best of our knowledge there are no structural reports in the literature of platinum complexes with phosphonite ligands showing *ortho*-metallation. Balakrishna has claimed the formation of an *ortho*-metallated platinum complex with $(PhCH_2O)_2P$-N(Ph)-$P(OCH_2Ph)_2$ coordinated as a (κ^3-P-P-C) chelating ligand, next to the expected *cis*-$PtCl_2$(PP) complex.[48b] This intramolecular rearrangement to the *ortho*-metallated species is suggested on the basis of the ^{31}P NMR spectrum, which showed two doublets with coupling constants J_{Pt-P} of 5381 Hz and 5363 Hz, respectively, for both inequivalent phosphorus atoms, coordinated in a *cis*-fashion. This implies that the *trans*-effect of a chlorine atom is virtually the same as that of a phenyl ligand, which seems unlikely and also clearly in contradiction to the spectroscopic data presented here, which is supported by an X-ray crystallographic study. Bennet *et al*. have reported on complexes containing orthoplatinated triphenylphosphine.[48c] Recently, Bedford has shown the application of *ortho*-platinated triaryl phosphite and phosphinite complexes in Suzuki biaryl coupling reactions.[48d]

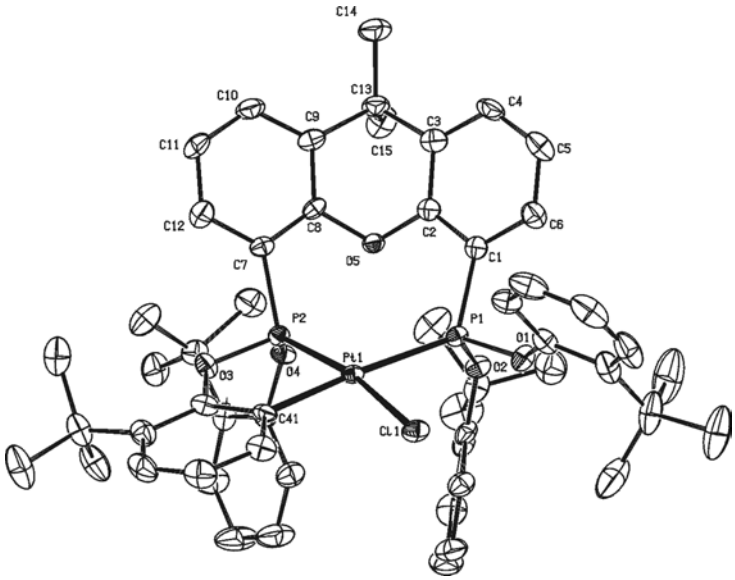

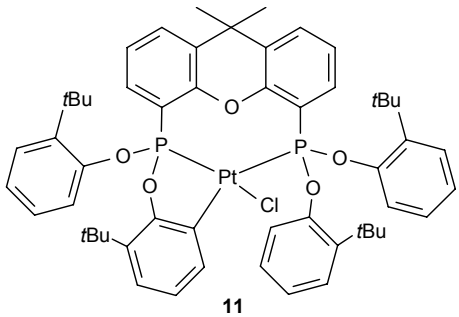

11

Figure 2.9: *ORTEP representation of complex **11**, [PtCl{κ^3(C-P-P)**1**}]. Displacement ellipsoids are drawn at the 50% probability level. All hydrogen atoms are omitted for clarity.*

The relatively high temperature applied during the reaction can explain the formation of this complex. The ligand coordinates in a *cis*-fashion to the platinum center, in order to accommodate the phosphonite ring as well as both phosphorus atoms. The bite angle, P_1-Pt-P_2, is found to be only 103.50(3)°, while the Cl-Pt-C_{41} angle is 89.86(10)°. The P-Pt bond lengths are 2.3680(11) Å for P_1-Pt and 2.1922(9) Å for P_2-Pt. This latter value is also found in the work of Dahlenburg[45] and Pringle[15] for a phosphonite moiety *trans* to chlorine. The C_{41}-Pt bond length is 2.073(4) Å, similar as found for other platinum-carbon single bonds.[49] The Pt-Cl bond length of 2.3408(9) Å is comparable with the few bond lengths reported so far in literature for other Pt-phosphonite complexes.[15,45] The platinum atom is located outside of the ligand plane, with the angles Pt-P_1-C_1 of 124.01° and Pt-P_2-C_7 of 122.19° and a dihedral angle between the Cl_1-Pd-C_{41} plane and the P_2-P_1-C_1-plane of 115°. The xanthene backbone is strongly bent, to accommodate the *cis*-configuration in the solid state, leading to a dihedral angle of 106.5° between the two aromatic rings of the xanthene moiety. The intramolecular P_1-P_2 distance is 3.5828(15) Å, which is significantly shorter than in the structure of the uncoordinated ligand **1** (*vide supra*) and also shorter than commonly found for Xantphos derived structures. The distance Pt-O_5 is found to 3.533(2) Å, too long to assume any platinum-oxygen interaction.

Table 2.4: *Selected bond lengths, distances and angles for complex **11**,* cis-*[PtCl{(κ^3(C-P-P)**1**}]*.

		Bond lengths (Å)			
Pt-P_1	2.3680(11)	Pt-P_2	2.1922(9)	Pt-Cl	2.3408(9)
Pt-C_{41}	2.073(4)	P_1-O_1	1.613(3)	P_1-O_2	1.606(3)
P_1-C_1	1.826(4)	P_2-O_3	1.613(3)	P_2-O_4	1.602(3)
P_2-C_7	1.803(4)	O_5-C_2	1.372(4)	O_5-C_8	1.387(4)
Pt-O_5	3.533(2)	P_1-P_2	3.5828(15)		
		Angles (°)			
Cl_1-Pt-C_{41}	89.87(10)	P_1-Pt-P_2	103.50(3)	Cl-Pt-P_1	86.64(3)
Cl-Pt-P_2	168.87(4)	P_1-Pt-C_{41}	176.12(10)	P_2-Pt-C_{41}	79.86(10)
O_1-P_1-O_2	97.64(14)	O_3-P_2-O_4	101.68(14)	Pt-P_1-O_1	116.34(10)
Pt-P_1-O_2	115.79(10)	Pt-P_2-O_3	108.04(9)	Pt-P_2-O_4	121.35(10)
Pt-P_1-C_1	124.01(13)	Pt-P_2-C_7	122.19(13)	C_2-O_5-C_8	112.2(3)
C_3-C_{13}-C_9	105.4(3)	O_1-P_1-C_1	100.35(15)	O_2-P_1-C_1	98.13(16)
O_3-P_2-C_7	102.66(16)	O_4-P_2-C_7	97.84(15)		

In an attempt to reactivate the platinum-carbon bond, complex **11** was subjected to 45 bar of H_2 for two hours, in benzene-d_6 at room temperature. The ^{31}P NMR spectrum of the depressurized

product did not show any new signals, implying that the formation of a Pt-H bond was not established under those conditions.

To prevent the undesired *ortho*-metallation and to draw an analogy with the palladium complexes described before, the reaction of $PtCl_2$(cod) with ligand **6** was investigated. The reaction proceeded at room temperature, with 43% conversion after 3 hours but complete disappearance of free ligand after reaction overnight. The ^{31}P NMR spectrum showed a singlet at δ = 86.8 ppm, flanked by two ^{195}Pt satellites, and a coupling constant $J_{Pt\text{-}P}$ of 5188 Hz. This clearly indicates that with this rigid and sterically constrained ligand, only *cis*-coordination occurs, as with ligand **2**. The ^{1}H NMR spectrum of this compound showed the same features as for *trans*-[$PdCl_2$(**6**)]. There are two signals for both the *tert*-butyl and the methoxy groups of the dioxaphosphepin units, showing chemical inequivalency. By slow diffusion of acetonitrile into a dichloromethane solution, single crystals could be grown and a crystallographic study was carried out. A side-view of the molecular structure of complex **12** is represented in Figure 2.10 while the full structure is shown in Figure 2.11. Table 2.5 contains selected data on bond lengths, distances and angles.

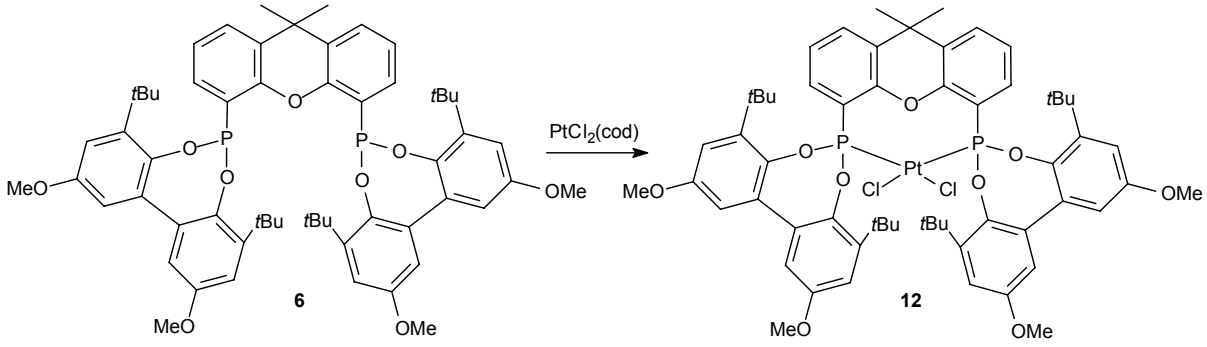

Scheme 2.4: *Reaction of ligand **6** with $PtCl_2$(cod) to yield complex **12,*** cis-*[$PtCl_2$(**6**)]*.

The solid state structure is in good agreement with the spectroscopic data obtained in solution, since the diphosphonite ligand is clearly coordinated in a *cis*-fashion to the platinum atom. The geometry around the platinum atoms is square planar, albeit heavily distorted due to the relatively large bite angle P_1-Pt-P_2 of 113.43(6)°. This leads to an angle Cl_1-Pt-Cl_2 of only 84.74(5)°, while the angle P_1-Pt-Cl_1 is even smaller at 80.61(5)°.

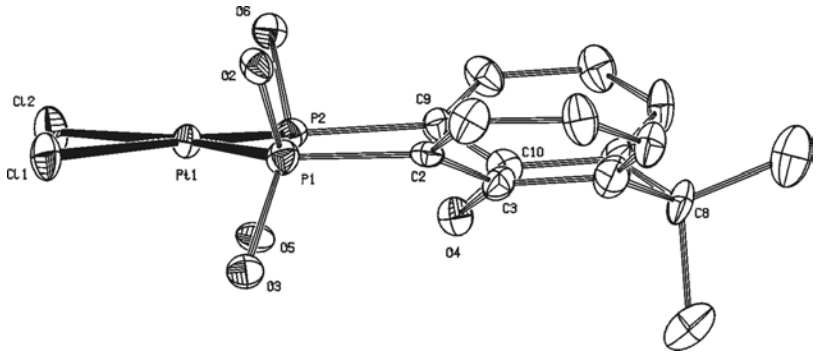

Figure 2.10: *Side view on the metallic core of complex **12**, showing the square-planarity around the platinum atom and the alignment of the P_1-Pt-P_2 plane and the P_1-P_2-C_2 plane.*

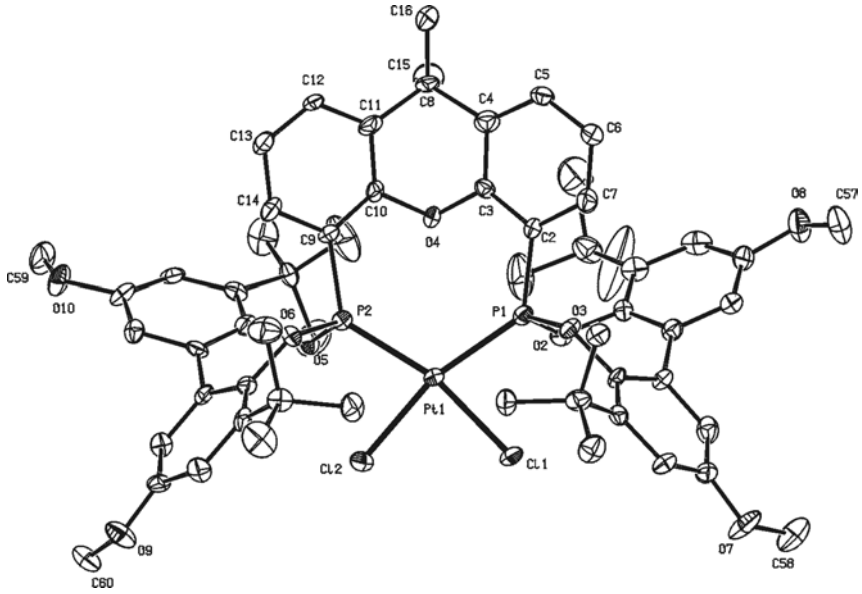

Figure 2.11: *ORTEP representation of complex **12**,* cis-*[$PtCl_2$(**6**)]. Displacement ellipsoids are drawn at the 50% probability level. All hydrogen atoms are omitted for clarity.*

The Pt-P bond lengths of 2.2725(16) Å and 2.2660(16) Å are longer than those in the *cis*-complexes reported by Dahlenburg,[45] Atherton[50] and Pringle.[15] This might be caused by the different electronic character of the aryl groups in complex **12** compared to the alkyl units (Dahlenburg) or the use of fluorinated phenyl substituents (Atherton). The discrepancy with the work of Pringle is not clear but might originate from the different backbone structure used. The dihedral angle between the P_1-Pt-P_2 plane and the P_1-P_2-C_9 plane is negligible at 5.1°. Also the bending of the xanthene backbone, leading to a dihedral angle between the two aromatic rings of 101.4°, is apparent. The Pt-O_4 distance of 3.466(4) Å is too large to assume any interaction.

Table 2.5: *Selected bond lengths, distances and angles for complex **12**,* cis-*[$PtCl_2$(**6**)]*.

Bond lengths (Å)					
Pt-P_1	2.2725(16)	Pt-P_2	2.2660(16)	Pt-Cl_1	2.3216(13)
Pt-Cl_2	2.3334(16)	P_1-O_2	1.612(5)	P_1-O_3	1.620(4)
P_1-C_2	1.826(6)	Pt-O_4	3.466(4)	P_1-P_2	3.794(2)
Angles (°)					
P_1-Pt-P_2	113.43(6)	Cl_1-Pt-Cl_2	84.74(5)	Cl_1-Pt-P_1	80.61(5)
Cl_2-Pt-P_1	165.32(5)	Cl_1-Pt-P_2	165.58(5)	Cl_2-Pt-P_2	81.14(6)
Pt-P_1-C_2	131.3(2)	Pt-P_1-O_2	114.24(15)	Pt-P_1-O_3	104.66(15)
O_2-P_1-O_3	107.1(2)	O_2-P_1-C_2	93.9(2)	O_3-P_1-C_2	103.6(2)

Atherton *et al.* have published on a series of [$PtCl_2(PEt_3)$L] complexes (L is a monophosphonite), all with coupling constants $J_{Pt\text{-}P}$ around 5200 Hz.[50] Puddephatt has described the synthesis of a monophosphonite, based on a calixresorcinarene backbone, as well as the molecular structure of its platinum complex $PtCl_2(SMe_2)$(P), which showed a coupling constant $J_{Pt\text{-}P}$ of 4966 Hz in the ^{31}P NMR spectrum.[51]

2.3.3 Rhodium

To continue the investigations of the coordination chemistry of these novel ligands, their Rh complexes were studied. These are particularly interesting, since the rhodium catalyzed hydroformylation with the same ligands will be studied (*vide infra*). When starting from the rhodium precursor [Rh(μ-Cl)$(CO)_2]_2$ and either ligand **1, 5** or **6**, which vary mainly in the steric properties (**1** vs. **5**) and electronic properties (**5** vs. **6**) a clean yellow/brown powder was obtained. The ^{31}P NMR spectrum in all cases showed only a doublet, giving rise to the formation of *trans*-[Rh(Cl)(CO)(P-P)] complexes, with a coupling constant $J_{Rh\text{-}P}$ of 184 Hz (**1**) and 192 Hz (**5** and **6**). In the IR-spectrum (ATR mode) of the respective solids the CO-stretch vibration is visible at ν = 1996 cm^{-1} (**1**), ν = 1999 cm^{-1} (**5**) and ν = 1998 cm^{-1} (**6**). This means that the ligands have similar σ-donor and π-acceptor character.[52] The values found are in-between those typical for RhCl(CO)(phosphite)[52a] complexes (ν_{CO} ~ 2015 cm^{-1}) and RhCl(CO)(phosphinite)[52b,c] complexes (ν_{CO} = 1990 cm^{-1}), confirming the similar trend as found for the coupling constant $J_{Pt\text{-}P}$ of *cis*-[$PtCl_2$(PP)] complexes (*vide supra*).

The group of Broussier has reported on a mixed phosphonite-phosphine ligand with a ferrocenyl backbone. In the corresponding RhCl(CO)(PP) complex, the carbonyl is believed to be positioned *trans* to the phosphonite moiety.

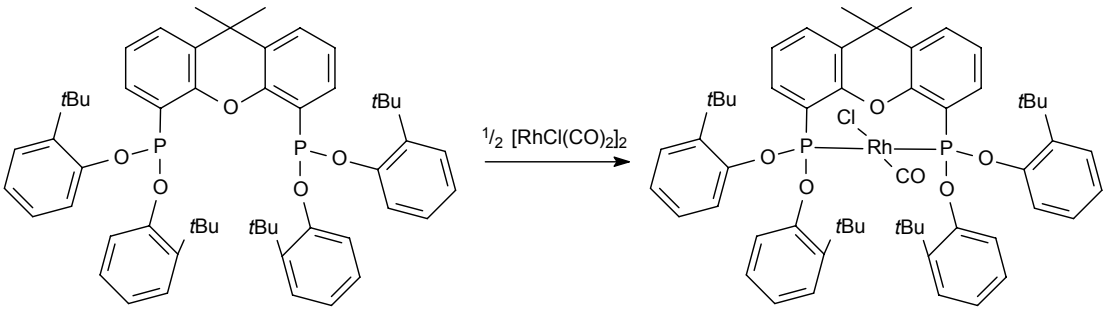

Scheme 2.5: *Reaction of ligand **1** with $[RhCl(CO)_2]_2$ to yield complex **13,*** trans-*[RhCl(CO)(**1**)]*.

This is supported by the observation that the CO stretch vibration appears as high as ν = 2041 cm^{-1}, measured in CH_2Cl_2.[53] This value seems unusually high for a 'normal' phosphonite. It might well be that there is a favourable interaction with the Fe-atom of the ferrocenyl backbone. For their calix[4]arene based diphosphonite system (*P*), Schmutzler and Börner claimed *cis*-coordination of the bidentate ligand in the complexes [Rh(nbd)(*P*)]BF_4 and [Rh(cod)(*P*)]BF_4 on the basis of the coupling constant $J_{Rh\text{-}P}$ of between 220 Hz and 240 Hz.[26] For the present system, a *trans*-relationship is expected to exist between both phosphorus atoms in every complex, since only one doublet is observed, without any splitting that would indicate an inequivalency of both phosphonite units.

The complexes *trans*-[Rh(Cl)(CO)(**1**)], *trans*-[Rh(Cl)(CO)(**5**)] and *trans*-[Rh(Cl)(CO)(**6**)] crystallized as yellow blocks from CH_2Cl_2/CH_3CN, and the molecular structures of these complexes **13**-**15** turned out to have the anticipated coordination of the chlorine *trans* to the carbonyl ligand and both phosphorus atoms *trans* to one another. The molecular structure of complex **13** is depicted in Figure 2.12, while table 2.6 contains data on selected bond lengths and angles for all three complexes.

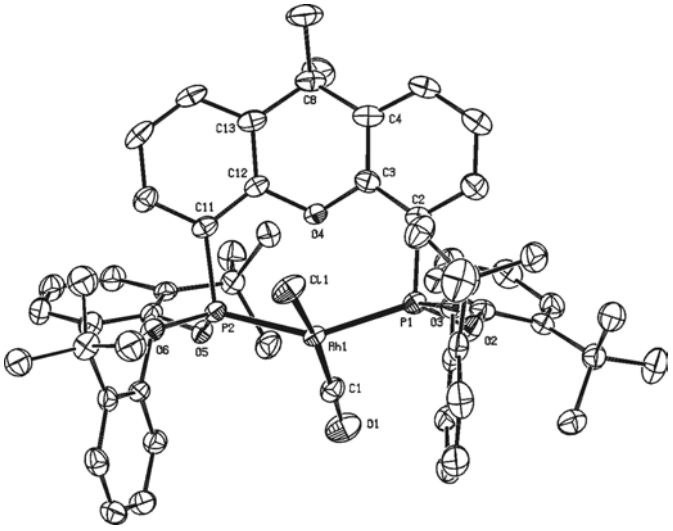

Figure 2.12: *ORTEP representations of complex **13**,* trans-*[RhCl(CO)(**1**)]. Displacement ellipsoids are drawn at the 50% probability level. All hydrogen atoms are omitted for clarity.*

For complex **13**, the geometry around the rhodium atom is clearly distorted square planar, possibly towards a square pyramidal configuration. This is shown in all angles around the rhodium atom. The P_1-Rh-P_2 bite angle is 147.19(3)°, while the Cl_1-Rh-C_1 angle is 166.11(8)°. A weak interaction between the Rh atom and oxygen atom O_4 can not be excluded, since the distance of only 2.7193(16) Å is significantly smaller than the sum of both atomic radii. The intramolecular P_1-P_2 distance is 4.3408(10) Å. The structural differences with complex **14** (and the very similar complex **15)** are found to be mainly in the orientation of the ancillary *tert*-butyl groups. The latter two complexes have an internal mirror plane. In complex **14** the geometry around the rhodium atom is also heavily distorted from square planar, with the P_1-Rh-P_2 bite angle at 149.40(2)° and the Cl_1-Rh-C_1 angle at 174.56(8)°. The intramolecular P_1-P_2 distance is 4.3534(7) Å. In each complex the Cl-Rh-P angles are all below 90° while the C_1-Rh-P angles are all well above 90°. All bond lengths for complexes **13-15** correlate nicely. The C_1-O_1 bond lengths are normal at around 1.14-1.15 Å. So far in literature, no examples of molecular structures of [Rh(Cl)(CO)(PP)] complexes with diphosphonites exist, so it is hard to compare bond lengths found for these complexes. The group of Pastor has reported a [Rh(acac)diphosphonite] complex.[54] Puddephatt has described the face-to-face dimer with a (CO)Rh-Cl-Rh(CO) core and the ligand $(PhO)_2PCH_2P(OPh)_2$.[55] Their reported values for the Rh-Cl and Rh-P bond lengths are not in agreement with those of complexes **13-15**, most likely due to the different electronic character of the backbones used and the dimeric geometry of their complex. Atherton has published the structural characterization of a $Rh^{(III)}$ complex with a monodentate phosphonite, with essentially similar bond lengths as above.[50] The best alternatives for comparison are similar complexes containing (di)phosphite ligands. In such structures with either mono- or bidentate ligands, normal Rh-P bond lengths are around 2.15 Å, while the Rh-Cl bond lengths are 2.36-2.37 Å. For the carbonyl ligand, the C-O bond length is 1.14 Å, on average.[56-60]

The complexes **13-15** can be considered as structural models for the four-coordinate species $Rh(H)(CO)(P)_2$, formed in the catalytic cycle of hydroformylation by CO dissociation from the catalyst resting state $Rh(H)(CO)_2(P)_2$. In an attempt to obtain the hydrido-carbonyl complex from complex **13**, the reaction with $LiB(Et)_3H$ (SuperHydride®) was tried. This compound was previously reported to be able to convert $NiCl_2$(dippe) to Ni(μ-$H)_2$(dippe)[61] and $MoCl_2(CO)_2(PMe_3)_3$ to $MoCl(H)(CO)_2(PMe_3)_3$.[62] Following the reaction in time by ^{31}P NMR spectroscopy, however, showed no significant change as complex **13** was still the major species.

Table 2.6: *Selected bond lengths, distances and angles for complex **13**,* trans-*[RhCl(CO)(**1**)], complex **14**,* trans-*[RhCl(CO)(**5**)] and complex **15**,* trans-*[RhCl(CO)(**6**)].*

	13	**14**	**15**		**13**	**14**	**15**
	Bond lengths (Å)				**Angles (°)**		
Rh-P_1	2.2583(7)	2.2567(5)	2.2554(9)	P_1-Rh-P_2	147.19(3)	149.40(2)	149.56(3)
Rh-Cl	2.3504(8)	2.3875(7)	2.3840(3)	P_1-Rh-Cl_1	88.49(3)	87.23(1)	87.89(2)
C_1-O_1	1.149(3)	1.142(4)	1.154(6)	Rh-C_1-O_1	174.1(2)	178.8(2)	179.1(4)
P_1-O_3	1.6141(17)	1.6202(13)	1.626(2)	Rh-P_1-O_3	124.61(7)	124.20(5)	125.74(8)
Rh-O_4	2.7193(16)	2.7091(17)	2.664(3)	O_2-P_1-O_3	97.80(9)	103.86(7)	103.70(11)
Rh-P_2	2.2668(7)	2.2567(5)	2.2554(9)	O_3-P_1-C_2	97.13(10)	97.13(8)	96.25(13)
Rh-C_1	1.818(3)	1.826(3)	1.818(5)	Cl_1-Rh-C_1	166.11(8)	174.56(8)	172.84(15)
P_1-O_2	1.6300(17)	1.6305(13)	1.621(2)	P_1-Rh-C_1	95.52(8)	94.17(2)	93.95(4)
P_1-C_2	1.826(3)	1.8348(19)	1.830(3)	Rh-P_1-O_2	120.30(7)	114.02(5)	113.26(8)
P-P	4.3408(10)	4.3534(7)	4.3526(13)	Rh-P_1-C_2	109.74(9)	108.22(7)	108.34(11)
				O_2-P_1-C_2	103.26(10)	107.27(8)	107.25(13)

2.4 Catalysis

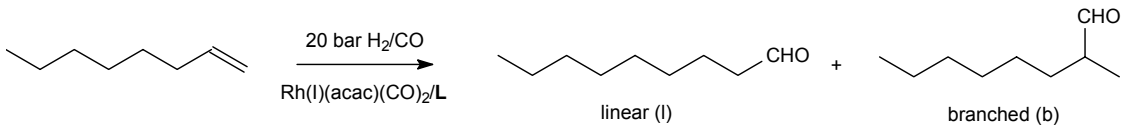

Scheme 2.6: *Schematic representation of the rhodium catalyzed hydroformylation of 1-octene.*

To obtain information on the catalytic activity of rhodium complexes containing these sterically constrained diphosphonites, some of the ligands **1**-**8** were tested in the rhodium catalyzed hydroformylation of 1-octene (Scheme 2.6). The reactions were carried out under typical hydroformylation conditions, at 20 bar of synthesis gas ($CO:H_2$ =1:1) and a temperature of 80 °C, using $Rh(CO)_2(acac)$ (acac = acetylacetonate) and 6 molar equivalents of ligand. The results of these catalytic runs are listed in Table 2.7. For a good comparison of all catalysts, conversion was kept low at approximately 20%, from which data the initial turnover frequencies are calculated (TOF).

Table 2.7: *Rhodium catalyzed hydroformylation of 1-octene using diphosphonite ligands.*[a]

Ligand	Time (h)	Conv [%][b]	Sel_{Ald} [%][b]	Hydrogenation [%][b]	Isomerization [%][b]	l/b ratio [b]	TOF[c]
1	2.5	24.8	92.9	6.0	1.1	8.9	256
2	1.5	31.4	93.2	6.5	0.3	6.7	530
4	1.5	27.4	93.5	6.2	0.3	7.7	419
5	2.5	18.4	96.6	1.9	1.5	7.4	181
6	2.5	12.7	96.8	2.0	1.1	4.8	127
8	2.5	15.9	95.7	3.3	1.0	5.1	160

[a]*Reaction conditions: 1-octene (23.7 mmol), decane (9.6 mmol), toluene (14.5 mL), T = 80 °C, p = 20 bar, [Rh(acac)(CO)$_2$] = 0.47 mM, substrate:Rh = 2500:1, ligand:Rh = 6:1;* [b]*determined by GC analysis;* [c]*turnover frequency, defined as (mol substrate converted)·(mol rhodium)$^{-1}$·h^{-1}.*

As can be seen from Table 2.7, especially with the sterically less hindered diphosphonites **2** and **4**, based on 3,5-di-*tert*-butylphenol, high activities are observed with good regioselectivities to the desired linear aldehyde. With the more bulky ligands **1** and especially with **4**-**6** and **8**, significantly lower activities but still good selectivities to the desired product 1-nonanal are obtained. The amounts of isomerization are slightly higher than with catalysts containing xanthene based diphosphines.[63] Whether this is due to electronic or steric effects is not clear. There seems to be a small difference between the xanthene and the phenoxathiin backbone, comparing the results obtained with ligand **2** and **4**. A possible explanation for this apparent difference in activity could be the slight distortion or flipping motion in the phenoxathiin backbone, as found by Goertz *et al.*[32] The catalysts containing ligands **1**-**8** clearly outperform those reported by Schmutzler and Börner using their calix[4]arene based diphosphonites, since the l/b ratio reported for their catalytic systems does not even reach 2.[26] This is most likely due to the large natural bite angle of the diphosphonites, as evidenced by the rhodium complexes **13**-**15**, which leads to an induced stability of *trans*-coordinated intermediate species in the catalytic cycle. Together with the steric hindrance, this leads to a reaction pathway beneficial for the formation of the linear aldehyde.[64]

Based on the promising results obtained for the hydroformylation of 1-octene, the possibilities of these diphosphonite ligands were investigated further by studying the rhodium catalyzed hydroformylation of 2-butene. The catalysis was performed at reaction temperatures of 120-160 °C while a pressure of 5 bar of synthesis gas was applied at room temperature, before heating. The reaction time was 4 hours, with $Rh(CO)_2(acac)$ as the metal precursor and 5 molar equivalents of

ligand. The results obtained for the hydroformylation of 2-butene under these conditions are listed in Table 2.8.

Table 2.8: *Rhodium catalyzed hydroformylation of 2-butene using diphosphonite ligands.*[a]

Entry	Ligand	Temperature [°C]	Conv [%][b]	Sel_{Ald} [%][b]	$Sel_{n\text{-}C5}$ [%][b]	l/b ratio[b]
1	**1**	140[c]	9	93	57	1.3
2	**2**	120	9	90	61	1.6
3	**2**	140[c]	66	94	62	1.6
4	**2**	160	54	87	55	1.2
5	**8**	160	10	76	50	1.0

[a]*Reaction conditions: 2-butene (178 mmol), toluene (11.6 mL),* $p_{ini\ (rt)}$ *= 5 bar,* $[Rh(acac)(CO)_2]$ *= 1.00 mM, substrate:Rh=15250:1, ligand:Rh = 5:1, t = 4h;* [b]*determined by GC analysis;* [c]*ligand:Rh = 10:1. Only other product found is butane.*

Higher temperatures and lower pressures are applied, compared to the hydroformylation of 1-octene, to enhance the rate of isomerization and to prevent the hydroformylation of internal alkenes. As is evident from Table 2.8, remarkably high selectivities of up to 62% to the desired linear product *n*-pentanal could be achieved with ligand **2**. With this ligand also the highest activity is recorded, with a TOF of up to 2500 h^{-1}. The overall aldehyde selectivity can be as high as 94% with this catalytic system. Conversions are low for the other ligands tested, which is probably due to steric hindrance by the bulky phosphonite groups. In all cases the linear product is favoured over the branched one, however at the cost of considerable amounts of hydrogenation, *i.e.* up to 24% of *n*-butane (entry 5). These results are among the best known in the open literature for the hydroformylation of the challenging substrate 2-butene. Electron deficient NAPHOS derivatives have been reported that give a l/b ratio of up to 19 at a TOF of about 900 h^{-1}.[24] Unfortunately nothing was reported about the hydrogenation side reaction of these systems. We conclude that the novel diphosphonite ligands form rhodium complexes that can be very efficient for the selective linear hydroformylation of internal alkenes such as 2-butene. It should be noted, that these diphosphonites can be easily varied in a wide range concerning sterics and electronics. This opens up a new range of applications for industrial feedstock such as Raffinate II and other internal alkenes.

In order to elucidate the coordination mode of the ligand during catalysis, the preformation of the catalytic resting state was monitored by *in situ* NMR studies under synthesis gas atmosphere. With high pressure NMR spectroscopy it is possible to distinguish between three major coordination modes, as depicted in Figure 2.13. Usually, CO bridging dimers are favoured at high rhodium concentration.[65-67f]

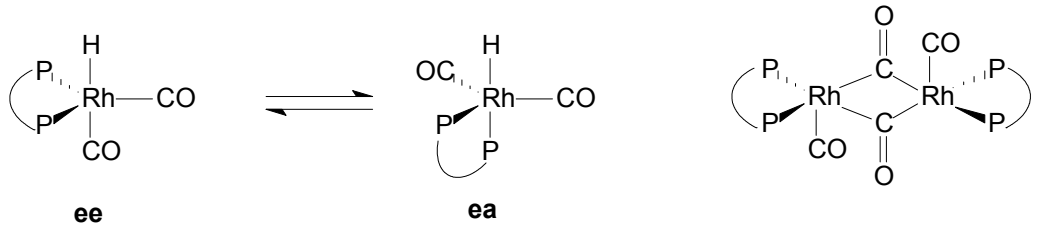

Figure 2.13: *Rh complexes formed during preformation: Ligand in equatorial-equatorial (**ee**) or equatorial-axial (**ea**) coordination, and the CO-bridged rhodium dimer.*

For the preformation, $Rh(acac)(CO)_2$ was reacted with a slight excess of the appropriate ligand under 20 bar of CO/H_2 (1:1), while the ^1H and ^{31}P NMR spectra were recorded. The results are listed in Table 2.9. There is a clear effect of the steric bulk of the ligand on the NMR spectra obtained. The flexible ligand **1** gives the most upfield signal, yet with the highest coupling constant in the ^{31}P NMR spectrum. This is probably due to the bulky *tert*-butyl groups, which point towards the center of the complex (*vide supra*). For the less crowded phosphorus atoms, ligands **2** and **4**, with the steric bulk directed away from the coordination center, lower coupling constants are obtained.

Table 2.9: *High pressure* in situ *NMR data of $Rh(H)(CO)_2$(ligand) complexes.*[a]

Ligand	δ ($^{31}P\{^1H\}$) (ppm)	δ (^1H) (ppm)	J_{Rh-P} (Hz)	$^1J_{Rh-H}$ (Hz)	$^2J_{P-H}$ (Hz)
1	150.9	-9.9	210.6	3.6	18.3
2	157.4	-9.9	195.2	nd	nd
4	156.6	-9.7	195.3	nd	nd
5	165.5	-9.8	207.5	2.5	23.2
6	166.0	-9.5	206.4	2.4	22.6
8	164.8	-9.7	206.4	3.2	22.4

[a]*Conditions: 1.5 mL toluene-d_8, $Rh(acac)(CO)_2$ (19.4 μmol), ligand:Rh=1.05:1, p = 20 bar H_2/CO (1:1); nd = not determinable. Preformation at 80 °C for 16 hours. Measurement at room temperature.*

The spectra obtained applying ligands **5**, **6** and **8** are similar, which seems plausible since these ligands are virtually identical in steric properties. In the hydride region of the ^1H NMR spectrum, in all cases a doublet of triplets is observed (Figure 2.14). From the measured coupling constants $^1J_{Rh-H}$ of around 3 Hz, and $^2J_{P-H}$ in the range of 18-23 Hz, it is evident that the diphosphonite ligands coordinate predominantly in an equatorial-equatorial (**ee**) fashion. An equatorial-axial coordination would lead to much higher coupling constants, due to the *trans* relationship of the hydride with P_{ax}, as seen with related phosphite systems.[68,69]

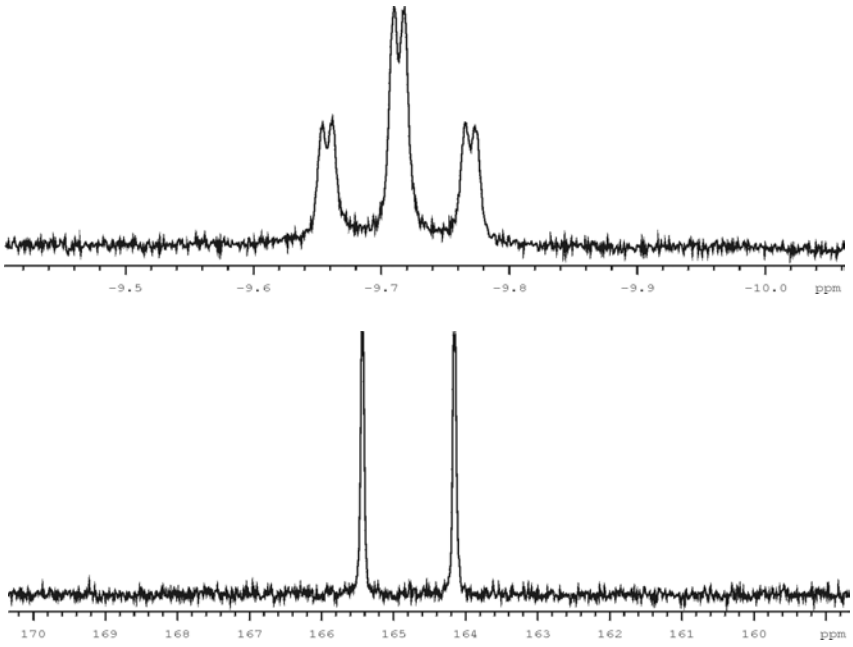

Figure 2.14: *High pressure NMR spectra of Rh(H)(CO)$_2$(**8**). Top: doublet of triplets in the hydride region of the ^{1}H NMR spectrum. Bottom: ^{31}P{^{1}H} NMR spectrum showing the characteristic doublet due to Rh-P coupling.*

For additional information on the complexation behaviour, IR spectra of the Rh(H)(CO)$_2$(PP) complexes were recorded under 20 bar of synthesis gas. The results of these experiments are listed in Table 2.10. It becomes clear that for all four ligands studied only one complex is present in solution under these conditions, although for ligand **1** two small shoulders are apparent. This is an indication that predominantly one species is present. From the equal intensities of both CO vibrations it is deduced that they represent the **ee** complex. This finding is markedly different from the studies by van der Veen *et al.* on Xantphos[63] and by Brown and Kent on Rh(H)(CO)$_2$(PPh$_3$)$_2$,[70] since with these systems mixtures of **ee** and **ea** complexes were found in various ratios.

Table 2.10: *High pressure* in situ *IR data of Rh(H)(CO)$_2$(ligand) complexes.*[a]

Ligand	ν_1 (cm^{-1})	ν_2 (cm^{-1})
1	2017 (2004)	2056 (2046)
2	2000	2055
5	2000	2064
6	2001	2066

[a]*Conditions: 15 mL cyclohexane, Rh(acac)(CO)$_2$ (15.5 μmol), ligand:Rh=2:1, p = 20 bar H$_2$/CO (1:1), T= 80 °C. Numbers between brackets correspond to shoulders.*

2.5 Conclusions

The coordination chemistry of novel sterically constrained diphosphonites has been explored with various transition metals. New features of the general class of diphosphonites could be deduced, such as the coupling constants of *cis*-platinum complexes and the stretching frequencies of the CO ligand ν_{CO} found for RhCl(CO) complexes. Several X-ray structures have been obtained. The mode of coordination of the specific ligands is clearly dependent on the transition metal used and on the amount of steric bulk present. With Pd and Rh, *trans*-coordination of the two phosphorus atoms is favoured, while with Pt *cis*-complexes are formed. Under specific conditions, *ortho*-metallation of one phenolate ring of ligand **1** occurs, with Pd (minor species) and Pt (only species formed).

This new class of diphosphonite ligands is shown to be promising, especially for use in industrially challenging processes like the hydroformylation of internal alkenes. Therefore further research on the modification of the phosphonite moieties should be undertaken. In the hydroformylation of 1-octene high activities and satisfactory selectivities, with l/b ratios up to 9, were found. High selectivity towards *n*-pentanal was observed with 2-butene as substrate, after 4 hours of reaction at a temperature of 140 °C. High pressure *in situ* spectroscopy (both IR and NMR) was used to identify the resting state of the catalytic active rhodium-hydride species to be predominantly an equatorial-equatorial species.

Acknowledgements

The National Research School for Catalysis (NRSCC) and BASF AG are thanked for financial support. OMG is acknowledged for a generous loan of various transition metal complexes. Dr. Ahlers and Dr. Wiebelhaus (BASF A.G.) are acknowledged for their interest. Dr. Rafaël Sablong is thanked for numerous valuable discussions, while Dr. Pieter Magusin and Eugène van Oers are acknowledged for assistance with the high pressure NMR experiments. This chapter is partly based on work by former co-worker Dr. Alison Hewat, who managed to synthesize the new family of diphosphonite ligands. X-ray crystal structure analyses were performed by Dr. Allison Mills and Dr. Huub Kooijman from the University of Utrecht (group of Prof. Anthony Spek) and by Drs. Auke Meetsma from the University of Groningen.

2.6 Experimental Section

General. All chemicals were purchased from Aldrich, Acros or Merck. Synthesis gas (CO/H_2 1:1) was purchased from Hoekloos. All preparations were carried out under an argon atmosphere using standard Schlenk techniques. Solvents were distilled from sodium/benzophenone (THF, diethyl ether, toluene, toluene-d_8 and hexanes) or calcium hydride (CH_2Cl_2 and $CDCl_3$) prior to use. All glassware was dried by heating under vacuum. The NMR spectra were recorded on a Varian Mercury 400 spectrometer. Chemical shifts are given in ppm referenced to solvent (^1H, $^{13}C\{^1H\}$) or an 85% aqueous solution of H_3PO_4 ($^{31}P\{^1H\}$). Part of the high pressure NMR spectra were recorded on a Bruker 200 MHz spectrometer. High pressure IR spectra were recorded on a Shimadzu FTIR 8300 spectrometer. GC spectra were recorded on a Shimadzu 17A Chromatograph equipped with a 50 m PONA column. $PdCl_2(cod)$,[71] $PdCl(CH_3)(cod)$,[72] and $PtCl_2(cod)$[73] were prepared according to literature procedures. Ligands **1** to **8** were prepared in our laboratories and have been reported by Hewat.[27a]

$PdCl_2$(1).
$PdCl_2(cod)$ (28.2 mg, 9.88 μmol) and ligand **1** (87.4 mg, 10.08 μmol) were dissolved in 5 mL of toluene and the solution stirred at 70 °C overnight. The solvent was removed *in vacuo* to leave a yellow solid.
^1H NMR ($CDCl_3$) δ 7.75 (d, 4H, ^1J = 8.0 Hz), 7.63 (d, 4H, ^1J = 8.0 Hz), 7.33 (dd, 4H, ^1J = 8.0 Hz, ^2J = 1.6 Hz), 7.22 (dt, 4H, ^1J = 8.0 Hz, ^2J = 1.6 Hz), 7.15 (t, 2H, ^1J = 8.0 Hz), 7.09 (dt, ^1J = 8.0 Hz, ^2J = 1.6 Hz), 1.64 (s, 6H, CH_3), 1.36 (s, 36H, tBu).
$^{31}P\{^1H\}$ NMR ($CDCl_3$) δ 109.7 (s).
Anal. Calcd for $C_{55}H_{64}Cl_2O_5P_2Pd$:C, 63.25; H, 6.18. Found: C, 63.18; H, 6.26.

trans-**[PdCl(CH_3)(1)] (complex 9).**
$PdCl(CH_3)(cod)$ (46.6 mg, 175.8 μmol) and ligand **1** (162.1 mg, 187.0 μmol) were dissolved in 5 mL of toluene and the solution was stirred at 75 °C overnight. The solvent was removed *in vacuo* to leave a pale-yellow solid. Single crystals, suitable for X-ray analysis, were grown by slow diffusion of acetonitrile into a CH_2Cl_2 solution.
^1H NMR ($CDCl_3$) δ 7.69 (dt, 4H, ^1J = 7.6 Hz), 7.64 (dq, 2H, ^1J = 4.0 Hz), 7.57 (dd, 2H, ^1J = 7.6 Hz, ^2J = 1.2 Hz), 7.3 (dd, 4H, ^1J = 7.6 Hz, ^2J = 1.2 Hz), 7.20 (dt, 4H, ^1J = 7.6 Hz), 7.10 (t, 2H, ^1J = 7.6 Hz), 7.07 (m, 2H), 1.63 (s, 3H, CCH_3), 1.57 (s, 3H, CCH_3), 1.39 (s, 36H, *t*Bu), 1.32 (s, 36H, *t*Bu), 0.79 (dt, 3H, $PdCH_3$).
$^{13}C\{^1H\}$ NMR ($CDCl_3$) δ 153.8, 152.2, 152.0, 140.0, 139.5, 134.0, 129.8, 128.8, 127.6, 127.5, 126.9, 124.0 (d, $^1J_{P\text{-}C}$ = 20.6 Hz), 123.5, 120.6, 119.9, 35.6, 34.8, 30.4, 30.3, 29.1, 27.4.
$^{31}P\{^1H\}$ NMR ($CDCl_3$) δ 123.1 (s).
Anal. Calcd for $C_{56}H_{67}ClO_5P_2Pd$: C, 65.69; H, 6.60. Found: C, 65.78; H, 6.67.

trans-**[$PdCl_2$(6)] (complex 10).**
$PdCl_2(cod)$ (16.1 mg, 56.4 μmol) and ligand **6** (56.1 mg, 57.0 μmol) were dissolved in 5 mL of dichloromethane and the solution stirred overnight at r.t. The solvent was then removed *in vacuo* to leave a yellow solid. Orange rectangles, suitable for X-ray crystallographic analysis were obtained by layering with CH_2Cl_2/CH_3CN.
^1H NMR ($CDCl_3$) δ 7.59 (d, 1H, ^1J = 7.6 Hz, ^2J = 1.2 Hz), 7.22 (m, 2H), 7.10 (dq, 2H, ^1J = 3.6 Hz, ^1J = 1.2 Hz), 7.00 (d, 2H, ^1J = 3.6 Hz), 6.952 (t, 3H, ^1J = 7.6 Hz), 6.78 (m, 3H), 6.67 (d, 1H, ^1J = 2.8 Hz), 3.88 (s, 6H, OCH_3), 3.81 (s, 6H, OCH_3), 1.71 (s, 3H, CCH_3), 1.47 (s, 36H, *t*Bu), 1.27 (s, 3H, CCH_3).
$^{31}P\{^1H\}$ NMR ($CDCl_3$) δ 136.5 (s) .

cis-**[$PtCl_2$(1)] (complex 11).**
$PtCl_2(cod)$ (155.1 mg, 414.5 μmol) and **1** (366.3 mg, 422.4 μmol) were stirred in 10 mL toluene at 75 °C overnight. During this period a white turbid mixture was formed. After removal of the solvent, a white solid remained. Single crystals, suitable for X-ray analysis, were grown from CH_2Cl_2/CH_3CN.
^1H NMR ($CDCl_3$) δ 8.39 (t, 1H, ^1J = 8.0 Hz), 7.69 (d, 2H, ^1J = 7.6 Hz), 7.66 (dd, 1H, ^1J = 8.0 Hz, ^2J = 0.4 Hz), 7.65 (dd, 1H, ^1J = 7.6 Hz, ^2J = 0.4 Hz), 7.57 (t, 2H, ^1J = 8.8 Hz), 7.38 (d, 1H, ^1J = 7.6 Hz), 7.30 (m, 2H), 7.22 (t, 1H, ^1J = 6.4 Hz), 7.16 (d, 1H, ^1J = 7.6 Hz), 7.09 (d, 1H, ^1J = 7.6 Hz), 7.01 (d, 2H, ^1J = 7.6 Hz), 6.97 (m, 2H), 6.89 (dt, 1H, ^1J = 8.4 Hz, ^2J = 1.6 Hz), 6.81 (t, 2H, ^1J = 7.6 Hz), 6.55 (br s, 1H), 1.96 (s, 3H, $C(CH_3)_2$), 1.60 (s, 3H, $C(CH_3)_2$), 1.58 (s, 9H, *t*Bu), 1.20 (s, 9H, *t*Bu), 1.17 (s, 9H, *t*Bu), 1.16 (s, 3H, *t*Bu).
$^{31}P\{^1H\}$ NMR ($CDCl_3$) δ 118.9 (br s, $J_{Pt\text{-}P}$ = 5270 Hz), 128.0 (br s, $J_{Pt\text{-}P}$ = 2517 Hz).

cis-**[$PtCl_2$(6)] (complex 12).**
$PtCl_2$(cod) (23.4 mg, 62.5 μmol) and ligand **6** (62.9 mg, 64.0 μmol) were dissolved in 5 mL of dichloromethane and the solution stirred overnight at r.t. The solution was filtered by cannula to remove insolubles and the solvent was then removed in vacuo to leave a yellow solid. An analytically pure and crystalline sample (cubic shaped) was obtained by layering with CH_2Cl_2/CH_3CN.
^{1}H NMR ($CDCl_3$) δ 7.49 (dd, 1H, ^1J = 7.2 Hz, ^2J = 1.2 Hz), 7.18 (m, 1H), 6.97 (d, 3H, ^1J = 7.2 Hz), 6.94 (t, 1H, ^1J = 7.2 Hz), 6.85 (d, 2H, ^1J = 2.4 Hz), 6.67 (d, 3H, ^1J = 2.8 Hz), 6.32 (d, 3H, ^1J = 2.8 Hz), 3.81 (s, 6H, OMe), 3.78 (s, 6H, OMe), 1.67 (s, 3H, CCH_3), 1.43 (s, 18H, $C(CH_3)_3$), 1.38 (s, 18H, $C(CH_3)_3$), 1.21 (s, 3H, CCH_3).
^{31}P{^{1}H} NMR ($CDCl_3$) δ 86.8 (s, J_{Pt-P} = 5188 Hz).

trans-**[Rh(Cl)(CO)(1)] (complex 13).**
[Rh(μ-Cl)$(CO)_2]_2$ (28.2 mg, 103.9 μmol) and ligand **1** (181.0 mg, 208.8 μmol) were dissolved in 5 mL of dichloromethane and the solution stirred overnight at r.t. The solution was filtered by cannula to remove insolubles and the solvent was then removed *in vacuo* to leave a yellow solid. An analytically pure sample was obtained by layering with CH_2Cl_2/CH_3CN.
^{1}H NMR ($CDCl_3$) δ 8.37 (dd, 2H, ^1J = 8.0 Hz, ^2J = 1.2 Hz), 7.81 (ddt, 2H, ^1J = 7.6 Hz, ^2J = 4.4 Hz, ^3J unresolved), 7.62 (dd, 2H, ^1J = 7.6 Hz, ^2J = 1.2 Hz), 7.41 (dd, 2H, ^1J = 7.6 Hz, ^2J = 1.2 Hz), 7.35 (dd, 1H, ^1J = 7.6 Hz, ^2J = 1.6 Hz), 7.33 (dd, 1H, ^1J = 7.6 Hz, ^2J = 1.6 Hz), 7.27 (m, 2H), 7.19 (t, 2H, ^1J = 7.6 Hz), 7.16 (dt, ^1J = 8.0 Hz, ^2J = 1.2 Hz), 7.01 (m, 4H), 1.90 (s, 3H, CCH_3), 1.42 (s, 18H, $C(CH_3)_3$), 1.37 (s, 3H, CCH_3), 1.25 (s, 18H, $C(CH_3)_3$).
^{13}C{^{1}H} NMR ($CDCl_3$) δ 152.2, 140.5, 139.5, 133.5, 129.4, 128.8, 127.5, 127.0 (d, $^1J_{P-C}$ = 25.5 Hz), 124.0 (d, $^1J_{P-C}$ = 12.8 Hz), 123.5, 121.5, 119.2, 35.5, 34.8, 34.6, 34.3, 30.2, 23.7.
^{31}P{^{1}H} NMR ($CDCl_3$) δ 138.4 (s, ^1J = 184.4 Hz).
FTIR (ATR mode, solid, cm^{-1}): ν 1996 (Rh(*CO*)).
Anal. Calcd for $C_{56}H_{64}ClO_6P_2Rh$: C, 65.09; H, 6.24. Found: C, 64.86; H, 6.31.

trans-**[Rh(Cl)(CO)(5)] (complex 14).**
Both [Rh(μ-Cl)$(CO)_2]_2$ (44.4 mg, 114.2 μmol) and ligand **5** (248.7 mg, 228.7 μmol) were dissolved in total 10 mL of dichloromethane and the solution stirred overnight at r.t. The solvent was then removed *in vacuo* to leave a yellow solid. Crystals suitable for X-ray analysis were obtained by layering with CH_2Cl_2/CH_3CN.
^{1}H NMR ($CDCl_3$) δ 7.58 (d, 2H, ^1J = 8.0 Hz), 7.50 (dd, 2H, ^1J = 7.6 Hz, ^2J = 1.6 Hz), 7.34 (d, 2H, ^1J = 2.8 Hz), 7.22 (d, 2H, ^1J = 2.8 Hz), 7.02 (m, 3H), 6.79 (t, 3H, ^1J = 7.6 Hz), 1.78 (s, 3H, CCH_3), 1.64 (s, 18H, $C(CH_3)_3$), 1.44 (s, 18H, $C(CH_3)_3$), 1.40 (s, 18H, $C(CH_3)_3$), 1.32 (s, 3H, CCH_3), 1.23 (s, 18H, $C(CH_3)_3$).
^{13}C{^{1}H} NMR ($CDCl_3$) δ 153.8, 149.8, 147.6, 146.9, 143.0, 142.2, 139.9, 136.3, 132.4, 129.3 (d, $^1J_{P-C}$ = 24.6 Hz), 127.0, 126.7, 125.3, 125.0 (d, $^1J_{P-C}$ = 10.5 Hz), 122.5, 122.4, 35.9, 35.3 (d, $^1J_{P-C}$ = 6.5 Hz), 34.7 (d, $^1J_{P-C}$ = 4.6 Hz), 32.2, 31.7, 31.6, 31.5, 29.7.
^{31}P{^{1}H} NMR ($CDCl_3$) δ 163.9 (s, ^1J = 191.5 Hz).
FTIR (ATR mode, solid, cm^{-1}): ν 1999 (Rh(*CO*)).

trans-**[Rh(Cl)(CO)(6)] (complex 15).**
[Rh(μ-Cl)$(CO)_2]_2$ (18.3 mg, 47.1 μmol) and ligand **6** (92.7 mg, 94.2 μmol) were dissolved in 5 mL of dichloromethane and the solution stirred for 2 hours at r.t. The solvent was then removed *in vacuo* to leave a yellow/red solid. Crystals suitable for X-ray analysis were obtained by layering with CH_2Cl_2/CH_3CN.
^{1}H NMR ($CDCl_3$) δ 7.54 (dd, 1H, ^1J = 3.6 Hz, ^2J = 1.2 Hz), 7.16 (m, 2H), 7.12 (d, 1H, ^1J = 3.2 Hz), 7.00 (d, 3H, ^1J = 3.2 Hz), 6.94 (t, 2H, ^1J = 7.6 Hz), 6.86 (d, 2H, ^1J = 1.2 Hz), 6.86 (d, 1H, ^1J = 7.6 Hz), 6.75 (d, 2H, ^1J = 3.2 Hz), 6.67 (d, 3H, ^1J = 2.8 Hz), 3.90 (s, 3H, OMe), 3.89 (s, 3H, OMe), 3.81 (s, 6H, OMe), 1.81 (s, 3H, CCH_3), 1.62 (s, 18H, $C(CH_3)_3$), 1.47 (s, 36H, $C(CH_3)_3$), 1.30 (s, 3H, CCH_3), 1.20 (s, 18H, $C(CH_3)_3$).
^{31}P{^{1}H} NMR ($CDCl_3$) δ 163.6 (s, J_{Rh-P} = 191.8 Hz).
FTIR (ATR mode, solid, cm^{-1}): ν 1998 (Rh(*CO*)).

Hydroformylation of 1-octene.
Reactions were performed using a 75 mL homemade autoclave equipped with an inner glass beaker. 1-Octene was filtered over neutral alumina before use to remove peroxides. In a typical experiment, Rh(acac)$(CO)_2$ (2.4 mg, 9.3 μmol) of and the appropriate amount of ligand (6 eq.) were each dissolved in 6 mL of toluene. The combined solution was transferred into the preheated autoclave (80 °C) under argon. The autoclave was then pressurized to 18 bar. After 1 hour the substrate solution, containing 1-octene (3.7 mL, 23.7 mmol) and decane

(1.8 mL, 9.2 mmol) in toluene (2.6 mL) After reaction the autoclave was cooled and the reaction mixture quenched by addition of an excess of $P(OEt)_3$ to form inactive rhodium species. A sample was withdrawn for GC analysis.

Hydroformylation of 2-butene.
Reactions were performed in 300 mL autoclaves. Typically, $Rh(acac)(CO)_2$ (3.0 mg, 11.6 μmol) and the appropriate amount of ligand (5 eq.) were each dissolved in 5.8 mL toluene and added to the autoclave under argon. The active catalyst was preformed under 10 bar of synthesis gas at 140 °C. After 30 minutes the autoclave was cooled, opened and 2-butene (9.99 g, 178 mmol) was added. At room temperature 5 bar synthesis gas was applied and then the autoclave was heated to the desired temperature while the pressure was kept constant. After reaction the volatiles were recovered in a cold trap. A sample was withdrawn for GC-analysis.

High pressure NMR experiments.
Measurements were performed in a 10 mm o.d. sapphire NMR tube, a home-made modification of the design described by Elsevier.[74] In a typical experiment $Rh(acac)(CO)_2$ (5 mg, 19.4 μmol) and 1.05 equivalents of ligand were dissolved in 1.5 mL of toluene-d_8. The solution was brought into an argon-flushed tube. The tube was then flushed four times with 4 bar of synthesis gas and then pressurized at 20 bar. Preformation was carried out at 60 ºC for 16 hours after which the tube was cooled down to r.t. and the desired spectra were recorded. Alternatively the chamber of a 10 mL autoclave was brought under an argon atmosphere after which the abovementioned solution was injected by syringe. After preformation at 80 ºC for 1 hour under stirring, the autoclave was depressurized, the contents transferred into a normal NMR tube and the spectra recorded at r.t.

High pressure IR experiments.
Measurements were performed using a homemade 50 mL stainless steel autoclave with an integrated flow-cell equipped with ZnSe windows, a mechanical stirrer and temperature control. Before use argon was flushed through the apparatus for 2 hours. The catalyst mixture, containing $Rh(acac)(CO)_2$ (4 mg, 15.5 μmol) and ligand (2 eq.) in 15 mL cyclohexane was brought into the autoclave under a stream of argon. The solution was flushed 3 times with 4 bar synthesis gas before pressurizing to 17 bar at room temperature. The autoclave was then heated up to 80 °C and spectra were recorded every 10 minutes for 2 hours.

Crystal structure determination of 1 and 9-15.
Intensity data were collected using graphite-monochromated MoKα radiation on a Nonius Kappa CCD diffractometer with rotating anode. The structures were solved by direct methods using SHELXS97,[75] and refined on *F*2 by least-squares procedures using SHELXL97.[76] All non-hydrogen atoms were refined with anisotropic displacement parameters. Hydrogen atoms were constrained to idealized geometries and allowed to ride on their carrier atoms with an isotropic displacement parameter related to the equivalent displacement parameter of their carrier atoms. The asymmetric unit cel of compound **1** contains half a molecule of acetonitrile; in the unit cel for complexes **10** and **15** one molecule of acetonitrile is present. Complex **12** contained four voids, two of 448 $Å^3$, incorporating 47 electrons, and two of 198 $Å^3$, with 34 electrons each. Contributions of the solvent molecules have been determined by the SQUEEZE method. Structure validation and molecular graphics preparation were performed with the PLATON package.[77] Crystal data are given in Table 2.11 and 2.12.

Crystal structure determination of 1A.
The data were collected on a *Bruker SMART APEX CCD*. Data integration and global cell refinement was performed with the program SAINT. Intensity data were corrected for Lorentz and polarization effects. The structure was solved by Patterson methods and extension of the model was accomplished by direct methods applied to difference structure factors using the program *DIRDIF*.[78] The positional and anisotropic displacement parameters for the non-hydrogen atoms were refined. A subsequent difference Fourier synthesis resulted in the location of all the hydrogen atoms, which coordinates and isotropic displacement parameters were refined. Final refinement on F^2 carried out by full-matrix least-squares techniques converged at $wR(F^2) = 0.1133$ for 12282 reflections and $R(F) = 0.0410$ for 10321 reflections with $F_o \geq 4.0\ \sigma(F_o)$ and 815 parameters. Crystal data are given in Table 2.11.

Table 2.11: *Selected crystallographic data for ligand **1**, the polymorph **1A** and complexes **9-11**.*

	1	**1A**	**9**	**10**	**11**
Formula	$C_{55}H_{64}O_5P_2 \cdot 0.5 \cdot CH_3CN$	$C_{55}H_{64}O_5P_2$	$C_{55}H_{63}ClO_5P_2Pd$	$C_{59}H_{68}Cl_2O_9P_2Pd \cdot CH_3CN$	$C_{55}H_{63}ClO_5P_2Pt$
FW ($g \cdot mol^{-1}$)	887.53	867.06	1007.84	1201.43	1096.53
Crystal size (mm)	0.09×0.12×0.48	0.52×0.49×0.37	0.03×0.12×0.36	0.18×0.24×0.45	0.03×0.06×0.33
Crystal system	Monoclinic	Triclinic	Monoclinic	Orthorhombic	Monoclinic
Space group	$P2_1/c$ (no. 14)	$P\bar{1}$ (no. 2)	$P2_1/c$ (no. 14)	*P*nma (no. 62)	$P2_1/c$ (no. 14)
a (Å)	10.9055(1)	12.2735(6)	9.4543(1)	11.5297(3)	9.4832(1)
b (Å)	26.3694(3)	14.0431(7)	26.6986(3)	20.7719(3)	26.6038(3)
c (Å)	20.0433(2)	15.0026(7)	21.5052(2)	24.2993(5)	21.4405(3)
α (°)		79.592(1)			
β (°)	118.3060(10)	73.871(1)	108.5200(6)		108.7890(6)
γ (°)		89.752(1)			
V ($Å^3$)	5074.68(10)	2440.3(2)	5147.15(9)	5819.5(2)	5120.96(11)
Z	4	2	4	4	4
d_{calc} ($g\ cm^{-3}$)	1.162	1.180	1.301	1.371	1.422
μ (Mo-Kα) (mm^{-1})	0.136	1.36	0.520	0.522	2.900
T (K)	150	100	150	150	150
Total reflections	54146	23323	45983	31225	43023
Unique reflections (R_{int})	11570 (0.061)	12282 (0.0171)	10085 (0.060)	5882 (0.063)	9900 (0.058)
wR_2 (F^2) (all data)	0.1196	0.1133	0.0774	0.0837	0.0676
λ (Å)	0.71073	0.71073	0.71073	0.71073	0.71073
R_1	0.0479	0.0410	0.0355	0.0352	0.0315
F(000)	1900	928	2104	4568	2232

$R_{int} = \sum [|F_o^2 - F_o^2(\text{mean})|] / \sum [F_o^2]$; $wR(F^2) = [\sum [w(F_o^2 - F_c^2)^2] / \sum [w(F_o^2)^2]]^{1/2}$; $R(F) = \sum (||F_o| - |F_c||) / \sum |F_o|$

Table 2.12: *Selected crystallographic data for complexes **12-15**.*

	12	**13**	**14**	**15**
Formula	$C_{59}H_{68}Cl_2O_9P_2Pt$	$C_{56}H_{64}ClO_6P_2Rh$	$C_{72}H_{92}ClO_6P_2Rh$	$C_{60}H_{68}ClO_{10}P_2Rh\cdot CH_3CN$
FW ($g\cdot mol^{-1}$)	1249.06	1033.37	1253.76	1190.50
Crystal size (mm)	0.10×0.15×0.25	0.08×0.14×0.23	0.10×0.17×0.28	0.05×0.10×0.20
Crystal system	Orthorhombic	Orthorhombic	Orthorhombic	Orthorhombic
Space group	$P2_12_12_1$ (no. 19)	$Pna2_1$ (no. 33)	*P*nma (no. 62)	*P*nma (no. 62)
a (Å)	9.0341(10)	16.8142(10)	20.7367(2)	11.6735(10)
b (Å)	21.647(2)	16.2527(11)	30.4055(3)	21.125(2)
c (Å)	32.496(3)	18.5497(12)	12.5622(1)	23.744(3)
V ($Å^3$)	6355.0(11)	5069.2(5)	7920.59(13)	5855.3(11)
Z	4	4	4	4
d_{calc} ($g\ cm^{-3}$)	1.3055	1.354	1.051	1.351
μ (Mo-Kα) (mm^{-1})	2.391	0.502	0.332	0.450
T (K)	150	150	150	150
Total reflections	152479	137931	65862	126110
Unique reflections (R_{int})	14566 (0.14)	11597 (0.0816)	9217 (0.062)	5515 (0.13)
wR_2 (F^2) (all data)	0.108	0.062	0.1148	0.099
λ (Å)	0.71073	0.71073	0.71073	0.71073
R_1	0.047	0.033	0.0391	0.042
F(000)	2544	2160	2656	2488

$R_{int} = \sum [|F_o^2 - F_o^2(\text{mean})|]/\sum [F_o^2]$; $wR(F^2) = [\sum [w(F_o^2 - F_c^2)^2]/\sum [w(F_o^2)^2]]^{1/2}$; $R(F) = \sum (||F_o| - |F_c||)/\sum |F_o|$

2.7 References

Parts of the work in this chapter have been published:
J.I. van der Vlugt, R. Sablong, P.C.M.M. Magusin and D. Vogt, *Angew.Chem. Int. Ed.,* submitted.
J.I. van der Vlugt, R. Sablong, A.M. Mills, H. Kooijman, A.L. Spek and D. Vogt, *J. Chem. Soc., Dalton Trans.,* submitted.
J.I. van der Vlugt, A.C. Hewat, S. Neto, R. Sablong, A.M. Mills, M. Lutz, A.L. Spek and D. Vogt, *to be submitted*.

1 C.A. Tolman and J.W. Faller, in *Homogeneous Catalysis with Metal Phosphine Complexes*; L.H. Pignolet, Ed.; Plenum, New York, **1983**, 81.
2 M. Beller, B. Cornils, C.D. Frohning and C.W. Kohlpainter, *J. Mol. Cat. A: Chem*., **1995**, *104*, 17.
3 For recent reviews see: a) F. Ungvary, *Coord. Chem. Rev.*, **2002**, *218*, 1; b) C.D. Frohning, C.W. Kohlpainter and H.N. Bohnen, in *Applied Homogeneous Catalysis with Organometallic Compounds*; B. Cornils, W.A. Herrmann, Ed.; VCH, Weinheim, **2002**, vol 1, 31; c) *Rhodium Catalyzed Hydroformylation*; P.W.N.M. van Leeuwen, C. Claver, Ed.; Kluwer, Amsterdam, **2001**.
4 a) T.J. Devon, G.W. Phillips, T.A. Puckette, J.L. Stavinoha and J.J. Vanderbilt (to Eastman Kodak), U.S. Pat. 4,694,109, **1987** [*Chem. Abstr.*, **1988**, *108*, 7890]; b) T.J. Devon, G.W. Phillips, T.A. Puckette, J.L. Stavinoha and J.J. Vanderbilt (to Eastman Kodak), U.S. Pat. 5,332,846, **1994** [*Chem. Abstr.*, **1994**, *121*, 280879].
5 H.Bahrmann, P. Lappe, W.A. Herrmann, G.P. Albanese and R.B. Manetsberger (to Hoechst AG) Eur. Pat. 646,588, **1994** [*Chem. Abstr.*, **1995**, *123*, 112408d] .
6 P.W.N.M. van Leeuwen, P.A.M. Grotenhuis and B.L. Goodall (to Shell) Eur. Pat. 309,056 **1989** [*Chem. Abstr.*, **1989**, *111*, 232086w].
7 C.P. Casey, G.T. Whiteker, M.G. Melville, L.M. Petrovich, J.A. Gavney Jr. and D.R. Powell, *J. Am. Chem. Soc.*, **1992**, *114*, 5535.
8 E. Billig, A.G. Abatjoglou and D.R. Bryant (to Union Carbide) U.S. Pat. 4,599,206, **1986** and U.S. Pat. 4,668,651, **1987** [*Chem. Abstr.*, **1988**, *109*, 233177 and **1987**, *107*, 7392].
9 K. Sato, Y.Karawagi, M. Takai and T. Ookoshi (to Mitsubishi) U.S. Pat. 5,235,113, **1993** [*Chem. Abstr.*, **1993**, *118*, 191183].
10 A. van Rooy, P.C.J. Kamer, P.W.N.M. van Leeuwen, K. Goubitz, J. Fraanje, N. Veldman and A.L. Spek, *Organometallics*, **1996**, *15*, 835.
11 P.C.J. Kamer, J.N.H. Reek and P.W.N.M. van Leeuwen in *Rhodium Catalyzed Hydroformylation*; P.W.N.M. van Leeuwen, C. Claver, Eds.; Kluwer, Dordrecht, **2000**, 35.
12 a) M.T. Reetz, A. Gosberg, R. Goddard and S.H. Kyung, *Chem. Commun.*, **1998**, 2077; b) M.T. Reetz, D. Moulin and A. Gosberg, *Org. Lett.*, **2001**, *3*, 4083.
13 A. Zanotti-Gerosa, C. Malan and D. Herzberg, *Org. Lett.*, **2001**, *3*, 3687.
14 A. Martorell, R. Naasz, B.L. Feringa, P.G. Pringle, *Tetrahedron: Asymmetry*, **2001**, *12*, 2497.
15 C. Claver, E. Fernandez, A. Gillon, K. Heslop, D.J. Hyett, A. Martorell, A. G. Orpen and P.G Pringle, *Chem. Commun.*, **2000**, 961.
16 D. Haag, J. Runsink and H.D. Scharf, *Organometallics*, **1998**, *17*, 398.
17 M.T. Reetz and M. Pastó, *Tetrahedron Lett.*, **2000**, *41*, 3315.
18 S. Hillebrand, J. Bruckmann, C. Krüger and M.W. Haenel, *Tetrahedron Lett.*, **1995**, *36*, 75.
19 M. Kranenburg, Y.E.M. van der Burgt, P.C.J. Kamer, P.W.N.M. van Leeuwen, K. Goubitz and J. Fraanje, *Organometallics*, **1995**, *14*, 3081.
20 a) P. Arnoldy, in *Rhodium Catalyzed Hydroformylation*; P.W.N.M. van Leeuwen, C. Claver, Eds; Kluwer, Amsterdam, **2001**, 203; b) D. Vogt, in *Applied Homogeneous Catalysis with Organometallic Compounds*; B. Cornils and W.A. Herrmann, Ed.; Wiley VCH, Weinheim, **2002**, vol 1, 240.
21 P.M. Burke, J.M. Garner, W. Tam, K.A. Kreutzer and A.J.J. Teunissen (to Du Pont/DSM) WO 97/33854, **1997** [*Chem. Abstr.*, **1997**, *127*, 294939]
22 L.A. van der Veen, P.C.J. Kamer and P.W.N.M. van Leeuwen, *Angew. Chem. Int. Ed.*, **1999**, *38*, 336.
23 a) D. Selent, K.D. Wiese, D. Röttger and A. Börner, *Angew. Chem. Int. Ed.*, **2000**, 3*9*, 1639; b) D. Selent, D. Hess, K.-D. Wiese, D. Röttger, C. Kunze and A. Börner, *Angew. Chem. Int. Ed.*, **2001**, 40, 1696.
24 H. Klein, R. Jackstell, K.D. Wiese, C. Borgmann and M. Beller, *Angew. Chem. Int. Ed.*, **2001**, *40*, 3408.
25 C.P. Casey and G.T. Whiteker, *Isr. J. Chem.*, **1990**, *30*, 299.

26 C. Kunze, D. Selent, I. Neda, M. Freytag, P.G. Jones, R. Schmutzler, W. Baumann and A. Börner, *Z. Anorg. Allg. Chem.*, **2002**, *628*, 779.

27 a) A.C. Hewat, *PhD.Thesis*, **2000**, RWTH Aachen; b) W. Ahlers, D. Wiebelhaus, R. Paciello, M. Bartsch, R. Baumann, D. Vogt and A.C. Hewat (to BASF AG) WO 02/22261, **2002** [*Chem. Abstr.*, **2002**, *136*, 249380]; c) W. Goertz, P.C.J. Kamer, P.W.N.M. van Leeuwen and D. Vogt, *Chem. Eur. J.*, **2001**, *7*, 1614.

28 A. Buhling, P.C.J. Kamer, P.W.N.M. van Leeuwen, J.W. Elgersma, K. Goubitz and J. Fraanje, *Organometallics*, **1997**, *16*, 3027.

29 A. Karaçar, M. Freytag, P.G. Jones, R. Bartsch and R. Schmutlzer, *Z. Anorg. Allg. Chem.*, **2001**, *627*, 1571.

30 a) S. Agbossou, M.C. Bonnet, F. Dahan and I. Tkatchenko, *Acta Cryst.*, **1989**, *C45*, 1149; b) M.C. Bonnet, S. Agbossou, I. Tkatchenko, R. Faure and H. Loiseleur, *Acta Cryst.*, **1987**, *C43*, 445.

31 P. Braunstein, F. Naud, A. Dedieu, M.-M. Rohmer, A. DeCian and S.J. Rettig, *Organometallics*, **2001**, *20*, 2966.

32 W. Goertz, W. Keim, D. Vogt, U. Englert, M.D.K. Boele, L.A. van der Veen, P.C.J. Kamer and P.W.N.M. van Leeuwen, *J. Chem. Soc., Dalton Trans.*, **1998**, 2981.

33 D.A. Albisson, R.B. Bedford, S.E. Lawrence and P.N. Scully, *Chem. Commun.*, **1998**, 2095.

34 V.I. Sokolov, L.A. Bulygina, O.Y. Borbulevych and O.V. Shishkin, *J. Organomet. Chem.*, **1999**, *582*, 246.

35 F.J. Parlevliet, M.A. Zuideveld, C. Kiener, H. Kooijman, A.L. Spek, P.C.J. Kamer and P.W.N.M. van Leeuwen, *Organometallics*, **1999**, *18*, 3394.

36 S.J. Sabounchei, A. Nagipour and J.F. Bickley, *Acta Cryst.*, **2000**, *C56*, e280.

37 M.A. Zuideveld, B.H.G. Swennenhuis, M.D.K. Boele, Y. Guari, G.P.F. van Strijdonck, J.N.H. Reek, P.C.J. Kamer, K. Goubitz, J. Fraanje, M. Lutz, A.L. Spek and P.W.N.M. van Leeuwen, *J. Chem. Soc., Dalton Trans.*, **2002**, 2308.

38 J. Yin and S.L. Buchwald, *J. Am. Chem. Soc.*, **2002**, *124*, 6043.

39 a) M.J. Green, G.J.P. Britovsek, K.J. Cavell, B.W. Skelton and AH. White, *Chem. Commun*, **1996**, 1563; b) P.L. Alsters, J. Boersma, W.J.J. Smeets, A.L. Spek and G. van Koten, *Organometallics*, **1993**, *12*, 1639; c) P.L. Alsters, J. Boersma, H. Kooijman, A. Sicherer-Roetman, A.L. Spek and G. van Koten, *Organometallics*, **1992**, *11*, 4124.

40 P.S. Pregosin and S.N. Sze, *Helv. Chim. Acta*, **1978**, *61*, 1848.

41 M. Stolmàr, C. Floriani, A. Chiesi-Villa and C. Rizzoli, *Inorg. Chem.*, **1997**, *36*, 1694.

42 C.G. Arena, D. Drommi, F. Faraone, C. Graiff and A. Tiripicchio, *Eur. J. Inorg. Chem.*, **2001**, 247.

43 C.J. Cobley and P.G. Pringle, *Inorg. Chim. Acta*, **1997**, *265*, 107.

44 a) R. van Duren, J.P.J. Huijbers, J.I. van der Vlugt, A.M. Mills, A.L. Spek and D. Vogt, *to be submitted*; b) See *Chapter* 3 of this thesis.

45 a) L. Dahlenburg and S. Mertel, *J. Organomet. Chem.*, **2001**, *630*, 221; b) L. Dahlenburg, C. Becker, J. Höck and S. Mertel, *J. Organomet. Chem.*, **1998**, *564*, 155.

46 M.E. Squires, D.J. Sardella and L.B. Kool, *Organometallics*, **1994**, *13*, 2970.

47 L. Manojlović-Muir, I.R. Jobe, B.J. Maya and R.J. Puddephatt, *J. Chem. Soc., Dalton Trans.*, **1987**, 2117.

48 a) F.H. Allen and A. Pidcock, *J. Chem. Soc. A*, **1968**, 2700; b) M.S. Balakrishna, *J. Chem. Res. (S)*, **2001**, 270; c) M.A. Bennett, S.K. Bhargava, M. Ke and A.C. Willis, *J. Chem. Soc., Dalton Trans*., **2000**, 3537; d) R.B. Bedford, S.L. Hazelwood and D.A. Albisson, *Organometallics*, **2002**, *21*, 2599.

49 a) G.P.C.M. Dekker, C.J. Elsevier, S.N. Poelsma, K. Vrieze, P.W.N.M. Van Leeuwen, W.J.J. Smeets and A.L. Spek, *Inorg. Chim. Acta*, **1992**, 195, 203; b) G.B. Deacon, K.T. Nelson and E.R.T. Tiekink, *Acta Cryst.*, **1991**, *C47*, 955; c) N.Bresciani-Phor, M. Plazzotta, L. Randaccio, G. Bruno, V. Ricetuvo, R. Romeo, U. Belluco, *Inorg. Chim. Acta*, **1978**, *31*, 171.

50 M.J. Atherton, J. Fawcett, A.P. Hill, J.H. Holloway, E.G. Hope, D.R. Russell, G.C. Saunders and R.M.J. Stead, *J. Chem. Soc., Dalton Trans.*, **1997**, 1137.

51 W. Xu, J.P. Rourke, J.J. Vittal and R.J. Puddephatt, *Inorg. Chem.*, **1995**, *34*, 323.

52 a) E. Fernández, A.Ruiz, C. Claver, S. Castillón, A. Polo, J.F. Piniella and A. Alvarez-Larena, *Organometallics*, **1998**, *17*, 2857; b) S.C. van der Slot, J. Duran, J. Luten, P.C.J. Kamer and P.W.N.M. van Leeuwen, *Organometallics*, **2002**, *21*, 3873; c) S.C. van der Slot, P.C.J. Kamer, P.W.N.M. van Leeuwen, J. Fraanje, K. Goubitz, M. Lutz and A.L. Spek, *Organometallics*, **2000**, *19*, 2504.

53 M. Laly, R. Broussier and B. Gauteron, *Tetrahedron Lett.*, **2000**, 1183.

54 S.P. Shum, S.D. Pastor and G. Rihs, *Inorg. Chem.*, **2002**, *41*, 127.

55 R. Kumar, R.J. Puddephatt and F.R. Fronczek, *Inorg. Chem.*, **1990**, *29*, 4850.
56 E. Fernández, A. Ruiz, C. Claver, S. Castillón, A. Polo, J.F. Piniella and A. Alvarez-Larena, *Organometallics*, **1998**, *17*, 2857.
57 R. Paciello, L. Siggel, H.J. Kneuper, N. Walker and M. Röper, *J. Mol. Cat. A: Chem.*, **1999**, *143*, 85.
58 E.K. van den Beuken, W.G.J. de lange, P.W.N.M. van Leeuwen, N. Veldman, A.L. Spek and B.L. Feringa, *J. Chem. Soc., Dalton Trans.*, **1996**, 3561.
59 A. Suárez, M.A. Méndez-Rojas and A. Pizzano, *Organometallics*, **2002**, *21*, 4611.
60 C.J. Cobley, D.D. Ellis, A. G. Orpen and P.G. Pringle, *J. Chem. Soc., Dalton Trans.*, **2000**, 1109.
61 D.A. Vicic and W.D. Jones, *J. Am. Chem. Soc.*, **1997**, *119*, 10855.
62 L. Contreras, A. Monge, A. Pizzano, C. Ruiz, L. Sánchez and E. Carmona, *Organometallics*, **1993**, *12*, 4228.
63 L.A. van der Veen, P.H. Keeven, G.C. Schoemaker, J.N.H. Reek, P.C.J. Kamer, P.W.N.M. van Leeuwen, M. Lutz and A.L. Spek, *Organometallics*, **2000**, *19*, 872.
64 P.C.J. Kamer, P.W.N.M. van Leeuwen and J.N.H. Reek, *Acc. Chem. Res.*, **2001**, *34*, 895.
65 Y. Pottier, A. Mortreux and F. Petit, *J. Organomet. Chem.*, **1989**, *370*, 333.
66 A. Castellanos-Páez, S. Castillón, C. Claver, P.W.N.M. van Leeuwen and W.G.J. de Lange, *Organometallics*, **1998**, *17*, 2543.
67 R. Ewalds, E.B. Eggeling, A.C. Hewat, P.C.J. Kamer, P.W.N.M. van Leeuwen and D. Vogt, *Chem. Eur. J.*, **2000**, *6*, 1496.
68 a) C.B. Dieleman, P.C.J. Kamer, J.N.H. Reek and P.W.N.M. van Leeuwen, *Helv. Chim. Acta*, **2001**, *84*, 3269; b) G.J.H. Buisman, L.A. van der Veen, P.C.J. Kamer and P.W.N.M. van Leeuwen, *Organometallics*, **1997**, *16*, 5681.
69 B. Moasser, W.L. Gladfelter and D.C. Roe, *Organometallics*, **1995**, *14*, 3832.
70 J.M. Brown and A.G. Kent, *J. Chem .Soc., Perkin Trans. 2*, **1987**, 1597.
71 D.R. Drew and J.R. Doyle, *Inorg. Synth.*, **1990**, *28*, 346.
72 F.T. Ladipo and G.K. Anderson, *Organometallics*, **1994**, *13*, 303.
73 H.C. Clark and L.E. Manzer, *J. Organomet. Chem.*, **1973**, *59*, 411.
74 C.J. Elsevier, *J. Mol. Cat.*, **1994**, *92*, 285.
75 G.M. Sheldrick, SHELXS97; University of Göttingen, Germany, **1997**.
76 G.M. Sheldrick, SHELXL97; University of Göttingen, Germany, **1997.**
77 A.L. Spek, PLATON, A Multipurpose Crystallographic Tool; Utrecht University, The Netherlands, **2002**.
78 P.T. Beurskens, G. Beurskens, R. de Gelder, S. García-Granda, R.O. Gould, R. Israël and J.M.M. Smits, The *DIRDIF*-99 program system; University of Nijmegen, The Netherlands, **1999**.

3

Rhodium Mediated Asymmetric Catalysis Using a Chiral Diphosphonite

Abstract *The improved synthesis of a chiral diphosphonite, XantBino **1**, with a xanthene backbone is described. The chirality is introduced by use of a binaphthyl unit on the phosphonite moieties. With this diphosphonite a complexation study is performed to get insight in the coordination behaviour towards palladium, platinum and rhodium. The ^{31}P NMR spectra of the three complexes obtained, show that the two phosphorus atoms become chemically inequivalent. Coupling constants $J_{P\text{-}P}$ are in the order of 15-50 Hz. For the platinum complex a coupling constant $J_{Pt\text{-}P}$ of 5200 Hz is found. Both* cis-*[$PdCl_2$(**1**)] (**2**) as well as* cis-*[$PtCl_2$(**1**)] (**3**) are characterized by X-ray crystallography. These studies confirm the unexpected* cis-*coordination of this bidentate ligand, leading to bite angles of around 100°. The metal atom is located outside the ligand plane in both complexes, leading to dihedral angles of the metal plane and the ligand plane of around 112-115°. The rhodium catalyzed asymmetric hydroformylation of styrene as well as the rhodium catalyzed asymmetric hydrogenation of methyl (Z)-2-acetamido-cinnamate are described applying the chiral diphosphonite. Low enantiomeric excesses of up to 33% are obtained in the asymmetric hydroformylation, while use of the catalytic system [Rh(cod)(**1**)]BF_4 resulted in an enantiomeric excess of 54% in the Rh catalyzed asymmetric hydrogenation.*

3.1 Introduction

The rhodium catalyzed asymmetric hydroformylation of vinylarenes, with styrene as a model substrate has been extensively studied during the past years, especially in academia. Several classes of ligands have been applied in this reaction, *e.g.* diphosphines,[1] phosphine-phosphites,[2] diphosphites,[3] aminophosphine-phosphinites[4] and other bifunctional systems.[5] Only few catalytic systems, however, show satisfactory enantioselectivity for the desired branched aldehyde. The best results have been obtained with the ligand BINAPHOS, a phosphine-phosphite, at high synthesis gas pressures of up to 100 bar.[2] The enantiomeric excess (ee) reached 98%. Drawback is that its synthesis is cumbersome, with little room for modularity. Work carried out at Union Carbide and later by the group of van Leeuwen on diphosphite ligands derived from (*2R,4R)*-pentane-2,4-diol led to enantioselectivities of up to 87%.[3]

The stereogenic aminophosphine-phosphinite (AMPP) ligands applied by Vogt *et al.* have proven to be powerful ligands for the hydroformylation of vinyl arenes as well, and ee's of up to 76% have been reported.[4]

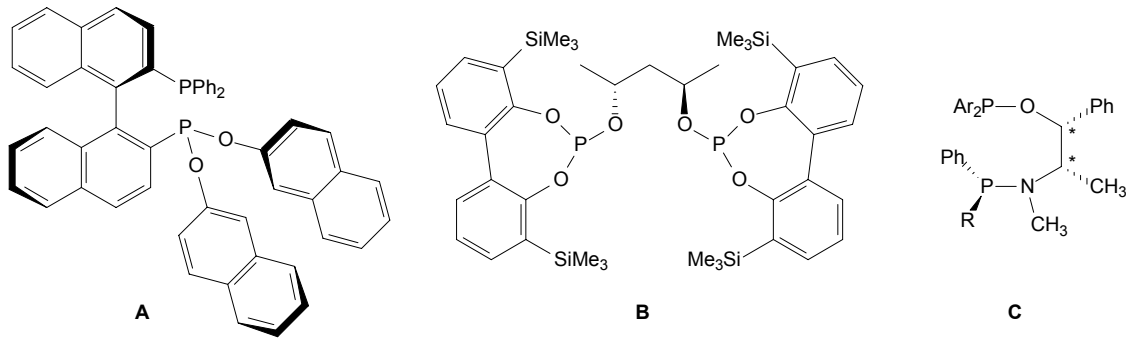

Figure 3.1: *Illustration of BINAPHOS (**A**), diphosphite derived from* (2R,4R)*-pentane-2,4-diol (**B**) and an amino-alcohol derived P-stereogenic AMPP ligand (**C**).*

Diphosphonites have been largely overlooked in homogeneous catalysis to date. Recently some reports have appeared about diphosphonites in asymmetric hydrogenation as well as in hydroboration, making use of several backbones.[6-8] Next to this, monophosphonites have attracted some attention, especially for the hydrogenation of enamides[9] and the copper catalyzed diethylzinc-addition to enones.[10] Also one report is known where a chiral diphosphonite, XantBino (Figure 3.2), based on a xanthene backbone, is applied in the asymmetric hydrocyanation of styrene.[11]

The results described in *Chapter* 2, on the use of achiral xanthene derived diphosphonites in the Rh catalyzed hydroformylation of alkenes, led to the consideration to study the applicability of a chiral diphosphonite based on this ligand backbone in asymmetric catalysis. In this chapter, the

synthesis of diphosphonite compound **1**, XantBino is described using a modified literature procedure.[11] The coordination chemistry of this ligand **1** with palladium, platinum and rhodium precursors is studied by NMR spectroscopy and X-ray crystallography. The applicability of the ligand in the rhodium catalyzed hydroformylation of styrene and in the asymmetric hydrogenation of methyl (*Z*)-2-acetamidocinnamate is evaluated.

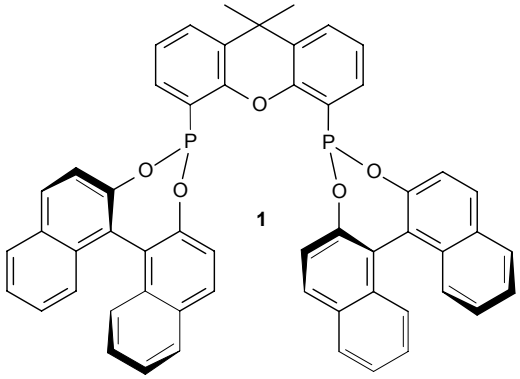

Figure 3.2: *Representation of compound **1**, XantBino.*

3.2 Synthesis

Diphosphonite **1** was prepared in a straightforward manner, using a two-step procedure, as illustrated in Scheme 3.1. The (bis(diethylamino))diphosphonite derivative of the commercial starting material 9,9-dimethylxanthene is prepared in moderate to good yield.[11] Subsequently, the chiral binaphthyl groups are introduced, to obtain the desired chiral diphosphonite. This reaction is catalyzed by tetrazole as protonation agent, which is a slight but important modification of the literature procedure. Addition of tetrazole shortened the reaction time considerably, in analogy to the synthesis of the sterically constrained diphosphonites described in *Chapter* 2. Work up to obtain the pure compound was done by layering a solution of the crude product in dichloromethane with acetonitrile. This has been omitted in the earlier methodology. In the present case however, the second reaction step always led to impurities (< 10%), most likely due to formation of only one phosphonite moiety. The ^{31}P NMR spectrum for the pure compound showed a singlet at δ = 178.0 ppm, which is even more low field than for the ligands described in the previous chapter. This value reflects the fact that both electronic factors as well as conformational influences strongly affect the chemical shift for the ^{31}P nucleus.

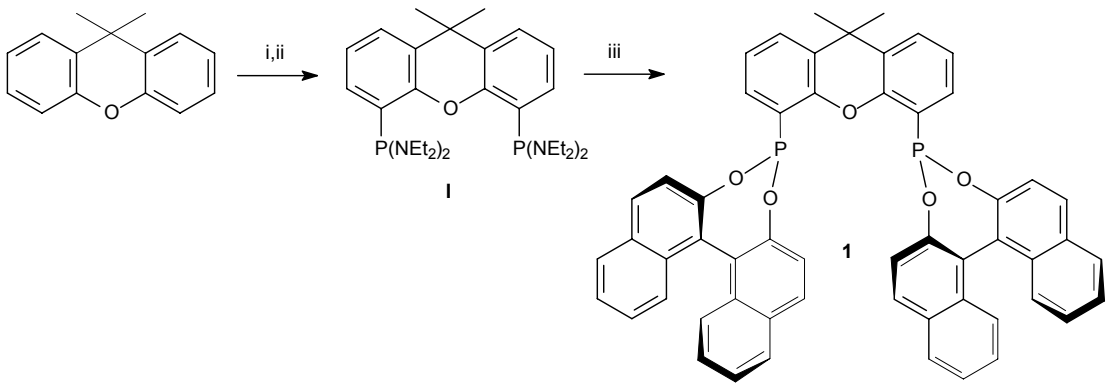

Scheme 3.1: *Synthetic route to compound **1** via compound **I**. i)* n-*BuLi, TMEDA, Et_2O, -40 ºC, 16 h; ii) $ClP(NEt_2)_2$, pentane, -60 ºC, 16 h; iii) 2,2'-dihydroxy-1,1'-binaphthyl (2 eq.), toluene, tetrazole, Δ, 1 day.*

3.3 Coordination Chemistry

To gain knowledge about the type of complexes formed with XantBino **1**, its coordination behaviour towards palladium, platinum and rhodium precursors is studied. Previously, only spectroscopic evidence for the formation of the 'bis-chelate' Ni(**1**)$_2$ has been described.[11]

3.3.1 Palladium

From the reaction of $PdCl_2$(cod) with ligand **1** (Scheme 3.2) at room temperature, a yellow compound was obtained, for which the ^{31}P NMR spectrum showed two doublets at 143.1 ppm and 137.4 ppm. The observed coupling constant $J_{P\text{-}P}$ was 46.5 Hz, indicating that the phosphorus atoms apparently are chemically inequivalent. This is probably due to the chiral, bulky binaphthyl units, making both phosphorus atoms distinctly different on the NMR timescale. From the ^{1}H NMR spectrum, it appears that also the methyl groups in the backbone are inequivalent, indicating that the aromatic skeleton of the xanthene is bent.[12]

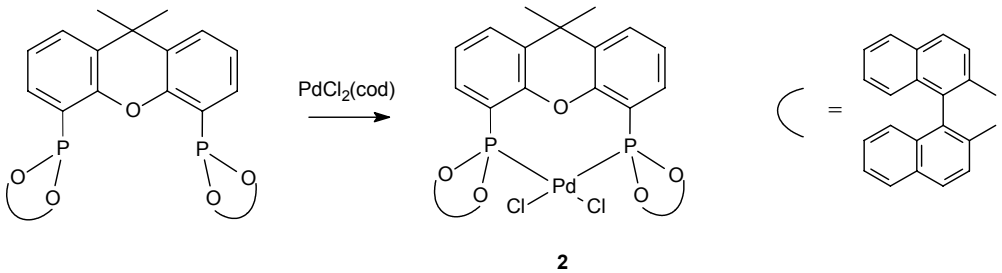

Scheme 3.2: *Reaction of XantBino with Pd precursor to form complex **2**.*

Single crystals suitable for X-ray analysis could be grown by layering a dichloromethane solution of complex **2** with acetonitrile. The molecular structure of *cis*-[$PdCl_2$(**1**)] is represented in Figure 3.3, while Table 3.1 contains selected bond lengths and angles. It is evident that ligand **1** acts as a bidentate ligand, coordinating in a *cis*-fashion to the palladium atom.

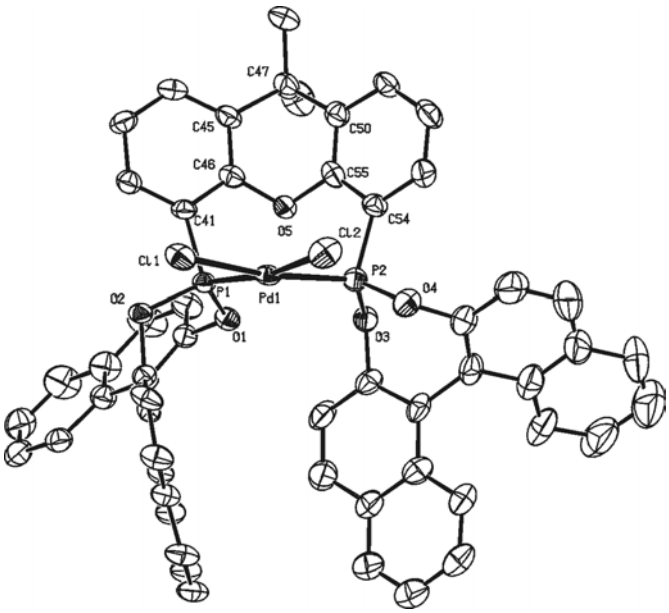

Figure 3.3: *ORTEP representation of complex **2**,* cis-*[$PdCl_2$(**1**)]. Displacement ellipsoids are drawn at the 50% probability level. All hydrogen atoms and solvent molecules are omitted for clarity.*

The coordination around the central palladium atom is distorted square planar, with a P_1-Pd-P_2 angle of 99.99(3)° while the angle Cl_1-Pd-Cl_2 is 90.15(4)°. There are few examples on palladium diphosphonite complexes known in literature. However, the bond lengths for Pd-P (~ 2.22 Å) and Pd-Cl (~2.35 Å) are normal, compared to the work of Agbossou[13] and Schmutzler.[14] Compared with crystal structures of Pd complexes known with Xantphos derivatives, the bite angle of nearly 100° for ligand **1** is unusually small.[15-17] The angles Pd-P_1-C_{41} and Pd-P_2-C_{54} were around 109°. The dihedral angle between the metal plane Cl_1-Pd-Cl_2 and the ligand plane P_1-P_2-C_{41} is 115.7°, indicating that the palladium is actually positioned outside the plane defined by the backbone and the phosphorus atoms, which is quite unusual for *cis*-Pd(PP) complexes. This makes that the palladium atom is fairly well accessible for further modifications or for catalysis. A similar structural disposition of the metal atom, together with a small bite angle P-Pd-P, was found for the *ortho*-metallated species described in *Chapter* 2, yet no such bond occurs in complex **2**. This phenomenon must therefore be based on steric crowding induced by the binaphthyl units. The dihedral angle of the two aromatic rings in the xanthene backbone is found to be 107.8°. The distance between the two phosphorus atoms is

3.4455(12) Å while the distance between the palladium atom and the oxygen in the backbone is 3.284(2) Å, too large to expect any interaction.

Table 3.1: *Selected bond lengths and angles for complex* ***2****,* cis-*[$PdCl_2$(**1**)]*.

Bond lengths (Å)					
Pd-P_1	2.2449(9)	Pd-P_2	2.2532(9)	Pd-Cl_1	2.3412(10)
Pd-Cl_2	2.3442(9)	P_1-O_1	1.613(2)	P_1-O_2	1.601(2)
P_2-O_3	1.800(3)	P_2-O_4	1.604(3)	P_1-C_{41}	1.800(3)
P_2-C_{54}	1.815(3)	O_5-C_{46}	1.380(4)	O_5-C_{55}	1.388(4)
Pd-O_5	3.284(2)	P_1-P_2	3.4455(12)		
Angles (°)					
Cl_1-Pd-Cl_2	90.15(4)	P_1-Pd-P_2	99.99(3)	Cl_1-Pd-P_1	82.70(3)
Cl_1-Pd-P_2	172.15(3)	Cl_2-Pd-P_1	170.01(3)	Cl_2-Pd-P_2	86.23(3)
O_1-P_1-O_2	102.46(12)	O_3-P_2-O_4	103.07(13)	Pd-P_1-O_1	116.50(9)
Pd-P_1-O_2	117.78(9)	Pd-P_2-O_3	123.91(9)	Pd-P_2-O_4	110.02(10)
Pd-P_1-C_{41}	109.87(11)	Pd-P_2-C_{54}	108.57(12)	C_{46}-O_5-C_{56}	112.6(3)
C_{45}-C_{47}-C_{50}	106.8(3)	O_1-P_1-C_{41}	106.07(13)	O_2-P_1-C_{41}	102.70(13)
O_3-P_2-C_{54}	102.50(14)	O_4-P_2-C_{54}	107.67(15)		

The reaction of **1** with the palladium precursor PdCl(CH_3)(cod) was monitored in time by *in situ* ^{31}P NMR spectroscopy. Initially, two doublets appeared at δ = 148.0 ppm and δ = 115.0 ppm, both with a coupling constant $J_{P\text{-}P}$ of 24 Hz, as the major species (~ 94%). In the corresponding ^{1}H NMR spectrum a broad doublet was observed at 2.71 ppm ($J_{P\text{-}H}$ = 10.4 Hz) for the methyl ligand coordinated to Pd. These observations indicate the formation of a *cis*-[PdCl(CH_3)(**1**)] complex. Next to this, a minor species showed two doublets at δ = 141.6 ppm and δ = 100.8 ppm, both with a coupling constant $J_{P\text{-}P}$ of 13 Hz. In the course of approximately 3 hours the former product completely disappeared and only the latter two doublets were apparent. This suggests a transformation from the kinetically controlled *cis*-complex to the more stable product with both phosphorus atoms coordinated to the palladium in a *trans*-fashion.

3.3.2 Platinum

After the reaction of $PtCl_2$(cod) with ligand **1**, a white solid was obtained. The ^{31}P NMR spectrum for this compound indicated that also in this complex the two phosphorus atoms are chemically inequivalent. The ^{31}P NMR spectrum (Figure 3.4) showed two doublets at δ = 113.1 ppm (A) and δ = 110.5 ppm (B), both flanked by ^{195}Pt satellites, and a coupling constant $J_{Pt\text{-}P}$ of 5040 Hz. The coupling constant $J_{P\text{-}P}$ is 15.9 Hz.

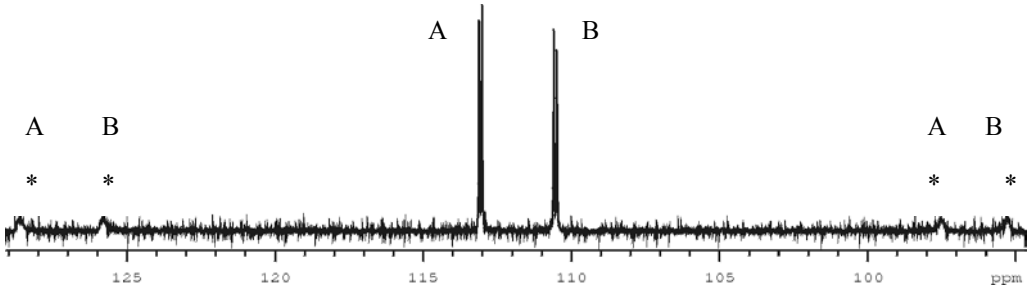

Figure 3.4: *The ^{31}P NMR of complex **3**,* cis-*[$PtCl_2$(**1**)], showing the two doublets at δ = 110.5 ppm and δ = 113.1 ppm. The P-P splitting is invisible here due to poor resolution. * denotes a ^{195}Pt satellite.*

Comparing this value with literature data for *cis*-$PtCl_2$(PP) complexes of diphosphites (J ~ 5800 Hz) and diphosphines (J ~ 3500 Hz)[18,19] and the values reported in *Chapter* 2, this spectrum can be assigned to originate from a *cis*-platinum diphosphonite complex. The value is also in agreement with the limited literature values reported so far. The groups of Schmutzler and Börner have prepared a new calix[4]arene based diphosphonite, starting from 6-chloro-dibenzo-1-oxa-$\sigma^3\lambda^3$-phosphorine as the phosphorus building block.[20] They also discussed the related Pt complex, for which the ^{31}P NMR spectrum showed two doublets (due to stereogenic P-atoms) and coupling constants $J_{Pt\text{-}P}$ of around 5060 Hz. A combined effort from the groups of Claver and Pringle has resulted in a study on the use of monophosphonites in asymmetric hydrogenation.[9] Herein, also the X-ray analyses of two Pt complexes, one bearing a chelating diphosphonite, the other complex containing two monophosphonites, are reported, but without any spectroscopic identification of these complexes in solution. Puddephatt has been able to characterize a *trans*-dimeric species, incorporating diethoxyphosphonitomethane as the ligand.[21] Work by Squires[22] and the group of Dahlenburg[23] on alkyl substituted phosphonites resulted in coupling constants $J_{Pt\text{-}P}$ for this subclass of diphosphonites of around 4700 Hz.

Single crystals, suitable for X-ray analysis, were obtained by layering a dichloromethane/chloroform solution of complex **3** with acetonitrile. The resulting molecular structure obtained is depicted in Figure 3.5, while selected bond lengths and angles are found in Table 3.2. The structure of the complex turned out to be almost isomorphous to that of complex **2**.

The geometry around the platinum atom is distorted square planar. The bite angle P_1-Pt-P_2 is 99.64(4)° while the Cl_1-Pt-Cl_2 is 87.99(4)°. The solid crystallized in a chiral space group $P2_12_12_1$. The angles Pt-P_1-C_{41} and Pt-P_2-C_{54} are 111.32(14)° and 108.92(14)°, respectively. The dihedral angle between the metal plane Cl_1-Pt-Cl_2 and the ligand plane P_1-P_2-C_{41} is 112.2°, so a similar structural motif as in complex **2** exists.

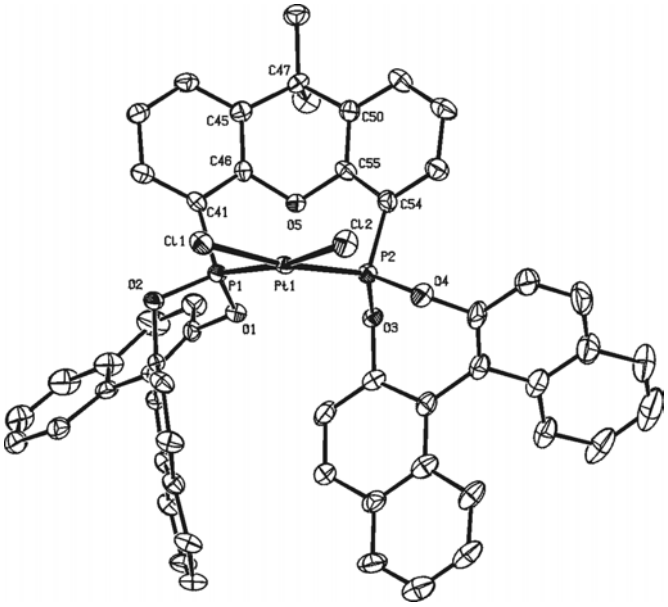

Figure 3.5: *Displacement ellipsoid plot of complex **3**,* cis-*[$PtCl_2$(**1**)]. Displacement ellipsoids are drawn at the 50% probability level. All hydrogen atoms and solvent molecules are omitted for clarity.*

This gives way to a very large accessibility of the platinum center. The distance between the two phosphorus atoms is 3.3980(15) Å while the distance between the platinum atom and the oxygen in the backbone is 3.335(3) Å, too large to expect any interaction. The Pt-Cl and the Pt-P bond lengths are ~2.348 Å and ~2.223 Å on average, respectively and as such in agreement with values reported by Dahlenburg.[23]

The displacement of the platinum plane relative to the ligand plane is clearly illustrated in Figure 3.6, which shows a front view on the complex. The sterically demanding binaphthyl units have been omitted for clarity, but both are pointing sideways of the molecule.

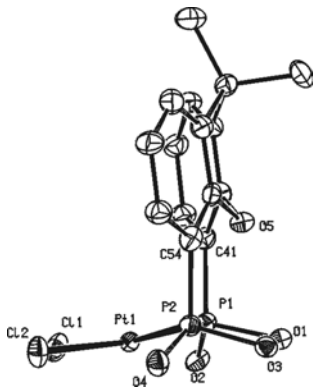

Figure 3.6: *Front view on the metallic core of complex **3**, showing the displacement of the square planar platinum from the ligand plane.*

Table 3.2: *Selected bond lengths, distances and angles for complex **3**,* cis-*[$PtCl_2$(**1**)]*.

Bond lengths (Å)					
Pt-P_1	2.2229(11)	Pt-P_2	2.2245(11)	Pt-Cl_1	2.3504(11)
Pt-Cl_2	2.3450(11)	P_1-O_2	1.604(3)	P_1-O_2	1.601(3)
P_2-O_3	1.603(3)	P_2-O_4	1.616(3)	P_1-C_{41}	1.798(4)
P_2-C_{54}	1.813(4)	O_5-C_{46}	1.388(5)	O_5-C_{55}	1.397(5)
Pt-O_5	3.335(3)	P_1-P_2	3.3980(15)		
Angles (°)					
Cl_1-Pt-Cl_2	87.99(4)	P_1-Pt-P_2	99.64(4)	Cl_1-Pt-P_1	84.32(4)
Cl_1-Pt-P_2	172.19(4)	Cl_2-Pt-P_1	170.59(4)	Cl_2-Pt-P_2	87.39(4)
O_1-P_1-O_2	102.54(14)	O_3-P_2-O_4	102.61(17)	Pt-P_1-O_1	116.58(11)
Pt-P_1-O_2	117.11(11)	Pt-P_2-O_3	122.51(12)	Pt-P_2-O_4	110.23(12)
Pt-P_1-C_{41}	111.32(14)	Pt-P_2-C_{54}	108.92(14)	C_{46}-O_5-C_{56}	112.6(3)
C_{45}-C_{47}-C_{50}	105.7(4)	O_1-P_1-C_{41}	105.87(16)	O_2-P_1-C_{41}	101.80(16)
O_3-P_2-C_{54}	104.24(16)	O_4-P_2-C_{54}	107.32(19)		

3.3.3 Rhodium

As rhodium is the metal of choice for both studied types of asymmetric catalysis in this chapter, the hydroformylation as well as the hydrogenation, it seemed worthwhile to investigate the complexation behaviour of ligand **1** with rhodium precursors as well. To get more comprehension for the cationic catalyst [Rh(cod)(P-P)]BF_4 which is normally applied for such hydrogenation reactions, an *in situ* NMR study was carried out. A small excess of the ligand was reacted with Rh(acac)(cod) by a standard procedure. For the final product [Rh(cod)(**1**)]BF_4 the ^{31}P NMR spectrum showed two doublets of doublets (Figure 3.7). The average signals appeared at δ = 169.7 ppm and at δ = 161.4 ppm, with coupling constants $J_{Rh\text{-}P}$ of 218 Hz and $J_{P\text{-}P}$ of 24 Hz. The existence of this ABX pattern

implies that the two phosphorus atoms are chemically inequivalent in the rhodium complex as well. The Rh-P coupling constant is similar to values reported by Börner,[20] Puddephatt[24] and Shum,[25] although the latter report dealt with a Rh(acac)-diphosphonite derivative, with a $^{1}J_{Rh\text{-}P}$ of 266 Hz.

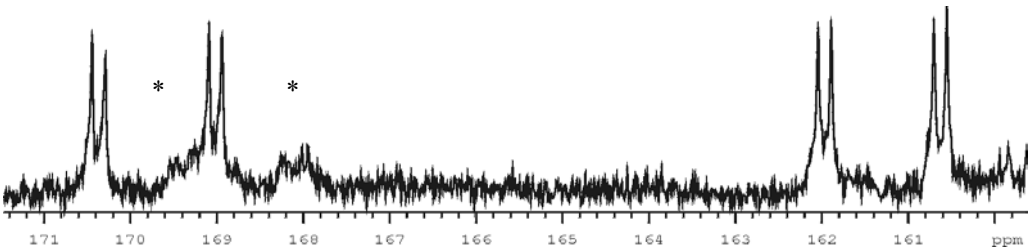

Figure 3.7: *^{31}P NMR spectrum of [Rh(cod)(**1**)]BF_4 showing the two doublets of doublets. * denotes an impurity.*

3.4 Catalysis

3.4.1 Asymmetric hydroformylation

In order to evaluate the catalytic properties of enantiomerically pure (*R,R*)-(**1**) it was applied in the rhodium catalyzed asymmetric hydroformylation of styrene (Scheme 3.3) using $Rh(acac)(CO)_2$. Before addition of the substrate, the catalyst system was activated for 1 hour in order to generate the catalytic resting state [$Rh(H)(CO)_2$(**1**)].

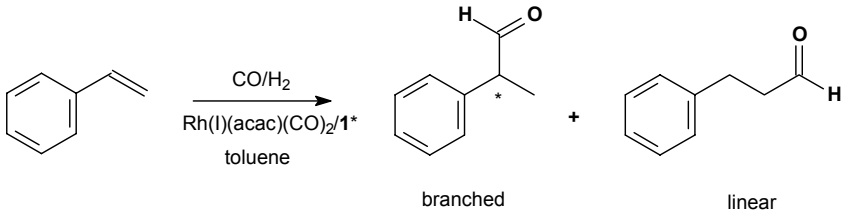

Scheme 3.3: *General reaction scheme for the rhodium catalyzed hydroformylation of styrene.*

Several hydroformylation experiments were performed at different synthesis gas pressures (10 and 20 bar) and at different temperatures (40-100 °C). The amount of hydrogenation was usually less than 1% and there were no other side products formed. The results obtained are summarized in Table 3.3. At 40 °C, a pressure of 20 bar instead of 10 bar led to an increase in the reaction rate of approximately 33%. The enantiomeric excess was found to be lower (entry 2 vs. 1). The selectivity for the branched aldehyde remained constant within experimental error. Turnover frequencies were determined from the linear increase of conversion in time (at conversion levels of about 20-40%). Several samples were taken throughout the reaction without pressure loss.

Table 3.3: *Rhodium catalyzed asymmetric hydroformylation of styrene, applying XantBino (R,R)-(**1**).*[a]

Entry	T [°C]	*p* [bar]	Time [h]	Conversion [%][b]	$Sel_{branched}$ [%][b]	ee [%][c]	TOF [h^{-1}][d]
1[e]	40	10	48	63	91	17 (*R*)	12
2[e]	40	20	72	90	92	13 (*R*)	17
3	60	10	5	54	85	22 (*R*)	260
4	60	20	8	93	87	16 (*R*)	140
5	80	10	3	99	80	27 (*R*)	880
6	80	20	3	100	85	20 (*R*)	720
7	100	10	2	94	56	33 (*R*)	n.d.
8	100	20	2	96	81	24 (*R*)	n.d.

[a]Reaction conditions: 1.55 mL styrene (13.5 mmol), 3.45 mL toluene, [Rh(acac)(CO)$_2$] = 0.9 mM, L:Rh = 1.2:1, substrate:Rh = 1000:1; [b]determined by GC analysis; [c]enantiomeric excess, determined by chiral GC analysis; [d]turnover frequency, defined as (mol substrate converted)·(mol rhodium)$^{-1}$·h^{-1}; [e]preformation time 15 h.

The effect of pressure on the reaction rate is more significant at temperatures of 60 °C and higher. In all cases the initial activity (TOF) is lower at higher pressures. Also lower values for the enantiomeric excess are found at higher pressures. The regioselectivity showed a reverse trend, *viz*. a positive effect of pressure on the regioselectivity to branched product and a negative influence of the reaction temperature. This is more pronounced at a pressure of 10 bar, as the regioselectivity is only 56% at 100 °C. In all cases the enantiomeric excess (ee) was poor, with a maximum of 33% at 100 °C. However, for the first time, a chiral diphosphonite has been applied in the asymmetric hydroformylation of styrene, leading to chiral induction.

No attempts were made to modify the ligand system in order to obtain higher values for the enantiomeric excess. Goertz *et al.* already showed for the asymmetric hydrocyanation, that the introduction of bulky substituents in the 3,3'-positions of the binaphthyl units can lead to higher ee's.[11] Buisman *et al.* observed a similar effect in the asymmetric hydroformylation of styrene, yet with diphosphites derived from less rigid backbones.[26] Furthermore too much steric crowding of these positions led to a significant decrease in enantioselectivity.

Van Rooij *et al.* have proposed a mechanism for the asymmetric hydroformylation of styrene with bulky monophosphites as ligands (Scheme 3.4).[27] With the assumption that the same mechanism is still correct for bidentate ligands such as (*R,R*)-(**1**), coordination of styrene to the metal center takes place in the equatorial plane (**1**). In order to interact with the hydride, a rotation of the substrate into the axial plane is needed (**2** and **6**).

The upper pathway proceeds via a linear alkyl intermediate (**3** and **4**) to yield the linear aldehyde (**5**), whereas the lower pathway ultimately leads to the branched chiral aldehyde (**9**) via a branched alkyl intermediate (**7** and **8**). Intermediate (**8**) is an allyl species; it is thought that the preference of styrene to be converted into the branched aldehyde is related to the formation of this stable allyl intermediate.

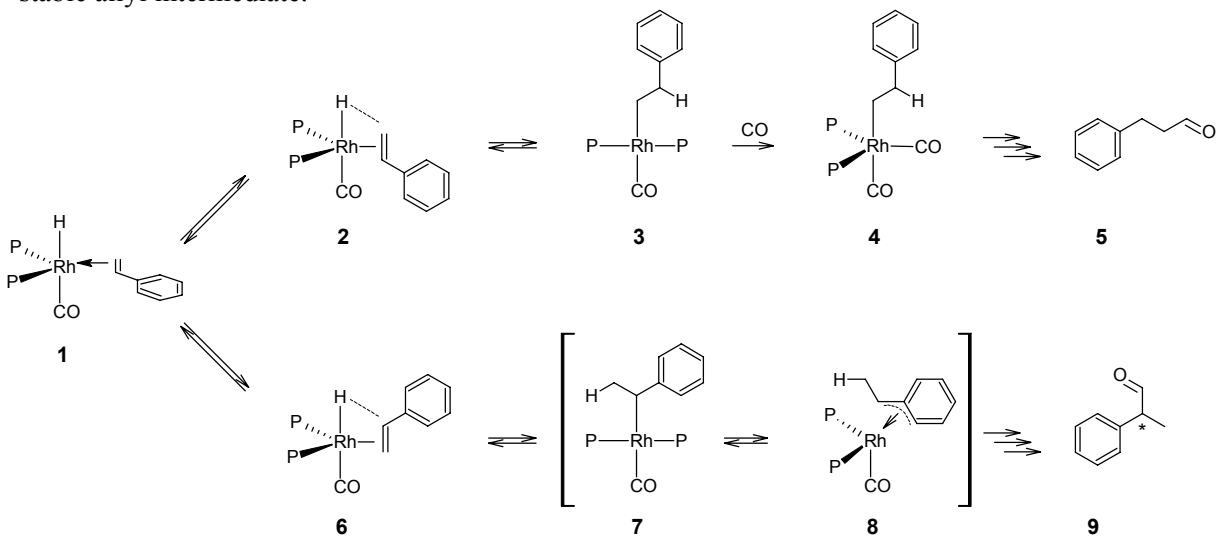

Scheme 3.4: *Proposed mechanism for the hydroformylation of styrene.*

Many systems in asymmetric hydroformylation show decreasing enantioselectivity when the temperature is increased. Therefore many experiments are conducted at low temperature in order to obtain high enantiomeric excesses.[28-30] In the experiments with **1** as the ligand the enantiomeric excess showed a positive dependency on the reaction temperature, as illustrated in Figure 3.8. The ee is lower at higher pressures (*e.g.* entries 3 and 4 vs. 5 and 6 in Table 3.3). Compared to the best systems known in literature the enantiomeric excess with this Rh-XantBino system is low at a maximum of 33% ee under the chosen reaction conditions.

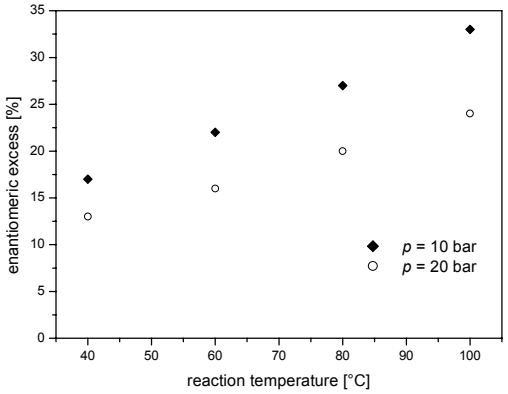

Figure 3.8: *Plot of the positive relationship between the ee and the reaction temperature, at two pressures.*

With the assumption that styrene coordinates in the way described before, it is likely that the two possible diastereomers that lead to the branched aldehyde are derived from the allyl complexes formed, as depicted in Scheme 3.5. The rhodium complex contains a ligand coordinated in a bis-equatorial fashion and in the allyl complex, styrene is coordinated in the axial plane. Furthermore, one should note that this is a simplified model, not considering internal rotations in the styrene moiety. Most probably, chirality is induced immediately when styrene coordinates to the rhodium center (from **1** to **6a** and **6b**). Which of the diastereomers is formed depends on which way the styrene coordinates, either with the benzyl group directed forward (**6a**) or backward (**6b**). When the allyl intermediate is formed (through intermediate **7a** to **8a** or from **7b** to **8b**), the earlier obtained chirality is maintained. These intermediates yield two different enantiomers (**9a** or **9b**) but which of these enantiomers will be formed is unknown. If the temperature dependency for k_1 is not equal to that for k_2 (k_i being the overall rate constant for the reaction steps that convert **8** into **9**), the enantiomeric excess can show a positive temperature dependency, as found for the Rh-XantBino system.

Daley *et al.*[31] very recently reported on the existence of diastereomeric alkoxide intermediates in asymmetric hydrogenation. The coordination of the substrate (an oxaloacetate ketone), which had three coordination positions, coordinated to the ruthenium (*R,R*)-BINAP complex and resulted in three diastereomers.

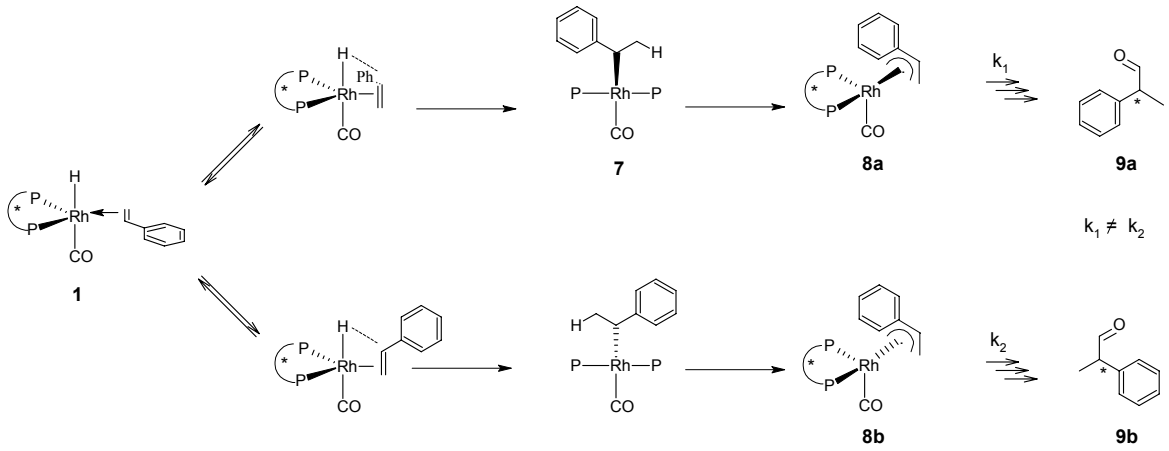

Scheme 3.5: *Overview of the two reaction pathways, each leading to a diastereomer and ultimately to one enantiomer of the branched aldehyde.*

The increase of enantiomeric excess with temperature, typical for a pre-equilibrium mechanism, has been observed earlier, for instance in the asymmetric hydroformylation of 2-butene, as a result of isomerization effects of the substrate rather than specific ligand effects.[32] Studies by Kollár *et al.*[33a] showed that certain catalysts in $Pt/SnCl_2$ catalyzed asymmetric hydroformylation of

styrene gave enantiomeric excess for (*S*)-2-phenylpropanal at low temperatures and enantiomeric excess for (*R*)-2-phenylpropanal at high temperatures. The enantiomeric excess appeared to decrease with temperature, but actually changed sign and the racemic product was formed only at even higher temperatures. NMR studies on these catalysts indicated that there were two species present in a temperature dependent equilibrium. They suggested that different conformations of the ligand resulted in two different species with different rate determining steps.[33b]

Tóth *et al.*[34] reported on several catalytic systems that showed similar strong temperature dependency as earlier reported. Although the structure of the ligands differed significantly in the type of backbone used, similar results were obtained. Therefore, changes in enantiomeric excess were probably caused by diastereomeric intermediates of one single catalytically active chelate conformation, via competing reaction pathways.

In conclusion, a chiral diphosphonite has been applied for the first time in the rhodium catalyzed asymmetric hydroformylation of styrene. The regioselectivity to branched aldehyde was normal at a reaction temperature of 40 °C and showed a negative dependency on temperature. The enantioselectivity reached moderate values, with a maximum of 33% at 100 °C. Further investigations should focus on the modification of the phosphorus substituent groups, varying for instance the steric bulk, as well as on mechanistic studies into the origin of the apparent linear dependency of enantiomeric excess with reaction temperature.

3.4.2 Asymmetric hydrogenation

As a second test reaction to investigate the applicability of the diphosphonite XantBino in asymmetric reactions, based on the literature that has appeared lately on the use of chiral diphosphonites in asymmetric hydrogenation reactions,[7-9] the Rh catalyzed asymmetric hydrogenation of methyl (*Z*)-2-acetamido-cinnamate (***I***) was studied. This substrate is a generally accepted model compound, mimicking the reaction leading to the product L-DOPA. The breakthrough in this research was the introduction of the chiral ligand DIPAMP, leading to 97.5 % enantiomeric excess in the product.[35] For this research, Knowles was rewarded the Nobel Prize in Chemistry in 2002. (Scheme 3.6).

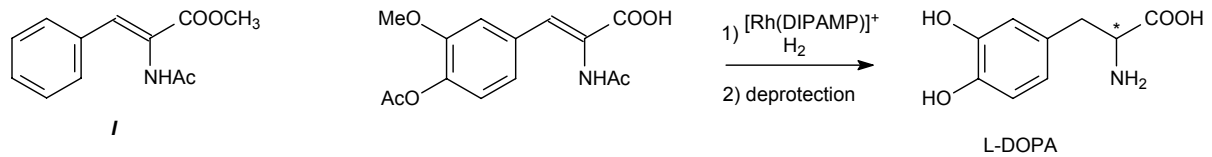

Scheme 3.6: *Schematic representation of substrate **I**, methyl (Z)-2-acetamido-cinnamate, (left) and the synthesis of L-DOPA, catalyzed with the cationic Rh-DIPAMP catalyst (right).*

The catalyst [Rh(cod)(**1**)]BF_4 is prepared in three steps from $RhCl_3 \cdot H_2O$ (Scheme 3.7). The ^{31}P NMR spectrum obtained for this complex was already shown in Figure 3.7.

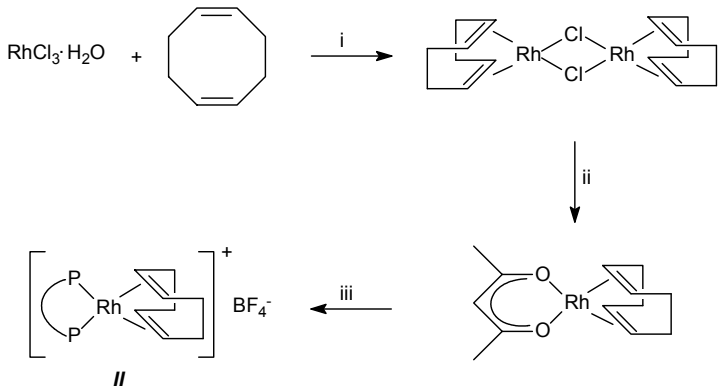

II

Scheme 3.7: *Synthetic route to [Rh(cod)(**1**)]BF_4 (**II**): i) ethanol, Δ, 3 h; ii) acetylacetone, KOH, diethyl ether, -77 °C, 30 minutes; iii) HBF_4, (S,S)-(**1**), diethyl ether, THF, 5 minutes.*

The catalysis was carried out at ambient temperature, with a substrate to rhodium ratio S/Rh of 100:1. Before addition of the substrate, a concentrated solution of ***II*** in methanol was stirred for 3 hours under 1.2 bar of H_2 in order to activate the catalyst. During catalysis a static H_2 pressure (1.2 or 5 bar) was applied. The reaction rate is constant up to 80% conversion, as can be seen from the graph in Figure 3.10 for the reaction with 1.2 bar of H_2, indicating that the catalytic system remains stable and active. Substrate depletion leads to the expected drop in reaction rate at even higher conversions.

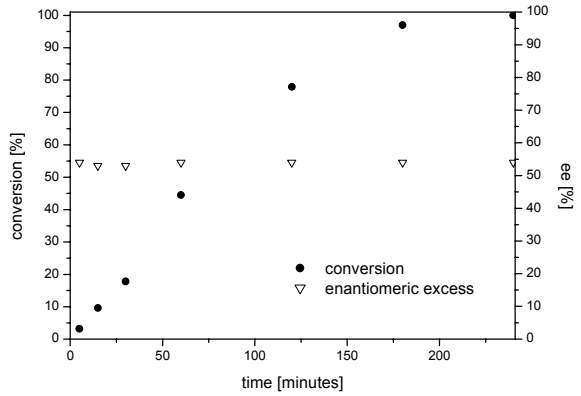

Figure 3.10: *Plots of the conversion (•) and the enantiomeric excess (▽) as a function of time for the reaction of **I** to the desired product, catalyzed by rhodium catalyst **II**. Reaction conditions: p =1.2 bar H_2, T = 25 °C, **I**:Rh = 100:1, 10 mL methanol, 3 h preformation, 4 h reaction time.*

This is in agreement with the generally accepted reaction mechanism for hydrogenation, since the addition of hydrogen to the substrate double bond is the rate limiting step. Up to about 80% conversion, the catalytic activity was constant but rather low under these non-optimized conditions,

with a turnover frequency of about 40 h^{-1}. However, also the data reported by Reetz[7] and Claver[8] suggested similar activities for their catalytic systems. Reetz however used different substrates, so a sound comparison is not possible. The paracyclophane based diphosphonite system employed by Zanotti-Gerosa[9] gave high activities with TON's of about 2000 h^{-1}.

The enantioselectivity of the present [Rh(cod)(**1**)]BF_4 system is promising, with an ee of 54%, which is however still moderate compared to the other diphosphonite systems reported in literature.[7-9] The (*S*)-enantiomer is formed in excess, starting with a catalyst containing (*S,S*)-(**1**). Similar catalytic results were obtained when applying a pressure of 5 bar H_2. After 2 hours of reaction the conversion was 94%, with an ee of 47%. The higher activity is expected since the concentration of hydrogen is evidently increased. No decisive explanation can be given for the lower enantioselectivity at higher H_2 pressure. It might originate from a rate acceleration of the formation of the (*R*)-enantiomer at higher H_2 concentration.

The results obtained with XantBino in the asymmetric hydrogenation are promising, since no optimization of reaction conditions was carried out during these catalytic runs. Further tuning of the reaction conditions as well as the use of other substrates might result in higher ee values.

3.5 Conclusions

In summary, the synthesis of the previously reported ligand XantBino (**1**) has been improved. The coordination chemistry of this ligand has been explored for palladium, platinum and rhodium. The molecular structures for *cis*-[$PdCl_2$(**1**)] and *cis*-[$PtCl_2$(**1**)] have been described, including the odd positioning of the metal atom at a dihedral angle of around 115° out of the ligand plane. The bite angle of the diphosphonite ligand was around 100° in both complexes, unusually small for a xanthene-derived phosphorus ligand. The first application of a chiral diphosphonite in the rhodium catalyzed asymmetric hydroformylation of styrene is reported, leading to high activities with turnover frequencies of up to 1420 h^{-1}. The maximum enantioselectivity obtained was low at 33% at 100°C. In the asymmetric hydrogenation of methyl (*Z*)-2-acetamidocinnamate, rather low activities were found, yet the enantioselectivity was promising, with an enantiomeric excess of 54%, which seems encouraging given the non-optimized reaction conditions.

Acknowledgements

The National Research School Combination for Catalysis (NRSCC) is kindly acknowledged for financial support. OMG is thanked for a generous loan of precious noble metals. Part of this research is carried out together with Jos Paulusse, whose input is highly appreciated for the work that brought this chapter to life. Prof. Carmen Claver (Tarragona, Spain) is thanked for the cooperation that enabled J.P. to do part of this project in her laboratories, supported by a travel grant from the Erasmius Program of the European Union. Jason Tijmensen is thanked for his work on the asymmetric hydrogenation. Scientific discussions with Dr. Rafaël Sablong are appreciated. Crystal structures were determined by Dr. Allison Mills from the group of Prof. Anthony Spek from the University of Utrecht.

3.6 Experimental Section

General. Chemicals were purchased from Aldrich, Acros and Merck and used as received. Synthesis gas (CO/H_2 1:1) was purchased from Carburos Metalicos. All preparations were carried out under an argon atmosphere using standard Schlenk techniques. Solvents were distilled from sodium/benzophenone (THF, diethyl ether, toluene, hexanes and ethanol) or calcium hydride (CH_2Cl_2 and $CDCl_3$) prior to use. All glassware was dried by heating under vacuum. The NMR spectra were recorded on a Varian Mercury 400 spectrometer (^1H, $^{13}C\{^1H\}$, $^{31}P\{^1H\}$). Chemical shift are given in ppm referenced to solvent (^1H, $^{13}C\{^1H\}$) or an 85% aqueous solution of H_3PO_4 ($^{31}P\{^1H\}$). GC spectra were recorded on a Hewlett Packard 5890A Chromatograph, equipped with a 50 m Cyclodex β-I/P column. $PdCl_2(cod)$,[36] $PdCl(CH_3)(cod)$,[37] $PtCl_2(cod)$,[38] $[Rh(cod)Cl]_2$[39] and [Rh(cod)(acac)][40] were prepared according to literature procedures.

(*R*,*R*)-4,5-Bis(dinaphtho[d,f][1,3,2]dioxaphosphepino)-9,9-dimethyl-xanthene (1).
This is a modification of a literature procedure[11]:
4,5-(Bis[bis-diethylamino]phosphonito)-9,9-dimethylxanthene, **I** (2,00 g, 3.58 mmol) and (*R*)-(+)-2,2'-dihydroxy-1,1'-binaphthyl (2,05 g, 7.16 mmol) were dissolved in 50 mL of toluene. A catalytic quantity of tetrazole was added as a protonation agent. The solution was heated to 90°C for 16 hours. Diethylamine formed during reaction was removed twice by applying vacuum. After reaction the solvent was removed *in vacuo* and the remaining crude product was dissolved in 5 mL of CH_2Cl_2 and layered with 20 ml of acetonitrile. The precipitated product was isolated by filtration and washed with 10 mL of acetonitrile. After drying, a yellow powder was obtained as a pure product (0,70 g, 31%). The other enantiomer can be obtained via the same procedure.
^{1}H NMR ($CDCl_3$) δ 7.94 (d, 2H, ^1J = 8.8 Hz, binolH), 7.90 (d, 2H, ^1J = 8.0 Hz, binolH), 7.84 (d, 2H, ^1J = 8.0 Hz, binolH), 7.63 (d, 2H, ^1J = 8.8 Hz, binolH), 7.58 (d, 2H, ^1J = 8.8 Hz, binolH), 7.55 (dd, 2H, ^1J = 8.0 Hz, ^2J = 0.8 Hz, binolH), 7.42 (t, 6H, ^1J = 8.8 Hz, ArH), 7.32 (d, 2H, ^1J = 8.4 Hz, binolH), 7.28 (dquin, 4H, ^1J = 8.0 Hz, ^2J = 1.2 Hz, binolH) 7.18 (d, 2H, ^1J = 8.8 Hz, binolH), 6.92 (d, 2H, ^1J = 8.8 Hz, binolH), 6.90 (d, 4H, ^1J = 7.2 Hz, binolH), 1.79 (s, 6H, $C(CH_3)_2$).
$^{13}C\{^1H\}$ NMR ($CDCl_3$) δ 152.6, 149.9, 149.1, 133.0, 132.5, 131.5, 130.9, 130.4, 129.9, 129.0 (d, $J_{P\text{-}C}$ = 16.8 Hz), 128.5, 128.2 (d, $J_{P\text{-}C}$ = 6.8 Hz), 126.9 (d, $J_{P\text{-}C}$ = 3.8 Hz), 125.8 (d, $J_{P\text{-}C}$ = 19.0 Hz), 124.6 (d, $J_{P\text{-}C}$ = 20.6 Hz), 123.3, 121.9 (d, $J_{P\text{-}C}$ = 5.3 Hz), 34.1 ($C(CH_3)_2$), 31.9 ($C(CH_3)_2$).
$^{31}P\{^1H\}$ NMR ($CDCl_3$) δ 178.0 (s).

***cis*-[$PdCl_2$(1)] (complex 2).**
$PdCl_2(cod)$ (13.2 mg, 46.2 μmol) and (*S,S*)-**1** (38.7 mg, 46.2 μmol) were dissolved in 5 mL of CH_2Cl_2 and stirred for 1 hour at r.t. The solvent was then removed *in vacuo* to leave a light-yellow solid. Yellow block-shaped crystals of complex **2** were grown by slow diffusion of acetonitrile into a solution of dichloromethane.
^{1}H NMR ($CDCl_3$) δ 8.37 (d, 1H, ^1J = 8.8 Hz), 8.20 (d, 1H, ^1J = 8.8 Hz), 8.16 (d, 1H, ^1J = 8.8 Hz), 8.08 (d, 1H, ^1J = 8.8 Hz), 8.03 (t, 1H, ^1J = 8.8 Hz), 8.00 (d, 1H, ^1J = 8.8 Hz), 7.95 (dd, 2H, ^1J = 8.0 Hz, ^2J = 4.8 Hz), 7.89 (d, 1H, ^1J = 8.8 Hz), 7.81 (m, 2H), 7.70 (m, 3H), 7.65 (dt, 1H, ^1J = 8.4 Hz, ^2J = 1.2 Hz), 7.58 (t, 1H, ^1J = 8.8 Hz), 7.56 (t, 2H, ^1J = 8.0 Hz), 7.51 (dd, 1H, ^1J = 7.2 Hz, ^2J = 1.2 Hz), 7.46 (m, 1H), 7.46 (t, 1H, ^1J = 8.0 Hz), 7.34 (m, 2H), 7.23 (m, 2H), 7.21 (t, 1H, ^1J = 6.8 Hz), 7.13 (m, 1H), 7.09 (dd, 1H, ^1J = 6.4 Hz, ^2J = 2.0 Hz), 6.90 (d, 1H, ^1J = 8.8 Hz), 6.09 (d, 1H, ^1J = 9.6 Hz), 1.96 (s 3H, CCH_3), 1.67 (s, 3H, CCH_3).
$^{31}P\{^1H\}$ NMR ($CDCl_3$) δ 143.1 (d, J_{PP} = 46.5 Hz), 137.4 (J_{PP} = 46.5 Hz).
Anal. Calcd for $C_{55}H_{36}Cl_2O_5P_2Pd$: C, 65.01; H, 3.57. Found: C, 65.34; H, 3.63.

***cis*-[$PtCl_2$(1)] (complex 3).**
$PtCl_2(cod)$ (72.3 mg, 193.2 μmol) and (*S,S*)-**1** (172.3 mg, 205.3 μmol) were dissolved in 10 mL CH_2Cl_2 and stirred for 1 hour at r.t. during which period a white solid precipitated. The solvent was then removed *in vacuo* to leave complex **3** as a pure solid. Colorless block-shaped crystals were grown by slow diffusion of acetonitrile (15 mL) into a $CH_2Cl_2/CHCl_3$ solution (5 mL/4 mL) of complex **3**.
^{1}H NMR ($CDCl_3$) δ 8.38 (d, 1H, ^1J = 8.8 Hz), 8.19 (d, 1H, ^1J = 8.8 Hz), 8.14 (d, 1H, ^1J = 8.8 Hz), 8.09 (t, 2H, ^1J = 8.8 Hz), 8.01 (t, 1H, ^1J = 8.8 Hz), 7.94 (dd, 2H, ^1J = 8.0 Hz, ^2J = 4.8 Hz), 7.89 (d, 1H, ^1J = 8.8 Hz), 7.79 (d, 2H, ^1J = 8.4 Hz), 7.68 (m, 4H), 7.59 (d, 1H, ^1J = 8.8 Hz), 7.56 (t, 2H, ^1J = 8.0 Hz), 7.50 (t, 2H, ^1J = 7.6 Hz), 7.45 (t, 2H, ^1J = 7.2 Hz), 7.32 (d, 2H, ^1J = 6.4 Hz), 7.22 (m, 2H), 7.12 (d, 1H, ^1J = 8.8 Hz), 7.08 (d, 1H, ^1J = 6.4 Hz), 6.88 (d, 1H, ^1J = 8.8 Hz), 6.03 (d, 1H, ^1J = 9.6 Hz), 1.96 (s 3H, CCH_3), 1.67 (s, 3H, CCH_3).

$^{31}P\{^{1}H\}$ NMR ($CDCl_3$) δ 113.1 (d, $^{1}J_{Pt\text{-}P}$ = 5052 Hz, $^{2}J_{PP}$ = 17.0 Hz), 110.6 (d, $^{1}J_{Pt\text{-}P}$ = 4948 Hz, $^{2}J_{PP}$ = 17.0 Hz). Anal. Calcd for $C_{55}H_{36}Cl_2O_5P_2Pt$: C, 59.79; H, 3.28. Found: C, 59.84; H, 3.42.

[Rh(cod)(1)]BF_4.
This is a modification of a literature procedure.[41] [Rh(cod)(acac)] (0.047 g, 0.15 mmol)[41] was dissolved in 2 mL THF. HBF_4 (54% solution in diethyl ether) (0.053 g, 0.60 mmol) was added. During addition the solution coloured darker. (*R,R*)-**1** (0.126 g, 0.15 mmol) was dissolved in 2 mL THF and then added to the solution, yielding an orange suspension. Approximately 20 mL of diethyl ether was added and the mixture was stirred vigorously for 5 minutes. The yellow precipitate formed, was isolated and washed with 10 mL of diethyl ether. Volatiles were removed *in vacuo* to leave a yellow/orange solid. Yield 68% (0.14 g, 0.10 mmol).
$^{31}P\{^{1}H\}$ NMR ($CDCl_3$) δ 169.3 (dd, $J_{Rh\text{-}P}$ = 219 Hz, $J_{P\text{-}P}$ = 24 Hz.), 161.1 (dd, $J_{Rh\text{-}P}$ = 216 Hz, $J_{P\text{-}P}$ = 24 Hz.).

Hydroformylation of styrene.
Reactions were performed using a stainless steel autoclave (75 mL) equipped with an inner glass beaker. Styrene was filtered over neutral alumina before use to remove peroxides. Generally $Rh(acac)(CO)_2$ (3.5 mg, 13.5 μmol) and **1** (1.2 eq.) were both dissolved in 5 mL of toluene and the combined solution was brought into the preheated autoclave. which was thereafter pressurized to 20 bar of synthesis gas. After the appropriate preformation time, the autoclave was depressurized and the substrate solution, containing 1-octene (1.55 mL, 13.5 mmol) in toluene (3.45 mL) was added and 20 bar of synthesis gas was applied. During catalysis, samples were withdrawn without pressure loss for GC analysis. After reaction, the autoclave was cooled, depressurized and the reaction mixture taken out. Oxidation of the aldehydes to the carboxylic acids was done directly afterwards, to prevent racemization and to allow for analysis by chiral GC.

Crystal structure determination of 2 and 3.
The data were collected on a Nonius Kappa CCD diffractometer with rotating anode The structures were solved by direct methods using SHELXS97,[42] and refined on *F*2 by least-squares procedures using SHELXL97.[43] All non-hydrogen atoms were refined with anisotropic displacement parameters. Hydrogen atoms were constrained to idealized geometries and allowed to ride on their carrier atoms with an isotropic displacement parameter related to the equivalent displacement parameter of their carrier atoms. Structure validation and molecular graphics preparation were performed with the PLATON package.[44] Crystal data are given in Table 3.4.

Table 3.4: *Selected crystallographic data for complexes **2** and **3**.*

	2	**3**
Formula	$C_{55}H_{36}Cl_2O_5P_2Pd$	$C_{55}H_{36}Cl_2O_5P_2Pt$
FW ($g \cdot mol^{-1}$)	1016.08	1104.76
Crystal size (mm)	0.06×0.12×0.30	0.06×0.24×0.32
Crystal system	Orthorhombic	Orthorhombic
Space group	$P2_12_12_1$ (no. 19)	$P2_12_12_1$ (no. 19)
a (Å)	11.3183(1)	11.2545(1)
b (Å)	17.4368(1)	17.1813(1)
c (Å)	27.4181(3)	27.4069(2)
V ($Å^3$)	5411.10(8)	5299.59(7)
Z	4	4
d_{calc} ($g\ cm^{-3}$)	1.247	1.385
μ (Mo-Kα) (mm^{-1})	0.544	2.583
T (K)	150	150
Total reflections	59674	60343
Unique reflections (R_{int})	12279 (0.064)	12174 (0.062)
wR_2 (F^2) (all data)	0.0975	0.0749
F(000)	2064	2192

$R_{int} = \sum [|F_o^2 - F_o^2(\text{mean})|]/\sum [F_o^2]$; $wR(F^2) = [\sum [w(F_o^2 - F_c^2)^2]/\sum [w(F_o^2)^2]]^{1/2}$; $R(F) = \sum (||F_o| - |F_c||)/\sum |F_o|$

3.7 References

Parts of the work described in this chapter have been published:
J.I. van der Vlugt, J.H.J. Paulusse, J.A. Tijmensen, C. Claver, A.M. Mills, A.L. Spek and D. Vogt, *manuscript in preparation*.
R. van Duren, J.P.J. Huijbers, J.I. van der Vlugt, A.M. Mills, A.L. Spek and D. Vogt, *manuscript in preparation*.

1 a) R. Stern, A. Hischauer and L. Sajus, *Tetrahedron Lett.*, **1973**, *35*, 3247; b) C. Salomon, G. Consiglio, C. Botteghi and P. Pino, *Chimia*, **1973**, *27*, 215.
2 N. Sakai, S. Mano, K. Nozaki and H. Takaya, *J. Am. Chem. Soc.*, **1993**, *115*, 7033.
3 a) G.J.H. Buisman, L.A. van der Veen, A. Klootwijk, W.G.J. de Lange, P.C.J. Kamer, P.W.N.M. van Leeuwen and D. Vogt, *Organometallics*, **1997**, *16*, 2929; b) J.E. Babin and G.T. Whiteker (to Union Carbide) U.S. Pat. 5,491,266, **1996** [*Chem. Abstr.,* **1993**, *119*, 159872]; c) J.E. Babin and G.T. Whiteker (to Union Carbide) WO 93/03939, **1993** [*Chem. Abstr*., **1993**, *119*, 159872].
4 R. Ewalds, E.B. Eggeling, A.C. Hewat, P.C.J. Kamer, P.W.N.M. van Leeuwen and D. Vogt, *Chem. Eur. J.*, **2000**, *6*, 1496.
5 a) M.T. Reetz and M. Pastó, *Tetrahedron Lett.*, **2000**, *41*, 3315; b) M. Laly, R. Broussier and B. Gautheron, *Tetrahedron Lett.*, **2000**, *41*, 1183.
6 For a recent review see: J. Ansell and M. Wills, *Chem. Soc. Rev.*, **2002**, *31*, 259.
7 a) M.T. Reetz, D. Moulin and A. Gosberg, *Org. Lett.*, **2001**, *3*, 4083; b) M.T. Reetz, A. Gosberg, R. Goddard and S.-H. Kyung, *Chem. Commun.*, **1998**, 2077.
8 A. Zanotti-Gerosa, C. Malan and D. Herzberg, *Org. Lett.*, **2001**, *3*, 3687.
9 C. Claver, E. Fernandez, A. Gillon, K. Heslop, D.J. Hyett, A. Martorell, A. G. Orpen and P.G. Pringle, *Chem. Commun.*, **2000**, 961.
10 A. Martorell, R. Naasz, B.L. Feringa and P.G. Pringle, *Tetrahedron: Asymmetry*, **2001**, *12*, 2497.
11 W. Goertz, P.C.J. Kamer, P.W.N.M. van Leeuwen and D. Vogt, *Chem. Eur. J.*, **2001**, *7*, 1614.
12 M. Kranenburg, Y.E.M. van der Burgt, P.C.J. Kamer, P.W.N.M. van Leeuwen, K. Goubitz and J. Fraanje, *Organometallics*, **1995**, *14*, 3081.
13 S. Agbossou, M.C. Bonnet, F. Dahan and I. Tkatchenko, *Acta Cryst.*, **1989**, *C45*, 1149.
14 A. Karaçar, M. Freytag, P.G. Jones, R. Bartsch and R. Schmutzler, *Z. Anorg. Allg. Chem.*, **2001**, *627*, 1571.
15 L.A. van der Veen, M.D.K. Boele, F.R. Bergman, P.C.J. Kamer, P.W.N.M. van Leeuwen, K. Goubtiz, J. Fraanje, H. Schenk and C. Bo, *J. Am. Chem. Soc.*, **1998**, *120*, 11616.
16 M.A. Zuideveld, B.H.G. Swennenhuis, M.D.K. Boele, Y. Guari, G.P.F. van Strijdonck, J.N.H. Reek, P.C.J. Kamer, K. Goubitz, J. Fraanje, M. Lutz, A.L. Spek and P.W.N.M. van Leeuwen, *J. Chem. Soc., Dalton Trans.*, **2002**, 2308.
17 J. Yin and S.L. Buchwald, *J. Am. Chem. Soc.*, **2002**, *124*, 6043.
18 C.J. Cobley and P.G. Pringle, *Inorg. Chim. Acta*, **1997**, *265*, 107.
19 P.S. Pregosin and S.N. Sze, *Helv. Chim. Acta*, **1978**, *61*, 1848.
20 C. Kunze, D. Selent, I. Neda, M. Freytag, P.G. Jones, R. Schmutzler, W. Baumann and A. Börner, *Z. Anorg. Allg. Chem.*, **2002**, *628*, 779.
21 L. Manojlović-Muir, I.R. Jobe, B.J. Maya and R.J. Puddephatt, *J. Chem. Soc., Dalton Trans.*, **1987**, 2117.
22 M.E. Squires, D.J. Sardella and L.B. Kool, *Organometallics*, **1994**, *13*, 2970.
23 a) L. Dahlenburg, S. Mertel, *J. Organomet. Chem.*, **2001**, *630*, 221; b) L. Dahlenburg, C. Becker, J. Höck and S. Mertel, *J. Organomet. Chem.*, **1998**, *564*, 155.
24 R. Kumar, R.J. Puddephatt and F.R. Fronczek, *Inorg. Chem.*, **1990**, *29*, 4850.
25 S.P. Shum, S.D. Pastor and G. Rihs, *Inorg. Chem.*, **2002**, *41*, 127.
26 G.J.H. Buisman, L.A. van der Veen, A. Klootwijk, W.G.J. de Lange, P.C.J. Kamer, P.W.N.M. van Leeuwen and D. Vogt, *Organometallics*, **1997**, *16*, 2929.
27 A. van Rooij, P.C.J. Kamer and P.W.N.M. van Leeuwen, *J. Organomet. Chem.*, **1997**, *535*, 201.
28 S. Cserépi-Szücs, and J. Bakos, *J. Chem. Soc., Chem. Commun.*, **1997**, 635.
29 P. Uriz, E. Fernández, N. Ruiz and C. Claver, *Inorg. Chem. Commun.*, **2000**, *3*, 515.
30 M. Diéguez, M.M. Pereira, A.M. Masdeu-Bultó, C. Claver and J.C. Bayón, *J. Mol. Cat. A: Chem.*, **1999**, *75*, 111.
31 C.J.A. Daley and S.H. Bergens, *J. Am. Chem. Soc.*, **2002**, *124*, 3680.

32 P. Haelg, G. Consiglio and P. Pino, *J. Organomet. Chem.*, **1985**, *296*, 281.

33 a) L. Kollár, J. Bakos, I. Tóth and B. Heil, *J. Organomet. Chem.*, **1988**, *350*, 277; b) L. Kollár, J. P. Sándor and G. Szalontai, *J. Mol. Cat. A: Chem.*, **1991**, *67*, 191; c) L. Kollár, T. Kégl and J. Bakos, *J. Organomet. Chem.*, **1993**, *453*, 155.

34 a) I. Tóth, I. Guo and B.E. Hanson, *Organometallics*, **1993**, *12*, 848; b) I. Tóth and B.E. Hanson, *Organometallics*, **1993**, *12*, 1506.

35 a) W.S. Knowles, M.J. Sabacky, B.D. Vineyard and D.J. Weinkauff, *J. Am. Chem. Soc.*, **1975**, *97*, 2567; b) W.S. Knowles and M.J. Sabacky, *J. Chem. Soc., Chem. Commun.*, **1968**, 1445.

36 D.R. Drew and J.R. Doyle, *Inorg. Synth.*, **1972**, *13*, 52.

37 F.T. Ladipo and G.K. Anderson, *Organometallics*, **1994**, *13*, 303.

38 H.C. Clark and L.E. Manzer, *J. Organomet. Chem.*, **1973**, *59*, 411.

39 J. Chatt and L.M. Venanzi, *J. Chem . Soc.*, **1957**, 4735.

40 R. Cramer, *J. Am. Chem.Soc.*, **1964**, *60*, 217.

41 J.M. Brown, P.A. Chaloner, A.G. Kent, B.A. Murrer, P.N. Nicholson, D. Parker and P.J. Sidebottom, *J. Organomet. Chem.*, **1981**, *216*, 263.

42 G.M. Sheldrick, SHELXS97; University of Göttingen, Germany, **1997**.

43 G.M. Sheldrick, SHELXL97; University of Göttingen, Germany, **1997.**

44 A.L. Spek, PLATON, A Multipurpose Crystallographic Tool; Utrecht University, The Netherlands, **2002**.

4

A New Class of Diphosphine Ligands Derived from Bisphenol A

Abstract *Easily accessible diphosphine compounds **1-4** based on Bisphenol A derived backbones, generally referred to as BPphos, are prepared, as well as compound **5** based on a terphenyl backbone, Terphos. A straightforward two-step synthetic route is employed to obtain these new compounds in good yields from cheap starting materials. X-ray crystal structures, showing the solid state conformation of the diphosphines **1-3** and **5** as well the phosphine oxide of ligand **2** (**6**·H_2O) are described. In the latter structure the oxo groups form hydrogen bonds with a water molecule acting as a template, thereby pre-organizing the phosphorus atoms. With ligand **2** derived from 1,1-bis(4-hydroxyphenyl)cyclohexane, as a specific example of this new family of ligands, the coordination to palladium, platinum and rhodium is studied in detail. X-ray crystal structures are determined for the dimeric face-to-face macrocyclic complexes **8**,* trans,trans-*[{PdCl(CH_3)(μ-**2**)}$_2$], **9**,* trans,trans-*[{$PtCl_2$(μ-**2**)}$_2$] and **10**,* trans,trans-*[{RhCl(CO)(μ-**2**)}$_2$]. Ligand **5** is shown to coordinate as a chelating bidentate ligand to form complex **11**,* cis-*[$PtCl_2$(**5**)], which is also structurally characterized. All ligands are applied in the rhodium catalyzed hydroformylation of 1-octene, to serve as a first example for their use in homogeneous catalysis. Under non-optimized conditions regioselectivities are low so far but activities are high with turnover frequencies of up to 3400 h^{-1} for ligand **5**, Terphos. In situ high pressure NMR and IR spectroscopy revealed the preference of an equatorial-axial coordination in the Rh(H)(CO)$_2$(**5**) species.*

4.1 Introduction

Homogeneous catalysis has proven to be a very powerful tool for the synthesis of various intermediates and fine chemicals.[1] The success of homogeneous transition metal catalysts strongly depends on the ligands used. A large number of the ligands applied in such reactions bear two phosphorus moieties since these atoms strongly coordinate to a wide range of transition metals. Accessibility to a wide range of ligand classes for different reactions is crucial. Moreover, these ligands should be modular and made from readily available materials. One focal point in both academia as well as in industry are diphosphine ligands.[2,3] Most of the currently available ligands lack one or more of these points mentioned above. The objective of the research described in this chapter therefore was to build up a new class of phosphorus containing compounds based on commercially available materials, to investigate their coordination towards palladium, platinum and rhodium precursors and to apply them in the rhodium catalyzed hydroformylation as a test-case of their potential for homogeneous catalysis.

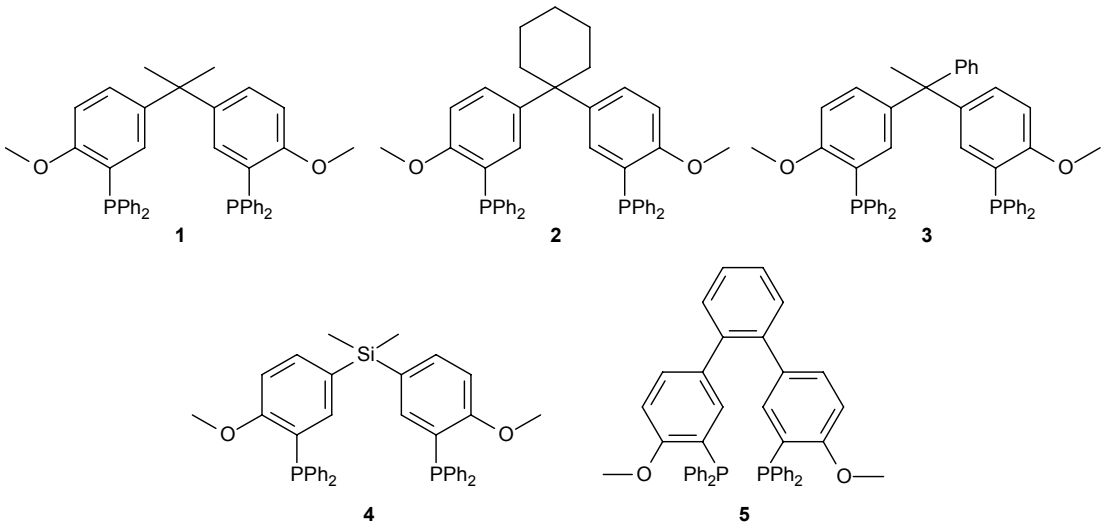

Figure 4.1: *Representation of the compounds used in this chapter.*

Bisphenol A was selected as a hitherto neglected yet promising starting material for the development of this new modular ligand class.[4] A wide range of these bisphenols is commercially available at low cost since they are used as components in epoxy resins.[5] Generic structures are easily available by simple acid-catalyzed condensation of a ketone with two molecules of a phenol. Based on these versatile compounds a simple straightforward two-step synthetic route was employed to obtain new phosphorus containing compounds, generally called BPphos. The coordination of these ligands towards palladium, platinum and rhodium is investigated, as well as the rhodium catalyzed hydroformylation of 1-octene.

The chosen synthetic approach is fundamentally different from the limited amount of earlier work dedicated to the synthesis and use of ligands based on Bisphenol A derived backbones. The approach by Arena *et al*. utilizes the phenolic OH-groups creating diphosphinites and diphosphites that are capable of forming metallamacrocycles.[6] The group of Bauer published a methodology of self-assembly, creating phosphite-bridged macrocycles.[7] Failla[8] and later Singh[9] as well have reported on the formation of phosphonate type compounds with Bisphenol A derived skeletons. The principal use of these molecules however is in the creation of macrocyclic hosts rather than in coordination chemistry and catalysis. Also their application as functional monomers for dental repair has been described.[10]

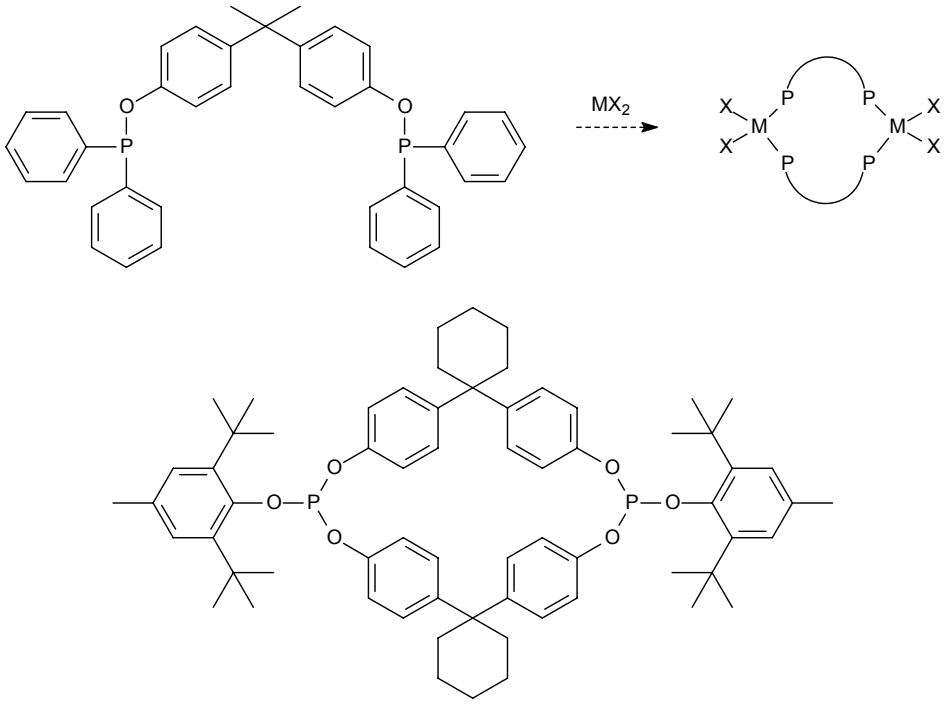

Figure 4.2: *Illustration of the systems described by Arena[6] and Bauer.[7]*

4.2 Synthesis

The first step in the synthesis of the BPphos family is the protection of the phenolic OH-groups by methylation with MeI, with isolated yields of about 80%. Subsequently, selective *ortho*-lithiation of both phenyl rings followed by reaction with an appropriate reagent, in this case $ClPPh_2$, led to the desired diphosphine compounds. The details of the reaction steps are given in Scheme 4.1.

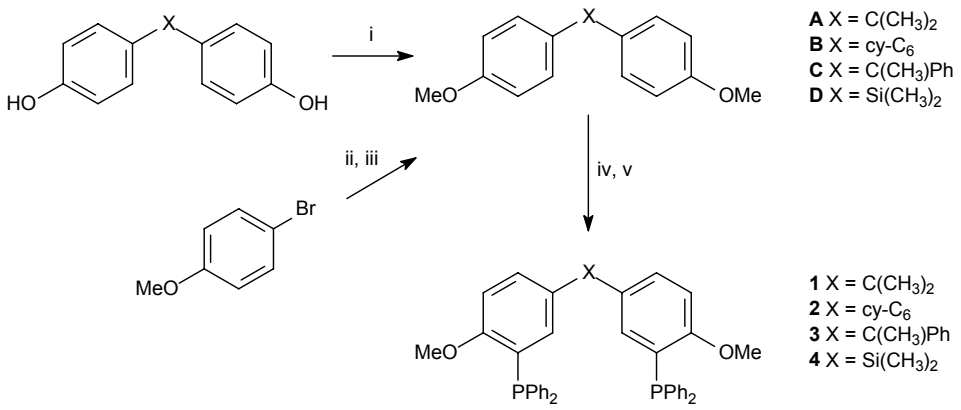

Scheme 4.1: *Synthetic methodology to compounds **1-4**: i) MeI, K_2CO_3, acetone, reflux 16 h, 85%; ii)* n-*BuLi, TMEDA, -15 °C, diethyl ether, 16 h (**A-C**); iii) 0.5 molar equivalents $SiCl_2(CH_3)_2$, -78 °C (1 min.), then r.t. (16 h), 80% (**D**); iv)* n-*BuLi, -78 °C, THF, 15 min; v) $ClPPh_2$, hexanes, 0 °C, 16 h, 60%.*

Filtration and evaporation of the solvent followed by washing of the crude product with a polar solvent such as methanol or acetonitrile afforded the pure compounds in overall yields of 40-50%. Using this method, compounds **1** to **3** based on derivatives of the Bisphenol A backbone were obtained. Furthermore, the silicon derivative **4** was synthesized in good yield starting from 4-bromoanisole and $SiCl_2(CH_3)_2$ via a modified two-step procedure. Compounds **1-4** were fully characterized by ^{1}H, ^{13}C and ^{31}P NMR spectroscopy, as well as by elemental analysis.

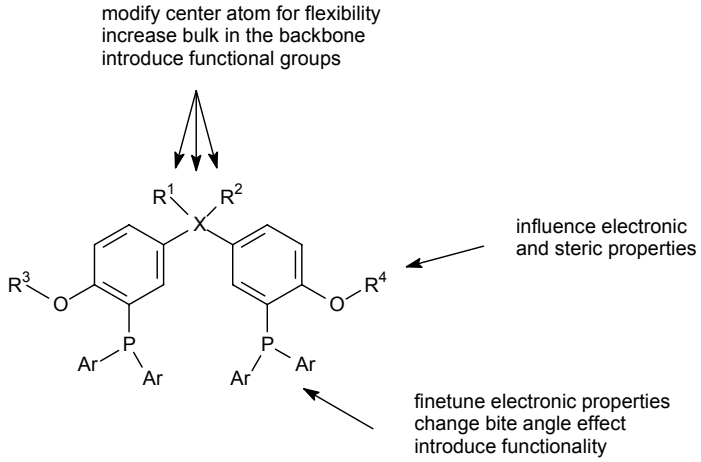

Figure 4.3: *Schematic picture indicating the modular approach possible with Bisphenol A backbones.*

There is high degree of modularity possible in our approach. Several derivatives of Bisphenol A with different center atoms and additional functional groups are commercially available. Possibly the protecting group can be altered for fine-tuning. This modular approach allows for variation in

rigidity, steric bulk and electronic properties of the ligands. Introduction of other phosphorus containing groups is also an option, leading to for instance diphosphonites. Applying the same general method also diphosphine compound **5** (Terphos) based on a terphenyl backbone was successfully synthesized in similar yield (Scheme 4.2). Both starting materials for this compound, *viz*. 1,2-dibromobenzene and 4-bromoanisole, are commercially available.

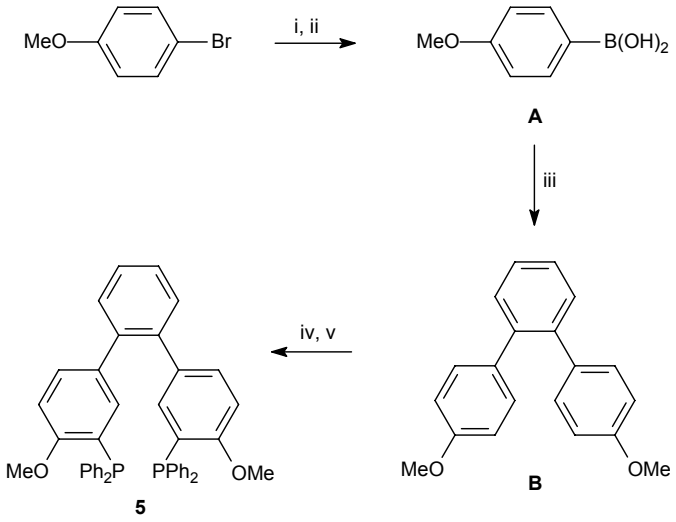

Scheme 4.2: *Synthetic route to compound* ***5:*** *i)* t-*BuLi, Et_2O, -60 °C, 15 min; ii) $B(OMe)_3$, -60 °C, 16 h, 74%; iii) 1,2-dibromobenzene, Na_2CO_3, $Pd(PPh_3)_4$, DME, H_2O, Δ, 16 h, 85%; iv)* n-*BuLi, TMEDA, -40 °C, diethyl ether, 16 h; v) $ClPPh_2$, hexanes, 0 °C, 16 h, 65%.*

The boronic acid of 4-bromoanisole was prepared using known synthetic procedures.[11a-c] The terphenyl backbone was synthesized via Pd catalyzed Suzuki-coupling.[11d-f] For this compound **B**, Blake *et al.* reported a yield of 66% using $Ba(OH)_2$ as the base.[12] The yield of this particular reaction could be improved to 85% using Na_2CO_3 as the base. Selective *ortho*-lithiation on both the outer phenyl rings followed by reaction with $ClPPh_2$ yielded the diphosphine ligand. Work up to obtain the product mainly consisted of removal of solvent *in vacuo* and washing of the crude product with methanol. Also this compound was fully characterized using spectroscopic techniques as well as elemental analysis.

Compounds **1**-**3** and **5** could be crystallized from either hot 1-propanol or acetonitrile to yield single crystals, suitable for X-ray structure analysis. Since the molecular structures for compounds **1**-**3** are nearly identical, only the molecular structure of compound **2** is depicted in Figure 4.4, together with the molecular structure of compound **5**, while selected bond lengths and bond angles for all compounds are summarized in Table 4.1.

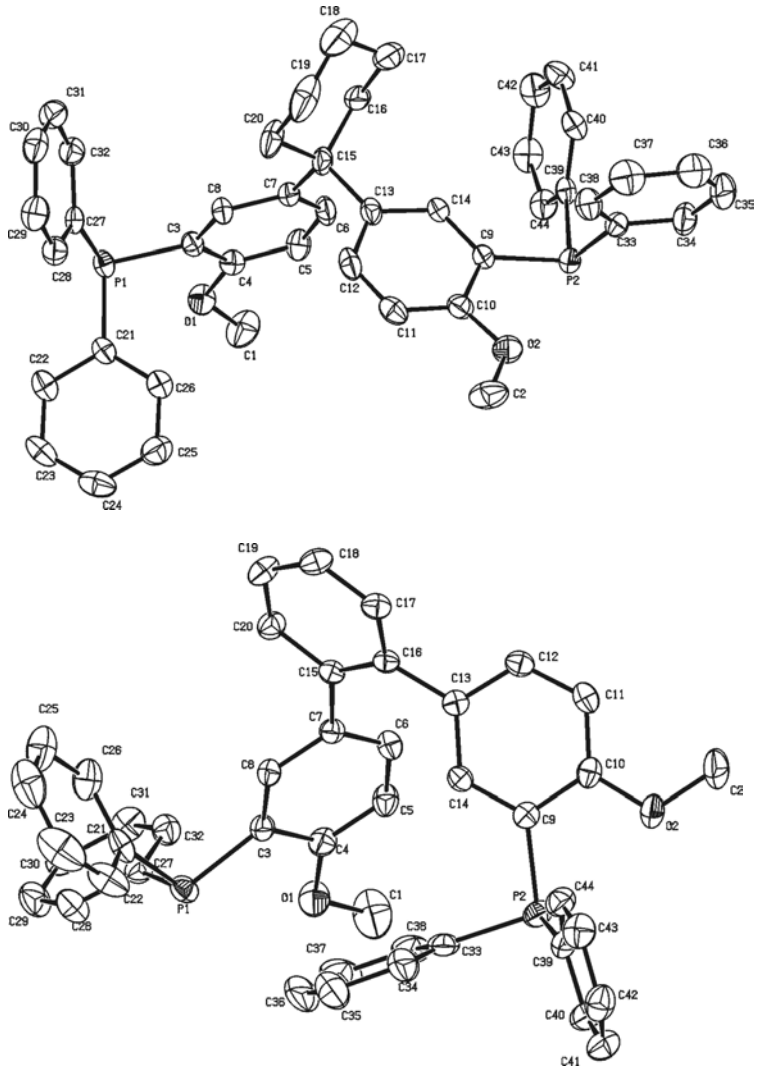

Figure 4.4: *ORTEP representation of compounds **2** (top) and **5** (bottom). Displacement ellipsoids are drawn at the 50% probability level. Hydrogen atoms are omitted for clarity.*

Because of the rotational freedom of the aromatic rings in both backbones, the diphenylphosphine groups are not constrained to any particular mutual orientation. The structure of compound **2** shows approximate C_2 symmetry. The sum of all angles around each phosphorus atom is about 305º. The through-space P_1-O_1 and P_2-O_2 distances are around 2.8-2.9 Å. The intramolecular P-P distance in this structure is found to be 9.7664(8) Å.

In compound **5**, the two peripheral aromatic rings are being tilted at angles of 48.22º and 49.70º with respect to the central ring. The molecule does not possess C_2 symmetry, since the two diphenylphosphino substituents are positioned at one side of the backbone, pointing in the same direction. The through-space intramolecular P-P distance in this conformation of **5** is 7.2841(8) Å.

The dihedral angles between the aromatic rings in the backbone are calculated to be 115.8° and 144.4° giving rise to the different spatial arrangements of the phosphorus atoms.

Table 4.1: *Selected bond lengths and angles for compounds **1-3** and **5**.*

	1	**2**	**3**	**5**
		Bond lengths (Å)		
P_1-C_3	1.8484(15)	1.840(2)	1.8354(16)	1.8322(19)
P_2-C_9	1.8428(16)	1.845(2)	1.8385(17)	1.8362(19)
O_1-C_1	1.429(2)	1.431(3)	1.413(3)	1.431(3)
O_1-C_4	1.374(2)	1.370(2)	1.375(2)	
O_2-C_2	1.429(3)	1.425(3)	1.424(2)	1.433(3)
O_2-C_{10}	1.372(2)	1.372(2)	1.376(2)	
		Angles (°)		
C_1-O_1-C_4	117.64(13)	117.52(17)	118.25(14)	117.83(18)
C_2-O_2-C_{10}	118.26(14)	117.86(16)	117.61(14)	116.34(16)
P_1-C_3-C_4	118.25(11)	118.01(14)	116.89(12)	119.45(14)
P_2-C_9-C_{10}	117.17(13)	118.72(15)	116.99(13)	117.60(13)
C_7-C_{15}-C_{13}	111.30(13)	106.96(14)	110.23(13)	
C_7-C_{15}-C_{16}				124.69(16)

4.3 Coordination Chemistry

4.3.1 BPphos family

Compound **2** was chosen as a representative example for the new family of BPphos compounds. To obtain the corresponding phosphine oxide, compound **2** was reacted with hydrogen peroxide, yielding compound **6**. In the ^{31}P NMR spectrum a singlet was observed at δ = 27.7 ppm, which is a normal value for diphenylphosphine oxides. Single crystals, suitable for X-ray analysis, were grown from a THF solution and from the crystallographic study the molecular structure as depicted in Figure 4.5 was obtained. Selected bond lengths and bond angles are listed in Table 4.2.

The structure for compound **6** represents the corresponding phosphine oxide of **2**, however with an additional molecule of water present in the asymmetric unit cell. There is hydrogen bonding between the oxo groups of compound **6** and the hydrogen atoms of the water molecule. The O-H…O(P) contacts are almost equivalent with H-O(P) bond lengths of 2.00 Å on average, O_5-O(P) distances of 2.83 Å on average and O_5-H-O(P) angles of 166.3º (P_1) and 168.0° (P_2), respectively.

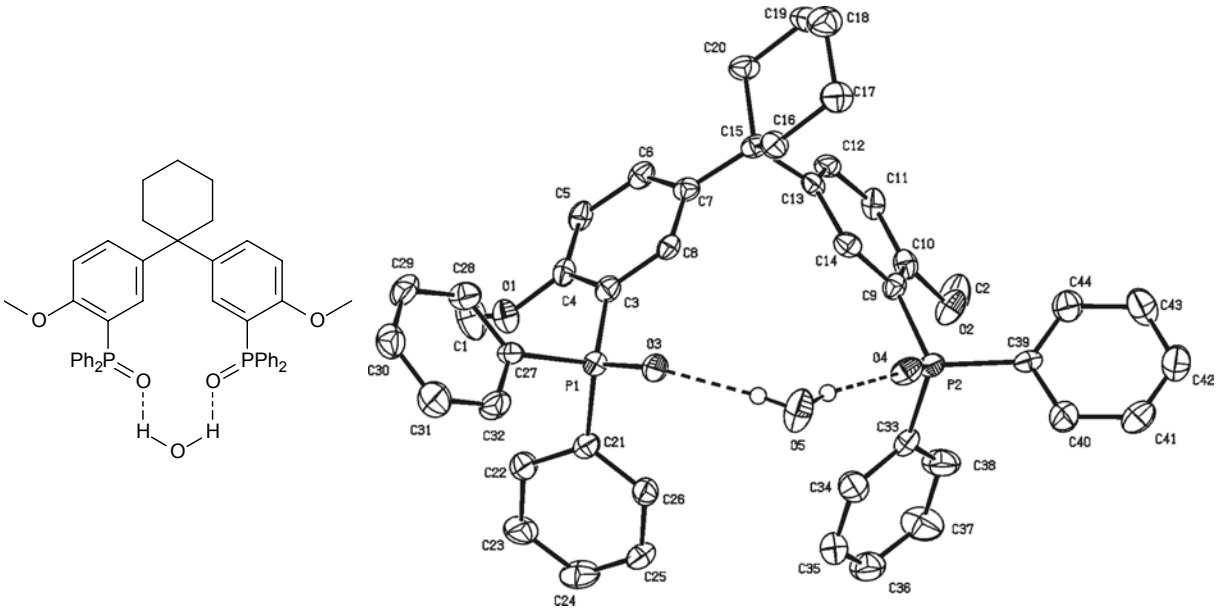

Figure 4.5: *ORTEP representation of compound* ***6***$\cdot H_2O$*. Displacement ellipsoids are drawn at the 50% probability level. All hydrogen atoms, except those of the water molecule, are omitted for clarity.*

The phosphorus atoms have a nearly perfect tetrahedral environment, as evidenced by the averaged O-P-C angles of 110.0° and C-P-C angles of 105.2º and 110.0°. Furthermore, the orientation of the two phosphorus atoms is dramatically altered relative to the structure for the free ligand (*vide supra*). Due to the template effect of the water molecule, both phosphorus atoms are located at the same side of the molecule, with the oxygen atoms pointing towards one another. This leads to a decreased P_1-P_2 distance of 6.579(2) Å. The bond lengths between the phosphorus and carbon atoms of the ligand backbone (P_1-C_3 and P_2-C_9) are slightly shorter, compared to compound **2**, due to a decrease of electron density on the phosphorus atoms in the oxidized state. The P-O bond lengths for both phosphine-oxide moieties are similar to those found in triphenylphosphine oxide hemihydrate[13] and tri-*p*-tolylphosphine oxide[14] but slightly lower in comparison with the mono-oxide of BINAP.[15]

It is well known that the coupling constant $J_{Se\text{-}P}$, observed in the ^{31}P NMR spectrum, of the analogous selenide is an indication of the basicity of the phosphine moiety. Compound **2** was therefore reacted with selenium, to convert the diphosphine into the corresponding diselenide **7**. The reaction proceeded smoothly at 60 °C in toluene within 15 minutes.

Table 4.2: *Selected bond lengths and angles for compound* ***6***$\cdot H_2O$.

Bond lengths (Å)		Angles (°)	
P_1-C_3	1.810(7)	C_1-O_1-C_4	117.4(6)
P_2-C_9	1.803(9)	C_2-O_2-C_{10}	118.9(6)
O_1-C_1	1.427(9)	P_1-C_3-C_4	125.4(5)
O_1-C_4	1.378(8)	P_2-C_9-C_{10}	125.6(5)
O_2-C_2	1.416(9)	C_7-C_{15}-C_{13}	105.1(5)
O_2-C_{10}	1.383(9)	O_3-P_1-C_3	110.1(3)
P_1-O_3	1.491(4)	O_4-P_2-C_9	109.9(3)
P_2-O_4	1.492(5)		

The ^{31}P NMR spectrum of **7** showed a singlet at δ = 37.6 ppm, flanked with ^{77}Se satellites and a coupling constant $J_{Se\text{-}P}$ of 726 Hz (in CH_2Cl_2). This value is normal for diphenylphosphine derived selenides, as reported in literature.[16,17] For triphenylphosphine selenide a coupling constant $J_{Se\text{-}P}$ of 732 Hz is reported. Compared to this benchmark ligand, the slightly lower value of **7** is most likely due to a higher σ-donor ability, originating from the methoxy-groups *ortho* of the phosphine moieties. Pinnell *et al.* have reported a value of 708 Hz for tris(4-methoxyphenyl)phosphine selenide.[18]

To evaluate the behaviour of the novel ligands towards various transition metals, ligand **2** was used as a specific example of this family. Its coordination chemistry with palladium, platinum and rhodium precursors is discussed, both by NMR spectroscopy as well as by X-ray crystallography. For a structural comparison within this chapter, some complexes with ligand **5** have also been characterized. Central issue is the assessment of the coordination mode of the ligand, *i.e.* monodentate or bidentate, via the phosphorus moieties. Coordination via the oxygen atoms of the methoxy groups present is not expected. Rauchfuss *et al.* already investigated the monophosphine diphenylphosphinoanisole and concluded that coordination of a metal such as palladium and platinum takes place only through phosphorus.[19] Marty *et al.* have claimed the formation of a monomeric *trans*-coordinated Pd complex using 3,3'-bis(diphenylphosphinito)methylbenzene, which is structurally related to our compounds **1**-**4**.[20]

After reaction of **2** with $PdCl_2$(cod) under very dilute conditions, 0.01 mM in both ligand and metal precursor, only a singlet at δ = 17.8 ppm was observed in the ^{31}P NMR spectrum. This chemical shift is indicative of a *trans*-coordination of the phosphorus atoms in the complex.[21] To confirm this, $PdCl(CH_3)$(cod) was used as well for the same reaction. In the ^{31}P NMR spectrum of the product from this reaction, a singlet was present at δ = 25.0 ppm. In the corresponding ^{1}H NMR spectrum a triplet

was present at δ = –0.05 ppm for the methyl ligand coordinated to the palladium, while in the ^{13}C NMR spectrum a singlet appeared at δ = 3.8 ppm for the same CH_3 unit. These observations are clear indications that a *trans*-coordinated species is present, which could be either monomeric or dimeric (Figure 4.6). For monomeric *trans*-coordinated $PdCl(CH_3)$(Xantphos)-complexes Zuideveld *et al.* have reported methyl proton signals at around –0.2 ppm.[22]

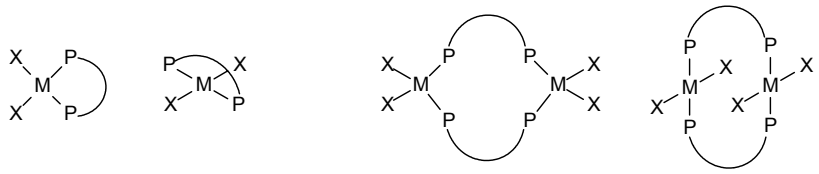

Figure 4.6: *Four possible modes of coordination: bidentate monomeric, cis and trans (left) and monodentate dimeric, cis and trans (right).*

Upon slow evaporation of the NMR solvent, yellow block-shaped single crystals, suitable for X-ray analysis, were obtained. The molecular structure for complex **8** is depicted in Figure 4.7, while selected bond lengths and bond angles are given in Table 4.3. The structure of complex **8,** *trans*,*trans*-[{$PdCl(CH_3)$(μ-**2**)}$_2$], is dimeric, forming a 20-membered macrocycle, with indeed a *trans*-coordination for two phosphorus atoms around each palladium atom and the ligands coordinated in a monodentate bridging fashion.

Complex **8** is centrosymmetric and the geometry around the palladium atoms is distorted square planar. The P_1-Pd-P_2 angle is 172.94(3)° and the C_1-Pd-Cl_1 angle is 171.64(13)°. The Pd-P bond lengths are normal for triaryl phosphines at 2.3250(9) Å (Pd-P_1) and 2.3248(9) Å (Pd-P_2),[23,24] and also in agreement with the values reported by Milstein *et al*.[25] and by the group of Hii.[26] Also the bond lengths between palladium and chlorine (2.4330(10) Å) and between palladium and the methyl ligand (1.836(3) Å) are in their expected ranges.[27] The intramolecular P_1-P_{2a} distance is found to be 7.4470(13) Å. Most binuclear palladium complexes with a face-to-face structure that have been described in literature have two chlorine ligands coordinated to the metal center instead of one chlorine and one methyl ligand. Pryde *et al.* reported on *trans*-type palladium dimers with P(*t*Bu)$(CH_2)_{10}$P(*t*Bu)) as a ligand[28] while the group of Housecroft described a $PdCl_2$(dpph) dimer (dpph = diphenylphosphinohexane).[29]

From these examples it is clear that there is a delicate balance between the formation of monomers or dimers dependent on the 'chelate-size', thereby defining the macrocycle that is formed. Davies *et al.* described a face-to-face dimer [$Pd_2Cl_2(CH_2NO_2)$(μ-dmpm)$_2$] (dmpm = $Me_2PCH_2PMe_2$).

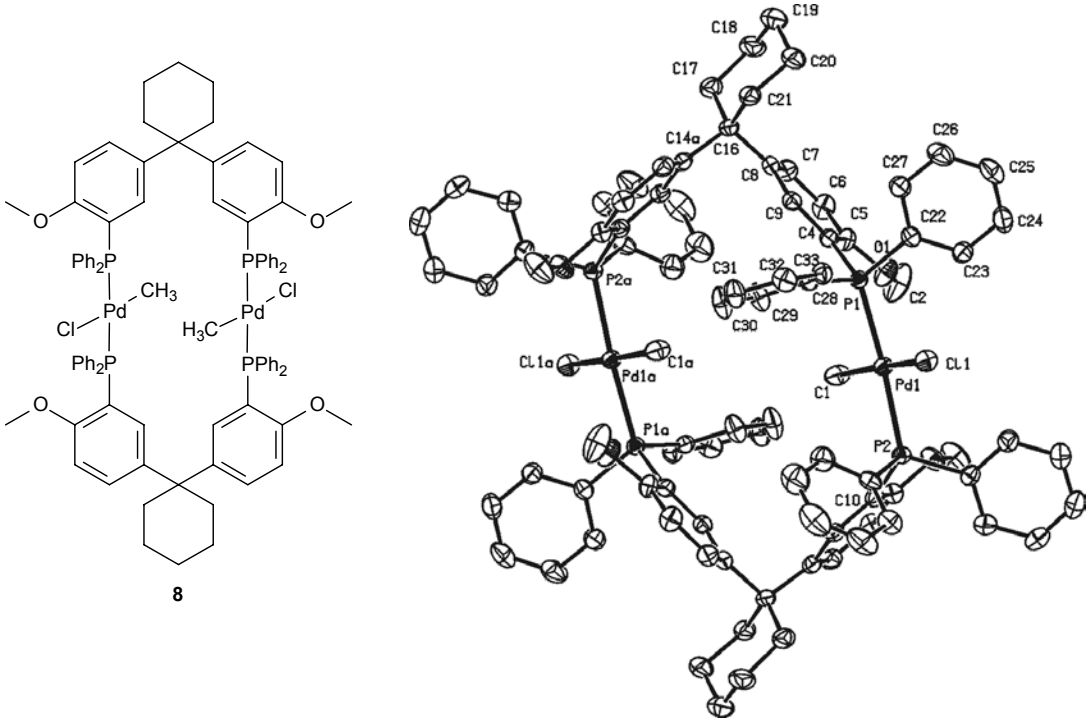

Figure 4.7: *ORTEP representation of complex **8**,* trans,trans-*[{PdCl(CH$_3$)(μ-**2**)}$_2$]. Displacement ellipsoids are drawn at the 50% probability level. Hydrogen atoms and solvent molecules are omitted for clarity.*

The bond distances between the palladium and the chlorine or the carbon atom of the nitromethyl-group turned out to be slightly shorter than in the case of complex **7**, due to the electron-withdrawing effect of the nitromethyl ligand.[30] Kemmitt and co-workers quite recently reported various dimeric palladium-diphosphine complexes with a chlorine and a phenyl group as the other ligands.[24]

Table 4.3: *Selected bond lengths and angles for complex **8**,* trans,trans-*[{PdCl(CH$_3$)(μ-**2**)}$_2$].*

Bond lengths (Å)					
Pd_1-P_1	2.3250(9)	Pd_1-P_2	2.3248(9)	Pd_1-Cl_1	2.4330(10)
Pd_1-C_1	2.075(4)	P_1-C_4	1.836(3)	P_2-C_{10}	1.830(3)
P_1-P_{2a}	7.4470(13)	Pd_1-Pd_{1a}	7.4972(4)		
Angles (°)					
P_1-Pd_1-P_2	172.94(3)	C_1-Pd_1-Cl_1	171.64(13)	P_1-Pd_1-Cl_1	88.18(3)
P_2-Pd_1-Cl_1	88.41(3)	P_1-Pd_1-C_1	92.30(9)	P_2-Pd_1-C_1	90.17(9)
C_8-C_{16}-C_{14a}	105.2(3)				

In order to verify if the formation of face-to-face dimeric complexes is favoured with other transition metals as well we decided to study the complexation of ligand **2** with two platinum precursors. For the product of the reaction with $PtCl_2$(cod) under dilute conditions (~ 3 mM), the ^{31}P NMR spectrum showed a singlet at δ = 7.93 ppm, flanked by ^{195}Pt satellites, and a coupling constant $J_{Pt\text{-}P}$ of 3820 Hz. This is a typical value for a *cis*-[$PtCl_2$(**2**)] complex.[31] The solubility of the this complex however was remarkably poor in common solvents such as toluene or CH_2Cl_2.

However, after reaction of **2** with $PtCl_2(CH_3CN)_2$, an off-white solid was obtained. By dissolving this compound in acetone and allowing slow evaporation of the solvent, one product could be isolated as yellow single crystals in good yield. The ^{31}P NMR spectrum of this compound showed a singlet at δ = 15.8 ppm, flanked by ^{195}Pt satellites, and a coupling constant $J_{Pt\text{-}P}$ of 2705 Hz. This clearly indicates a *trans*-coordination of two phosphorus atoms. These block-shaped crystals turned out to be suitable for X-ray analysis. The molecular structure for complex **9** is depicted in Figure 4.8. Selected bond lengths and bond angles are listed in Table 4.4.

Similar to the palladium complex **8**, the structure turned out to be dimeric and centrosymmetric. The coordination around the platinum atoms is distorted square planar, with a P_1-Pt-P_2 angle of 176.78(7) Å and a Cl_1-Pt-Cl_2 angle of 171.77(7) Å. The P-C bond length is slightly decreased to accommodate the transition metal. The geometry around the central atom C_{15} of the backbone is nearly perfectly tetrahedral, as indicated by the angle with both phenyl rings. Interestingly, the P_1-P_{2a} distance is larger than in the palladium-dimer **6** at 8.627(3) Å. The P-Pt and Cl-Pt bond lengths are in their expected ranges, compared to similar structures reported before.[32,33] Wood *et al.* showed that the reaction of 2,6-bis(diphenylphosphino)pyridine with $PtCl_2$ led to the formation of a *cis*-dimer while, when the chlorine is substituted for iodine, the phosphorus atoms are coordinated in a *trans*-fashion.[34] Armstrong *et al.* recently synthesized two diphosphine ligands (2,7-bis(3-diphenylphosphino-propoxy)naphthalene and 2,7-bis(3-diphenylphosphino-ethoxy)naphthalene and prepared the corresponding platinum complexes. They were able to show that under the proper conditions either the *cis,cis*-dimer or the *trans,trans*-dimer could be crystallized.[35]

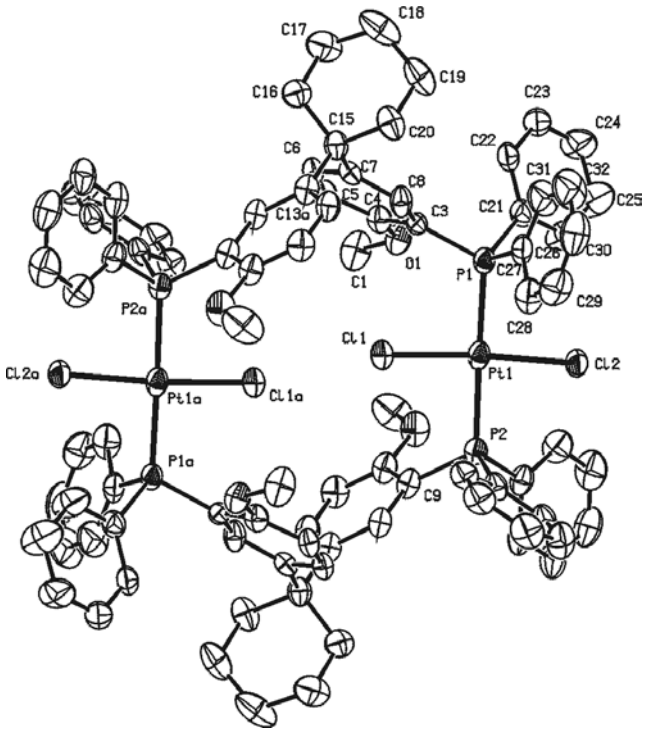

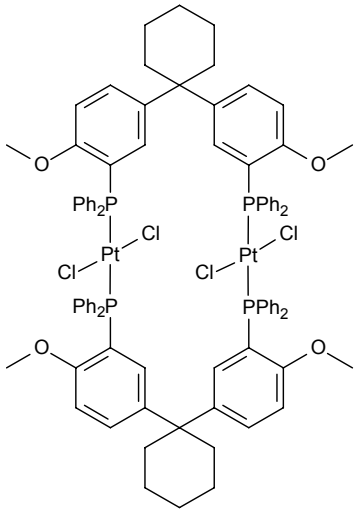

9

Figure 4.8: *ORTEP representation of complex **9**,* trans,trans-*[{PtCl$_2$(μ-**2**)}$_2$]. Displacement ellipsoids are drawn at the 50% probability level. Hydrogen atoms and solvent molecules are omitted for clarity.*

Table 4.4: *Selected bond lengths, distances and angles for complex **9**,* trans,trans-*[{PtCl$_2$(μ-**2**)}$_2$].*

Bond lengths (Å)					
Pt_1-P_1	2.320(2)	Pt_1-P_2	2.315(2)	Pt_1-Cl_1	2.294(2)
Pt_1-Cl_2	2.3270(18)	P_1-C_3	1.835(7)	P_2-C_9	1.827(7)
P_1-P_2	8.627(3)	Pt_1-Pt_{1a}	8.6391(5)		
Angles (°)					
P_1-Pt_1-P_2	176.78(7)	P_1-Pt_1-Cl_1	92.33(8)	P_1-Pt_1-Cl_2	90.09(7)
Cl_1-Pt_1-Cl_2	171.77(7)	P_2-Pt_1-Cl_1	88.80(7)	P_2-Pt_1-Cl_2	88.38(7)
C_7-C_{15}-C_{13a}	108.9(7)				

To further elucidate the formation of these face-to-face dimers, the rhodium precursor [Rh(μ-Cl)(CO)$_2$]$_2$ was chosen. Complexes prepared from this metal source normally result in a *trans*-coordination for the phosphorus atoms. After reaction of this rhodium species with ligand **2**, a doublet was observed in the ^{31}P NMR spectrum at δ = 23.7 ppm, with a coupling constant $J_{Rh\text{-}P}$ of 128.3 Hz, which is a normal value for rhodium diphenylphosphine complexes. In the carbonyl region of the IR spectrum (ATR-mode) obtained from the solid, the CO stretch-vibration was present at ν_{CO} = 1976 cm^{-1}. This is in good agreement with the data reported for the complex RhCl(CO)(P(o-An)Ph$_2$) (An =

anisyl) with ν_{CO} = 1974 cm^{-1},[36] but slightly lower than the values found for [RhCl(CO)($PPh_2(C_6F_5)$)] with ν_{CO} = 1982 cm^{-1},[37] and for Rh(Cl)(CO)(PPh_3)$_2$, with ν_{CO} = 1980 cm^{-1}.[38] *Note:* Moloy and Petersen have touched upon the discrepancy in literature with respect to the CO stretching frequency for Rh(Cl)(CO)(PPh_3)$_2$. Their own experiments showed a single band at ν = 1965 cm^{-1} in CH_2Cl_2.[38b] The value of 1976 cm^{-1} demonstrates that the ligands of the BPphos family are slightly more basic than the aforementioned two ligand systems. However, the value of ν = 1976 cm^{-1} is significantly higher than in Rh(Cl)(CO)(P) complexes with alkyldiarylphosphines such as described by Zhang *et al.*[39] and by the group of Dilworth (1957 cm^{-1}).[40]

By slow diffusion of acetonitrile into a dichloromethane solution of this compound, single crystals could be grown that were suitable for an X-ray crystallographic study. The molecular structure for complex **10** is shown in Figure 4.9. Similar to the Pd and Pt complexes, the face-to-face dimeric structure is apparent, so the complex is denoted as *trans,trans*-[{RhCl(CO)(μ-**2**)}$_2$]. Selected bond lengths and bond angles are listed in Table 4.5.

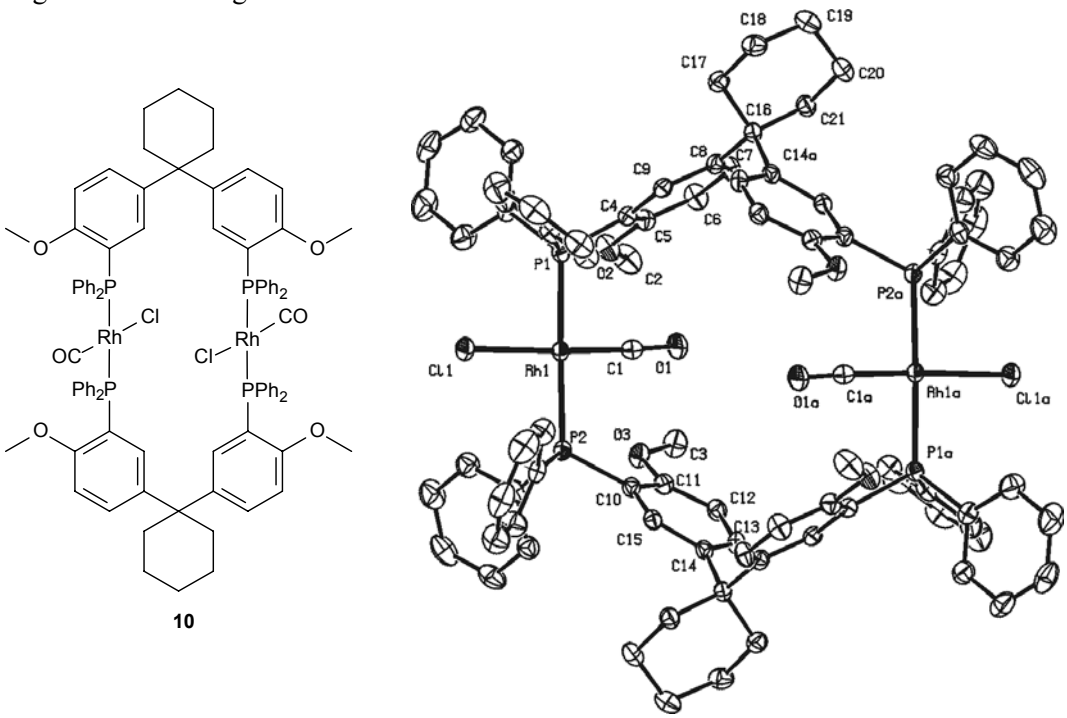

Figure 4.9: *ORTEP representation of complex **10**,* trans,trans-*[{RhCl(CO)(μ-**2**)}$_2$]. Displacement ellipsoids are drawn at the 50% probability level. Hydrogen atoms are omitted for clarity.*

The geometry around the rhodium atom is distorted square planar, with the P-Rh-P angle at 171.01º and a Cl-Rh-C(O) angle of 176.99º. The average Rh-P bond length of 2.32 Å is normal. The Rh-Cl and Rh-C(O) bond lengths come down to 2.3795(5) Å and 1.810(2) Å respectively. The C-O distance of 1.145(2) Å is normal.[39-44] The intramolecular P_1-P_{2a} distance of 8.8150(12) Å as well as

the corresponding Rh-Rh distance of 9.0005(11) Å are similar as the distances found in the palladium and platinum complexes.

In the literature, many *trans*-[RhCl(CO)(P)] complexes with (di)phosphine ligands have been described, yet most of these systems are solely mononuclear. Relatively few examples are known where a dimeric compound is formed exclusively and structurally characterized by X-ray crystallography.[44-48]

Table 4.5: *Selected bond lengths and angles for complex **10**,* trans,trans-*[(RhCl(CO)(μ-**2**)$_2$]*.

Bond lengths (Å)					
Rh_1-P_1	2.3153(5)	Rh_1-P_2	2.3345(6)	Rh_1-Cl_1	2.3795(5)
Rh_1-C_1	1.810(2)	C_1-O_1	1.145(2)	P_1-C_4	1.8349(17)
P_2-C_{10}	1.8352(18)	P_1-P_{2a}	8.8150(12)	Rh_1-Rh_{1a}	9.0005(11)
Angles (°)					
P_1-Rh_1-P_2	171.01(3)	P_1-Rh_1-Cl_1	87.85(3)	P_2-Rh_1-Cl_1	90.36(3)
Cl_1-Rh_1-C_1	176.99(7)	P_1-Rh_1-C_1	89.80(7)	P_2-Rh_1-C_1	92.24(7)
Rh_1-C_1-O_1	177.33(18)	Rh_1-P_1-C_4	116.75(6)	C_8-C_{16}-C_{14a}	110.19(15)

It is clear that the tertiary arylphosphines in BPphos, illustrated using ligand **2** as a representative example, show very different behaviour towards transition metals than for instance the wide angle ligand reported by Venanzi[49] as well as the structurally more related family of ligands based on xanthene.[22,50] Transition metal complexes incorporating one of these ligands are strictly mononuclear.

4.3.2 Terphos

In order to be able to draw conclusions about the structural motif of the design of the new backbone class, the behaviour of ligand **5**, Terphos, with palladium and platinum was studied under the same reaction conditions. Here as well predominantly *trans*-coordination was observed with both $PdCl_2$(cod) as well as with $PdCl(CH_3)$(cod), as indicated by the chemical shifts of δ = 17.1 and δ = 24.7 ppm, respectively, in the ^{31}P NMR spectra of the resulting complexes. As a minor species (~ 10%) a *cis*-coordinated species was observed at δ = 32.6 ppm. A MALDI-TOF spectrum of the [$PdCl_2$(**5**)] complex showed the presence of both dimeric and monomeric fragments.

The reaction of **5** with $PtCl_2(CH_3CN)_2$ showed the formation of only a *trans* coordinated platinum-(di)phosphine complex, *viz.* a singlet at δ = 16.2 ppm, together with ^{195}Pt satellites and a coupling constant $J_{Pt\text{-}P}$ of 2694 Hz.

However, from the reaction of $PtCl_2$(cod) with **5**, performed under very dilute conditions (~3 mM in both reagents), only a signal for a *cis*-[$PtCl_2$(**5**)] complex was found at δ = 9.9 ppm, flanked by ^{195}Pt satellites, and a corresponding coupling constant $J_{Pt\text{-}P}$ of 3810 Hz.

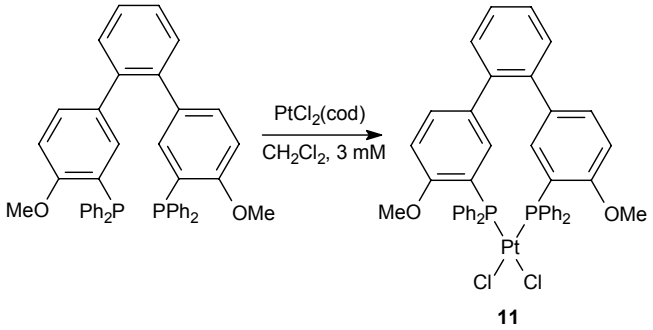

Scheme 4.3: *Formation of complex **11**,* cis-*[$PtCl_2$(**5**)] under dilute conditions.*

In the ^{1}H NMR spectrum the signal for the methoxy groups shifts upfield to 3.61 ppm and the signals for the phenyl substituents on the phosphines become rather broad due to fluxional behaviour, yet the protons of the backbone are well resolved. In time, evaporation of the NMR solvent yielded colorless single crystals that were subjected to a crystallographic study using X-ray diffraction. The molecular structure obtained for complex **11** is depicted in Figure 4.10. Table 4.6 contains data on selected bond lengths and angles.

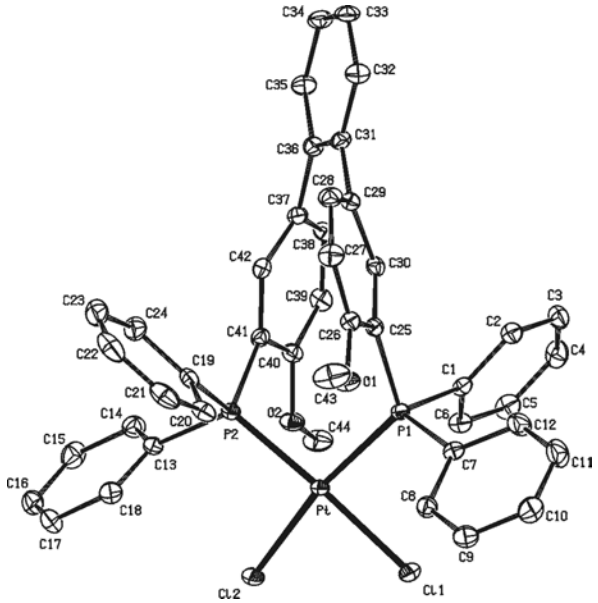

Figure 4.10: *ORTEP representation of complex **11**,* cis-*[$PtCl_2$(**5**)]. Displacement ellipsoids are drawn at the 50% probability level. Hydrogen atoms and solvent molecules are omitted for clarity.*

The *monomeric* complex **11**, *cis*-[$PtCl_2$(**5**)], shows unambiguously that ligand **5**, Terphos, is able to act as a chelating bidentate ligand. The structure obtained is in good agreement with the observed structure in solution, indicated by the coupling constant $J_{Pt\text{-}P}$. The geometry around the platinum atom is distorted square planar. This is evident from the angles P_1-Pt-Cl_2 and P_2-Pt-Cl_1 of 170.90(2)º and 172.80(3)º, respectively. The bite angle observed, P_1-Pt-P_2, is 98.74(2)º and consequently the Cl_1-Pt-Cl_2 angle is small at only 84.93(2)º. The sums of all angles around each phosphorus atom are 311.91º (P_1) and 313.80º (P_2). Compared to other complexes of this type, the Pt-P and Pt-Cl bond lengths are in their expected ranges, at 2.26-2.28 Å and 2.34-2.36 Å, respectively.[51-53] The aromatic rings of the terphenyl backbone have torsion angles C_{28}-C_{29}-C_{31}-C_{36} of 135.7º and C_{31}-C_{36}-C_{38}-C_{39} of 128.2º, showing that there is slight distortion from local C_2 symmetry of the backbone. The intramolecular P_1-P_2 distance is 3.4517(9) Å, significantly smaller than reported for various metal complexes (not including platinum) incorporating Xantphos.[54] This indicatess that there is an effect of the different degree of rigidity of the corresponding ligand backbones.

Table 4.6: *Selected bond lengths, distances and angles for complex **11**,* cis-*[$PtCl_2$(**5**)]*.

Bond lengths (Å)					
Pt-P_1	2.2847(7)	Pt-P_2	2.2635(7)	Pt-Cl_1	2.3565(6)
Pt-Cl_2	2.3358(7)	O_1-C_{26}	1.352(3)	O_2-C_{40}	1.356(3)
P_1-C_{25}	1.832(3)	P_2-C_{41}	1.818(3)	P_1-P_2	3.4517(9)
Angles (°)					
P_1-Pt-P_2	98.74(2)	Cl_1-Pt-Cl_2	84.93(2)	P_1-Pt-Cl_1	86.34(2)
P_1-Pt-Cl_2	170.90(2)	P_2-Pt-Cl_1	172.80(3)	P_2-Pt-Cl_2	89.73(2)
Pt-P_1-C_{25}	122.03(9)	Pt-P_2-C_{41}	110.75(9)	C_8-C_{16}-C_{14a}	110.19(15)

4.4 Catalysis

Molecular structures of metal complexes such as described for ligand **2** provide insight in the coordination behaviour of ligands in the solid state but they do not tell the (whole) story of the solution behaviour of said complexes. Therefore, to illustrate the applicability of the newly developed family of phosphorus ligands, the rhodium catalyzed hydroformylation of 1-octene was chosen as a model reaction (Scheme 4.3). The catalysis was carried out under typical hydroformylation conditions, at 20 bar of synthesis gas (CO/H_2 1:1) and a reaction temperature of 80 °C. The results of these catalytic tests are listed in Table 4.7.

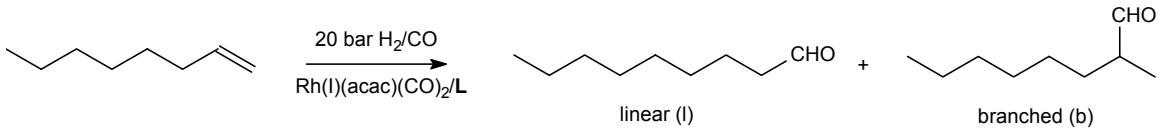

Scheme 4.4: *General illustration of the rhodium catalyzed hydroformylation of 1-octene.*

The flexibility and steric crowding of the central atom in the backbone greatly effect the initial activity of the corresponding catalyst. The least rigid ligand **1** (entry 1) gave a turnover frequency (TOF) of only 718 h^{-1}. The activity was higher when a cyclohexyl moiety was present in the backbone, ligand **2** (entry 2). In that case a TOF of 1029 h^{-1} was found. With ligand **3** (both a methyl and a phenyl group on the central carbon atom of the backbone) an even higher activity was found, with a TOF of 1418 h^{-1} (entry 3). The regioselectivity for the terminal aldehyde is low with a linear to branched (l/b) ratio of about 3. This is expected, as these ligands nor the reaction conditions were optimized. For ligand **4**, with the central silicon atom in the backbone, (entry 4) the activity was unexpectedly high since it was thought to resemble ligand **1** in structure.

Table 4.7: *Hydroformylation of 1-octene catalyzed by [Rh(acac)(CO)$_2$]/**1-5** [a].*

Entry	Ligand	Time [min]	Temperature [°C]	*p* [bar]	Conversion [%][b]	$Sel_{Aldehyde}$ [%][b]	l/b ratio[b]	TOF[c]
1	**1**	60	80	20	18.8	97.9	2.8	735
2	**2**	60	80	20	26.8	99.0	2.9	1029
3	**3**	60	80	20	35.4	99.2	2.7	1418
4	**4**	60	80	20	31.6	99.3	2.9	1250
5	**5**	15	80	20	21.8	98.1	3.0	3485
6	**5**	60	80	30	40.0	97.6	2.9	1615
7	**5**	60	70	20	20.3	98.4	3.0	800
8	**5**	60	60	20	8.3	98.3	3.0	325
9	**5**	60	60	20[d]	15.8	98.9	2.4	620

[a]Reaction conditions: [Rh(acac)(CO)$_2$] (0.39 mM), 1-octene (31.0 mmol), decane (12.5 mmol), toluene (12.7 mL), 1-octene:Rh=4000:1, preformation time 1 h, ligand:Rh = 6:1; [b]determined by GC; [c]turnover frequency, defined as (mol substrate converted)·(mol rhodium)$^{-1}$·h^{-1}; [d]p(CO):p(H$_2$) = 1:3.

Ligand **5** turned out to give the highest activity, with a turnover frequency up to almost 3500 h^{-1} which leads to a conversion of nearly 22% after 15 minutes (entry 5). No side reactions such as hydrogenation and isomerization of the substrate occurred, which is a common observation for diphosphine ligands.[33] Furthermore, the catalytic system based on Terphos (ligand **5**) shows the typical behaviour expected for diphosphine related catalysts concerning the influence of temperature,

pressure and CO/H_2 ratio on the conversion (entries 6-9). At a higher pressure of 30 bar, the activity is about 50% lower with a TOF of 1650 h^{-1} (entry 6). When lowering the reaction temperature to 70 °C, the conversion shows the expected trend (entry 7). Upon a further decrease of the temperature to 60 °C and at 20 bar CO/H_2 (1:1) the conversion dropped considerably to 8% (entry 8) but when the partial pressure of H_2 was increased to reach a CO/H_2 mixture of ratio 1:3, the conversion increased to 15.8%, indicative of the negative first order dependence in CO (entry 9).

Since ligand **5** proved to be able to coordinate as a bidentate ligand, the hydride formation under hydroformylation conditions was monitored by high-pressure NMR spectroscopy in order to investigate the structure of the catalytic resting state. Complexation was achieved using $Rh(acac)(CO)_2$ in the presence of a slight excess of ligand (typically 1.05 molar equivalents) under 20 bar of CO/H_2 (1:1) at 80 °C. In the ^{31}P NMR spectrum a doublet was observed at 18.5 ppm with a typical coupling constant $J_{Rh\text{-}P}$ of 128 Hz, while the ^{1}H NMR spectrum shows a triplet of doublets at –9.0 ppm. This is characteristic of a hydrido-dicarbonyl complex $Rh(H)(CO)_2(PP)$. The coupling constants $^{1}J_{Rh\text{-}H}$ of 4 Hz and $^{2}J_{P\text{-}H}$ of 41.5 Hz suggest a predominantly equatorial-apical (**ea**) coordination mode of the bidentate ligand.

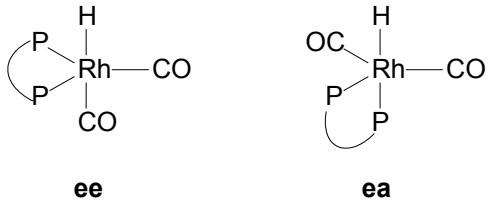

Figure 4.11: *Schematic representation of the equatorial-equatorial (**ee**) and equatorial-axial (**ea**) coordination modes possible for the catalytic resting state during hydroformylation.*

This is verified using high-pressure IR spectroscopy. Under hydroformylation conditions (20 bar and 80 °C) two bands of unequal intensities appear in the carbonyl region at 1952 and 1995 cm^{-1}, which is typical for a bis-equatorial coordination of the CO molecules, leading to an **ea**-complex, in accordance with findings of van der Veen *et al.*[55] From the combination of these spectroscopic observations, it can be concluded that the low regioselectivity is probably due to this preferred equatorial-apical (**ea**) coordination in the resting state of the catalyst. It is generally accepted that diphosphines with a preference for an equatorial-equatorial mode of coordination show a higher selectivity for the desired linear aldehyde.[56]

4.5 Conclusions

In summary, the development of novel modular diphosphine ligands **1**-**4** based on commercially available and cheap raw materials, derived from Bisphenol A, was successful. Based on a modified procedure, also ligand **5,** containing a terphenyl backbone, was prepared. X-ray crystallographic studies of these compounds were undertaken. In the molecular structure of the phosphine oxide **6** derivative of ligand **2**, hydrogen bonding to a water molecule occurred, directing the phosphorus atoms into a bidentate fashion. For ligands **2** and **5**, the coordination towards various transition metals was studied. From complexation studies undertaken with ligand **2**, several face-to-face dimeric macrocycles with palladium, platinum and rhodium were obtained and characterized by NMR spectroscopy as well as X-ray crystallography. Ligand **5** was shown to be able to coordinate in a bidentate manner to platinum, both by NMR spectroscopy as well as by an X-ray diffraction study, revealing the molecular structure of *cis*-[$PtCl_2$(**5**)]. The novel ligands have been applied in the rhodium catalyzed hydroformylation of 1-octene. Under non-optimized conditions regioselectivities are low at linear to branched ratios of around 3. High activities with turnover frequencies of up to 3600 h^{-1} were obtained for ligand **5.**

Acknowledgements

The National Research School Combination for Catalysis (NRSCC) is thanked for financial support and OMG for a generous loan of metal precursors. Drs. Michiel Grutters is gratefully acknowledged for his work on the phosphine oxide **6** and for valuable discussions. Josep Bonet assisted in the work related to the catalytic activity of the ligands described. His stay in Eindhoven was made possible by a grant from the Erasmus program of the European Union. Help from Dr. Pieter Magusin and Eugène van Oers during the HP NMR experiments is highly appreciated. Dr. Rafaël Sablong and Ir. Ruben van Duren contributed greatly in scientific discussions. Dr. Wolfgang Ahlers and Dr. Rocco Paciello (BASF AG.) are thanked for initial catalytic tests. X-ray crystallography was performed by Dr. Allison Mills and Dr. Huub Kooijman from the University of Utrecht (group of Prof. Anthony Spek) and by Drs. Auke Meetsma from the University of Groningen.

4.6 Experimental Section

General. Chemicals were purchased from Aldrich, Acros or Merck and used as received. Synthesis gas (CO/H_2 1:1) was purchased from Hoekloos. All preparations were carried out under an argon atmosphere using standard Schlenk techniques. Solvents were distilled from sodium/benzophenone (THF, diethyl ether, toluene and hexanes) or calcium hydride (CH_2Cl_2 and $CDCl_3$) prior to use. All glassware was dried by heating under vacuum. $PdCl_2(cod)$,[57] $PdCl(CH_3)(cod)$[58] and $PtCl_2(cod)$[59] were synthesized according to literature procedures. NMR spectra were recorded on a Varian Mercury 400 spectrometer (^1H, $^{13}C\{^1H\}$, $^{31}P\{^1H\}$). Chemical shifts are given in ppm referenced to solvent (^1H, $^{13}C\{^1H\}$) or to an 85% aqueous solution of H_3PO_4 ($^{31}P\{^1H\}$). GC analyses were performed on a Shimadzu 17A chromatograph equipped with a 50 m PONA column. Elemental analysis was performed by Kolbe Mikroanalytisches Laboratorium, Germany. High Pressure NMR spectra were recorded on a Bruker 200 MHz spectrometer. IR spectra were recorded on a Shimadzu 7300 FT-IR spectrometer.

2,2-Bis(4-methoxyphenyl)propane (A).
To a solution of Bisphenol A (2,2'-bis(4-hydroxyphenyl)propane) (11.48 g, 50 mmol) in 120 mL of acetone were added K_2CO_3 (27.69 g, 200 mmol) and CH_3I (21.69 g, 150 mmol) as well as NBu_4I (0.88 g, 2.38 mmol). The heterogeneous mixture was stirred for 16 h under reflux. The suspension was filtered over Celite and poured into a mixture of 100 mL of diethyl ether and 100 mL of a 15 w% aqueous KOH-solution. The organic phase was separated and further washed with saturated brine (100 mL) and water (50 mL) after which $MgSO_4$ was added and the organic phase stirred overnight. After filtration over Celite the solvent was removed *in vacuo* and 40 mL of ethanol was added to the remaining oil. After stirring, the ethanol was removed *in vacuo* to yield 9.44 g (36.8 mmol) (73 %) as pure off-white powder.
^{1}H NMR ($CDCl_3$) δ 7.15 (d, 4H, J_1 = 8.8 Hz), 6.81 (d, 4H, J_1 = 8.8 Hz), 3.79 (s, 6H, -OCH_3), 1.65 (s, 6H, -$C(CH_3)_2$).
^{13}C{1H} NMR ($CDCl_3$) δ 157.4, 143.1, 127.7, 113.2, 55.2 (OCH_3), 41.6 ($C(CH_3)_2$), 31.1 ($C(CH_3)_2$).

1,1-Bis(4-methoxyphenyl)cyclohexane (B).
Starting from 28.8 g (110 mmol) Bisphenol Z (1,1-bis(4-hydroxyphenyl)cyclohexane), compound **B** was obtained as a white crystalline solid, using the same procedure as described for **A**. Yield 83.5% (27.7 g, 93.5 mmol).
^{1}H NMR ($CDCl_3$) δ 7.18 (d, 4H, J_1 = 8.8 Hz), 6.81 (d, 4H, J_1 = 8.8 Hz), 3.77 (s, 6H, -OCH_3), 2.23 (m, 4H), 1.55 (m, 6H).
^{13}C{1H} NMR ($CDCl_3$) δ 157.1, 141.0, 128.0, 113.4, 55.1 (-OCH_3), 45.0 (C_{ipso}), 37.4, 26.4, 22.9.

2,2-Bis(4-methoxyphenyl)ethylbenzene (C).
Starting from 20.0 g (68.9 mmol) Bisphenol AP ((2,2-bis(4-hydroxyphenyl)ethyl)benzene), compound **C** was obtained as a pure off-white powder, using the same procedure as described for **A**. Yield 64 % (13.92 g, 43.7 mmol).
^{1}H NMR ($CDCl_3$) δ 7.26 (m, 2H), 7.20 (m, 1H), 7.09 (m, 2H), 7.00 (d, 4H, J_1 = 8.8 Hz), 6.79 (d, 4H, J_1 = 8.8 Hz), 3.79 (s, 6H, OCH_3), 2.14 (s, 6H, -$C(CH_3)$).
^{13}C{1H} NMR ($CDCl_3$) δ 157.6, 141.5, 129.7, 128.6, 127.8, 125.8, 113.1, 55.2 (-OCH_3), 30.7 (-$C(CH_3)_2$).

Bis(4-methoxyphenyl)dimethylsilane (D).
4-Bromoanisole (5.79 g, 31.0 mmol) was dissolved in 100 mL THF and the solution was cooled to –78 °C. Subsequently *n*-BuLi (12.4 mL, 31.0 mmol) as a 2.5 M solution in hexanes was added dropwise. The reaction mixture was stirred for 1 h followed by addition of $SiCl_2(CH_3)_2$ (2.00 g, 31.0 mmol). The reaction mixture was allowed to warm up to r.t. and stirring was continued overnight. Solvents were removed *in vacuo* and the crude product was dissolved in 30 mL of CH_2Cl_2. Washing with 40 mL distilled water afforded a turbid white organic layer. This phase was separated and the solvent removed *in vacuo* to yield a yellow oil. Upon addition of 25 mL of hexanes a brown precipitate was formed. The solution was isolated and dried with $MgSO_4$. After filtration and subsequent removal of solvent, an off-white solid was obtained. Yield 71% (3.00 g, 22.0 mmol).
^{1}H NMR ($CDCl_3$) δ 7.48 (d, 4H, J_1 = 8.8 Hz), 6.93 (d, 4H, J_1 = 8.8 Hz), 3.83 (s, 6H, OCH_3), 0.54 (s, 6H, -$Si(CH_3)$).
^{13}C{1H} NMR ($CDCl_3$) δ 160.4, 135.6, 129.4, 113.5, 55.0 (-OCH_3), -2.0 (-$Si(CH_3)_2$).

4-Methoxyphenylboronic acid (E).
4-Bromoanisole (2.66 g, 14.22 mmol) was dissolved in 30 mL Et_2O and the mixture cooled to –78 °C before *t*-BuLi (19.0 mL, 28.44 mmol) as a 1.5 M solution in pentane was added dropwise. The reaction mixture was stirred for 1 hour. $B(OMe)_3$ (5.91 g, 57.0 mmol) was added at -60 °C and the reaction allowed to warm up to r.t. overnight. 50 mL of a 1M HCl solution was added and the mixture stirred for 1 hour. This solution was extracted with 3 volumes of 20 mL CH_2Cl_2, the organic phases combined and dried over $MgSO_4$. After filtration the solvents were removed *in vacuo* to leave a white solid. Yield 1.60 g (75%). The obtained product was used without further purification or characterization.

1,2(Bis-4-methoxyphenyl)benzene (F).
E (1.60 g, 10.53 mmol) and 1,2-dibromobenzene (0.83 g, 5.26 mmol) were added to a degassed 2 M solution of Na_2CO_3 (30 mL) and 90 mL of dimethoxy ethane, together with a catalytic amount of $Pd(PPh_3)_4$. The reaction mixture was refluxed overnight. The reaction was brought to a pH of 7 by addition of a 4 M HCl solution. The solution was concentrated to approx. 40 mL and the product extracted by 3 volumes of 25 mL CH_2Cl_2. The organic phases were dried over $MgSO_4$, decanted by cannula and dried to leave a yellow oil. Upon addition of 10 mL of MeOH a white precipitate was obtained that was separated, washed twice with 10 mL of acetonitrile and dried to 0.72 g (73 %) of a white crystalline powder.
^{1}H NMR ($CDCl_3$) δ 7.38 (d, 4H, J_1 = 2.4 Hz), 7.07 (dt, 4H, J_1 = 8.3 Hz, J_2 = 1.2 Hz), 6.77 (dt, 4H, J_1 = 8.4 Hz, J_2 = 1.2 Hz) 3.79 (s, 6H, OCH_3).
^{13}C{1H} NMR ($CDCl_3$) δ 158.2, 140.0, 134.1, 130.9, 130.5, 127.1, 113.5, 55.2 (O*C*H_3).

2,2-Bis((3-diphenylphosphino-4-methoxy)phenyl)propane (1).
TMEDA (12.95 g, 0.11 mol) was added to *n*-BuLi (2.5 M solution in hexanes) (44.6 mL, 0.11 mol). At –15 °C a solution of **A** (13.29 g, 0.052 mol) in 75 mL diethyl ether was added dropwise over a period of 1.5 h. The mixture was allowed to slowly warm up to r.t. and stirred overnight to yield a yellow suspension. At 0 °C $ClPPh_2$ (24.6 g, 0.11 mol) in 30 mL of hexanes was added dropwise over a period of 1 h. Solvents were removed *in vacuo* and 60 mL of CH_2Cl_2 was added, together with 50 mL of saturated brine. The organic phase was separated and dried over $MgSO_4$. After filtration over Celite, the solvents were removed *in vacuo* to yield a pink oil that solidified on standing overnight at r.t. under argon. 40 mL of ethanol was added to give an orange solution and a white precipitate. The solid was washed with ethanol, filtered and dried. Yield 54% (17.46 g, 28.1 mmol).
^{1}H NMR ($CDCl_3$) δ 7.24 (m, 20H, PPh_2), 7.04 (dd, 2H, J_1 = 8.8 Hz, J_2 = 2 Hz), 6.73 (dd, 2H, J_1 = 8.8 Hz, J_2 = 4.8 Hz), 6.40 (dd, 2H, J_1 = 5.2 Hz, J_2 = 2.4 Hz) 3.73 (s, 6H, OCH_3), 1.24 (s, 6H, $C(CH_3)_2$).
^{13}C{1H} NMR ($CDCl_3$) δ 159.0 (d, $J_{P\text{-}C}$ = 14.5 Hz), 143.0, 136.9 (d, $J_{P\text{-}C}$ = 10.7 Hz), 133.7 (d, $J_{P\text{-}C}$ = 19.8 Hz), 132.4, 128.4, 128.3, 128.2 (d, $J_{P\text{-}C}$ = 6.8 Hz), 124.3, 109.5, 55.7 (O*C*H_3), 41.6 (*C*$(CH_3)_2$) 30.3 (C(*C*$H_3)_2$).
^{31}P{^{1}H} NMR ($CDCl_3$) δ -14.8 (s).
Anal. Calcd for $C_{41}H_{38}O_2P_2$: C, 78.83; H, 6.13; P, 9.92. Found: C, 78.65; H, 6.08; P, 9.98.

1,1-Bis((3-diphenylphosphino-4-methoxy)phenyl)cyclohexane (2).
Starting from **B** (4.99 g, 16.8 mmol), compound **2** was obtained as a white powder, using the same procedure as described for compound **1**. Yield 56% (6.34 g, 9.4 mmol).
^{1}H NMR ($CDCl_3$) δ 7.24 (m, 20H, PPh_2), 6.99 (dd, 2H, J_1 = 8.8 Hz, J_2 = 2.4 Hz), 6.72 (dd, 2H, J_1 = 8.8 Hz, J_2 = 4.8 Hz), 6.47 (dd, 2H, J_1 = 5.6 Hz, J_2 = 2.4 Hz), 3.71 (s, 6H, -OCH_3), 1.73 (m, 4H, cy-C_6), 1.23 (m, 6H, cy-C_6).
^{13}C{1H} NMR ($CDCl_3$) δ 159.0 (d, $J_{P\text{-}C}$ = 14.5 Hz), 140.9, 137.0, 133.7 (d, $J_{P\text{-}C}$ = 19.8 Hz), 132.9, 128.8, 128.3 (d, $J_{P\text{-}C}$ = 13.0 Hz), 128.2, 125.7, 109.8, 55.6 (-O*C*H_3), 45.2, 37.0, 26.2, 22.7.
^{31}P{^{1}H} NMR ($CDCl_3$) δ -15.2 (s).
Anal. Calcd for $C_{44}H_{42}O_2P_2$: C, 79.50; H, 6.37; P, 9.32. Found: C, 79.39; H, 6.39; P, 9.31.

2,2-Bis((3-diphenylphosphino-4-methoxy)phenyl)ethylbenzene (3).
Starting from **C** (12.4 g, 38.9 mmol), compound **3** was obtained as a white powder, using the same procedure as described for compound **1**. Yield 61 % (16.5 g, 23.7 mmol).
^{1}H NMR ($CDCl_3$) δ 7.18 (m, 20H, PPh_2), 7.07 (m, 3H, $C(C_6H_5)$), 6.91 (dd, 2H, J_1 = 8.8 Hz, J_2 = 2.4 Hz), 6.81 (m, 2H, $C(C_6H_5)$), 6.67 (dd, 2H, J_1 = 8.8 Hz, J_2 = 4.8 Hz), 6.33 (dd, 2H, J_1 = 5.6 Hz, J_2 = 2.4 Hz), 3.72 (s, 6H, -OCH_3), 1.74 (s, 3H, CH_3).

^{13}C{1H} NMR ($CDCl_3$) δ 159.1 (d, J_{P-C} = 14.5 Hz), 149.0, 141.3, 136.7 (d, J_{P-C} = 10.7 Hz), 134.1, 133.6 (d, J_{P-C} = 19.8 Hz), 130.2, 128.3 (d, J_{P-C} = 3.1 Hz), 128.2 (d, J_{P-C} = 6.8 Hz), 127.6, 125.5, 124.2 (d, J_{P-C} = 13.0 Hz), 109.3, 55.6 (-O*C*H$_3$), 51.2, 30.0.
^{31}P{^{1}H} NMR ($CDCl_3$) δ -15.3 (s).
Anal. Calcd for $C_{46}H_{40}O_2P_2$: C, 80.45; H, 5.87; P, 9.02. Found: C, 80.52; H, 5.76; P, 9.05.

Bis((3-diphenylphosphino-4-methoxy)phenyl)dimethylsilane (4).
Starting from **D** (3.00 g, 11.0 mmol), compound **4** was obtained as a white powder, using the same procedure as described for compound **1**. Yield 65 % (4.58 g, 7.2 mmol).
^{1}H NMR ($CDCl_3$) δ 7.28 (m, 20H, PPh_2), 6.81 (dd, 4H, J_1 = 8.0 Hz, J_2 = 4.4 Hz), 6.69 (dd, 4H, J_1 = 8.0 Hz, J_2 = 4.4 Hz), 3.75 (s, 6H, O*CH$_3$*), 0.09 (s, 6H, -Si(*CH$_3$*)).
^{13}C{1H} NMR ($CDCl_3$) δ 161.9 (d, J_{P-C} = 15.9 Hz), 139.5, 136.7 (d, J_{P-C} = 9.9 Hz), 136.3, 133.8 (d, J_{P-C} = 19.8 Hz), 129.5, 128.5, 128.2 (d, J_{P-C} = 6.8 Hz), 124.7, 109.7, 55.5 (-O*C*H$_3$), -2.6 (Si(*C*H$_3$)$_2$).
^{31}P{^{1}H} NMR ($CDCl_3$) δ -16.1 (s).
Anal. Calcd for $C_{40}H_{38}O_2P_2Si$: C, 74.98; H, 5.98; P, 9.67. Found: C, 75.06; H, 5.93; P, 9.63.

1,2-Bis((3-diphenylphosphino-4-methoxy)phenyl)benzene [Terphos] (5).
To a solution of **F** (2.20 g , 7.57 mmol) in 75 mL diethyl ether and TMEDA (2.5 mL, 16.7 mmol) at –40 °C was added *n*-BuLi (6.7 mL, 16.7 mmol) as a 2.5 M solution in hexanes in a dropwise fashion. The reaction mixture was allowed to warm up to room temperature and stirred overnight. $ClPPh_2$ (3.68 g, 16.7 mmol) in 15 mL of hexanes was added dropwise at 0 °C. The reaction mixture was warmed to r.t. and stirred overnight. Volatiles were removed *in vacuo*. 50 mL of THF and 75 mL of a 25% brine-solution were added and the organic phase was washed twice with 30 mL of water. After drying with $MgSO_4$, the solvent was removed and the precipitate washed 3 times with 25 mL of methanol to give a white powder. Yield 60% (2.11 g, 4.54 mmol).
^{1}H NMR (C_6D_6), δ 7.32 (m, 16H, PPh_2), 7.27 (dd, 2H, ^1J = 5.6 Hz, ^2J = 3.2 Hz), 7.19 (dd, 2H, ^1J = 5.6 Hz, ^2J = 3.2 Hz), 7.16 (m, 4H), 7.06 (dd, 2H, ^1J = 8.4 Hz, ^2J = 2.0 Hz), 6.82 (dd, 2H, ^1J = 8.4 Hz, ^2J = 4.8 Hz), 6.41 (dd, 2H, ^1J = 4.8 Hz, ^2J = 2.0 Hz), 3.72 (s, OCH_3).
^{13}C{1H} NMR (C_6D_6), δ 159.6, 145.5, 140.2, 136.5 (d J_{P-C} = 9.8 Hz), 135.1, 134.3, 134.0 (d, J_{P-C} = 20.4 Hz), 131.4, 130.4, 128.5, 128.4 (d, J_{P-C} = 6.8 Hz), 128.4, 126.9, 110.0, 55.8.
^{31}P{^{1}H} NMR (C_6D_6), δ -16.5 (s).
Anal. Calcd. for $C_{44}H_{36}O_2P_2$: C, 80.23; H, 5.51; P, 9.40. Found: C, 80.16; H, 5.43: P, 9.55.

Bis(2,2'-methoxy-5,5'-cyclohexyl)diphenylphosphine oxide (6).
Ligand **2** (0.65 g, 0.98 mmol) was dissolved in 25 mL of CH_2Cl_2 and H_2O_2 (0.20 mL, 1.96 mmol) (30 wt% aqueous solution in 20 mL of H_2O was added dropwise at 0 °C after which the two-phase system was stirred at r.t. overnight. The organic layer was washed with 20 mL of a 0.1 M NaOH-solution and with 20 mL of water. After drying over $MgSO_4$ and subsequent filtration, the solvent was removed *in vacuo* to leave a white powder. Yield 85 % (0.58 g, 0.83 mmol).
^{1}H NMR ($CDCl_3$) δ 7.69 (q, 8H, J = 4.8 Hz), 7.65 (d, 2H, J = 2.4 Hz), 7.51 (dt, 4H, J_1 = 8.4 Hz, J_2 = 1.2 Hz), 7.41 (dt, 8H, J_1 = 8.0 Hz, J_2 = 2.4 Hz), 7.32 (dd, 2H, J_1 = 8.8 Hz, J_2 = 2.4 Hz), 6.81 (dd, 2H, J_1 = 8.8 Hz, J_2 = 5.6 Hz), 3.55 (s, 6H, -O*C*H$_3$), 2.18 (s, 4H), 1.46 (s, 6H).
^{13}C{1H} NMR ($CDCl_3$) δ 158.6 (d, J_{P-C} = 3.7 Hz), 141.0, 133.9, 133.2, 132.8, 131.3 (d, J_{P-C} = 10.8 Hz), 128.0 (d, J_{P-C} = 12.3 Hz), 111.3 (d, J_{P-C} = 7.6 Hz), 55.2 (-OCH_3), 45.3 (C_{ipso}), 37.0, 26.1, 22.7.
^{31}P{^{1}H} NMR ($CDCl_3$) δ 27.7 (s).
Anal. Calcd for $C_{44}H_{42}O_4P_2$: C, 75.85; H, 6.08. Found: C, 76.04; H, 6.14.

Bis(2,2'-methoxy-5,5'-cyclohexyl)diphenylphosphine selenide [BPC$_6$Phos-selenide] (7).
Ligand **2** (57.8 mg, 8.75 mmol) and an excess of selenium were suspended in 5 mL of toluene and stirred for 15 minutes at 60°C. After cooling to r.t., the solution was filtered off to remove insolubles and the solvent was evaporated *in vacuo* to leave a yellow oil. Upon addition of 5 mL of hexanes, a white precipitate was formed that was isolated by filtration and then redissolved in 5 mL of dichloromethane. Removal of the solvent left a pure white solid. Yield 93.2% (66.8 mg, 8.16 mmol).
^{1}H NMR ($CDCl_3$) δ 7.95 (d, 1H, ^1J = 2.8 Hz), 7.91 (d, 1H, ^1J =2.8 Hz), 7.78 (dq, 8H, ^1J = 6.8 Hz, ^2J = 2.4 Hz), 7.45 (dq, 4H, ^1J = 8.4 Hz, ^2J = 2.4 Hz), 7.40 (dq, 8H, ^1J = 8.0 Hz, ^2J = 2.4 Hz), 7.21 (dd, 2H, ^1J = 8.0 Hz, ^2J = 2.4 Hz), 6.81 (dd, 2H, ^1J = 8.4 Hz, ^2J = 2.4 Hz), 3.49 (s, 6H, -O*C*H$_3$), 2.18 (s, 4H), 1.45 (s, 6H).

^{13}C{1H} NMR ($CDCl_3$) δ 158.2, 135.7 (d, $J_{P\text{-}C}$ = 12.2 Hz), 133.3 (d, $J_{P\text{-}C}$ = 3.7 Hz), 133.0, 132.2 (d, $J_{P\text{-}C}$ = 12.2 Hz), 132.1 (d, $J_{P\text{-}C}$ = 3.7 Hz), 131.0 (d, $J_{P\text{-}C}$ = 3.0 Hz), 128.1 (d, $J_{P\text{-}C}$ = 12.2 Hz), 111.9 (d, $J_{P\text{-}C}$ =6.3 Hz), 55.2 (-OCH_3), 45.6 (C_{ipso}), 37.1, 26.2, 22.8.
^{31}P{^{1}H} NMR ($CDCl_3$) δ 33.1 (s, $J_{Se\text{-}P}$ = 717 Hz).

trans-**[$PdCl_2$(2)].**
$PdCl_2$(cod) (83.4 mg, 2.92 mmol) was dissolved in 15 mL of CH_2Cl_2 and to this ligand **2** (194.3 mg, 2.92 mmol) in 15 mL of CH_2Cl_2 was added dropwise. The solution was stirred overnight at room temperature. After evaporation of the solvent a yellow remaining solid was analysed by NMR.
^{31}P{^{1}H} NMR ($CDCl_3$) δ 17.8 (s).

trans,trans-**[{$PdCl(CH_3)$(μ-2)}$_2$] (complex 8).**
Ligand **2** (40.2 mg, 60.5 mmol) and $PdCl(CH_3)$(cod) (13.9 mg, 52.4 mmol) were dissolved in 0.5 mL of $CDCl_3$ and the solution was stirred for 2 h before the solution was analyzed by NMR. Single crystals were obtained by slow evaporation from the NMR-solution.
^{1}H NMR ($CDCl_3$) δ 7.71 (bs, 16H, PPh_2), 7.30 (m, 24H, PPh_2), 7.04 (d, 8H, J_1 = 8 Hz), 6.71 (d, 4H, J_1 = 8 Hz), 3.61 (s, 12H, OCH_3), 1.80 (bs, 8H), 1.26 (bs, 12H), -0.05 (t, 6H, PdCH_3).
^{13}C{1H} NMR ($CDCl_3$) δ 157.9, 140.4, 135.0, 133.3, 131.6, 130.9, 129.2, 127.5, 119.2, 119.0, 110.8, 55.5 (OCH_3), 45.1, 37.1, 26.3, 22.8, 3.8.
^{31}P{^{1}H} NMR ($CDCl_3$) δ 25.0 (s).
Anal. Calcd for $C_{90}H_{90}Cl_2O_4P_4Pd_2$: C, 65.78; H, 5.52. Found: C, 65.60; H, 5.46.

cis-**[$PtCl_2$(2)].**
$PtCl_2$(cod) (85.2 mg, 227.7 mmol) and ligand **2** (154.1 mg, 231.8 mmol) were dissolved in 1 mL of $CDCl_3$ and the solution was stirred for 2 h at room temperature. During this period a white precipitate formed that remained insoluble, probably oligomeric material. After filtration the filtrate was analyzed by ^{31}P{1H} NMR spectroscopy.
^{31}P{^{1}H} NMR ($CDCl_3$) δ 7.93 (s, $J_{Pt\text{-}P}$ = 3820 Hz).

trans,trans-**[{$PtCl_2$(μ-2)}$_2$] (complex 9).**
$PtCl_2$ (170.3 mg, 640.5 mmol) was refluxed in 10 mL of acetonitrile until the solid was completely dissolved. Ligand **2** (425.8 mg, 640.5 mmol) was added and the mixture stirred under reflux overnight. After cooling to r.t., the solvent was removed *in vacuo* to leave a yellow powder. Single crystals were obtained from acetone, by slow evaporation of the solvent.
^{1}H NMR ($CDCl_3$) δ 7.73 (q, 16H, PPh_2), 7.37 (br m, 24H, PPh_2), 7.09 (d, 4H), 7.01 (d, 4H), 6.67 (d, 4H), 3.63 (s, 12H, OCH_3), 1.71 (br s, 8H, cy-C_6), 1.23 (m, 12H, *c*-C_6).
^{31}P{^{1}H} NMR ($CDCl_3$) δ 15.8 (s, $J_{Pt\text{-}P}$ = 2705 Hz, 40 %, *trans*-dimer), 15.2 (s, $J_{Pt\text{-}P}$ = 2705 Hz, 60 %, *trans*-oligomer).
Anal. Calcd for $C_{88}H_{84}Cl_4O_4P_4Pt_2$: C, 56.78; H, 4.55. Found: C, 56.65; H, 4.45.

trans,trans-**[{RhCl(CO)(μ-2)}$_2$] (complex 10).**
$[RhCl(CO)_2]_2$ (170.3 mg, 640.5 mmol) and ligand **2** (425.8 mg, 640.5 mmol) were dissolved in 10 mL of CH_2Cl_2 and the reaction mixture stirred for 2 h. Evaporation of the solvent yielded a yellow solid. Single crystals were obtained by slow diffusion of CH_3CN into a CH_2Cl_2 solution of the solid.
^{1}H NMR ($CDCl_3$) δ 7.82 (br s, 16H, PPh_2), 7.46 (q, ^1J = 7.2 Hz, 8H, PPh_2), 7.38 (t, ^1J = 7.2 Hz, 16H, PPh_2), 7.00 (d, ^1J = 6.4 Hz, 4H), 6.87 (br s, 4H), 6.65 (d, ^1J = 8.8 Hz, 4H), 3.61 (s, 12H, OCH_3), 1.64 (br s, 8H, *o*-CH_2, *c*-C_6), 1.20 (br s, 12H, *m,p*-CH_2, *c*-C_6).
^{31}P{^{1}H} NMR ($CDCl_3$) δ 23.7 (d, $J_{Rh\text{-}P}$ = 128 Hz).
IR (ATR mode, carbonyl region) ν 1976 cm^{-1} (Rh*CO*).
Anal. Calcd for $C_{90}H_{84}Cl_2O_6P_4Rh_2$: C, 65.03; H, 5.09. Found: C, 64.88; H, 4.96.

cis-**[$PtCl_2$(5)], (complex 11).**
$PtCl_2$(cod) (35.9 mg, 95.9 mmol) was dissolved in 15 mL of CH_2Cl_2, and to this was slowly added ligand **5** (65.1 mg, 95.5 mmol), also dissolved in 15 mL of CH_2Cl_2. The solution was stirred overnight. The solvent was removed *in vacuo* and a white powder was obtained. Single crystals, suitable for X-ray analysis, could be obtained by slow evaporation of $CDCl_3$ from an NMR tube.

^{1}H NMR ($CDCl_3$) δ 7.83 (br s, 8H, PPh_2), 7.51 (dd, 2H, ^1J = 5.2 Hz, ^2J = 2.8 Hz), 7.44(dd, 2H, ^1J = 5.2 Hz, ^2J = 2.8 Hz), 7.23 (dd, 14H, Ph and PPh_2, ^1J = 8.8 Hz, ^1J = 2.4 Hz), 6.57 (dd, 2H, Ph, ^1J = 8.4 Hz, ^2J = 4.8 Hz), 6.35 (d, 2H, Ph, ^1J = 9.2 Hz), 5.64 (d, 2H, Ph), 3.63 (s, 6H, OCH_3).
^{31}P{^{1}H} NMR ($CDCl_3$) δ 16.1 (s, J_{Pt-P} = 2705 Hz).

Hydroformylation of 1-octene.
Hydroformylation experiments were performed in tailor-made 75 mL stainless steel autoclaves equipped with an inner glass-beaker. 1-Octene was filtered over neutral alumina before use, to remove peroxides. $Rh(acac)(CO)_2$ (2.00 mg, 7.75 μmol) and the appropriate amount of ligand (6 eq.) were both dissolved in 5 ml of toluene. The combined solution was transferred under argon into the autoclave, equipped with a glass inner beaker, which was preheated to 80 °C. The autoclave was then pressurized to 18 bar. After 1 hour 10 mL of the substrate solution of 1-octene (4.86 mL, 31.0 mmol) and decane (2.43 mL, 12.5 mmol) in toluene was added to the reaction mixture under 20 bar of synthesis gas. After reaction the autoclave was cooled and the reaction mixture quenched by addition of an excess of $P(OEt)_3$ to form inactive rhodium species.

High pressure NMR experiments.
Measurements were performed in a 10 mm outer diameter sapphire NMR tube, a home-made modification of the design described by Elsevier.[60] In a typical experiment 5.00 mg of $Rh(acac)(CO)_2$ and 1.05 equivalents of ligand were dissolved in 1.5 mL of toluene-d_8. The solution was brought into an argon-flushed tube. The tube was then flushed four times with 4 bar of synthesis gas and then pressurized at 20 bar. Preformation was carried out at 60 ºC for 16 h after which the tube was cooled down to r.t. and the desired spectra were recorded. Alternatively the chamber of a 10 mL autoclave was brought under an argon atmosphere after which the abovementioned solution was injected by syringe. After preformation at 80 ºC for 1 hour under stirring, the autoclave was depressurized, the contents transferred into a normal NMR tube and the spectra recorded at r.t.

High pressure FT-IR experiments.
Measurements were performed using a tailor-made 50 mL stainless steel autoclave with an integrated flow cell equipped with ZnSe windows, a mechanical stirrer and temperature control. Before use, argon was flushed through the apparatus for 2 h. The catalyst-containing mixture was transferred to the autoclave under a stream of argon. The solution was flushed 3 times with 4 bar synthesis gas before pressurizing to 17 bar at r.t. The autoclave was then heated to 80 °C and spectra were recorded every 10 minutes for 2 h.

Crystal structure determination of 1-3, 5, 6 and 8-10.
The data were collected on a Nonius Kappa CCD diffractometer with rotating anode. The structure was solved by direct methods using SHELXS97,[61] and refined on *F*2 by least-squares procedures using SHELXL97.[62] All non-hydrogen atoms were refined with anisotropic displacement parameters. Hydrogen atoms were constrained to idealized geometries and allowed to ride on their carrier atoms with an isotropic displacement parameter related to the equivalent displacement parameter of their carrier atoms. Compound **3** contains one phenyl ring on one of the phosphines which is disordered over two positions. Compound **8** contains four molecules of $CDCl_3$ in the unit cell. Compound **9** contains one acetone molecule, which is disordered over two positions. Structure validation and molecular graphics preparation were performed with the PLATON package.[63] Crystal data are given in Table 4.8 and Table 4.9.

Crystal structure determination of 11.
The data for **11** was collected on a *Bruker SMART APEX CCD*. Data integration and global cell refinement was performed with the program *SAINT*. Intensity data were corrected for Lorentz and polarization effects. The structure was solved by Patterson methods and extension of the model was accomplished by direct methods applied to difference structure factors using the program *DIRDIF*.[64] The positional and anisotropic displacement parameters for the non-hydrogen atoms were refined. The unit cell contains one molecule of $CDCl_3$, which is disordered over two positions. The hydrogen atoms were included in the final refinement riding on the C-atom as appropriate with $U_{iso} = c \times U_{equiv}$. Final refinement on F^2 carried out by full-matrix least-squares techniques converged at $wR(F^2) = 0.0673$ for 10560 reflections and $R(F) = 0.0275$ for 9320 reflections with $F_o \geq 4.0\ \sigma(F_o)$ and 677 parameters. Crystal data are given in Table 4.9.

Table 4.8: *Selected crystallographic data for compounds **1-3**, **5** and **6**.*

	1	**2**	**3**	**5**	**6**
Formula	$C_{41}H_{38}O_2P_2$	$C_{44}H_{42}O_2P_2$	$C_{46}H_{40}O_2P_2$	$C_{44}H_{36}O_2P_2$	$C_{44}H_{42}O_5P_2{\cdot}H_2O$
FW / M_r	624.65	664.72	686.72	658.67	714.73
Crystal size (mm)	0.12×0.27×0.42	0.12×0.15×0.45	0.21×0.39×0.48	0.27×0.15×0.09	0.09×0.21×0.24
Crystal system	Monoclinic	Monoclinic	Triclinic	Triclinic	Monoclinic
Space group	*C*2/*c* (no. 15)	$P2_1/c$ (no. 14)	$P\bar{1}$ (no. 2)	$P\bar{1}$ (no. 2)	$P2_1/c$ (no. 14)
A (Å)	28.1693(3)	17.4156(2)	11.1456(1)	9.4589(1)	12.2410(10)
B (Å)	8.2166(1)	7.8636(1)	12.0144(2)	10.8619(3)	11.9950(10)
c (Å)	32.3533(4)	28.3503(4)	15.0980(2)	18.4500(3)	27.398(3)
α (°)			89.1746(9)	80.1013(7)	
β (°)	115.7420(4)	113.2940(10)	70.6049(9)	76.3222(6))	114.279(11)
γ (°)			80.4301(5)	78.9500(10)	
V (A^3)	6745.21(14)	3566.08(8)	1878.66(4)	1791.68(5)	3667.1(7)
Z	8	4	2	2	4
d_{calc} (g cm^{-3})	1.230	1.238	1.214	1.221	1.295
μ (Mo-Kα) (mm^{-1})	0.164	0.159	0.153	0.158	0.165
T (K)	150	150	150	150	150
Total reflections	26580	28637	27481	28679	4661
Unique reflections (R_{int})	7617 (0.058)	8121 (0.055)	8452 (0.054)	8182 (0.058)	4661 (0.085)
wR_2 (F^2) (all data)	0.1025	0.1063	0.1159	0.1193	0.1921
λ (Å)	0.71073	0.71073	0.71073	0.71073	0.71073
R_1	0.0411	0.0452	0.0431	0.0467	0.0785
F(000)	2640	1408	724	692	1512

$R_{int} = \sum [|F_o^2 - F_o^2 (\text{mean})|] / \sum [F_o^2]$; $wR(F^2) = [\sum [w(F_o^2 - F_c^2)^2] / \sum [w(F_o^2)^2]]^{1/2}$; $R(F) = \sum (||F_o| - |F_c||) / \sum |F_o|$

Table 4.9: *Selected crystallographic data for complexes **8-11**.*

	8	**9**	**10**	**11**
Formula	$C_{90}H_{90}O_4P_4Pd_2 \cdot 4 \cdot CDCl_3$	$C_{88}H_{84}O_4P_4Pt_2 \cdot 4 \cdot CH_3C(O)CH_3$	$C_{90}H_{84}O_6P_4Cl_2Rh_2$	$C_{44}H_{36}Cl_2O_2P_2Pt \cdot CDCl_3$
FW / M_r	1643.34	1977.57	1662.17	1045.08
Crystal size (mm)	0.06×0.12×0.18	0.21×0.30×0.36	0.21×0.30×0.36	0.40×0.16×0.13
Crystal system	Triclinic	Monoclinic	Monoclinic	Monoclinic
Space group	$P\bar{1}$ (no.2)	$P2_1/c$ (no.14)	$P2_1/c$ (no.14)	$P2_1/n$ (no.14)
A (Å)	11.3951(2)	14.4501(2)	14.3323(10)	14.1508(6)
B (Å)	14.6487(2)	19.5893(3)	19.9531(12)	20.5058(8)
c (Å)	16.5314(2)	16.5611(2)	16.4423(19)	14.7262(6)
α (°)	63.8137(6)			
β (°)	77.9245(6)	112.0310(6)	112.66(2)	90.897(1)
γ (°)	79.6576(8)			
V (A^3)	2409.47(6)	4345.60(11)	4339.1(9)	4272.6(3)
Z	1	2	2	4
d_{calc} (g cm^{-3})	1.462	1.511	1.272	1.623
μ (Mo-Kα) (mm^{-1})	0.877	3.465	0.565	0.371
T (K)	150	150	150	100
Total reflections	37005	42286	82640	38867
Unique reflections (R_{int})	10960 (0.061)	8532 (0.072)	9954 (0.0505)	10560 (0.0338)
wR_2 (F^2) (all data)	0.1176	0.1106	0.070	0.0673
λ (Å)	0.71073	0.71073	0.71073	0.71073
R_1	0.0479	0.0587	0.029	0.0275
F(000)	1080	1984	1712	2064

$R_{int} = \sum [|F_o^2 - F_o^2 (\text{mean})|] / \sum [F_o^2]$; $wR(F^2) = [\sum [w(F_o^2 - F_c^2)^2] / \sum [w(F_o^2)^2]]^{1/2}$; $R(F) = \sum (||F_o| - |F_c||) / \sum |F_o|$

4.7 Notes and References

Parts of the work described in this chapter have been published:
W. Ahlers, R. Paciello, D. Vogt and J.I. van der Vlugt, (to BASF AG) U.S. Pat. 111,517, **2002** [*Chem. Abstr.*, **2002**, *137*, 169060].
J.I. van der Vlugt, J.M. Bonet, A.M. Mills, A.L. Spek and D. Vogt, *Tetrahedron Lett.*, **2003**, *44*, 4389.
J.I. van der Vlugt, M.M.P. Grutters, A.M. Mills, H. Kooijman, A.L. Spek and D. Vogt, *Eur. J. Inorg. Chem,* accepted.
J.I. van der Vlugt, R. van Duren, A. Meetsma and D. Vogt, *manuscript in preparation.*
M.M.P. Grutters, J.I. van der Vlugt, A.M. Mills, A.L. Spek and D. Vogt, *manuscript in preparation.*

1 C.D. Frohning, C.W. Kohlpainter and H.W. Bohnen, in *Applied Homogeneous Catalysis with Organometallic Compounds*; B. Cornils and W.A. Herrmann, Ed.; VCH, Weinheim, **2002**, vol. 1, 31.
2 P.C.J. Kamer, P.W.N.M. van Leeuwen and J.N.H. Reek, *Acc. Chem. Res.*, **2001**, *34*, 895.
3 a), T. J. Devon, G.W. Phillips, T.A. Puckette, J.L. Stavinoha and J.J. Vanderbilt (to Eastman Kodak), U.S. Pat. 4694109, **1987** [*Chem. Abstr.*, **1988**, *108*, 7890] b) T.J. Devon, G.W. Phillips, T.A. Puckette, J.L. Stavinoha and J.J. Vanderbilt (to Eastman Kodak), U.S. Pat. 5,332,846, **1994** [*Chem. Abstr.*, **1994**, *121*, 280879].
4 W. Ahlers, R. Paciello, D. Vogt and J.I. van der Vlugt (to BASF AG), U.S. Pat. 111,517, **2002** [*Chem. Abstr.*, **2002**, *137*, 169060].
5 Ullmann's Encyclopedia of Industrial Chemistry, 6th electronic edition, Wiley-VCH, Weinheim, **2002**.
6 a) C.G. Arena, D. Drommi, F. Faraone, C. Graiff and A.Tiripicchio, *Eur. J. Inorg. Chem.*, **2001**, 247; b) C.G. Arena, D. Drago and F. Faraone, *J. Mol. Cat. A: Chem.*, **1999**, *144*, 379; c) C.G Arena, D. Drago, M. Panzalorta, G. Bruno and F. Faraone, *Inorg. Chim. Acta*, **1999**, *292*, 84.
7 I. Bauer and W.D. Habicher, *Tetrahedron Lett.*, **2002**, *43*, 5245.
8 G.A. Consiglio, S. Failla, P. Finocchiaro and V. Siracusa, *Phosphorus, Sulfur and Silicon*, **1998**, *134-135*, 413.
9 L. Mou, G. Singh and J.W. Nicholson, *Chem. Commun.*, **2000**, 345.
10 T. Grawe, T. Scharader, P. Finocchiaro, G. Consiglio and S. Failla, *Org. Lett.*, **2001**, *3*, 1597.
11 a) H.C. Brown, *Organic Syntheses via Boranes*; Wiley, New York, **1975**, 104; b) E.A. Ivanova, S.I. Panchenko, I.I. Kolodkina and A.M. Yurkevich, *Zh. Obsch. Khim.*, **1975**, *45*, 786; c) A. Mendoza and D.S. Matteson, *J. Org. Chem.*, **1978**, *44*, 1352; d) A. Suzuki, *J. Organomet. Chem.*, **1999**, *576*, 147; e) N. Miyaura, A. Suzuki, *Chem. Rev.*, **1995**, *95*, 2457; f) A. Suzuki, *Pure Appl. Chem.*, **1994**, *66*, 213.
12 A.J. Blake, P.A. Cooke, K.J. Doyle, S. Gair and N.S. Simpkins, *Tetrahedron Lett.*, **1998**, *39*, 9093.
13 P.W. Baures and J.V. Silverton, *Acta Cryst.*, **1990**, *C46*, 715.
14 M.R. Churchill, R.F. See, S.L. Randall and J.D. Atwood, *Acta Cryst.*, **1993**, *C49*, 345.
15 S. Gladiali, S. Pulacchini, D. Fabbri, M. Manassero and M. Sansoni, *Tetrahedron: Asymmetry*, **1998**, *9*, 391.
16 A. Suárez, M.A. Méndez-Rojas and A. Pizzano, *Organometallics*, **2002**, *21*, 4611.
17 D.W. Allen and B.F. Taylor, *J. Chem. Soc., Dalton Trans.*, **1982**, 51.
18 R.P. Pinnell, C.A. Megerle, S.L.Manatt and P.A. Kroon, *J. Am. Chem. Soc.*, **1973**, *95*, 977.
19 T.B. Rauchfuss, F.T. Patino and D.M. Roundhill, *Inorg. Chem.*, **1975**, *14*, 652.
20 W. Marty, P.N. Kapoor, H.B. Bürgi and E. Fischer, *Helv. Chim. Acta,* **1987**, *70*, 158.
21 C.A. Bessel, P. Aggarwal, A.C. Marschilok and K.J. Takeuchi, *Chem. Rev.*, **2001**, *101*, 1031.
22 M.A. Zuideveld, B.H.G. Swennenhuis, M.D.K. Boele, Y. Guari, G.P.F. van Strijdonck, J.N.H. Reek, P.C.J. Kamer, K. Goubitz, J. Fraanje, M. Lutz, A.L. Spek and P.W.N.M. van Leeuwen, *J. Chem. Soc., Dalton Trans.*, **2002**, 2308.
23 K. Takenaka, Y. Obora, L.H. Jiang and Y. Tsuji, *Organometallics*, **2002**, *21*, 1158.
24 A. Mentes, R.D.W. Kemmitt, J. Fawcett and D.R. Russeli, *Polyhedron*, **1999**, *18*, 1141.
25 S.J. Young, B. Kellenberger, J.H. Reibenspies, S.E. Himmel, M. Manning, O.P. Anderson and J.K. Stille, *J. Am. Chem. Soc.*, **1988**, *110*, 5744.
26 A. Pryde, B.L. Shaw and B. Weeks, *J. Chem. Soc., Dalton Trans.*, **1976**, 322.
27 C.E. Housecroft, B.A.M. Shaykh, A.L. Rheingold and B.S. Haggerty, *Inorg. Chem.*, **1991**, *30*, 125.
28 J.A. Davies, S. Dutremez, A.A. Pinkerton and M. Vilmer, *Organometallics*, **1991**, *10*, 2956.
29 M.E. van der Boom, M. Gozin, Y. Ben-David, L.J.W. Shimon, F. Frolow, H.B. Kraatz and D. Milstein, *Inorg. Chem.*, **1996**, *35*, 7068.
30 K.K. Hii, M.Thornton-Pett, A. Jutand and R.P. Tooze, *Organometallics*, **1999**, *18*, 1887.

31 C.J. Cobley and P.G. Pringle, *Inorg. Chim. Acta*, **1997**, *265*, 107.
32 N.W. Alcock, L. Judd and P.G. Pringle, *Inorg. Chim. Acta*, **1986**, *113*, L13.
33 F.C. March, R. Mason, K.M. Thomas and B.L. Shaw, *J. Chem. Soc. Chem Commun.*, **1975**, 584.
34 F.E. Wood, J. Hvoslef, H. Hope and A.L. Balch, *Inorg. Chem.*, **1984**, *23*, 4309.
35 S.K. Armstrong, R.J. Cross, L.J. Farrugia, D.A. Nichols and A. Perris, *Eur. J. Inorg. Chem.*, **2002**, 141.
36 P. Suomalainen, S Jääskeläinen, M. Haukka, R.H. Laitinen, J. Pursiainen and T.A. Pakkanen, *Eur. J. Inorg. Chem.*, **2000**, 2607.
37 M.J. Atherton, K.S. Coleman, J. Fawcett, J.H. Holloway, E.G. Hope, A. Karaçar, L.A. Peck and G.C. Saunders, *J. Chem. Soc., Dalton Trans*., **1995**, 4029.
38 a) L. Vaska and J. Peone Jr., *J. Chem. Soc., Chem. Comm.*, **1971**, 418; b) K.G. Moloy and J.L. Petersen, *J. Am. Chem. Soc.*, **1995**, *117*, 7696.
39 F.B. Xu, Q.S. Li, X.S. Zeng, X.B. Leng and Z.Z. Zhang, *Organometallics*, **2002**, *21*, 4894.
40 J.R. Dilworth, Y. Zheng and D.V. Griffiths, *J. Chem. Soc., Dalton Trans.*, **1999**, 1877.
41 C.M. Thomas, R. Mafua, B. Therrien, E. Rusanov, H. Stœckli-Evans, G. Süss-Fink, *Chem. Eur. J.*, **2002**, *8*, 3343.
42 T.W. Graham, A. Llamazares, R. McDonald and M. Cowie, *Organometallics*, **1999**, *18*, 3502.
43 N.W. Alcock, J.M. Brown and J.C. Jeffery, *J. Chem. Soc., Dalton Trans.,* **1977**, 888.
44 a) D.C. Smith Jr., E.D. Stevens and S.P. Nolan, *Inorg. Chem*., **1999**, *38*, 5277; b) E. Valls, J. Suades, R. Mathieu and N. Lugan, *Eur. J. Inorg. Chem.*, **2003**, 3047.
45 A.L. Balch, L.A. Fossett, M.M. Olmstead, D.E. Oram and P.E. Reedy Jr., *J. Am. Chem. Soc.*, **1985**, *107*, 5272.
46 X. Liu, A.H. Eisenberg, C.L. Stern and C.A. Mirkin, *Inorg. Chem.*, **2001**, *40*, 2940.
47 M.F.M. Al-Dulaymmi, D.L. Hughes and R.L. Richards, *J. Organomet. Chem.*, **1992**, *424*, 79.
48 a) M. Cowie, S.K. Dwight and A.R. Sanger, *Inorg. Chim. Acta*, **1978**, *31*, L407; b) M. Cowie and S.K. Dwight, *Inorg. Chem.*, **1980**, *19*, 2500.
49 M. Camalli, F. Caruso, S. Chaloupka, P.N. Kapoor, P.S. Pregosin and L.M. Venanzi, *Helv. Chim. Acta*, **1984**, *67*, 1603.
50 J. Yin and S.L. Buchwald, *J. Am. Chem. Soc.*, **2002**, *124*, 6043.
51 M.H. Johannson and S. Otto, *Acta Cryst.*, **2000**, *C56*, e12.
52 E.K. van den Beuken, A. Meetsma, H. Kooijman, A.L. Spek and B.L. Feringa, *Inorg. Chim. Acta*, **1997**, *264*, 171.
53 F. Maienza, M. Wörle, P. Steffanut, A. Mezzetti and F. Spindler, *Organometallics*, **1999**, *18*, 1041.
54 M. Kranenburg, J.G.P. Delis, P.C.J. Kamer, P.W.N.M. van Leeuwen, K. Vrieze, N. Veldman, A.L. Spek, K. Goubitz and J. Fraanje, *J. Chem. Soc., Dalton Trans.*, **1997**, 1839.
55 L.A. van der Veen, P.H. Keeven, G.C. Schoemaker, J.N.H. Reek, P.C.J. Kamer, P.W.N.M. van Leeuwen, M. Lutz and A.L. Spek, *Organometallics*, **2000**, *19*, 872.
56 C.P. Casey, G.T. Whiteker, M.G. Melville, L.M. Petrovich, J.A. Gavney Jr. and D.R. Powell, *J. Am. Chem. Soc.*, **1992**, *114*, 5535.
57 D.R. Drew and J.R. Doyle, *Inorg. Synth.*, **1990**, *28*, 346.
58 F.T. Ladipo and G.K. Anderson, *Organometallics*, **1994**, *13*, 303.
59 H.C. Clark and L.E. Manzer, *J. Organomet. Chem.*, **1973**, *59*, 411.
60 C.J. Elsevier, *J. Mol. Cat.*, **1994**, *92*, 285.
61 G.M. Sheldrick, SHELXS97; University of Göttingen, Germany, **1997**.
62 G.M. Sheldrick, SHELXL97; University of Göttingen, Germany, **1997**.
63 A.L. Spek, PLATON, A Multipurpose Crystallographic Tool; Utrecht University, The Netherlands, **2002**.
64 P.T. Beurskens, G. Beurskens, R. de Gelder, S. García-Granda, R.O. Gould, R. Israël and J.M.M. Smits, The *DIRDIF*-99 program system; University of Nijmegen, The Netherlands, **1999**.

5

Novel Silsesquioxane Based Phosphorus Containing Ligands

Abstract O*ligosilsesquioxanes are employed as ligand backbones for the synthesis of novel phosphorus-containing compounds* ***2-4*** *and* ***6-9****. Both mono- and bidentate phosphinites and phosphites are prepared in good yields. Two types of silsesquioxanes are employed as starting materials, viz. the completely condensed, thallium silsesquioxide (*c-$C_5H_9)_7Si_7O_{12}$*SiOTl, and the incompletely condensed, monosilylated disilanol (*c-$C_5H_9)_7Si_7O_9(OSiMePh_2)(OH)_2$*. Density Functional Theory has been used to get insight into the electron-withdrawing character of the resulting ligands. The coordination of these compounds, especially of the bidentate derivatives, towards various transition metals is studied, both by NMR spectroscopy as well as by X-ray crystallography. Unprecedented molecular structures of palladium, platinum, molybdenum and rhodium complexes with these novel silsesquioxane based phosphorus containing ligands are described. With the monophosphite ligand* ***7*** *a* trans-*[$PtCl_2$(**7**)$_2$]complex is formed. The bidentate diphosphinite ligand* ***8*** *shows a clear tendency to coordinate in a* cis*-fashion to Pd, Pt and Mo.* Trans*-coordination is observed only in the complex* trans*-[RhCl(CO)(**8**)], which is also structurally characterized. With the diphosphite ligand* ***9*** *bearing bulky groups, various modes of coordination are possible. The molecular structures for the complexes* trans*-[$PdCl_2$(**9**)],* cis*-[$Mo(CO)_4$(**9**)] and the dinuclear complex [{Rh(*μ*-Cl)(CO)}$_2$(*κ^2*-**9**)] have been determined. In the rhodium catalyzed hydroformylation of 1-octene high activities with turnover frequencies of up to 6800 h^{-1} are obtained with these new nanostructured phosphorus ligands.*

5.1 Introduction

Silsesquioxane is the general name for a family of molecular spherosilicates with the formula $[RSiO_{3/2}]_n$. R stands for an inorganic or organic group, n ranging from 4 to 30, with typical values of 6, 8, 10 or 12. A common synthetic route towards these polyhedral oligomeric silsesquioxanes (also referred to as **POSS**) uses the hydrolytic multiple condensation of $RSiY_3$ in an acetone/water mixture to form dimers, tetramers, *etc*.[1] Usually, the substituent Y is a highly reactive group such as chloride or alkoxide, while R is an alkyl group such as isobutyl, cyclopentyl or cyclohexyl.

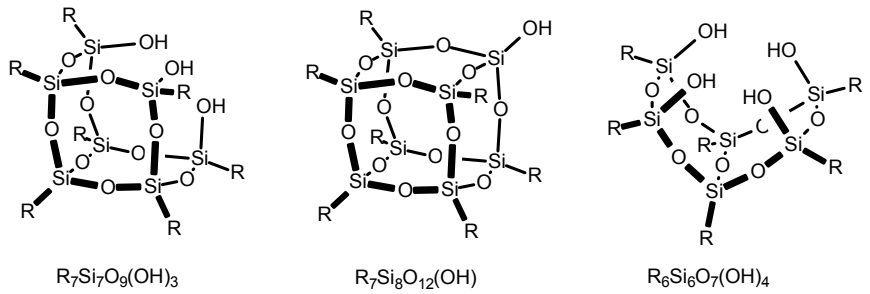

Figure 5.1: *Schematic overview of different types of silsesquioxane structures.*

Because the preparation of these compounds via hydrolytic condensation of trifunctional silanes is often a very slow process, other synthetic routes are preferred. It has recently been shown that incompletely condensed silsesquioxanes can be prepared in high yield and short reaction times by base-mediated cleavage of fully condensed $[RSiO_{3/2}]$ frameworks, which are instead easily available.[2]

Silsesquioxanes have been extensively studied for several years, either as homogeneous models for silica supports,[3] as building blocks for inorganic or hybrid materials[4-6] or as ligand backbones for (transition) metal complexes.[7,8] However, the synthesis and application of phosphorus ligands based on silsesquioxane frameworks has hardly received any attention to date. The few systems reported so far are mainly several peripherally functionalized (dendritic) silsesquioxanes containing phosphorus moieties, tethered by various (alkyl) spacers.[9-12]

In addition, silsesquioxanes are known to have electron-withdrawing properties similar to conventional silica.[13] Previous studies with simple π-acidic phosphites which have already showed interesting effects on the regioselectivity and rates in hydroformylation.[14] Research interest was therefore the development of new phosphorus ligands based on silsesquioxane backbones, in order to study whether such backbones could have beneficial effects. Mono- and bidentate phosphorus compounds, both phosphinite and phosphite, were synthesized. Their coordination towards various metal precursors was investigated as well as their application in the rhodium catalyzed hydroformylation of 1-octene.

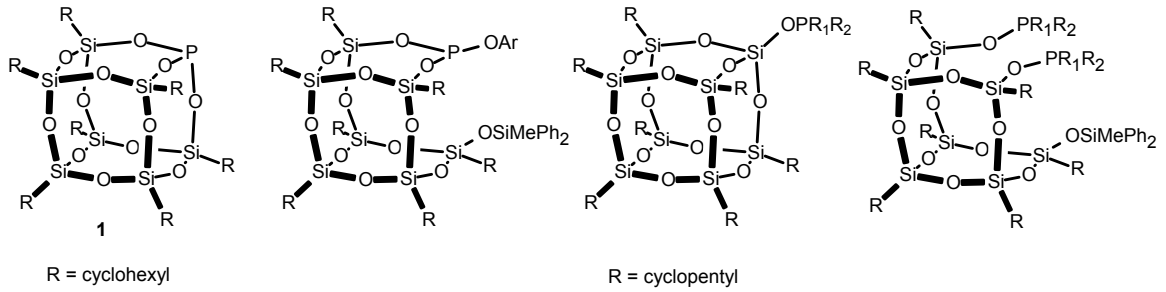

Figure 5.2: *General representation of the phosphorus containing silsesquioxane-based compounds applied.*

First examples for phosphite ligands in rhodium catalyzed hydroformylation of 1-alkenes were reported by Pruett and Smith at Union Carbide.[15] Phosphites are generally better π-acceptors than phosphines and therefore have great potential in hydroformylation, because the metal-CO bond is weakened, leading to accelerated CO dissociation and higher reaction rates. Other advantages are the easier synthesis and decreased sensitivity towards oxidation of the phosphorus atoms. On the other hand, phosphites are more sensitive to side reactions such as hydrolysis, alcoholysis, Arbuzov reaction[16] and C-O cleavage. Phosphinites resemble phosphines in their σ-donor character, yet their synthesis is more straightforward, since it does not require the lithiation of the backbone as an intermediate step.

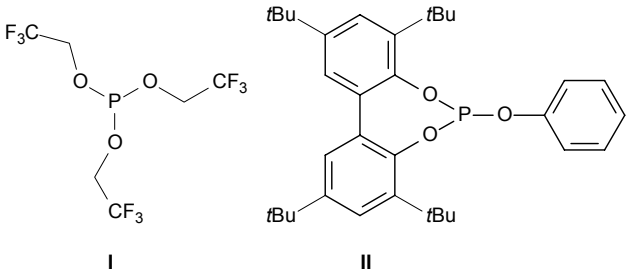

Figure 5.3: *Two representative examples of monophosphites from the literature.*[14,17]

Often the selectivity for the linear aldehyde increases when electron-withdrawing ligands are applied. This can be exemplified by the difference between the ligands $P(OEt)_3$ and tris(2,2,2-trifluoroethyl)phosphite, **I**.[14] Applying 1-heptene as the substrate, the rhodium catalyst containing $P(OEt)_3$ gave a poor regioselectivity (*i.e.* low l/b ratio), while with ligand **I** the linear to branched (l/b) ratio was 19. The observed rate of this latter reaction however was rather low. By using bulky phosphites like tris(2-*tert*-butyl-4-methylphenyl)phosphite **II**, very high reaction rates up to 85,000 h^{-1} in the hydroformylation of 1-octene were achieved, albeit with lower l/b ratios. It was shown that mono-ligated complexes were formed which led to enhanced activities.[17,18]

Other reports based on bulky monophosphites[19,20] often showed high reaction rates, but most systems suffered from a low regioselectivity, which is still a common feature of monodentate ligands. Bidentate diphosphite ligands have been developed to circumvent this problem,[21-23] whereby the bridge length between the two phosphorus atoms appeared to have a large influence on the catalytic results.

This chapter describes the synthesis of novel silsesquioxane based phosphorus containing monodentate ligands **2**-**4**, **6** and **7** and bidentate compounds **8** and **9**. The coordination of these latter two ligands towards various transition metals, *viz.* Pd, Pt, Mo and Rh, is described. Also the application of the silsesquioxane derived phosphites as ligands in the Rh catalyzed hydroformylation of 1-octene is investigated.

5.2 Synthesis

5.2.1 Monodentate ligands

Two routes to arrive at monodentate ligands have been explored. The first was based on the work reported by Feher *et al.* describing the synthesis of compound **1**, which will be used as a reference compound in the rhodium catalyzed hydroformylation. No catalytic results are known for this ligand to date.[24] Starting from the incompletely condensed silsesquioxane trisilanol $(c\text{-}C_5H_9)_7Si_7O_9(OH)_3$,[25] the monophosphite compounds **2-4** (generally named POSSphites) were synthesized in a three step reaction in good yield (Scheme 5.1).

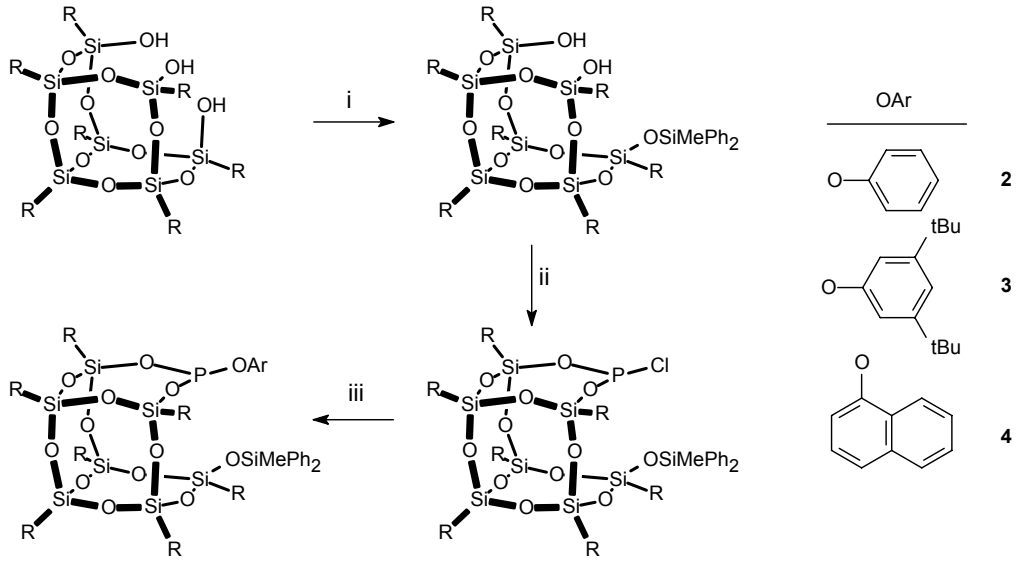

Scheme 5.1: *Synthetic route to compounds **2-4**: i) $ClSiMePh_2$, NEt_3, THF, 1h; ii) PCl_3, NEt_3, THF, -15 °C, 30 min; iii) for **2**: ArOH, THF, -78 °C, 15 min, then r.t., 16 h; R = (c-C_5H_9).*

After initial monosilylation of the trisilanol,[26] the resulting disilanol was reacted with PCl_3 in the presence of NEt_3 to generate a phosphorochloridite functionalized silsesquioxane. This compound was converted *in situ* to the desired monophosphite by reaction with the appropriate phenol in the presence of NEt_3. The incorporation of the phosphorus moiety into the silsesquioxane skeleton was monitored by NMR. The C_s symmetry of the silsesquioxane framework is evident from the ^{13}C and ^{29}Si NMR spectra, indicative of a structure where the two remaining siloxy groups are attached to a phosphorus atom.

To compare the reactivity and electron-withdrawing character of the synthesized monodentate phosphites **2-4** based on silsesquioxanes with that of simple siloxane based systems, the disilanol $Ph_2Si(OH)OSi(OH)Ph_2$ **III** was chosen as starting material. Despite various attempts, the selective synthesis of any (di)phosphite, diphosphinite or monophosphonite based on this skeleton failed, due to an intrinsic difference in the electronic character of the compound.[27] Therefore the commercially available tris(*tert*-butyl-dimethylsilyl)phosphite **5** is used as a reference compound for catalysis.

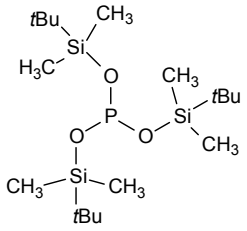

5

The relative instability of the phosphorochloridite resulting from the reaction of the disilanol $(c\text{-}C_5H_9)_7Si_7O_9(OH)_2OSiMePh_2$ with PCl_3 could easily lead to inseparable impurities. Therefore the straightforward reaction of a monosilanol with the desired PCl-compound was studied. Monosilanol **A** can be obtained from the incompletely condensed silsesquioxane trisilanol $(c\text{-}C_5H_9)_7Si_7O_9(OH)_3$ in two steps.[28] To enhance the reactivity of the siloxy group, the silanol is then converted into a thallium silsesquioxide.[29] Reaction with the appropriate phosphorochloridite gave the desired compounds **6** and **7** in high yields (Scheme 5.2). As expected, the ^{13}C NMR spectrum reflects the 4:3:1 ratio between the *ipso*-carbons of the cyclopentyl groups.

So far little chemistry has been performed with such completely condensed monofunctionalized silsesquioxanes. Duchateau has described on titanium and zirconium complexes covalently linked to the framework by an oxo group.[29a] Furthermore, some zirconocene complexes have been prepared and structurally characterized by Duchateau, however with a CH_2 group instead of an oxo bridge.[29b,c] The group of Edelmann has reported very recently on attempts to synthesize a phosphorusdiamide based on the same monosilanol, as depicted in Scheme 5.2, by reaction with $P(NMe_2)_3$.[30] So far no structural characterization of any siloxy functionalized completely condensed silsesquioxane has been published.

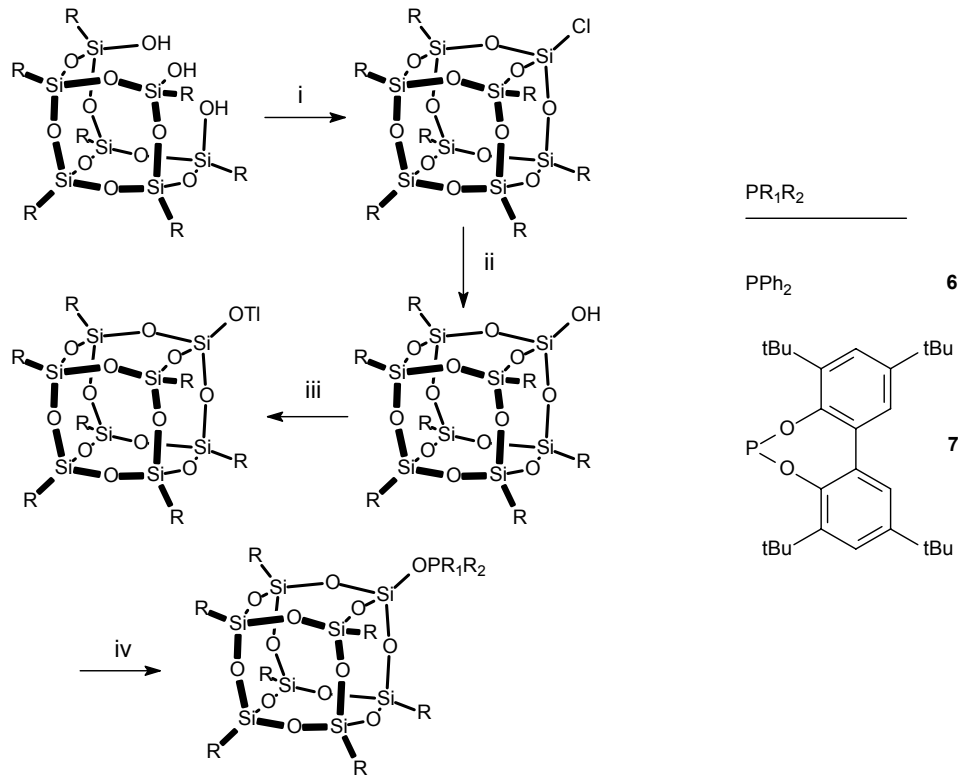

Scheme 5.2: *Synthetic-route to compounds **6** and **7**: i) $SiCl_4$, 3 eq. NEt_3, THF; ii) H_2O; iii) TlOEt; iv) $ClPPh_2$ (for **6**) or phosphorochloridite $ClPO_2C_{28}H_{40}$ (for **7**), NEt_3, toluene, 16 h; R = (c-C_5H_9).*

5.2.2 Bidentate ligands

To evaluate the results – both in cooordination chemistry and in catalysis – of the monodentate compounds based on the completely condensed silsesquioxide framework, the diphosphinite **8** and diphosphite **9** were synthesized (Scheme 5.3). Compounds **8** and **9** were prepared from the incompletely condensed silsesquioxane disilanol $(c\text{-}C_5H_9)_7Si_7O_9(OH)_2OSiMePh_2$ in a one-step reaction, which in turn is available by selective monosilylation of the corresponding trisilanol $(c\text{-}C_5H_9)_7Si_7O_9(OH)_3$.[25] The methyldiphenylsilyl group is used instead of the more commonly known trimethylsilyl unit because of crystal engineering reasons, as silsesquioxanes containing this former group have a higher tendency to crystallize.[26] Yields varied from 86% for the diphosphinite **8** to 79% for the bulky diphosphite **9**. Both compounds were fully characterized by ^{1}H, ^{13}C and ^{31}P NMR spectroscopy as well as by elemental analysis.

The corresponding reaction of Cl_2PPh with the tetrasilanol $(c\text{-}C_5H_9)_7Si_6O_7(OH)_4$[31] failed to give one well-defined product, probably due to scrambling of thermodynamic and kinetic reaction products. An attempt to synthesize a tridentate phosphinite ligand, by reaction of $(c\text{-}C_5H_9)_7Si_7O_9(OH)_3$ with three equivalents of $ClPPh_2$ lead to an inseparable mixture of products.

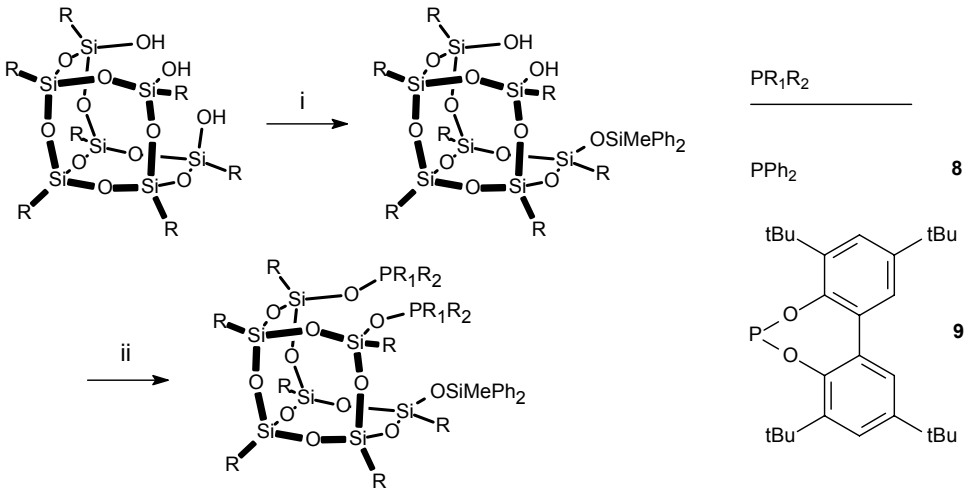

Scheme 5.3: *Synthetic route to compounds **8** and **9**: i) 2 eq. $ClPPh_2$ (for **8**) or phosphorochloridite (for **9**), NEt_3, toluene, 16 h; R = (c-C_5H_9).*

In the ^{13}C NMR spectrum of both compounds **8** and **9**, the expected 2:2:1:1:1 ratio was observed for the signals of the *ipso*-carbons of the cyclopentyl groups on the silicon atoms in the silsesquioxane framework. Single crystals, suitable for X-ray analysis, were obtained for compound **9**, by recrystallization from a hot dichloromethane/acetonitrile mixture. The molecular structure for this compound is depicted in Figure 5.4, while selected bond lengths and angles are listed in Table 5.1.

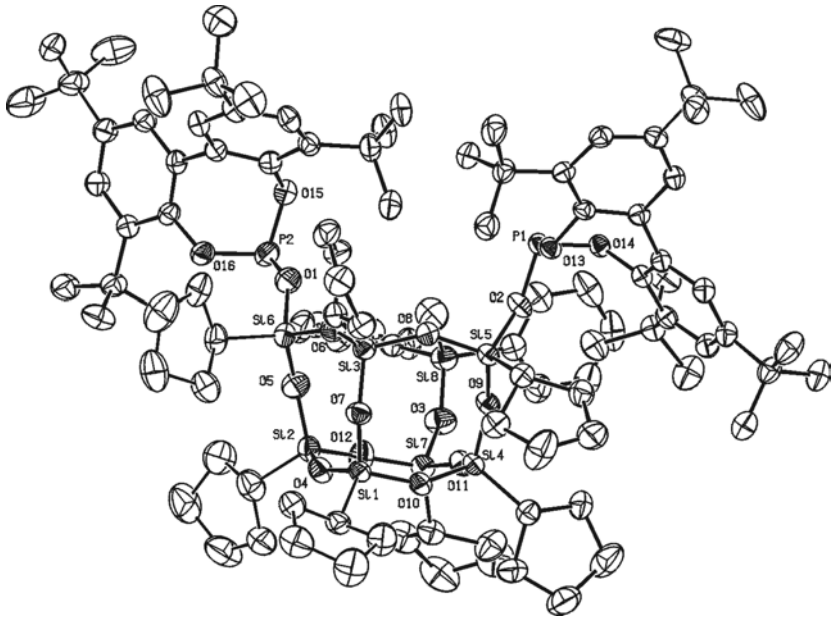

Figure 5.4: *ORTEP representation of compound **9**. Displacement ellipsoids are drawn at the 50% probability level. All hydrogen atoms are omitted for clarity.*

Due to rotational freedom around the P-O(silsesquioxane) bonds the phosphite groups are not constrained to any particular mutual orientation. The intramolecular P-P distance of 7.6782 Å in the solid state seems rather large, but coordination to transition metals in a chelating manner may still be possible and can not be excluded as yet. As is normally observed for silsesquioxane framework structures, the oxygen atoms are bent outward slightly, with an average Si-O-Si angle of around 150°.[3a]

Table 5.1: *Selected bond lengths, distances and angles for compound **9**.*

Bond lengths (Å)					
P_1-O_2	1.5911(18)	P_2-O_1	1.589(2)	Si_5-O_2	1.6404(18)
Si_6-O_1	1.636(2)	Si_4-O_9	1.6217(18)	Si_5-O_9	1.6149(18)
Si_7-O_3	1.609(3)	Si_8-O_3	1.630(2)	P_1-P_2	7.6782(8)
Angles (°)					
Si_5-O_2-P_1	144.11(11)	Si_6-O_1-P_2	143.17(13)	Si_4-O_9-Si_5	152.30(11)
		Si_7-O_3-Si_8	150.05(14)		

Diphosphinite compound **8** was allowed to react with elemental selenium, in order to convert both phosphinite groups into the corresponding selenides. If there is a noticeable influence of the electronic properties of the silsesquioxane framework, this might be indicated by the value for the coupling constant $J_{Se\text{-}P}$. Since the stability towards oxidation is fairly low for most phosphinites, the reaction went to completion in approximately 1 hour in toluene at 100 °C. In the ^{31}P NMR spectrum of diselenide **10**, a singlet was found at δ = 69.8 ppm together with ^{77}Se satellites and a corresponding coupling constant $J_{Se\text{-}P}$ of 816 Hz (in CH_2Cl_2). This value is in agreement with the few available literature data.[32-34] However, due to the limited amount of reference data and the fact that NMR chemical shift values are not only influenced by electronic effects it is hard to draw definite conclusions on the electron-withdrawing character of the silsesquioxane backbone.

5.3 DFT calculations on model compounds.

To get insight into the electronic implications of applying the silanol groups of silsesquioxanes as an anchor for phosphorus ligands instead of 'standard' hydroxyl functionalities, DFT calculations were performed on some simple models. Therefore compound **IV**, the simplest phosphinite with an alkoxy group and compound **V**, as model for the silsesquioxane based diphosphinite compound **8**, were compared with respect to their Mulliken electron density distributions.

5.3.1 Models.

Silsesquioxanes are reported to have electron-withdrawing character.[13] In order to compare the electronic properties of the silyl based phosphinite ligand **8** with a 'normal' alkoxy based phosphinite, the electron density on the phosphorus atoms of two respective model compounds were calculated using DFT methods. As simple model precursors CH_3OPPh_2 (**IV**) and $H_2P(O(HSiOH))_2OPPh_2$ (**V**) have been considered (Figure 5.5). The silyl chain is long enough to avoid electronic influence from the opposite end side of the molecule and, at the same time, will provide information on the differences between the PH_2 group, commonly used in modelling, and the more realistic PPh_2 group, the former normally chosen for obvious restrictions by the computational capabilities.

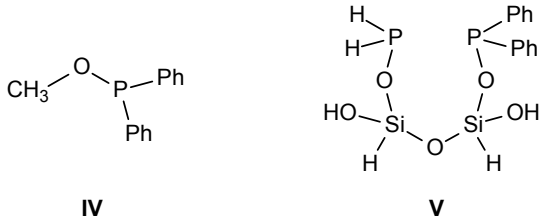

IV **V**

Figure 5.5: *Illustration of the two model compounds **IV** and **V** used in the DFT calculations.*

5.3.2 Geometries.

From the calculations run on the model compounds as depicted in Figure 5.5, the optimized geometries gave the selected geometric parameters (bond lengths and angles) as listed in Table 5.2. From the listed bond lengths it is clear that there is a slight difference in the P-$C_{\alpha,Ph}$ length of 0.1 Å found for the two compounds ($C_{\alpha,Ph}$ is the *ipso*-carbon of the phenyl group attached to phosphorus). This difference can be considered within the error limit of the calculated quantities. The P-O bond lengths are the same. A sensible difference, as expected, has been found between the P-O bond length of the $H_2P(O(HSiOH))_2OPPh_2$ molecule when P is attached to a phenyl group (0.184 nm) or to a hydrogen atom (0.162 nm).

The only comparable angles between the two molecules, the $C_{\alpha,Ph}$-P-O angles, are shown to yield a difference of ~1° with the CH_3OPPh_2 being higher in value. From the preceding geometrical analysis, little can be deduced on the difference between the PPh_2 moieties present in the silyl based model compound **V** and in the CH_3OPPh_2 reference system **IV**. A following charge distribution could give a better estimation of the difference between the phosphorus atoms in the two model compounds.

Table 5.2: *Selected bond lengths and angles for the optimized geometries of compounds **IV** and **V**.*

CH_3OPPh_2 (IV)		$H_2P(O(HSiOH))_2OPPh_2$ (V)	
Bond lengths (Å)			
P-$C_{\alpha, Ph}$	1.85	P-$C_{\alpha, Ph}$	1.84
P-O	1.68	P_{Ph}-O	1.68
C-O	1.43	Si-O	1.66
C-H	1.09	P_H-O	1.62
		P-H	1.42
		Si-H	1.46
Angles (°)			
$C_{\alpha, Ph}$-P-O	99.19	$C_{\alpha, Ph}$-P-O	98.17
P-O-CH_3	117.28	P_{Ph}-O-Si	127.73
		Si-O-Si	168.50
		Si-O-P_H	128.29
		O-P-H	97.65

Charges. The electronic distributions in the modelled compounds were analyzed through an electrostatic charge analysis. Although atomic charges are not a quantum mechanical observable, they are appropriate to get an idea of the electron distribution. Different schemes and algorithms can be employed. In this study the Mulliken population analysis was considered.[35] This method assigns charges by partitioning the orbital overlap evenly between the two atoms which are involved. In Table 5.3 the Mulliken atomic charges between the two compounds **IV** and **V** are reported and compared.

Table 5.3: *Selected Mulliken Atomic Charges[a] for model compounds **IV** and **V**.*

CH_3OPPh_2 (IV)		$H_2P(O(HSiOH))_2OPPh_2$ (V)[b]	
P	0.192	**P**Ph_2	0.260
O	-0.516	Ph_2P**O**	-0.580
CH_3	-0.238	Si	1.050
		OPH_2	-0.689
		PH_2	0.389

[a] Electron Units (charge of electron is equal to -1).

[b] Atoms considered in the Mulliken Population analysis are bold face.

A slight difference between the charge on the phosphorus atom of **IV** and the **P**Ph_2 atom of **V** is calculated (|0.068|) due to the higher electron-withdrawing effect of the siloxy skeleton. This relates to the charges found for the oxygen atoms, since a higher negative charge (|0.064|) is present in **V**.

Also the positive charge present on the silicon atom of the silyl based model compound supports this, compared to the negative charge situated on the carbon of the methoxy group in compound **IV**. The two central Si atoms of the $H_2P(O(HSiOH))_2OPPh_2$ model show the same charges, while the oxygens attached to the two phosphorus atoms have a difference of |0.109|. Remarkable is the difference between the two phosphorus atoms in compound **V**, in the PPh_2 group and the PH_2 group, reaching a value of |0.129|, which states as evidence for the large difference between the two systems. In the limit of the Mulliken analysis and of the model compounds considered here, the charge distributions showed a clear difference between the two systems, *i.e.* whether the P atom is followed by an alkoxy or a siloxy chain. This may serve as an approximation for the electron-withdrawing character expected for silsesquioxane frameworks such as present in compound **8** and as such indicate that silsesquioxanes can be regarded as models for silica surfaces.[3,13] As an interesting intermediate between the two 'extremes' **IV** and **V**, the model compound $R_3SiOPPh_2$ should be investigated next, to allow for a more precise comparison between the electron-withdrawing abilities of the model compounds and the effect on the phosphorus atoms present.

5.4 Coordination Chemistry

5.4.1 Monodentate ligands

Edelmann and co-workers have recently claimed the formation of a *cis*-$PtCl_2(P)_2$ compound, P being a silsesquioxane based phosphorodiamide $(c\text{-}C_6H_{11})_7Si_8O_{12}OP(NMe_2)_2$. Their conclusions are, however, based on an incorrect interpretation of the observed coupling constant $J_{Pt\text{-}P}$ of 2730 Hz, since such a value typically indicates a complex with both phosphorus ligands in a mutual *trans*-fashion.[30,36]

Based on these findings, also the complexation behaviour of ligand **7** towards platinum was investigated. After reaction with $PtCl_2$(cod), the ^{31}P NMR spectrum of the corresponding white solid showed a singlet at δ = 80.3 ppm, together with ^{195}Pt satellites and a coupling constant $J_{Pt\text{-}P}$ of 4680 Hz, which is characteristic for two phosphites coordinated in a *trans*-fashion (Scheme 5.4).[36,37] No dealkylation was observed.

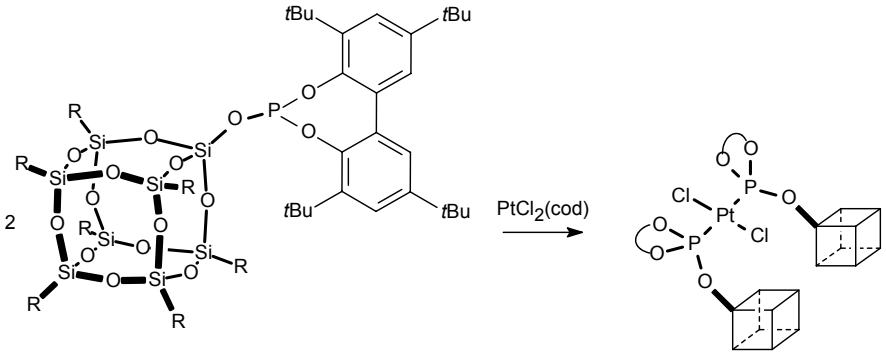

Scheme 5.4: *Reaction of compound **7** with $PtCl_2$(cod) to form complex **11**,* trans-*[$PtCl_2$(**7**)$_2$]*.

By slow diffusion of CH_3CN into a CH_2Cl_2 solution of this compound, single crystals could be grown that were suitable for X-ray analysis. From the crystallographic study, it is clear that this complex is indeed *trans*-[$PtCl_2$(**7**)$_2$], as is evident from the molecular structure, depicted in Figure 5.7. Relevant bond lengths and bond angles are listed in Table 5.4.

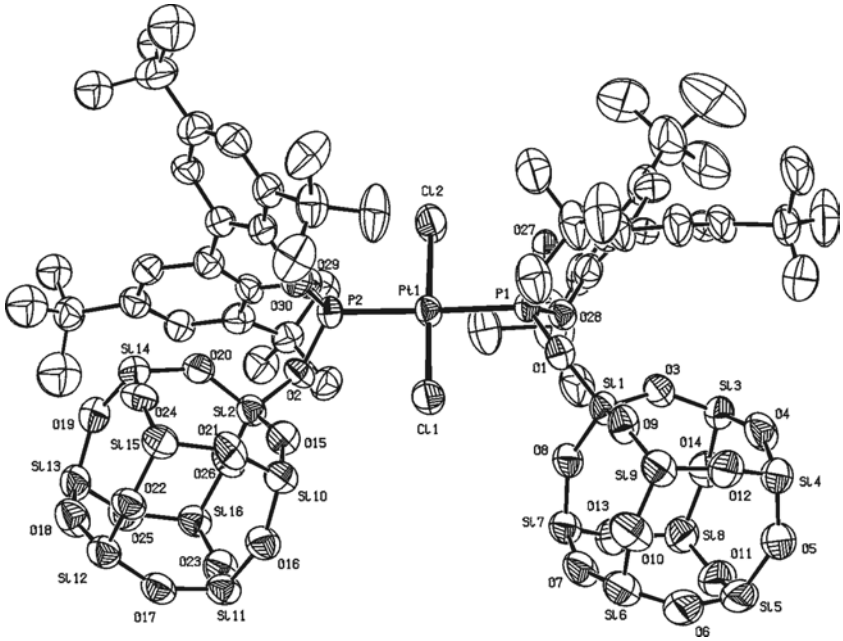

Figure 5.6: *ORTEP representation of complex **11**,* trans-*[$PtCl_2$(**7**)$_2$]. Displacement ellipsoids are drawn at the 50% probability level. All hydrogen atoms and all cyclopentyl substituents are omitted for clarity.*

The geometry around the platinum atom in complex **11** is only slightly distorted square planar, as can be concluded from the angles P_1-Pt-P_2 of 178.36(9)° and Cl_1-Pt-Cl_2 of 178.74(12)°. Both silsesquioxane groups are located on the same side of the molecule. This rather unexpected phenomenon must result from favourable packing interactions that dominate over steric constraints in the solid state configuration only. The closest intramolecular Si-Si distance between the two

silsesquioxane moieties is Si_7-Si_{10} of 7.635(5) Å. The slight distortion from ideal square planarity is also apparent from the angles P_1-Pt-Cl_1 (91.00(10)°) and P_1-Pt-Cl_2 (87.82(10)°). The intramolecular P-P distance is 4.529(4) Å. The Pt-P bond lengths (2.267(3) Å for Pt-P_1 and 2.262(3) Å for Pt-P_2) are slightly but significantly longer than for other platinum-phosphite complexes reported in literature, while the Pt-Cl bond lengths (2.279(3) Å for Pt-Cl_1 and 2.304(3) Å for Pt-Cl_2) on the contrary are somewhat elongated in comparison with these reference-compounds.[38,39] This is believed to be a clear indication of the electron-withdrawing character of the silsesquioxane framework.

Table 5.4: *Selected bond lengths, distances and angles for complex **11**,* trans-*[$PtCl_2(7)_2$]*.

Bond lengths (Å)					
Pt-P_1	2.267(3)	Pt-P_2	2.262(3)	Pt-Cl_1	2.279(3)
Pt-Cl_2	2.304(3)	P_1-O_1	1.567(6)	P_2-O_2	1.569(6)
Si_1-O_1	1.635(6)	Si_2-O_2	1.646(6)	Si_1-O_3	1.601(7)
Si_2-O_{15}	1.604(7)	P_1-O_{27}	1.583(7)	P_1-O_{28}	1.601(7)
P_2-O_{29}	1.581(7)	P_2-O_{29}	1.598(7)	P_1-P_2	4.529(4)
Angles (°)					
Cl_1-Pt-Cl_2	178.74(12)	P_1-Pt-P_2	178.36(9)	P_1-Pt-Cl_1	91.00(10)
P_1-Pt-Cl_2	87.82(10)	P_2-Pt-Cl_1	90.31(10)	P_2-Pt-Cl_2	90.87(10)
Si_1-O_1-P_1	139.6(4)	Si_2-O_2-P_2	141.4(4)	Pt-P_1-O_1	118.4(3)
Pt-P_2-O_2	117.4(3)	Si_1-O_3-Si_3	145.3(4)	Si_2-O_{15}-Si_{10}	150.2(5)

5.4.2 Complexes with diphosphinite 8

Transition metal complexes containing silyl based phosphinite ligands are rare.[40a] To date, only four complexes have been structurally characterized, all using the $SiR_1R_2(OPPh_2)_2$ skeleton with various substituents for R_1 and R_2.[40b-42] To show the applicability of compound **8** as a new silyl based diphosphinite ligand for the preparation of such metal complexes, its coordination behaviour towards platinum, palladium, molybdenum and rhodium precursors was studied.

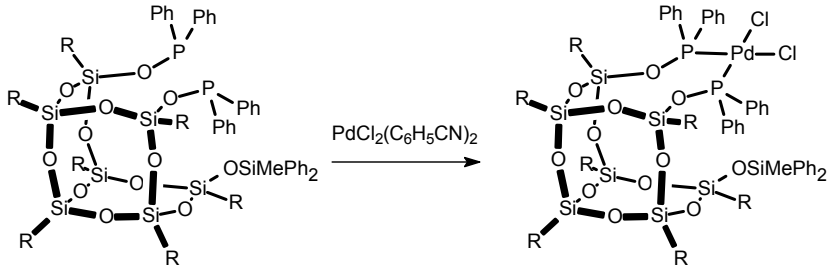

Scheme 5.5: *Illustration of the reaction of diphosphonite **8** with $PdCl_2(C_6H_5CN)_2$.*

Palladium. Reaction of $PdCl_2(C_6H_5CN)_2$ with **8** (Scheme 4), for 2 hours at room temperature, resulted in a yellow solid compound [$PdCl_2\{(c\text{-}C_5H_9)_7Si_7O_9(OPPh_2)_2OSiMePh_2\}$], for which the ^{31}P NMR spectrum showed a singlet at δ = 91.8 ppm. The ^{13}C NMR spectrum showed the typical pattern 2:1:1:2:1 for the *ipso*-carbons of the cyclopentyl groups. This indicates that the original silsesquioxane framework is still intact. Single crystals, suitable for analysis by X-ray diffraction, were obtained by layering a dichloromethane solution of $PdCl_2$(**8**) with acetonitrile. The molecular structure is depicted in Figure 5.7. Selected bond lengths and angles can be found in Table 5.5. Clearly, diphosphinite **8** has coordinated to Pd as a bidentate ligand, adopting a *cis*-configuration at the palladium atom. The complex *cis*-[$PdCl_2$(**8**)] crystallized in the triclinic spacegroup $P\bar{1}$.

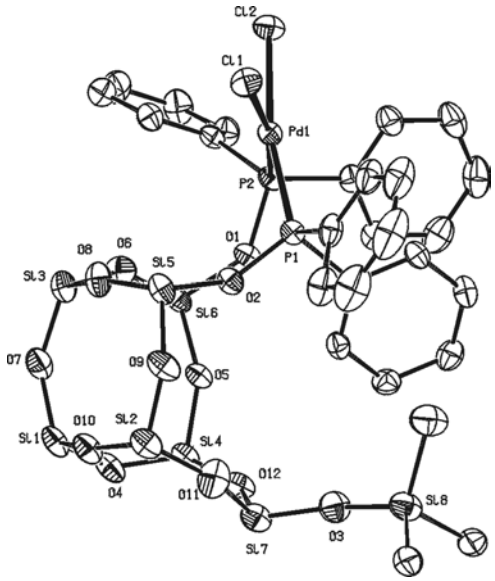

Figure 5.7: *ORTEP representation of complex **12**,* cis-*[$PdCl_2$(**8**)]. Displacement ellipsoids are drawn at the 50% probability level. All hydrogen atoms and all cyclopentyl substituents are omitted for clarity.*

The geometry around the palladium atom in complex **12** is slightly distorted square planar. This is evident from the bite angle P_1-Pd-P_2 of 92.35(3)°, while the Cl_1-Pd-Cl_2 angle is 89.71(3)°. The P_1-Pd-Cl_2 angle is only 168.86(3)°, similar to the angle P_2-Pd-Cl_1 of 168.44(3)°. Viewed along the Pd-P bond, the geometry around each phosphorus atom is clearly pyramidal, with total sums of all angles of 345.51° (P_1) and 343.16° (P_2). Four of the cyclopentyl rings as well as one phenyl ring of the $SiMePh_2$ moiety are disordered over two conformations of equal distribution. The intramolecular P-P distance is 3.2500(13) Å. The bond lengths between palladium and phosphorus Pd_1-P_1 and Pd_1-P_2 are 2.2497(9) and 2.2550(10) Å, respectively. These bond lengths fall within the expected range, compared to other $PdCl_2(P)_2$ complexes described in literature.[43-46] The *trans*-[$PdCl_2(P)_2$] complex (P being a calix[4]arene derived monophosphinite) by Faidherbe *et al.* showed the largest deviation, with a Pd-P bond length of 2.3251(6) Å.[43] Furthermore, the palladium-chloride bond distances Pd_1-Cl_1

(2.3589(10) Å) and Pd_1-Cl_2 (2.3591(10) Å) are in their normal range.[43-46] The lower electron density in the silyl ether bonds Si_5-O_2 and Si_6-O_1 is reflected in longer bond lengths of 1.672(3) Å and 1.660(2) Å compared to the average Si-O bond lengths of the silsesquioxane framework (average 1.62 Å). The $SiMePh_2$ substituent leads to a Si_8-O_3 bond length of 1.636(3) Å, similar as in complexes reported by Duchateau[47] and slightly longer compared to values found with a $SiMe_3$ substituent.[48] Other silyl oxygen bond lengths and Si-O-Si angles are normal, within the wide range known for silsesquioxane complexes. There is a significant tetrahedral distortion in the coordination plane around the palladium atom, illustrated by the calculated dihedral angle between the P_1-Pd-P_2 plane and the Cl_1-Pd-Cl_2 plane of 18°. The P-O bond lengths of 1.584(2) (P_1-O_2) and 1.601(2) Å (P_2-O_1) are found to be smaller than the values normally reported in the literature for phosphinites coordinated to palladium.[43-46,49] This might again indicate that the silsesquioxane framework indeed possesses electron-withdrawing character.

Table 5.5: *Selected bond lengths, distances and angles for complex **12**,* cis-*[$PdCl_2$(**8**)]*.

Bond lengths (Å)					
Pd-P_1	2.2497(9)	Pd-P_2	2.2550(10)	Pd-Cl_1	2.3589(10)
Pd-Cl_2	2.3591(10)	P_1-O_2	1.584(2)	P_2-O_1	1.601(2)
Si_5-O_2	1.672(3)	Si_6-O_1	1.660(2)	Si_4-O_9	1.620(3)
Si_5-O_9	1.622(3)	Si_7-O_3	1.611(3)	Si_8-O_3	1.636(3)
P_1-P_2	3.2500(13)				
Angles (°)					
Cl_1-Pd-Cl_2	89.71(3)	P_1-Pd-P_2	92.35(3)	Cl_1-Pd-P_1	92.47(3)
Cl_2-Pd-P_2	87.57(3)	P_1-Pd-Cl_2	168.86(3)	P_2-Pd-Cl_1	168.44(3)
Si_5-O_2-P_1	139.12(16)	Si_6-O_1-P_2	139.20(15)	Pd-P_1-O_2	114.96(9)
Pd-P_2-O_1	115.92(9)	Si_4-O_9-Si_5	147.52(17)	Si_7-O_3-Si_8	158.93(19)

Platinum. To establish if the structural motif found for complex **12** also occurs in complexes with other metals of the same group, the structure of the analogous platinum complex was investigated. Reaction of $PtCl_2$(cod) with ligand **8** yielded the straightforward formation of the white solid compound [$PtCl_2${(c-C_5H_9)$_7Si_7O_9$($OPPh_2$)$_2$$OSiMePh_2$}]. The ^{31}P NMR spectrum of $PtCl_2$(**8**) showed a singlet at δ = 64.5 ppm, flanked by ^{195}Pt satellites and a coupling constant $J_{Pt\text{-}P}$ of 4246 Hz. This value is a clear indication of a *cis*-coordination of the two phosphorus atoms to the platinum center, comparable to other Pt-diphosphinite systems known in literature.[37,46,50-52] The chemical shift difference with the uncoordinated ligand in the ^{31}P NMR spectrum Δδ = 34.2 ppm, considerably more than found from the reaction to yield complex **12**, were Δδ is only 5.9 ppm. In the ^{13}C NMR spectrum,

the characteristic signals for the *ipso*-carbons of the cyclopentyl substituents appeared in the normal region, in a 1:1:1:2:2 ratio. This indicates that the silsesquioxane framework remained intact during the complexation.

In addition, single crystals could be obtained by slow diffusion of acetonitrile into a CH_2Cl_2 solution of $PtCl_2$(**8**). A crystallographic study confirmed the structure of *cis*-[$PtCl_2$(**8**)], complex **13**, to be isomorphous with that of complex **12**. The molecular structure for complex **13** is represented in Figure 5.8. Selected bond lengths and angles can be found in Table 5.6.

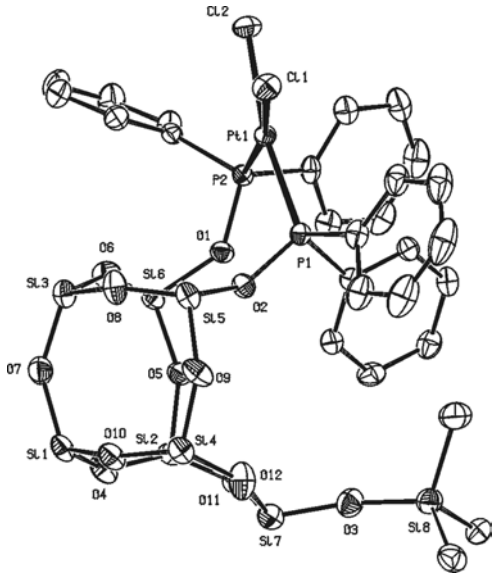

Figure 5.8: *ORTEP representation of complex **13**,* cis-*[$PtCl_2$(**8**)]. Displacement ellipsoids are drawn at the 50% probability level. All hydrogen atoms and all cyclopentyl substituents are omitted for clarity.*

The geometry around the platinum atom in complex **13** is distorted square planar. The bite angle for the diphosphinite ligand, P_1-Pt-P_2, is 92.80(3)°, while the Cl_1-Pt-Cl_2 angle turned out to be 87.34(3)°. Similar values are found for P_1-Pt-Cl_1 (93.25(3)°) and P_2-Pt-Cl_2 (88.28(3)°). The *trans* P-Pt-Cl angles are only 168.85(3)° and 170.31(3)°, respectively. Four of the cyclopentyl rings as well as one phenyl ring of the $SiMePh_2$ moiety are disordered over two conformations of equal distribution. The intramolecular P-P distance is 3.2341(10) Å, marginally smaller than the distance found in complex **12**. The total sums of the angles around the phosphorus atoms, viewed along the Pt-P bonds, are 346.35° (P_1) and 343.64° (P_2). The Pt-P bond lengths (2.2290(7) Å for Pt-P_1 and 2.2372(8) Å for Pt-P_2) and the Pt-Cl bond lengths (2.3640(8) Å for Pt-Cl_1 and 2.3621(8) Å for Pt-Cl_2) are in their expected ranges, respectively, as reported for other platinum-phosphinite structures.[37,40,43,46,50,53] In the platinum-(silyl-diphosphinite) compound *cis*-[$PtCl_2(SiPh_2(OPPh_2)_2)$] (**VI**) described by the group of Pringle and depicted in Figure 5.9, the P-O and Si-O bond lengths are

1.637 Å (P_1-O_2 is 1.615(4) Å and P_2-O_1 is 1.658(3) Å) and 1.691 Å (Si-O_1 is 1.735(4) Å and Si-O_2 is 1.652(3) Å), on average, respectively.[40]

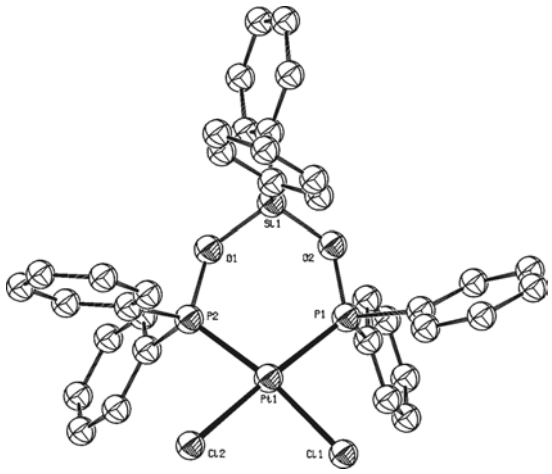

Figure 5.9: cis-*[$PtCl_2$(silyl-diphosphinite)] complex **VI** reported by Pringle* et al.[40]

In complex **13**, the P-O bond lengths are considerably shorter at 1.591(2) Å (P_1-O_2) and 1.603(2) Å (P_2-O_1). The average Si-O bond length found in **VI** is significantly longer than the values found for Si_5-O_2 (1.666(2) Å and Si_6-O_1 (1.662(2) Å) in complex **13**. Comparison of these silicon atoms, however, is hampered by their different respective substitution pattern. Regarding the different Si-O bonds present in complex **13**, similar considerations can be made as for complex **12**. The bonds Si_5-O_2 and Si_6-O_1 are considerably longer than those of the silsesquioxane framework, such as Si_5-O_9 (1.618(2) Å) or Si_7-O_3 (1.614(2) Å).

The 10-membered chelate ring, depicted in Figure 5.10, as present in complex **13** resembles the structure reported by Balakrishna *et al.* for a $PtCl_2$(PP) complex, bearing a diphosphinite ligand PP derived from bis(2-hydroxy-1-naphthyl)methane.[37] In the molecular structure for this specific compound, the metal atom is pointing upwards with respect to the remaining atoms of the chain.

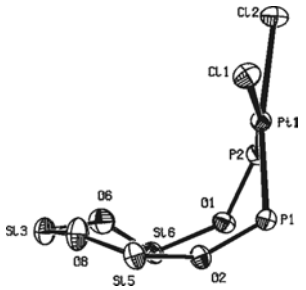

Figure 5.10: *10-membered chelate ring of complex **13**, showing the tetrahedral distortion around the square planar platinum atom and the conformation of the chelating silsesquioxide diphosphinite ring.*

The strong disposition of the platinum coordination plane from the silsesquioxane chelate ring in complex **13**, is evident from the dihedral angle between the P_1-Pt-P_2 plane and the O_1-O_2-Si_5 plane of 61.1°.The dihedral angle between the P_1-Pt-P_2 plane and the O_1-O_2-Si_6 plane is even larger at 90.0°. In complex **13**, a similar, albeit slightly smaller, tetrahedral distortion is evident as found in complex **12**. The angle between the P_1-Pt-P_2 plane and the Cl_1-Pt-Cl_2 plane is 16°. This solid state geometry has been reported before, for instance with a diphosphine ligand synthesized by Armstrong *et al.*[54]

Table 5.6: *Selected bond lengths, distances and angles for complex **13**,* cis-*[$PtCl_2$(**8**)]*.

Bond lengths (Å)					
Pt-P_1	2.2290(7)	Pt-P_2	2.2372(8)	Pt-Cl_1	2.3640(8)
Pt-Cl_2	2.3621(8)	P_1-O_2	1.591(2)	P_2-O_1	1.603(2)
Si_5-O_2	1.666(2)	Si_6-O_1	1.662(2)	Si_4-O_9	1.623(2)
Si_5-O_9	1.618(2)	Si_7-O_3	1.614(2)	Si_8-O_3	1.633(2)
P_1-P_2	3.2341(10)				
Angles (°)					
Cl_1-Pt-Cl_2	87.34(3)	P_1-Pt-P_2	92.80(3)	Cl_1-Pt-P_1	93.25(3)
Cl_2-Pt-P_2	88.28(3)	P_1-Pt-Cl_2	170.31(3)	P_2-Pt-Cl_1	168.85(3)
Si_5-O_2-P_1	137.62(14)	Si_6-O_1-P_2	138.94(14)	Pt-P_1-O_2	115.84(8)
Pt-P_2-O_1	115.48(9)	Si_4-O_9-Si_5	147.38(16)	Si_7-O_3-Si_8	161.04(17)

Molybdenum. The structures found for complexes **12** and **13** clearly showed that the bidentate ligand **1** is capable of forming square planar complexes with late transition metals. To investigate whether the scope of complexes formed with ligand **8** could be extended to earlier transition metals, the switch to an octahedral surrounded metal precursor, *viz*. $Mo(CO)_4(L)_2$ was made. Ligand **8** reacted readily with $Mo(CO)_4(pip)_2$ (pip = piperidine) at room temperature in CH_2Cl_2. A light-yellow precipitate [$Mo(CO)_4${(c-C_5H_9)$_7Si_7O_9$($OPPh_2$)$_2$$OSiMePh_2$}] was obtained after addition of acetonitrile.

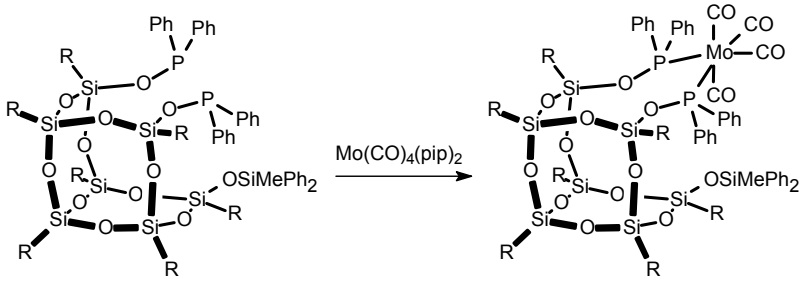

Scheme 5.6: *Schematic illustration of the reaction between **8** and $Mo(CO)_4(pip)_2$.*

The corresponding ^{31}P NMR spectrum showed only one singlet at δ = 130.4 ppm. This downfield shift with Δδ = 31.7 ppm compared to the free ligand is markedly different from the Pd and Pt complexes, where an upfield shift is observed in the ^{31}P NMR spectrum. In the carbonyl region of the ^{13}C NMR spectrum only three carbonyl signals were present (as triplets, due to phosphorus carbon coupling), indicative of two chemically inequivalent CO ligands in this complex. Based on literature values for the chemical shifts of both kinds of CO ligands in such Mo complexes [55], the signal at δ = 215.5 ppm is attributed to two carbonyl moieties in the equatorial (*trans* to P) positions. The two signals at δ = 210.2 ppm and δ = 209.3 ppm then correspond to the CO ligands in the axial positions, which have become inequivalent because of unsymmetrical arrangements within the molecule. In the carbonyl range of the infrared spectrum (ATR mode), three distinct vibrations were present at 2020, 1934, 1895 cm^{-1} and one shoulder at 1872 cm^{-1}, consistent with a *cis*-$Mo(CO)_4(PP)$ complex. No traces of the precursor $Mo(CO)_4(pip)_2$ remained in the IR spectrum, indicative that complete conversion to the diphosphinite species has taken place. This was confirmed by a crystallographic study on colorless single crystals, obtained from slow diffusion of acetonitrile in a dichloromethane solution of the product. The molecular structure of *cis*-[$Mo(CO)_4$(**8**)] is represented in Figure 5.11. Table 5.7 contains selected bond lengths and angles for this complex.

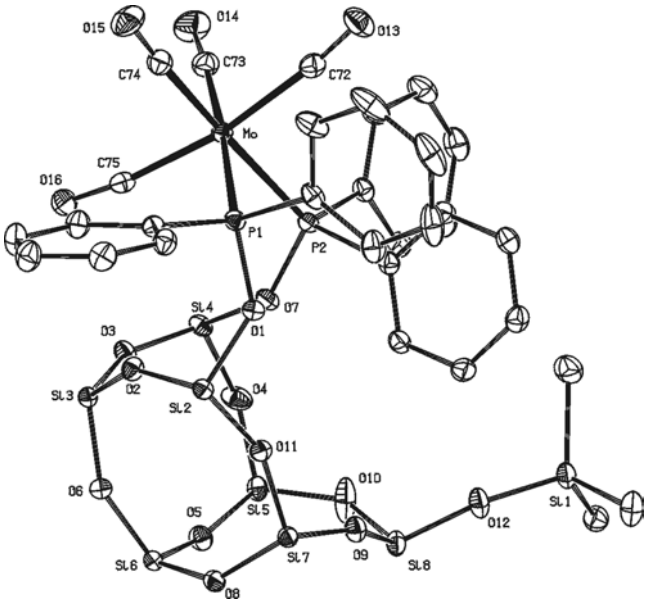

Figure 5.11: *ORTEP representation of complex **14**,* cis-*[$Mo(CO)_4$(**8**)]. Displacement ellipsoids are drawn at the 50% probability level. All hydrogen atoms, cyclopentyl substituents and solvent molecules are omitted for clarity.*

The geometry around the molybdenum atom of complex **14** is distorted octahedral. The C_{72}-Mo-C_{75} angle is only 170.37(8)°, while the representative C_{73}-Mo-C_{74} angle is 91.00(8)°. The bite

angle for the diphosphinite ligand, P_1-Mo-P_2, was found to be 87.94(1)°. The distortion is also apparent from the angle Mo-C_{72}-O_{13} of only 173.62(17)°. There is only little disorder in the molecule, as one of the cyclopentyl groups is disordered over two conformations. The intramolecular P-P distance is 3.4892(6) Å, distinctly larger than for both complexes **12** and **13**, a clear indication that the silsesquioxane framework of ligand **8** is quite flexible and able to accommodate various conformations. The Mo-P bond lengths of 2.5196(5) Å (Mo-P_1) and 2.5059(5) Å (Mo-P_2) are in the expected range as found for other molybdenum phosphinite complexes.

Both Gray and co-workers[41] as well as the group of Roesky[42] have described molecular structures of complexes with the general formula $[Mo(CO)_4(SiR_1R_2(OPPh_2)_2)]$. The values reported for the Mo-P bond lengths are slightly lower than those for complex **14**. Compared to the two other molybdenum phosphinite complexes described, the values found in complex **14** agree well.[55,56] The Mo-C bond lengths (avg. value of ~2.02 Å) as well as the P-O bond lengths of 1.6217(13) Å (P_1-O_1) and 1.6173(14) Å (P_2-O_7) are all in good agreement with reported literature values.[41,42,55,56] The Si-O(P) bond lengths found compare well with those found in the molybdenum-silylphosphinite complexes reported by Gray and Roesky.[41,42]

Table 5.7: *Selected bond lengths, distances and angles for complex **14**,* cis-*[Mo(CO)$_4$(**8**)]*.

Bond lengths (Å)					
Mo-P_1	2.5196(5)	Mo-P_2	2.5059(5)	Mo-C_{72}	2.031(2)
Mo-C_{73}	2.005(2)	Mo-C_{74}	1.999(2)	Mo-C_{75}	2.044(2)
C-O	1.14-1.15	P_1-O_1	1.6217(13)	P_2-O_7	1.6173(14)
Si_2-O_1	1.6462(14)	Si_4-O_7	1.6467(14)	Si_7-O_{11}	1.6315(14)
Si_2-O_{11}	1.6191(13)	Si_8-O_{12}	1.6039(16)	Si_1-O_{12}	1.6289(16)
P_1-P_2	3.4892(6)				
Angles (°)					
P_1-Mo-P_2	87.94(1)	C_{73}-Mo-C_{74}	91.00(8)	C_{72}-Mo-C_{75}	170.37(8)
C_{73}-Mo-P_1	176.64(6)	C_{74}-Mo-P_2	174.67(6)	P_1-Mo-C_{74}	87.90(6)
P_2-Mo-C_{73}	93.33(6)	P_1-Mo-C_{72}	93.51(6)	P_2-Mo-C_{75}	94.49(6)
Mo-C_{72}-O_{13}	173.62(17)	Mo-C_{73}-O_{14}	176.61(19)	Mo-P_1-O_1	118.35(5)
Mo-P_2-O_7	115.63(5)	Si_2-O_1-P_1	136.59(9)	Si_4-O_7-P_2	139.80(9)
Si_2-O_{11}-Si_7	153.83(10)	Si_1-O_{12}-Si_8	163.59(11)		

Rhodium. All three aforementioned complexes containing ligand **8** show a clear preference for *cis*-coordination of the diphosphinite ligand. The intramolecular P-P distances, however, are shown to range from 3.2341(10) to 3.4892(6) Å, *i.e.* 0.25 Å difference. To validate if *trans*-coordination would be feasible with this ligand, $[Rh(\mu\text{-}Cl)(CO)_2]_2$ was employed as a rhodium precursor for the reaction with diphosphinite **8**.

Upon addition of the ligand to a CH_2Cl_2 solution of the rhodium precursor, the solution immediately turned yellow. After six hours of reaction at room temperature, removal of volatiles left a clear yellow microcrystalline solid. The ^{31}P NMR spectrum of this complex showed a doublet at δ = 110.1 ppm, and a corresponding coupling constant $J_{Rh\text{-}P}$ of 145 Hz. In the IR spectrum, one single vibrational band ν_{CO} at 1995 cm^{-1} was present in the carbonyl region. Both measurements clearly indicate the selective formation of the complex *trans*-[RhCl(CO)(**8**)].

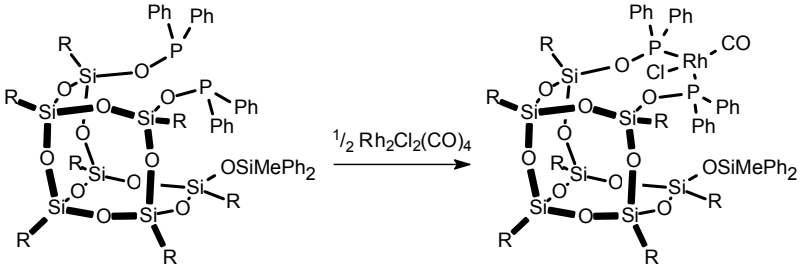

Scheme 5.7: *Illustration of the formation of* trans-*[RhCl(CO)(**8**)]*.

Other RhCl(CO)(phosphinite)$_2$ or RhCl(CO)(diphosphinite) complexes characterized by X-ray analysis have been reported before. Nolan has reported on the monophosphinite ligand $CF_3(CF_2)_5CH_2CH_2OPPh_2$, and a vibration ν_{CO} of 1990 cm^{-1} was found in the IR spectrum of the corresponding Rh complex.[57] Burrows has presented a face-to-face dimer with the diphosphoxane ligand (Ph_2POPPh_2) and for the Rh complex ν_{CO} = 1964 cm^{-1}.[58] In the former example, electron-withdrawing fluorine containing tails are employed, leading to a similar value for the CO stretch vibration. The value of ν = 1995 cm^{-1} for RhCl(CO)(**8**) is also similar to the one observed for Rh(Cl)(CO)(PPh_2(pyr))$_2$ at ν = 1992 cm^{-1}, (pyr = pyrrolyl), in which the pyrrole unit induces electron-withdrawing character in the phosphine ligand.[59]

However, also for complex [RhCl(CO)(PPh_2(OPh))$_2$],[60] the value for the CO stretch vibration is similar at ν_{CO} = 1991 cm^{-1}, which is remarkable given the difference that exists between the RhCl(CO)-complexes with the 'phosphite' $P(OPh)_3$ (2016 cm^{-1})[61] and $P(pyr)_3$ (2024 cm^{-1}).[59] Also for other ligand systems based on calix[4]arenes[46] and amino-alcohols[62] with no electron-withdrawing character, the ν_{CO} is around 1990 cm^{-1} for the Rh(Cl)(CO)(PP) complexes. It is therefore probably not

possible to determine the electronic properties of the silsesquioxane framework by such IR measurements alone.

Single crystals of the rhodium-compound could be obtained as yellow plates by slow diffusion of CH_3CN into a CH_2Cl_2 solution, and a crystallographic study was undertaken. The molecular structure of complex **15** thus unraveled by X-ray diffraction is shown in Figure 5.12, while Table 5.8 lists selected bond lengths and angles.

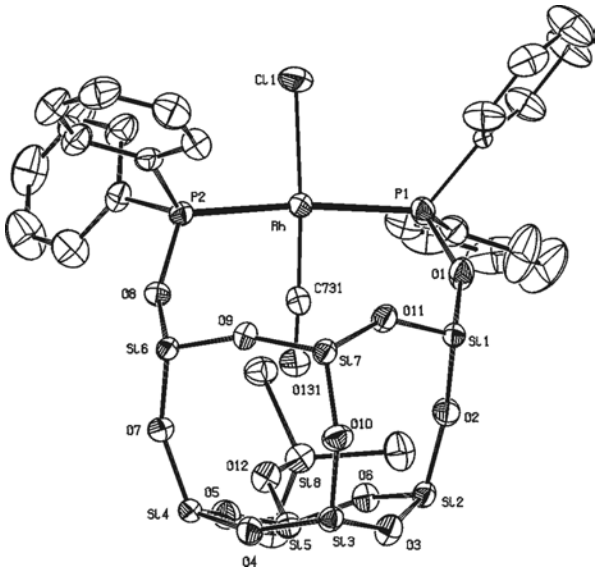

Figure 5.12: *ORTEP representation of complex **15**,* trans-*[RhCl(CO)(**8**)]. Displacement ellipsoids are drawn at the 50% probability level. All hydrogen atoms and the cyclopentyl substituents are omitted for clarity.*

The geometry around the rhodium atom is clearly square planar with only slight distortion and a *trans*-coordination of the phosphorus atoms of ligand **8**. The bite angle P_1-Rh-P_2 is 171.75(2)°, while the angle Cl_1-Rh-C_{731} is 175.6(2)°. The distortion is most pronounced in the angles P_1-Rh-Cl_1 of 95.75(3)° and P_1-Rh-C_{731} of 87.18(19)°, respectively. The Rh-P bond lengths of 2.23039(7) Å (Rh-P_1) and 2.2913(6) Å (Rh-P_2) are in the range reported for rhodium-phosphinite complexes.[58,60,63,64] The same holds for the Rh-Cl_1 an Rh-C_{731} bond lengths, although the latter falls short compared with the values of around 1.82-1.83 Å found in literature.[58,60] The lengths for the phosphorus-oxygen bonds P_1-O_1 (1.6023(19) Å) and P_1-O_8 (1.6108(16 Å) are in reasonable agreement with reported values for other phosphinite containing Rh complexes. The various silicon-oxygen bonds present in complex **15** are only slightly shorter than those in complexes **12**, **13**, and **14**. The Cl and CO ligands are both disordered over two positions, with a major fraction for both ligands of 88%. The intramolecular P-P distance in complex **15** is significantly larger at 4.5832(9) Å than the distances found in complexes **12**, **13** and **14** as a result of the *trans*-disposition.

Table 5.8: *Selected bond lengths, distances and angles for complex **15**,* trans-*[RhCl(CO)(**8**)].*

Bond lengths (Å)					
Rh-P_1	2.3039(7)	Rh-P_2	2.2913(6)	Rh-Cl_1	2.3483(15)
Rh-C_{731}	1.793(5)	C_{731}-O_{131}	1.152(6)	P_1-O_1	1.6023(19)
P_2-O_8	1.6108(16)	Si_1-O_1	1.6365(19)	Si_6-O_8	1.6504(16)
Si_1-O_2	1.6091(18)	Si_2-O_2	1.6171(18)	Si_5-O_{12}	1.6201(18)
Si_8-O_{12}	1.6390(18)	P_1-P_2	4.5832(9)		
Angles (°)					
P_1-Rh-P_2	171.75(2)	C_{731}-Rh-Cl_1	175.6(2)	C_{731}-Rh-P_1	87.18(19)
C_{731}-Rh-P_2	87.15(19)	P_1-Rh-Cl_1	95.75(3)	P_2-Rh-Cl_1	90.28(3)
Rh-C_{731}-O_{131}	174.8(6)	Rh-P_1-O_1	112.83(7)	Rh-P_2-O_8	113.21(6)
P_1-O_1-Si_1	147.24(12)	P_2-O_8-Si_6	138.18(11)	Si_1-O_2-Si_2	162.21(12)
Si_5-O_{12}-Si_8	137.30(11)				

5.4.3 Complexes with diphosphite 9

To evaluate whether the diphosphite **9**, with its sterically constrained 1,1'-biphenyldioxaphosphepine substituents, would show a different coordination behaviour compared to diphosphinite **8**, similar complexation reactions were carried out with palladium, molybdenum and rhodium precursors.

Palladium. Complexation of **9** with $PdCl_2$(cod) at room temperature resulted in a clean yellow powder and the ^{31}P NMR spectrum showed a singlet at δ = 88.9 ppm. From this data alone no conclusion can be drawn as to which isomer is formed. There is no general relationship for the chemical shifts of either *cis* or *trans* (palladium) complexes to validate the mode of coordination of the bidentate ligand on the basis of the position of the NMR signal.

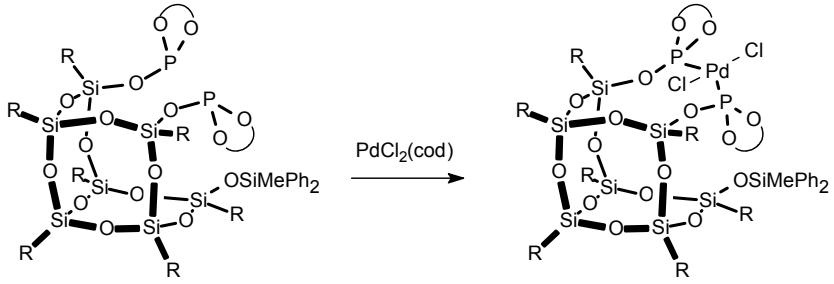

Scheme 5.8: *Formation of palladium complex **16** from the reaction of $PdCl_2$(cod) with diphosphite **9**.*

In order to deduce the exact configuration of complex **16** a crystallographic study was carried out on some single crystals, obtained from slow diffusion of acetonitrile into a dichloromethane solution of $PdCl_2$(**9**). The molecular structure for complex **16** is depicted in Figure 5.13, while for selected bond lengths and angles the reader is referred to Table 5.9.

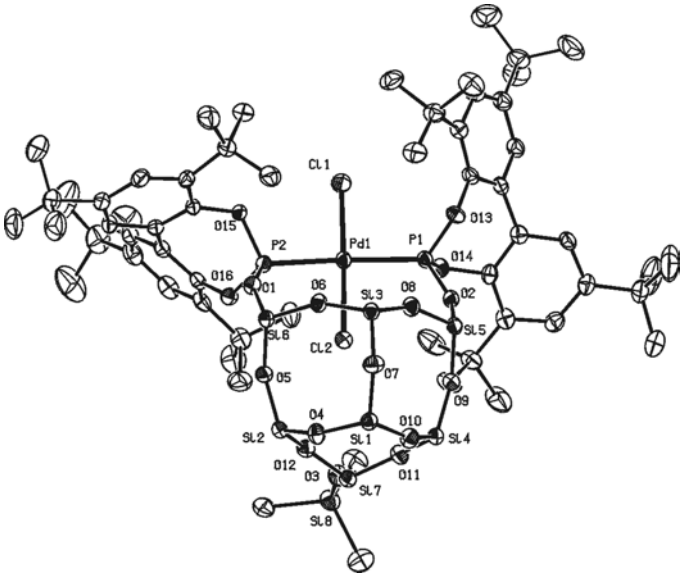

Figure 5.13: *ORTEP representation of complex **16**,* trans-*[$PdCl_2$(**9**)]. Displacement ellipsoids are drawn at the 50% probability level. All hydrogen atoms, cyclopentyl substituents and solvent molecules are omitted for clarity.*

The molecular structure shows that the palladium atom of complex **16** is in a square planar coordination, with the phosphite units in a *trans* relationship, giving rise to a bite angle for the diphosphite ligand P_1-Pd-P_2 of 171.45(5)° while the Cl_1-Pd-Cl_2 angle is 171.55(5)°. The P-Pd-Cl angles correspond to 90.41(4)° (P_1-Pd-Cl_1) and 85.12(4)° (P_2-Pd-Cl_2). To date, characterization of palladium-diphosphite complexes by X-ray analysis has been rare. The Pd-P bond lengths of 2.2859(12) Å (Pd-P_1) and 2.2821(10) Å (Pd-P_2) as well as the Pd-Cl bond lengths of 2.2980(13) Å (Pd-Cl_1) and 2.2924(13) Å (Pd-Cl_2) correspond well with other complexes with (bulky) diphosphite structures.[65,66] Dehnicke has reported on the synthesis and X-ray structural analysis of $PdCl_2${$P(OSiMe_3)_3$}. The Pd-P (2.229(1) Å), Pd-Cl (2.342(2) Å) and P-O (1.543(3) Å) bond lengths are all comparable.[67] The various bond lengths and bond angles for the silsesquioxane framework are in the normal ranges with little difference to the case of free ligand **9** (*vide supra*).

Table 5.9: *Selected bond lengths, distances and angles for complex **16**,* trans-*[$PdCl_2$(**9**)]*.

Bond lengths (Å)					
Pd-P_1	2.2859(12)	Pd-P_2	2.2821(10)	Pd-Cl_1	2.2980(13)
Pd-Cl_2	2.2924(13)	P_1-O_2	1.560(3)	P_2-O_1	1.560(3)
Si_5-O_2	1.654(3)	Si_6-O_1	1.654(3)	Si_4-O_9	1.623(3)
Si_5-O_9	1.603(3)	Si_7-O_3	1.610(3)	Si_8-O_3	1.633(3)
P_1-P_2	4.5554(15)				
Angles (°)					
Cl_1-Pd-Cl_2	171.55(4)	P_1-Pd-P_2	171.45(5)	Cl_1-Pd-P_1	90.41(4)
Cl_2-Pd-P_2	85.12(4)	P_1-Pd-Cl_2	90.69(4)	P_2-Pd-Cl_1	94.82(5)
Si_5-O_2-P_1	144.9(2)	Si_6-O_1-P_2	151.3(2)	Pd-P_1-O_2	115.98(12)
Pd-P_2-O_1	112.63(11)	Si_4-O_9-Si_5	154.7(2)	Si_7-O_3-Si_8	152.0(2)

Molybdenum. To examine if bidentate coordination in a *cis*-fashion is actually a real possibility for this sterically congested diphosphite ligand, $Mo(CO)_4(pip)_2$ was allowed to react with a small excess of ligand **9** in dichloromethane for 4 hours at room temperature. From the concentrated solution a white powder was obtained after addition of acetonitrile. The IR spectrum of the solid showed four absorption bands in the carbonyl region at 2041, 1948, 1935 and 1922 cm^{-1}. These values agree reasonably well with other *cis*-$Mo(CO)_4$(phosphite)$_2$ complexes.[55c,68] In the ^{31}P NMR spectrum a singlet was observed at δ = 149.6 ppm. To get a confirmation of the actual coordination of the ligand to the molybdenum atom a crystallographic study was undertaken, since single crystals could be grown by slow diffusion of acetonitrile into a dichloromethane solution of $Mo(CO)_4$(**9**). The molecular structure, as determined by X-ray diffraction, is depicted in Figure 5.14. Selected bond lengths and angles can be found in Table 5.10. To date, the number of X-ray structures as found in the Cambridge Crystallographic Database for other $Mo(CO)_4$((di)phosphite) complexes is limited to thirteen, of which only four contain $P(OR)(OAr)_2$ moieties, (Ar = any arylgroup, R = any non-aryl related substituent).

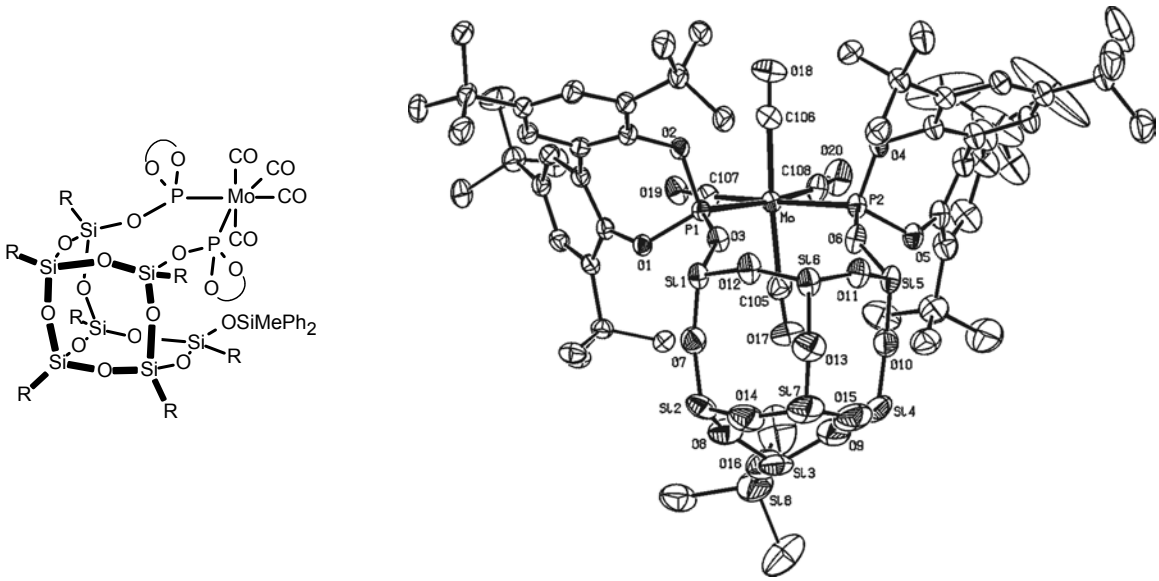

Figure 5.14: *ORTEP representation of complex **17**,* cis-*[Mo(CO)$_4$(**9**)]. Displacement ellipsoids are drawn at the 50% probability level. All hydrogen atoms, cyclopentyl substituents and solvent molecules are omitted for clarity.*

The geometry around the molybdenum atom of complex **17** is distorted octahedral, similar to the analogous diphosphinite complex **14**. In agreement with the IR spectrum measured the ligand coordinates in a bidentate manner to the molybdenum atom, adopting a *cis*-configuration. This means however, that there is significant crowding around the center of the molecule, with the biphenyl derived moieties positioned at the far sides of the molecule. The bite angle P_1-Mo-P_2 is 99.67(3)°, which causes the C_{107}-Mo-C_{108} angle to become as small as 82.00(16)°. This bite angle is significantly larger than the ideal 90° for a true *cis*-coordination, most likely due to steric constraints of the phosphite moieties. The geometry around the Mo in the equatorial plane (Mo-P_1-P_2-C_{107}-C_{108}) is slightly deviated from-planarity as evidenced by the angles C_{108}-Mo-P_1 of 169.69(13)°) and C_{107}-Mo-P_2 of (171.76(11)°), leading to a dihedral angle between the Mo-P_1-P_2 plane and the Mo-C_{107}-C_{108} plane of 3.4°. The CO-ligands in the axial positions are deviated from the ideal plane because the C_{105}-Mo-C_{106} angle is only 171.76(11)°. These distortions are significantly larger than those found for *cis*-[Mo(CO)$_4$(P(OPh)$_3$)$_2$].[68] Furthermore it is clear that both axially placed CO ligands experience completely different steric environments in the complex, which also makes them inequivalent in the ^{13}C NMR spectrum. The Mo-P bond lengths of 2.4771(10) Å (Mo-P_1) and 2.4509(10) Å (Mo-P_2) are in good agreement with the structures reported by Gray *et al.*[41,55] and by Kee and co-workers[69] on Mo-complexes containing silyl-diphosphites. The phosphorus-oxygen bond lengths of 1.574(3) Å for P_1-O_3 and 1.575(3) Å for P_2-O_6 found in complex **17** tend to be somewhat shorter compared to these same systems, which generally have P-O bond lengths of 1.60 Å or higher. The silylphosphite type of

ligands reported so far are structurally identical to a compound used in the work reported by Pringle.[40] This implies that the P-O-Si angles found in complex **17**, P_1-O_3-Si_1 at 147.62(19)° and P_2-O_6-Si_5 at 146.0(2)°, are considerably larger than found in the literature, where the P-O-Si angles are in between 129.9° and 138.5°. Compared to the Mo complex described by Kee *et al.*, the difference is even larger, since the P-O-Si angles within the silyl-triphosphite $SiR(OP)_3$ are around 124-125°.[68c]

Table 5.10: *Selected bond lengths, distances and angles for complex **17**,* cis-*[Mo(CO)$_4$(**9**)]*.

Bond lengths (Å)					
Mo-P_1	2.4771(10)	Mo-P_2	2.4509(10)	Mo-C_{105}	2.0471(5)
Mo-C_{106}	2.050(4)	Mo-C_{107}	2.023(4)	Mo-C_{108}	2.009(4)
C-O	1.13-1.15	P_1-O_3	1.574(3)	P_2-O_6	1.575(3)
Si_1-O_3	1.653(3)	Si_5-O_6	1.650(3)	Si_5-O_{10}	1.614(3)
Si_4-O_{10}	1.627(4)	Si_3-O_{16}	1.615(5)	Si_8-O_{16}	1.628(5)
P_1-P_2	3.7661(14)				
Angles (°)					
P_1-Mo-P_2	99.67(3)	C_{107}-Mo-C_{108}	82.00(16)	C_{105}-Mo-C_{106}	171.07(16)
C_{108}-Mo-P_1	169.69(13)	C_{107}-Mo-P_2	171.76(11)	P_1-Mo-C_{105}	88.99(11)
P_2-Mo-C_{106}	89.77(12)	P_1-Mo-C_{106}	87.90(11)	P_2-Mo-C_{105}	83.09(12)
Mo-C_{107}-O_{13}	173.62(17)	Mo-C_{105}-O_{14}	176.61(19)	Mo-P_1-O_3	119.14(11)
Mo-P_2-O_6	118.35(11)	P_1-O_3-Si_1	147.62(19)	P_2-O_6-Si_5	146.0(2)
Si_5-O_{10}-Si_4	150.3(2)	Si_3-O_{16}-Si_8	161.4(3)		

Rhodium On addition of 2 equivalents of **9** to 1 equivalent of $[Rh(\mu\text{-}Cl)(CO)_2]_2$, three broad doublets could be distinguished in the ^{31}P NMR spectrum after reaction at ambient temperature for 2 hours in CH_2Cl_2, demonstrating the formation of several species. Two doublets, at δ = 120.8 ppm and δ = 118.0 ppm each had a coupling constant $J_{Rh\text{-}P}$ of 217 Hz while the major species (~50%) at δ = 113.5 ppm showed a coupling constant $J_{Rh\text{-}P}$ of 299 Hz. To drive the reaction to completion the reaction was continued overnight in refluxing toluene. A second ^{31}P NMR spectrum showed that the latter species had increased to ~90%. The IR spectrum of the solid product showed two CO stretch vibrations at 2019 and 2009 cm^{-1}. To interpret the spectroscopic data correctly, a crystallographic study was performed on single crystals grown by slow diffusion of acetonitrile into a concentrated CH_2Cl_2 solution of RhCl(CO)(**9**). The molecular structure of complex **18** thus obtained is depicted in Figure 5.15, while important bond lengths and angles are listed in Table 5.11.

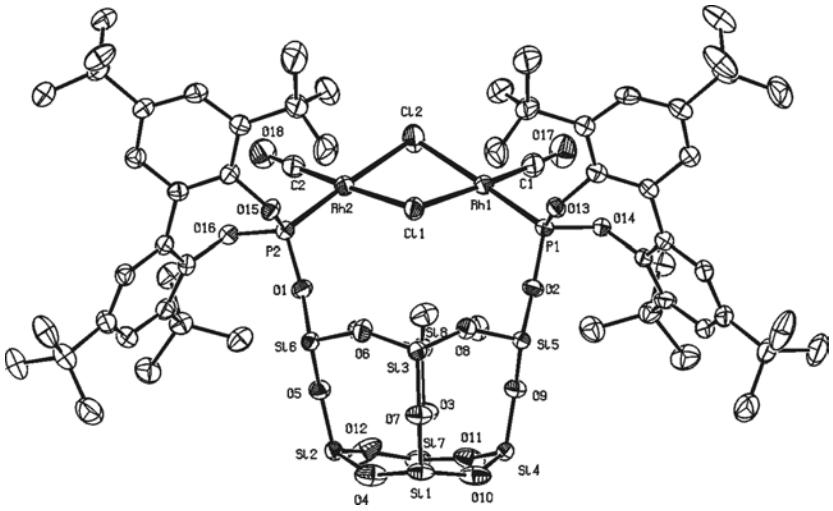

Figure 5.15: *ORTEP representation of complex **18**, [{Rh(μ-Cl)(CO)}$_2$(κ^2-**9**)]. Displacement ellipsoids are drawn at the 50% probability level. All hydrogen atoms and cyclopentyl substituents are omitted for clarity.*

Complex **18** is a rhodium dimer, with the two phosphite moieties of the ligand each coordinated to one rhodium atom. There is one terminal CO molecule present per rhodium atom, with two bridging chlorine atoms. The two phosphorus atoms are mutually *cis* to one another. This structure does explain why two CO bands are observed in the infrared spectrum with a splitting of ~10 cm^{-1}. This is due to the non-planarity of the Rh_1-Cl_1-Rh_2-Cl_2 ring, leading to a so-called 'butterfly-angle' between the Cl_1-Rh_1-Cl_2 plane and the Cl_1-Rh_2-Cl_2 plane of 20.5°. This existence of two vibrations was already observed by the group of Poilblanc.[70] Since no free ligand was present in solution after reaction, complex **18** can not be the major product formed.

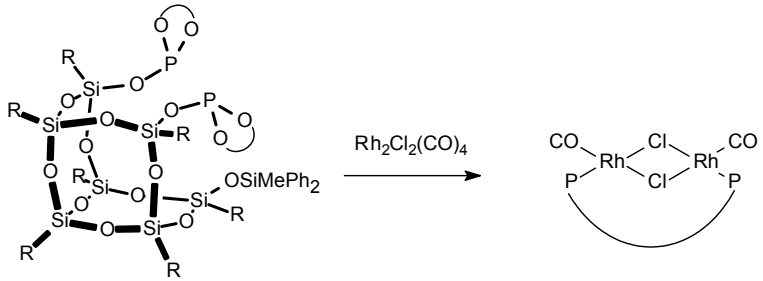

Scheme 5.9: *Formation of the minor product **18** from the reaction of **9** with Rh-dimer precursor.*

The geometry around each rhodium atom is square planar, with the P_1-Rh-P_2 angles at 177.70(3)° and 176.82(3)°. These features of the molecular structure of complex **18** are especially visible from a side-view, as presented in Figure 5.16.

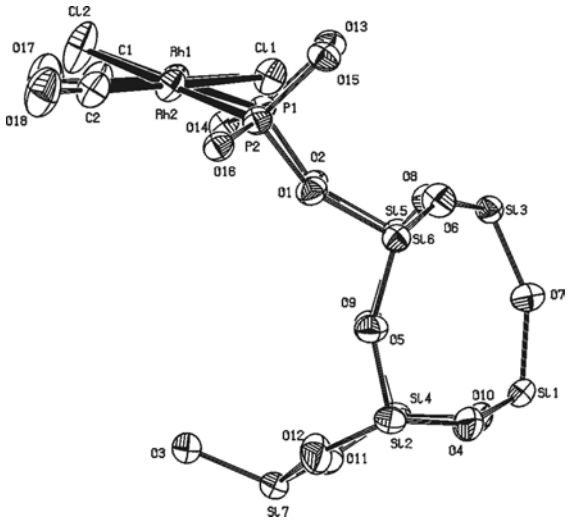

Figure 5.16: *Front view of complex **18**, showing the symmetry of the rhodium atoms in the dimeric species and the butterfly shape of the Cl_1-Rh_1-Cl_2-Rh_2 cycle.*

The skeletal core of the molecule, not regarding any cyclopentyl groups or the biphenyl-derivatives on the phosphorus atoms, is highly symmetric. The Cl_1-Rh-*C* angles are nearly identical at 176.58(10)° and 177.58(11)°. The Rh-P bond lengths are around 2.18 Å, while the Rh-*C* and Rh-Cl lengths are around 1.80-1.81 Å and 2.41-2.42 Å, respectively. All these data compare well with the values found in the mononuclear complex $[RhCl(CO)\{P(OPh)_3\}_2]$,[71] with the exception of the Rh-P bonds which are about ~0.1 Å shorter in complex **18**. The Rh-Cl bond lengths are slightly elongated in comparison to the value (2.370(3) Å) for the terminal Cl in $[RhCl(CO)\{P(OPh)_3\}_2]$. The intramolecular Rh_1-Rh_2 distance is 3.5163 Å, which might indicate a weak metal-metal interaction. The geometry around each phosphorus atom is tetrahedral, as indicated by the angles Rh_1-P_1-O_2 of 115.89(8)° and Rh_2-P_2-O_1 of 114.10(8)°.

Two other dinuclear rhodium-phosphite complexes with a similar conformation have been characterized by X-ray crystallography. Cobley *et al.* have described the reaction of a calix[4]arene based monophosphite with $[Rh(\mu\text{-}Cl)(CO)_2]_2$ at different stoichiometries, always ending up with a mixture of two complexes in the ratio 1 to 4, based on the ^{31}P NMR spectrum. The authors proposed an equilibrium between the *trans* and *cis*-isomer. The only product obtained as crystals turned out to be the *cis*-isomer.[72] The existence of such an equilibrium in solution between the two isomers was also proposed by Poilblanc for other dinuclear rhodium phosphite complexes.[70] Shum *et al.* have speculated on the formation of a dinuclear structure applying a tripodal phosphite that acted as a bidentate ligand, but so far only some NMR spectroscopic data has been reported to support this suggestion.[72c,d]

Table 5.11: *Selected bond lengths, distances and angles for complex **18**, [{Rh(μ-Cl)(CO)}$_2$(κ^2-**9**)].*

Bond lengths (Å)					
Rh_1-P_1	2.1820(8)	Rh_2-P_2	2.1768(8)	Rh_1-Cl_1	2.4135(8)
Rh_1-Cl_2	2.4213(10)	Rh_2-Cl_1	2.4179(9)	Rh_2-Cl_2	2.4154(10)
Rh_1-C_1	1.809(3)	Rh_2-C_2	1.814(3)	C_1-O_{17}	1.155(4)
C_2-O_{18}	1.140(4)	P_1-O_2	1.563(2)	P_2-O_1	1.564(2)
Si_5-O_2	1.650(2)	Si_6-O_1	1.652(2)	Si_4-O_9	1.630(2)
Si_5-O_9	1.619(2)	Si_7-O_3	1.612(2)	Si_8-O_3	1.643(2)
P_1-P_2	6.5417(14)	Rh_1-Rh_2	3.5163(5)		
Angles (°)					
P_1-Rh_1-Cl_2	177.70(3)	P_2-Rh_2-Cl_2	176.82(3)	Cl_1-Rh_1-C_1	176.58(10)
Cl_1-Rh_2-C_2	177.58(11)	P_1-Rh_1-Cl_1	93.51(3)	P_2-Rh_2-Cl_1	92.65(3)
C_1-Rh_1-Cl_2	92.41(10)	C_2-Rh_2-Cl_2	93.50(10)	Cl_1-Rh_1-Cl_2	84.18(3)
Cl_1-Rh_2-Cl_2	84.22(3)	P_1-Rh_1-C_1	89.90(10)	P_2-Rh_2-C_2	89.64(10)
Rh_1-Cl_1-Rh_2	93.40(3)	Rh_1-Cl_2-Rh_2	93.27(4)	Si_5-O_2-P_1	156.62(14)
Si_6-O_1-P_2	155.57(15)	Rh_1-P_1-O_2	115.89(8)	Rh_2-P_2-O_1	114.10(8)
Si_4-O_9-Si_5	148.66(15)	Si_7-O_3-Si_8	142.59(15)		

Furthermore, Gavrilov and co-workers have published a similar structural motif, employing a catechol based monophosphite. The Rh-Cl bond lengths were around 2.40 Å, the Rh-P bond lengths around 2.15 Å.[73] Tilley recently reported on a rhodium dimer with two ligand molecules present, together with two bridging chlorine atoms, originating from the rhodium precursor $RhCl_2(cod)_2$.[74] Similar bond lengths as in complex **18** are found for these structures, especially the Rh-P bond length and the Rh-Rh distance. Structurally related halide bridged complexes containing phosphites coordinated to palladium and platinum have been reported as well, with different co-ligands.[75-81]

5.5 Catalysis

5.5.1 Monophosphites 1-5

In order to get a first impression on the behaviour of the novel ligands **2**-**4** versus the known compounds **1** and tris(*tert*-butyl-dimethylsilyl)phosphite **5** under catalytic conditions, the rhodium catalyzed hydroformylation of 1-octene was the reaction of choice. The catalysis was carried out under standard conditions, applying 20 bar of syngas (1:1), a catalyst preformation time of 1 hour and a reaction temperature of 80 °C. Results of these catalytic tests are summarized in Table 5.12.

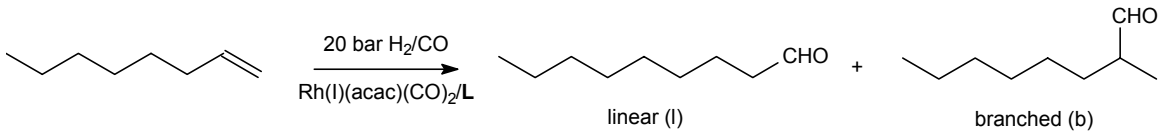

Scheme 5.10: *Rhodium catalyzed hydroformylation of 1-octene.*

With monophosphite **2** (Silsphite) the catalytic system showed very high activity with a turnover frequency of around 5000 h^{-1} and a conversion of 30% after 15 minutes (entry 2). Even when increasing the substrate to catalyst ratio the activity remained nearly constant, indicative of a stable catalytic complex (entry 3). The selectivity to the desired linear aldehyde *n*-nonanal is low with a linear to branched ratio of 2.1, as expected for a simple sterically unconstrained monophosphite.

Ligands **3** and **4** were designed to have greater bulk around the phosphorus center in an attempt to influence the preferred coordination mode and hence the activity of the corresponding rhodium catalyst. The initial activity decreased significantly when these ligands were applied (entry 4 and 5 respectively). Exclusive formation of a monoligated complex, ensuring high reaction rates,[18] is therefore not likely to occur with these ligands.

Table 5.12: *Rhodium catalyzed hydroformylation of 1-octene with monophosphites **1-5**.*[a]

Entry	Ligand	Time (min)	Conversion [%][b]	Selectivity [%][b]	l/b[b]	TOF[c]
1	**1**	60	<1[d]	-	-	-
2	**2**	15	31.5	94.5	2.2	5000
3[e]	**2**	15	14.5	95.5	2.1	4500
4[f]	**3**	20	22.9	94.4	2.1	2800
5	**4**	20	17.8	94.8	2.1	2200
6	**5**	20	2.2	nd	nd	-

[a]*Reaction conditions: 1-octene (31.0 mmol), decane (12.5 mmol), toluene (12.7 mL), p = 20 bar , T = 80 °C, [Rh(acac)(CO)$_2$] = 0.39 mM, S:Rh = 4000:1, ligand:Rh = 10:1;* [b]*determined by GC analysis;* [c]*turnover frequency, defined as (mol substrate converted)·(mol rhodium)$^{-1}$·h^{-1};* [d]*below detection limit;* [e]*[Rh(acac)(CO)$_2$] = 0.20 mM, S:Rh = 8000:1;* [f]*ligand:Rh = 5:1.*

Interestingly, under these conditions the reference material **1** showed no catalytic activity at all, even after 1 hour of reaction (entry 1). No decisive explanation as to why this ligand shows no activity at all can be given. It might originate from the poor electron-donating character of the ligand or from unfavourable coordination to the metal center arising from a large Tolman angle and the rigidity observed in the solid state structure.[25] Tris(*tert*-butyl-dimethylsilyl)phosphite **5** (entry 6) turned out relatively inactive as well in this reaction, probably due to the different electronic character of this ligand compared to ligands **2-4**, which prevent favourable coordination to the rhodium atom.

5.5.2 Monophosphite 7 vs. diphosphite 9

The results of the catalytic tests applying either ligand **7** or ligand **9** in the same reaction as above and under the same reaction conditions are shown in Table 5.13. With the monophosphite **7** a high activity is achieved (entry 1), with an initial turnover frequency of around 5100 h^{-1}. In addition, an influence of the ligand to metal ratio on the catalytic performance was observed. While increasing this ratio from 5 to 10, the activity was also increased by 33% to a turnover frequency of 6800 h^{-1} (entry 2). This activity is an order higher as observed with catalysts based on electron-withdrawing monophosphites-such as the ligand $P(OCH_2CF_3)_3$ (**I**).[14] However, it does not compete yet with the sterically constrained ligand **II** in terms of activity.[17] The regioselectivity remained low with an l/b-ratio of around 2.2, as expected for a monodentate ligand. With the bidentate ligand **9**, a significantly lower activity is observed (entry 3). This is expected for such a sterically constrained chelating ligand, yet the regioselectivity remains low, possibly because of too much steric crowding around the metal center, leading to an unselective catalyst and a low activity.

Table 5.13: *Rhodium catalyzed hydroformylation of 1-octene using ligands 7 and 9.*[a]

Entry	Ligand	Time [min]	Conversion [%][b]	Selectivity [%][b]	l/b[b]	TOF[c]
1	**7**	20	41.7	68.7	2.2	5100
2[d]	**7**	20	55.2	63.7	2.2	6800
3	**9**	60	11.3	80.1	2.3	500

[a]*Reaction conditions: 1-octene (31.0 mmol), decane (12.5 mmol), toluene (12.7 mL), p = 20 bar , T = 80 °C, [Rh(acac)(CO)$_2$] = 0.39 mM, S:Rh = 4000:1, ligand:Rh = 5:1;* [b]*determined by GC analysis;* [c]*turnover frequency, defined as (mol substrate converted)·(mol rhodium)$^{-1}$·h^{-1};* [d]*ligand:Rh = 10:1.*

5.5 Conclusions

The synthesis of five monodentate compounds **2**-**4**, **6** and **7** as well as two bidentate derivatives **8** and **9**, all based on silsesquioxane frameworks, is described. Limitations in the synthetic possibilities have been identified. The partial functionalization of PCl_3 with an incompletely condensed, monosilylated silsesquioxane offered possibilities for a new modular class of monophosphites. The bidentate compounds were easily obtained from reaction of similar silsesquioxane structures with chlorophosphines or phosphorochloridites. An exploratory DFT study gave insight in the electronic character of the phosphorus atoms present in these nanostructured compounds.

The coordination chemistry with especially the bidentate ligands **8** and **9** proved versatile, as indicated by the molecular structures obtained for the palladium, platinum, molybdenum and rhodium

complexes. The diphosphinite **8** showed a clear tendency to form *cis*-complexes, while for the diphosphite **9** various modes of coordination were observed. This can be rationalized in terms of steric crowding and an intrinsic large flexibility range for the silyloxy functionalized ligands. Silsesquioxanes offer many possibilities for the development of new families of phosphorus ligands, with additional new opportunities for catalyst immobilization and recycling.

Acknowledgements

The National Research School Combination for Catalysis (NRSCC) is thanked for financial support. OMG is acknowledged for a generous loan of various transition metal complexes. Dr. Tessa Dijkstra has introduced the 'T_8-compound' (c-$C_5H_9)_7Si_7O_{12}SiOTl$ into these investigations. Dr. Rob Hanssen is thanked for scientific discussions as well as for providing samples of (c-$C_5H_9)_7Si_7O_9(OH)_3$ and (c-$C_6H_{11})_7Si_7O_9(OH)_3$, while Gijsbert Gerritsen donated (c-$C_5H_9)_6Si_6O_7(OH)_4$. Input from Dr. Erik Abbenhuis and Dr. Rafaël Sablong in lively discussions was very welcome. The huge amount of experimental efforts of Drs. Michiel Grutters, who also co-initiated this research, as well as the scientific input during the whole project are warmly appreciated. Enthusiastic assistance of Jens Ackerstaff in experimental work is gratefully acknowledged. Dr. Marco Fioroni performed the DFT calculations of various metal complexes. Crystal structure analyses were carried out by Dr. Allison Mills, Dr. Huub Kooijman and Prof. Anthony Spek (Univ. Utrecht) and by Drs. Auke Meetsma (Univ. Groningen). Their work has been essential for a thorough study on the coordination chemistry of the silsesquioxane based phosphorus containing ligands.

5.6 Experimental Section

General. Chemicals were purchased from Aldrich, Acros or Merck and used as received. . Synthesis gas (CO/H_2 1:1) was purchased from Hoekloos. All preparations were carried out under an argon atmosphere using standard Schlenk techniques. Solvents were distilled from sodium/benzophenone (THF, diethyl ether, toluene and hexanes) or calcium hydride (CH_2Cl_2 and $CDCl_3$) prior to use. All glassware was dried by heating under vacuum.
The NMR spectra were recorded on a Varian Mercury 400 spectrometer (^1H, $^{13}C\{^1H\}$, $^{31}P\{^1H\}$) or a Varian Inova 500 spectrometer (^{29}Si). Chemical shifts are given in ppm referenced to solvent (^1H, $^{13}C\{^1H\}$), to an 85% aqueous solution of H_3PO_4 ($^{31}P\{^1H\}$) or to $SiMe_4$ (^{29}Si). GC analyses were performed on a Shimadzu 17A chromatograph equipped with a 50 m PONA column. Elemental analysis was performed by Kolbe Mikroanalytisches Laboratorium, Germany. IR spectra were taken on an AVATAR E.S.P. 360 FTIR spectrometer. Dibenzo[d,f]-2,2´,4,4´-tetra-tert-butyl-[1,3,2]-dioxa-phosphepin-P-chloride[82] as well as the metal precursors $PdCl_2(cod)$,[83] $PdCl(CH_3)(cod)$,[84] $PtCl_2(cod)$[85] and $Mo(CO)_4(pip)_2$[86] were prepared according to literature procedures. Monodentate phosphite **1** ($(c\text{-}C_6H_{11})_7Si_7O_9O_3P$), $(c\text{-}C_5H_9)_7Si_7O_9(OH)_3$ and $(c\text{-}C_5H_9)_7Si_8O_{13}Tl$ were previously prepared by other group members according to literature procedures.[24,25,29]
***CAUTION**: Thallium-containing compounds are poisonous. Handling of such compounds should be done with utmost care, also regarding the waste disposal of thallium containing compounds.*

$(c\text{-}C_5H_9)_7Si_7O_9(OH)_2OSiMePh_2$ (A).
Trisilanol $(c\text{-}C_5H_9)_7Si_7O_9(OH)_3$ (10.96 g, 12.52 mmol) was dried under vacuum in a 250 mL roundbottom flask. At r.t. 50 mL of THF was added and the solid dissolved by applying heat. NEt_3 (6.33 g, 62.60 mmol) was added to the clear solution and thereafter $SiClMePh_2$ (3.21 g, 13.77 mmol) was added dropwise to the stirred mixture. After complete addition, the reaction mixture was heated to reflux for 5 min and stirred under slow argon flow over night at r.t.. The solvent was evaporated and the residu was extracted with 80 mL of hexanes. All solvents were removed by evaporation and **A** was obtained as a white powder. A small amount was dissolved again in 15 mL of hexanes and after cooling down in the freezer gave colourless crystals.
Yield: 94% (12.56 g, 11.77 mmol).
^1H NMR ($CDCl_3$) δ 7.69 - 7.40 (m, C_6H_5); 1.79, 1.65 - 1.45, 0.96 (br m, $c\text{-}C_5H_9$); 0.1 (s, $SiMePh_2$).
$^{13}C\{^1H\}$ NMR ($CDCl_3$) δ 137.9, 134.0, 129.7, 127.9 (C_6H_5); 27.5, 27.4, 27.3, 27.1, 27.0, 23.8, 23.0, 22.5, 22.3, 22.2 (1:2:2:1:1 ratio for C_{ipso}), -1.1 ($SiMePh_2$).

$(c\text{-}C_5H_9)_7Si_7O_9(OSiMePh_2)O_2PObenzene$ (2).
To a solution of **A** (1.76 g, 1.64 mmol) in 25 mL of THF, NEt_3 (0.83 g, 8.20 mmol) was added. At –15 °C, PCl_3 (236.0 mg, 1.72 mmol) was added dropwise. After stirring for 1 h at r.t., the solution was cooled to –78 °C and phenol (161.9 mg, 1.72 mmol) in 5 mL of THF was added dropwise. After addition an extra 5 mL of THF was added via the same syringe. The solution was allowed to warm up to r.t. overnight. The solvent was removed *in vacuo* and the residue extracted with 10 mL of hexanes. The solution was concentrated by removal of solvents to leave 1.74 g (1.46 mmol) of a turbid colorless oil that solidified upon standing. Yield 89% of **2**.
^1H NMR ($CDCl_3$) δ 7.63 (dd, ^1J = 7.3 Hz, ^1J = 2.2 Hz), 7.31 (m), 7.11 (t), 6.95 (t), 6.80 (d, ^1J = 8.8 Hz), 1.77 (br m, *c-C5H9*), 1.58 (br m, $c\text{-}C_5H_9$), 1.28 (br m, $c\text{-}C_5H_9$), 0.15 (s, $SiCH_3Ph_2$).
$^{13}C\{^1H\}$ NMR ($CDCl_3$) δ 137.9, 134.2, 129.1, 127.4, 123.0, 121.0, 120.9, 31.7, 27.6, 27.5, 27.4, 27.3, 27.2, 27.1, 27.0, 26.9, 24.0, 23.0, 22.6, 22.3, 21.9 (1:2:2:1:1 for $C_{ipso}H$), -0.6 ($SiMePh_2$).
$^{31}P\{^1H\}$ NMR ($CDCl_3$) δ 122.6 (s).
^{29}Si NMR ($CDCl_3$) δ -10.58 ($SiMePh_2$), -64.01, -65.02, -65.06, -66.60, -67.65 (1:2:1:1:2).

$(c\text{-}C_5H_9)_7Si_7O_9(OSiMePh_2)O_2PO$(3,5-di-*tert*-butyl)benzene (3).
In 20 mL of THF, **A** (0.86 g, 0.80 mmol) was dissolved and to this solution NEt_3 (0.56 ml, 4.0 mmol) was added. The clear solution was cooled to -15 °C. Under rapid stirring PCl_3 (0.11 g, 0.80 mmol) was added dropwise. The reaction mixture was stirred for 1 h at -15 °C and then further cooled to -77 °C. 3,5-di-*tert*-butylphenol (0.17 g, 0.80 mmol) was dissolved in 1 mL of THF and the solution was added dropwise to the stirred reaction mixture. Stirring was continued over night at r.t. and then all solvents were removed *in vacuo*. The residue was stripped with 10 mL of THF and extracted by addition of 20 mL of hexanes. After removal of the solvents, a turbid yellow oil was obtained, containing **3** in 80% purity. Yield: 78% (0.82 g).

^{1}H NMR ($CDCl_3$) δ 7.62, 7.25 (m, C_6H_3); 1.89 - 0.81 (br m, *c*-C_5H_9); 1.34 (s, t-Bu); 0.05 (s, $SiMePh_2$).
^{31}P{^{1}H} NMR ($CDCl_3$) δ 123.7 (s).

(*c*-C_5H_9)$_7$$Si_7O_9$(OSiMe$Ph_2$)$O_2$POnaphtalene **(4).**
Based on the same procedure as for **2**, dry **A** (1.40 g, 1.30mmol), NEt_3 (1.0 mL, 7.17 mmol) and PCl_3 (0.18 g, 1.30 mmol) were used. Then a solution of 1-naphthol (188.1 mg, 1.30 mmol) in 2 mL of THF was added dropwise and the mixture slowly warmed up to r.t.. Following the known procedure, product **4** was obtained 86 % pure as sticky white oil. It was stored at –18 °C. Yield: 82% (1.33 g, 1.07 mmol).
^{1}H NMR ($CDCl_3$) δ 8.10 (d, ^{1}J = 8.4 Hz, 1H), 7.78 (d, ^{1}J = 8.4 Hz), 7.67 – 7.64 (m), 7.62 – 7.60 (m), 7.53 (d, ^{1}J = 8.4 Hz), 7.45 (t, J_3 = 7.6 Hz), 7.41 – 7.24 (br m), 7.06 (d, ^{1}J = 7.6 Hz), 1.81 – 1.31 (br m), 1.17 – 0.90 (br m), 0.07 (s, $SiMePh_2$).
^{13}C{^{1}H} NMR ($CDCl_3$) δ 137.9, 134.6, 134.1, 129.0, 127.4, 127.2, 126.1, 125.5, 123.1, 115.4, 27.5, 27.4, 27.3, 27.1, 27.0, 23.0, 22.6, 22.3, 21.8 (1:2:2:1:1 ratio for C_{ipso}H), -0.7 ($SiMePh_2$).
^{31}P{^{1}H} NMR ($CDCl_3$) δ 123.3 (s).

(*c*-C_5H_9)$_7$$Si_8O_{12}OPPh_2$ (6).
(c-C_5H_9)$_7$$Si_8O_{12}$(OTl) (0.42 g, 0.37 mmol) was dissolved under heating in 20 mL of toluene giving a colloidal white solution. $ClPPh_2$ (0.08 g, 0.37 mmol) was dissolved in 4 mL of hexanes and this solution was added dropwise to the stirred suspension via syringe. The reaction mixture was stirred overnight at r.t. and the suspension was filtered over Celite to remove salts. After evaporation of the solvents *in vacuo*, **6** was obtained pure as a white powder. Yield: 82% (1.33 g, 1.07 mmol).
^{1}H NMR ($CDCl_3$) δ 7.54 (dt, 4H, ^{1}J = 7.6 Hz, ^{2}J = 1.6 Hz), 7.35 (dq, 6H, ^{1}J = 7.6 Hz, ^{1}J = 1.6 Hz), 1.77 (br s, *c*-C_5H_9), 1.61 – 1.49 (br m, *c*-C_5H_9), 1.00 (m, *c*-C_5H_9).
^{13}C{^{1}H} NMR ($CDCl_3$) δ 132.6 (d, $J_{P\text{-}C}$ = 2.4 Hz), 130.7(d, $J_{P\text{-}C}$ = 11.4 Hz), 129.5, 129.3, 129.0, 128.8, 128.1 (d, $J_{P\text{-}C}$ = 7.6 Hz), 126.4, 125.3, 124.9, 124.0, 31.6, 31.5, 31.3, 29.7, 27.3, 27.2, 27.1, 27.0, 26.9, 22.2, 22.1, 22.0 (1:4:3 ratio for C_{ipso}H).
^{31}P{^{1}H} NMR ($CDCl_3$) δ 101.6 (s).
Anal. Calcd for $C_{47}H_{73}O_{13}PSi_8$:C, 51.24; H, 6.68. Found: C, 51.35; H 6.78.

(*c*-C_5H_9)$_7$$Si_8O_{12}$O-dibenzo[d,f]-2,2´,4,4´-tetra-tert-butyl-[1,3,2]-dioxa-phosphepin (7).
(*c*-C_5H_9)$_7$$Si_8O_{13}$Tl (0.37 g, 0.39 mmol) was suspended in 20 mL of toluene. While stirring at r.t., a solution of dibenzo[d,f]-2,2´,4,4´-tetra-tert-butyl-[1,3,2]-dioxa-phosphepin-P-chloride (0.16 g, 0.39 mmol) in 4 mL of toluene was added dropwise via syringe and the reaction mixture was stirred for 16 hours. Then salts were removed by filtration and the filtrate was concentrated by removal of the solvents *in vacuo*. The product was extracted by addition of 15 mL of hexanes. Solvents were removed by evaporation, leaving **7** as a brown solid. Yield: 79% (0.42 g, 0.31 mmol).
^{1}H NMR ($CDCl_3$) δ 7.44 (d, 4H, ^{1}J = 2.4 Hz), 7.18 (d, 4H, ^{1}J = 2.4 Hz), 1.78 – 1.33 (br m, *c*-C_5H_9), 1.00 (m, *c*-C_5H_9)
^{13}C{^{1}H} NMR ($CDCl_3$) δ 146.0, 145.3 (d, $J_{P\text{-}C}$ = 16.8 Hz), 126.4, 125.3, 124.9, 124.0, 31.6, 31.5, 31.3, 29.7, 27.3, 27.2, 27.0, 26.9, 22.2, 22.1, 22.0 (1:4:3 ratio for C_{ipso}H).
^{31}P{^{1}H} NMR ($CDCl_3$) δ 132.6 (s).

(*c*-C_5H_9)$_7$$Si_7O_9$(OSiMe$Ph_2$)bisdiphenylphosphinite (8).
A (1.03 g, 0.96 mmol) was dissolved under heating in 20 mL of toluene and NEt_3 (0.19 g, 1.92 mmol) was added. Under stirring at -15 °C $ClPPh_2$ (0.42 g, 1.91 mmol) in 3 mL of toluene was added dropwise via syringe and the reaction mixture was allowed to warm to r.t. All solvents were removed *in vacuo* and the product was extracted by addition of 10 mL hexanes. After removal of the solvents **8** was obtained as a solid. Yield: 86% (1.19 g, 0.83 mmol).
^{1}H NMR ($CDCl_3$) δ 7.53 (dd, 8H, H_{ortho} P*Ph*$_2$, ^{1}J = 7.6 Hz, ^{2}J = 1.2 Hz), 7.44 (m, 4H, H_{ortho} SiMe*Ph*$_2$), 7.29 (m, 6H, SiMe*Ph*$_2$), 7.16 (m, 12H, P*Ph*$_2$), 1.80 – 1.34 (br m, *c*-C_5H_9), 1.02 (dsextet, 6H, *c*-C_5H_9, ^{1}J = 4.4 Hz, ^{2}J = 1.2 Hz), 0.90 (dquintet, 6H, *c*-C_5H_9, ^{1}J = 4.4 Hz, ^{2}J = 1.2 Hz), 0.53 (s, 3H, Si*Me*Ph_2).
^{13}C{^{1}H} NMR ($CDCl_3$) δ 137.9, 134.2, 130.0, 12989 (d, $J_{P\text{-}C}$ = 8.5 Hz), 129.6, 129.0, 128.5 (d, $J_{P\text{-}C}$ = 8.5 Hz), 127.9 (t), 127.4, 27.4 (t), 27.3, 27.0 (d), 26.9 (d), 24.1, 24.0, 23.5, 23.4, 22.4 (1:2:2:1:1 ratio for C_{ipso}H), -0.5 ($SiMePh_2$).
^{31}P{^{1}H} NMR ($CDCl_3$) δ 98.7 (s).
Anal. Calcd for $C_{72}H_{96}O_{12}P_2Si_8$: C, 60.05; H, 6.72. Found: C, 60.19; H 6.68.

(*c*-C_5H_9)$_7$$Si_7O_9$(OSiMe$Ph_2$) bis-dibenzo[d,f]-2,2´,4,4´-tetra-tert-butyl-[1,3,2]-dioxa-phosphepin (9).
A (1.30 g, 1.21 mmol) was dissolved in 20 mL of toluene and NEt_3 (0.36 g, 3.59 mmol) was added. While stirring at r.t. dibenzo[d,f]-2,2´,4,4´-tetra-tert-butyl-[1,3,2]-dioxa-phosphepin-P-chloride (1.15 g, 2.42 mmol) in 5 mL of toluene was added dropwise via syringe and the reaction continued for 16 hours. The solution was concentrated to about 5 mL and then extracted by addition of 10 mL of hexanes. After removal of solvents *in vacuo*, 2.12 g (90%) of the product was obtained as a slightly brown solid. Recrystallization from a hot mixture of CH_2Cl_2/CH_3CN (1:2) afforded **9** as colourless rectangular single crystals, suitable for X-ray analysis.
^{1}H NMR ($CDCl_3$) δ 7.64 (d, 2H, ^1J = 2.4 Hz), 7.62 (d, 2H, ^1J = 2.4 Hz), 7.45 (d, 2H, ^1J = 2.4 Hz), 7.38 (d, 2H, ^1J = 2.4 Hz), 7.32 (dd, 6H, ^1J = 5.6 Hz, ^2J = 2.4 Hz), 7.16 (d, 2H, ^1J = 2.4 Hz), 7.14 (d, 2H, ^1J = 2.4 Hz), 1.82 – 1.68 (br s, *c*-C_5H_9), 1.63 – 1.40 (br m, *c*-C_5H_9), 1.56 (s), 1.38 (s), 1.36 (s), 1.28 (s), 0.98 – 0.89 (br m, *c*-C_5H_9), 0.15 (s, SiMePh_2).
^{13}C{^{1}H} NMR ($CDCl_3$) δ 152.8, 146.0, 145.6 (d, J_{P-C} = 16.8 Hz), 140.5 (d, J_{P-C} = 24.5 Hz), 137.8, 134.1, 133.5, 129.2, 127.7, 126.1 (d, J_{P-C} = 13.7 Hz), 123.8, 35.4, 35.0, 34.6 (d), 31.6 (d), 31.2 (d), 27.8 (d, J_{P-C} = 3.0 Hz), 27.6 (d, J_{P-C} = 4.5 Hz), 27.3, 27.0, 26.9, 26.8, 26.7, 24.8, 24.2, 24.1, 23.6, 22.4 (2:1:1:2:1 ratio for C_{ipso}H), -0.4 (Si*Me*Ph_2).
^{31}P{^{1}H} NMR ($CDCl_3$) δ 131.3 (s).
Anal. Calcd for $C_{104}H_{156}O_{16}P_2Si_8$: C, 64.09; H, 8.07. Found: C, 63.85; H, 7.95.

(*c*-C_5H_9)$_7$$Si_7O_9$(OSiMe$Ph_2$)bis((diphenylphosphino)oxy) selenide (10).
8 (65.9 mg, 45.8 μmol) was dissolved in 5 mL of toluene and excess selenium was added. The reaction mixture was stirred for 1 hour at 90 °C. Excess selenium was removed by filtration and the filtrate solution was evaporated to dryness, leaving **10** as a pinkish solid. Yield: 98% (71.7 mg, 44.8 mmol).
^{1}H NMR ($CDCl_3$) δ 7.84-7.75 (m, 8H, H_{ortho} PPh_2), 7.49 (dd, 4H, H_{ortho} SiMePh_2, ^1J = 7.6 Hz, ^2J = 1.6 Hz), 7.35–7.30 (m, 6H, SiMePh_2), 7.11(br t, 12H, PPh_2), 178 (m, *c*-C_5H_9), 1.60-1.35 (m, *c*-C_5H_9), 0.98 (m, *c*-C_5H_9), 0.83 (m, *c*-C_5H_9), 0.16 (s, SiMePh_2).
^{13}C{^{1}H} NMR ($CDCl_3$) δ 137.4, 137.1 (d, ^1J = 4.5 Hz), 136.1 (d, ^1J = 4.5 Hz), 134.0, 131.3 (d, ^1J = 3.0 Hz), 131.2 (d, ^1J = 3.0 Hz), 130,8 (d, ^1J = 10.7 Hz), 130.7 (d, ^1J = 10.7 Hz), 129.5, 128.2 (d, ^1J = 6.8 Hz), 128.1 (d, ^1J = 6.8 Hz), 127.6, 27.6, 27.5, 27.3, 27.2, 26.9 (d), 26.8, 26.7, 25.1, 24.3, 23.7, 23.6, 22.5, (2:1:2:1:1 ratio for C_{ipso}H), -0.85 (Si*Me*Ph_2).
^{31}P{^{1}H} NMR ($CDCl_3$) δ 69.8 (s, J_{Se-P} = 805 Hz).
Anal. Calcd for $C_{72}H_{96}O_{12}P_2Se_2Si_8$: C, 54.11; H, 6.05. Found: C, 54.02; H, 6.12.

trans-**[$PtCl_2$(7)$_2$] (complex 11).**
$PtCl_2$(cod) (22.4 mg, 0.06 mmol) and **7** (162.7 mg, 0.12 mmol) were dissolved in 5 mL of CH_2Cl_2 and stirred for 2 hours at r.t. After removal of the solvent, complex **11** was obtained as a yellow solid. By slow diffusion of CH_3CN into a CH_2Cl_2 solution of this compound, colourless cubic single crystals could be grown, suitable for X-ray analysis.
^{1}H NMR ($CDCl_3$) δ 7.43 (d, 2H, ^{1}J = 2.4 Hz), 7.41 (d, 2H, ^1J = 2.4 Hz), 7.15 (d, 2H, ^1J = 2.4 Hz), 7.10 (d, 2H, ^1J = 2.4 Hz), 1.83 – 1.26 (br m, c-C_5H_9), 1.63 (s, *t*Bu), 1.60 (s, *t*Bu), 1.47 (s, *t*Bu), 1.36 (s, *t*Bu), 1.34 (s, *t*Bu), 1.06-0.85 (br m, c-C_5H_9)
^{31}P{^{1}H} NMR (toluene-*d8*) δ 81.5 (s, J_{Pt-P} = 4680 Hz).
Anal. Calcd for $C_{126}H_{206}Cl_2O_{30}P_2PtSi_{16}$: C, 50.81; H, 6.97. Found: C, 50.68; H, 7.10.

cis-**[$PdCl_2$(8)] (complex 12).**
$PdCl_2(C_6H_5CN)_2$ (19.0 mg, 50.0 μmol) and **8** (72.0 mg, 50.0 μmol) were dissolved in 5 mL of CH_2Cl_2 and stirred for 2 hours at r.t. Solvents were then evaporated *in vacuo* to leave **12** as a pure yellow solid. Yield: 95% (76.8 mg, 47.5 μmol). Layering with CH_2Cl_2/CH_3CN under slight argon flow gave yellow rectangular single crystals, suitable for X-ray analysis.
^{1}H NMR ($CDCl_3$) δ 7.73 (dd, 4H, J_1 = 12.8 Hz, J_2 = 7.2 Hz), 7.44 (d, 4H, J_1 = 7.2 Hz), 7.37 (t, 8H, J_1 = 7.2 Hz), 7.26 (t, 8H, J_1 = 7.2 Hz), 6.99 (t, 4H, J_1 = 7.2 Hz), 6.91 (t, 2H, J_1 = 7.2 Hz), 1.83 (br s, *c*-C_5H_9), 1.60 (br s), 1.31 (br s), 1.05 (m, *c*-C_5H_9), 0.83 (m, *c*-C_5H_9), 0.03(s, Si*Me*Ph_2).
^{13}C{^{1}H} NMR ($CDCl_3$) δ 137.1, 133.9, 132.4 (d, J_{P-C} = 5.2 Hz), 132.1, 131.2, 130.6 (d, J_{P-C} = 5.2 Hz), 130.4, 129.5, 129.1, 128.1 (d, J_{P-C} =5.2 Hz), 127.5, 127.3 (d, J_{P-C} = 5.2 Hz), 27.6, 27.3, 27.4, 27.2, 27.1, 27.0, 26.9, 26.7 (d), 24.8, 23.4 (d), 23.2, 22.2 (2:*1*:*1*:2:1 ratio for C_{ipso}H), -0.9 (Si*Me*Ph_2).
^{31}P{^{1}H} NMR ($CDCl_3$) δ 91.8 (s).

***cis*-[$PtCl_2$(8)] (complex 13).**

$PtCl_2$(cod) (15.5 mg, 41.5 μmol) and **8** (59.7 mg, 41.5 μmol) were dissolved in 5 mL of CH_2Cl_2 and stirred for 2 hours at r.t. Then the solvent was removed *in vacuo*. After that the remaining traces of solvent were removed by stripping 2 times with 5 mL hexanes to leave **13** as a white powder. Yield: 92% (65.1 mg, 38.5 μmol). Upon slow diffusion of acetonitrile into a dichloromethane solution of this compound, colourless cubic single crystals were obtained, suitable for X-ray analysis.

^{1}H NMR ($CDCl_3$) δ 7.69 (dd, 4H, J_1 = 12.0 Hz, J_2 = 7.6 Hz), 7.42 (d, 4H, J_1 = 6.8 Hz), 7.36 (t, 4H, J_1 = 6.8 Hz), 7.33 (d, 4H, J_1 = 7.2 Hz), 7.26 (d, 4H, J_1 = 7.2 Hz), 7.24 (t, 4H, J_1 = 7.6 Hz), 6.97 (t, 4H, J_1 = 7.2 Hz), 6.88 (t, 2H, J_1 = 7.2 Hz), 1.97-1.17 (br m, *c*-C_5H_9), 1.04 (quintet, J_1 = 8.8 Hz, *c*-C_5H_9), 0.83 (m, *c*-C_5H_9), 0.20 (br m, *c*-C_5H_9), -0.03(s, Si*Me*Ph_2).

^{13}C{^{1}H} NMR ($CDCl_3$) δ 137.1, 133.9, 132.7 (d), 132.3, 131.1, 130.6 (d), 130.2, 129.5, 128.7, 127.9 (d), 127.5, 127.0 (d),30.9, 28.0, 27.6, 27.5, 27.4, 27.3, 27.1 (d), 26.9, 26.8, 26.7, 24.8, 23.5 (d), 23.2, 22.2 (1:*1*:*1*:2:2 ratio for C_{ipso}H), -1.0 ($SiMePh_2$).

^{31}P{^{1}H} NMR ($CDCl_3$) δ 64.5 (d, $J_{Pt\text{-}P}$ = 4246 Hz).

Anal. Calcd for $C_{72}H_{96}O_{12}P_2PtSi_8$: C, 50.69; H, 5.67. Found: C, 50.75; H, 5.62.

***cis*-[$Mo(CO)_4$(8)] (complex 14).**

$Mo(CO)_4(pip)_2$ (53.5 mg, 141.4 μmol) and **8** (204.6 mg, 142.0 μmol) were dissolved in 10 mL of CH_2Cl_2 and stirred for 2 hours at r.t. Then the solvent was concentrated to approx. 3 mL *in vacuo* and 5 mL of acetonitrile were added to precipitate the desired product as an off-white powder. After isolation of the powder, further washing with 4 mL of acetonitrile followed by drying *in vacuo* yielded **14** as a white powder. Yield: 78% (182.6 mg, 110.8 μmol). Upon slow diffusion of acetonitrile into a dichloromethane solution, yellow, parallelepiped single crystals were obtained, suitable for X-ray analysis.

^{1}H NMR ($CDCl_3$) δ 7.70 (m, 4H), 7.49 (dd, 4H, ^1J = 7.6 Hz, ^2J = 1.2 Hz), 7.41 (t, 2H, ^1J = 7.6 Hz, ^2J = 1.2 Hz), 7.34 (dt, 10H, ^1J = 7.6 Hz, ^2J = 3.2 Hz), 7.17 (dd, 4H), 7.00 (t, 4H, ^1J = 7.6 Hz), 6.68 (t, 2H, ^1J = 7.6 Hz), 1.95-1.14 (br m, c-C_5H_9), 1.06 (quintet, ^1J = 8.8 Hz, c-C_5H_9), 0.84 (m, c-C_5H_9), 0.1 (s, $SiMePh_2$).

^{13}C{^{1}H} NMR ($CDCl_3$) δ 215.5 (t, $J_{P\text{-}C}$ = 10.5 Hz), 210.2 (t, $J_{P\text{-}C}$ = 11.5 Hz), 209.3 (t, $J_{P\text{-}C}$ = 10.0 Hz), 142.6 (t, $J_{P\text{-}C}$ = 14.6 Hz), 141.5 (t, $J_{P\text{-}C}$ = 19.9 Hz), 137.5, 134.0, 131.3 (t, $J_{P\text{-}C}$ = 7.5 Hz), 130.3, 129.5, 128.8 (t, $J_{P\text{-}C}$ = 7.5 Hz), 128.3, 127.8 (t), 127.6 (t), 127.6, 27.8, 27.6, 27.5, 27.4, 27.3 (d), 27.1 (d), 27.0, 26.9, 26.7, 26.6 (d), 25.1, 24.1, 23.6, 22.4, 22.3 (1:2:2:1:1 ratio for C_{ipso}H), -1.2 ($SiMePh_2$).

^{31}P{^{1}H} NMR ($CDCl_3$) δ 130.4 (s).

FTIR (ATR mode, solid, cm^{-1}) ν (carbonyl region) 1872.2 (s), 1894.6 (st) 1934.1 (m), 2019.8 (m).

Anal. Calcd for $C_{76}H_{96}MoO_{16}P_2Si_8$:C, 55.39; H, 5.87. Found: C, 55.18; H, 5.83.

***trans*-[Rh(Cl)(CO)(8)] (complex 15).**

[Rh(μ-Cl)$(CO)_2]_2$ (21.2 mg, 54.5 μmol) and **8** (158.5 mg, 110.1 μmol) were stirred in 8 mL of CH_2Cl_2 for 6 hours, giving a light yellow solution. After removal of the solvent *in vacuo*, complex **15** remained as a microcrystalline yellow solid. Slow diffusion of CH_3CN into a CH_2Cl_2 solution of this compound led to yellow platelet crystals, suitable for X-ray analysis.

^{1}H NMR ($CDCl_3$) δ 7.97 (m, 2H), 7.81 (d, 4H), 7.40 (m, 10H), 7.06 (q, 4H, ^1J = 7.2 Hz), 2.00 – 1.18 (br m, *c*-C_5H_9), 1.15 (m, *c*-C_5H_9), 0.94 (br m, *c*-C_5H_9), 0.35(s, $SiMePh_2$).

^{31}P{^{1}H} NMR ($CDCl_3$) δ 110.1 (d, $J_{Rh\text{-}P}$ = 145 Hz).

FTIR (ATR mode, solid, cm^{-1}): ν 1995 (Rh(*CO*)).

***trans*-[$PdCl_2$(9)] (complex 16).**

$PdCl_2$(cod) (8.4 mg, 29.4 μmol) and **9** (58.7 mg, 30.1 μmol) were stirred in 5 mL of CH_2Cl_2 for 1.5 h. After removal of the solvent, **16** was obtained as a yellow solid. Layering with CH_2Cl_2/CH_3CN gave yellow rectangular single crystals, suitable for X-ray analysis .

^{1}H NMR ($CDCl_3$) δ 7.66 (dd, 4H, ^1J = 7 6 Hz, ^2J = 1.2 Hz), 7.43 (d, 2H, ^1J = 2.4 Hz), 7.38 (t, 8H, ^1J = 7.2 Hz), 7.19 (d, 2H, ^1J = 2.4 Hz), 7.04 (d, 2H, ^1J = 2.4 Hz), 1.83 – 1.18 (br m, *c*-C_5H_9), 1.61 (s, *t*Bu), 1.49 (s, *t*Bu), 1.36 (s, *t*Bu), 1.34 (s, *t*Bu), 1.31 (br s), 0.92 (s, $SiMePh_2$), 0.80 (m, *c*-C_5H_9).

^{13}C{^{1}H} NMR ($CDCl_3$) δ 146.7, 141.3, 139.7, 137.7, 134.4, 134.1, 132.5, 130.9, 129.3, 128.8, 127.5, 126.3, 124.9, 124.1, 36.1, 35.3, 34.6, 32.4, 31.5 (d), 31.2, 30.4, 28.9, 27.9, 27.7, 27.6, 27.5, 27.3, 27.1, 27.0, 26.9, 26.4, 26.3, 24.4, 24.3, 23.8, 23.0, 22.5 (1:2:2:1:1 ratio for C_{ipso}H), 1.1 ($SiMePh_2$).

^{31}P{^{1}H} NMR ($CDCl_3$) δ 88 9 (s).

Anal. Calcd for $C_{104}H_{156}Cl_2O_{16}P_2PdSi_8$:C, 58.75; H, 7.39. Found: C, 58.68; H, 7.42.

cis-**[Mo(CO)$_4$(9)] (complex 17).**
$Mo(CO)_4(pip)_2$ (27.2 mg, 71.9 μmol) and **9** (154.6 mg, 79.0 μmol) were dissolved in 10 mL of CH_2Cl_2 and stirred for 2 hours at r.t. Then the solvent was concentrated to approx. 3 mL *in vacuo*. 5 mL of acetonitrile were added to precipitate the desired product as an off-white powder. After isolation of the powder, further washing with 4 mL of acetonitrile followed by drying *in vacuo* yielded **16** as a pure product. Upon slow diffusion of acetonitrile into a CH_2Cl_2 solution, yellow, parallelepiped single crystals were obtained, suitable for X-ray analysis.
^{1}H NMR ($CDCl_3$) δ 7.68 (dd, 4H, ^1J = 7 6 Hz, ^2J = 1.2 Hz), 7.44 (dd, 6H, ^1J = 7.6 Hz, ^1J = 3.2 Hz), 7.41 (d, 4H, ^1J = 7.2 Hz), 7.10 (d, 2H, ^1J = 2.4 Hz), 7.01 (d, 2H, ^1J = 2.4 Hz), 1.84 – 1.68 (br m, *c*-C_5H_9), 1.62 (s, *t*Bu), 1.61-1.07 (br m, *c*-C_5H_9), 1.50 (s, *t*Bu), 1.35 (s, *t*Bu), 1.32 (s, *t*Bu), 1.05-0.83 (br m, *c*-C_5H_9), 0.80 (br m, *c*-C_5H_9), 0.75 (s, *t*Bu), 0.11 (s, Si*CH*$_3$Ph$_2$).
^{13}C{^{1}H} NMR ($CDCl_3$) δ 146.7, 146.3, 140.0, 139.4, 137.5, 134.3, 134.0, 133.0, 132.1, 129.5, 127.8, 127.6, 126.7, 126.0, 123.8, 36.2, 35.7, 34.5, 34.4, 33.0, 32.3, 31.5 (d), 31.3, 31.2, 28.2, 28.1, 28.0, 27.7, 27.4, 27.2, 27.1, 27.0, 26.9, 26.8, 26.7, 26.6, 26.2 (d), 25.7, 24.9, 24.0, 22.6, 22.1 (1:2:2:1:1 ratio for $C_{ipso}H$), 1.1 ($SiMePh_2$).
^{31}P{^{1}H} NMR ($CDCl_3$) δ 149.6 (s).
FTIR (ATR mode, solid, cm^{-1}) ν (carbonyl region) 2041.3 (m), 1947.9 (st) 1935.2 (st), 1922.3 (st).

[RhCl(CO)(9)] (complex 18).
[Rh(μ-Cl)$(CO)_2]_2$ (13.6 mg, 3.50 μmol) and **9** (136.6 mg, 7.01 μmol) were stirred in 5 mL of CH_2Cl_2 for 2 hours, giving a reddish brown solution. The ^{31}P{1H} NMR showed the existence of three species, all as doublets in a ratio of 1:1:2. By further reaction in toluene overnight at reflux, the signal for the major product **A** (~ 90 %) was present at 110.4 ppm with a coupling constant J_{Rh-P} of 299 Hz while the minor product **B** appeared at 119.4 ppm with a coupling constant J_{Rh-P} of 217 Hz. Layering a dichloromethane solution of the solid with acetonitrile yielded **18** as yellow cubic single crystals, suitable for X-ray analysis, showing the minor product.
^{1}H NMR ($CDCl_3$) δ 7.78 (br s, 2H), 7.66 (dd, 2H, ^1J = 7.6 Hz, ^2J = 2.4 Hz), 7.55 (br d, 2H), 7.49 (br s, 2H), 7.42 (br d, 4H, ^1J = 7.2 Hz), 7.37 (br d, 2H), 7.15 (br s, 2H), 7.12 (br s, 2H), 1.83 – 1.18 (br m, *c*-C_5H_9), 1.61 (s, *t*Bu), 1.49 (s, *t*Bu), 1.36 (s, *t*Bu), 1.34 (s, *t*Bu), 1.31 (br s), 0.92 (s, $SiMePh_2$), 0.80 (m, *c*-C_5H_9).
^{31}P{^{1}H} NMR ($CDCl_3$) δ 119.4 (d, J_{Rh-P} = 217 Hz), 110.4 (d, J_{Rh-P} = 299 Hz).
FTIR (ATR mode, solid, carbonyl range, cm^{-1}): ν 2019 (s), 2009 (s).

Hydroformylation of 1-octene.
Experiments were performed in tailor-made 75 mL stainless steel autoclaves. 1-Octene was filtered over neutral alumina before use, to remove peroxides. Rh(acac)$(CO)_2$ (2.00 mg, 7.75 μmol) and the appropriate amount of ligand (6 eq.) were both dissolved in 5 mL of toluene. The combined solution was transferred under argon into the autoclave, equipped with a glass inner beaker, which was preheated to 80 °C. The autoclave was pressurized to 18 bar. After 1 hour 10 mL of the substrate solution, containing 1-octene (4.86 mL, 31.0 mmol), decane (2.43 mL, 12.5 mmol) in toluene was added to the reaction mixture under 20 bar. After reaction the autoclave was cooled and the reaction mixture quenched by addition of an excess of $P(OEt)_3$ to form inactive rhodium species. A sample was withdrawn for GC analysis.

Computational Methods.
For all the presented calculations, the use of the Gaussian98 series of computer programs have been used.[87]

Density Functional Methods.
Standard computational methods based on the density functional theory have been employed.[88] The used functional is the three-parameter exchange functional of Becke[89] together with the correlation functional of Lee, Yang and Parr (B3LYP).[90] For the P, C, O, Si, and H the basis set used is the Pople style basis set 6-31G[91] with diffuse (+) s- and p- functions added on the heavy atoms[92] and polarization function[93] (d,p), adding one d function on the heavy atoms and one p function on the hydrogens [6-31+G(d,p)].
The geometries of all the model compounds have been fully optimized using analytical gradients technique at the B3LYP level of theory previously cited. No symmetry constraints have been introduced. The optimized stationary points have been confirmed through an harmonic vibrational analysis (B3LYP level), using analytical or numerical differentiation of the obtained analytical energy first derivative.

Crystal structure determination of 9, 12, 13, 16 and 18.

For **12** a correction for absorption was considered unnecessary. This structure was solved by automated direct methods using SIR97,[94b] and refined on F^2 using SHELXL97.[95] For **13** an empirical absorption correction was applied using PLATON/DELABS (0.550-0.894 transmission).[96] Compound **13** is isomorphous with its Pd analogue **12**; the atomic positions of the latter compound were used as the initial model for **13**. Four of the seven cyclopentyl rings and one of the six phenyl rings are disordered over two conformations and refined with a disorder model. The crystal structure contains voids (495.7 Å^3/ unit cell) filled with disordered solvent molecules (dichloromethane/acetonitrile). Their contribution to the structure factors was ascertained using PLATON/SQUEEZE (158 e/unit cell).[96] All non-hydrogen atoms were refined with anisotropic displacement parameters. All hydrogen atoms were constrained to idealized geometries and allowed to ride on their carrier atoms with an isotropic displacement parameter related to the equivalent displacement parameter of their carrier atoms. Structure validation and molecular graphics preparation were performed with the PLATON package.[96] For **13** the structure was refined on F^2 using SHELXL97.[95] Four of the seven cyclopentyl rings and one of the six phenyl rings are disordered over two conformations and were refined with a disorder model. The crystal structure contains voids (404.2 Å^3/ unit cell) filled with disordered solvent molecules (dichloromethane/acetonitrile). Their contribution to the structure factors was ascertained using PLATON/SQUEEZE (122 e/unit cell).[96] All non-hydrogen atoms were refined with anisotropic displacement parameters. All hydrogen atoms were constrained to idealized geometries and allowed to ride on their carrier atoms with an isotropic displacement parameter related to the equivalent displacement parameter of their carrier atoms. Structure validation and molecular graphics preparation were performed with the PLATON package.[96]
For **9**, **16** and **18** diffraction data were collected on a Nonius KappaCCD diffractometer with rotating anode at 150 K. PLATON/DELABS was used to correct the data of complex **16** for absorption. The structures were solved by Direct Methods (SHELXS97[94a] for **9** and SIR97[94b] for **16**) and Patterson methods (DIRDIF99[94c] for **18**). Least-squares refinement of F^2 was done with SHELXL97.[95] Hydrogen atoms were introduced at calculated positions and refined riding on their carrier atom. Several of the *tert*-butyl and cyclopentyl moieties were refined with a disorder model in all three structures. Structures **9** and **18** contain voids (393 Å^3/unit cell for **9** and 2460 Å^3 for **18**, with 83 and 418 recovered electrons respectively) filled with severily disordered solvents (CH_2Cl_2/CH_3CN). Their contribution to the structure factors was taken into account in the least-squares refinement using the PLATON/SQUEEZE[96] procedure. Structure validation and molecular graphics were performed with the PLATON package.[96] Intensity data were collected on a Nonius Kappa CCD diffractometer with rotating anode. The structures were solved by direct methods using SHELXS97,[94a] and refined on F^2 by least-squares procedures using SHELXL97.[95] All non-hydrogen atoms were refined with anisotropic displacement parameters. Hydrogen atoms were constrained to idealized geometries and allowed to ride on their carrier atoms with an isotropic displacement parameter related to the equivalent displacement parameter of their carrier atoms. The unit cells also contained voids filled with disordered solvent (CH_2Cl_2/CH_3CN). The solvent contribution was taken into account using PLATON/SQUEEZE (158 Å^3/unit cell). Structure validation and molecular graphics preparation were performed with the PLATON package.[96] Crystal data are given in Table 5.10 and 5.11.

Crystal structure determination of 14, 15 and 17.
Intensity data were collected on a *Bruker SMART APEX CCD*. Data integration and global cell refinement was performed with the program *SAINT*. Intensity data were corrected for Lorentz and polarization effects. The structure was solved by Patterson methods and extension of the model was accomplished by direct methods applied to difference structure factors using the program DIRDIF99.[94c] The positional and anisotropic displacement parameters for the non-hydrogen atoms were refined. Refinement was frustrated by disorder problems, since several cyclopentyl groups, one phenyl groups as well as one of the dichloromethane solvent molecules were highly disordered and probably partly occupied. displacement parameters and bond restraints were applied in the final refinement to establish 1,2 and 1,3 distances, but unfortunately the applied two-sited disorder model could not account for all the observed residual density (dynamic disorder). No discrete successful model could be fitted in the residual density. Final refinement on F^2 carried out by full-matrix least-squares techniques converged at $wR(F^2)$ = 0.2312 for 29433 reflections and $R(F)$ = 0.0808 for 21648 reflections with $F_o \geq 4.0\ \sigma(F_o)$ and 1453 parameters and 35 restraints. The hydrogen atoms were included in the final refinement riding on the C-atom as appropriate with $U_{iso} = c \times U_{equiv}$. Final refinement on F^2 carried out by full-matrix least-squares techniques converged at $wR(F^2)$ = 0.1057 for 21387 reflections and $R(F)$ = 0.0375 for 18554 reflections with $F_o \geq 4.0\ \sigma(F_o)$ and 975 parameters. Crystal data are given in Table 5.10 and 5.11.

Crystal structure determination of 11.

Intensity data were collected on a Nonius Kappa CCD diffractometer with rotating anode. The structure was solved by direct methods using SHELXS97,[94a] and refined on F^2 by least-squares procedures using SHELXL97.[95] All non-hydrogen atoms were refined with anisotropic displacement parameters. Hydrogen atoms were constrained to idealized geometries and allowed to ride on their carrier atoms with an isotropic displacement parameter related to the equivalent displacement parameter of their carrier atoms. Most cyclopentyl and *tert*-butyl groups were disordered and restraints were necessary to obtain reasonable geometries. The unit cells also contained voids filled with disordered solvent (CH_2Cl_2/CH_3CN). The solvent contribution was taken into account using PLATON/SQUEEZE (1920 $Å^3$/unit cell and 629 electrons). Structure validation and molecular graphics preparation were performed with the PLATON package.[96] Some crystallographic details: wR_2 = 0.299, R_1 = 0.098, total reflections 164,471, unique reflections 25029, R_{int} = 0.143.

Table 5.10: *Selected crystallographic data for complexes **12-15**.*

	12	**13**	**14**	**15**
Formula	$C_{72}H_{94}Cl_2O_{12}P_2PdSi_8$	$C_{72}H_{94}Cl_2O_{12}P_2PtSi_8$	$C_{76}H_{94}Cl_2O_{16}P_2MoSi_8$ ·2·CH_2Cl_2	$C_{73}H_{94}ClO_{13}P_2RhSi_8$
FW (g·mol^{-1})	1617.45	1706.14	1747.12	1606.55
Crystal size (mm)	0.12×0.15×0.30	0.06×0.24×0.51	0.49×0.35×0.30	0.33×0.29×0.09
Crystal system	Triclinic	Triclinic	Triclinic	Monoclinic
Space group	*P*$\bar{1}$ (no. 2)	*P*$\bar{1}$ (no. 2)	*P*$\bar{1}$ (no. 2)	$P2_1/a$, (no. 14)
a (Å)	12.9272(1)	12.9593(1)	13.5557(5)	20.2345(8)
b (Å)	17.7140(2)	17.6366(1)	17.5982(7)	15.8819(6)
c (Å)	19.4640(2)	19.4061(2)	19.2276(7)	24.428(1)
α (°)	89.1056(4)	88.9667(3)	73.275(1)	
β (°)	76.6436(4)	76.5243(3)	79.557(1)	91.356(1)
γ (°)	78.2285(5)	77.4749(5)	78.516(1)	
V (Å^3)	4243.03(7)	4208.19(6)	4267.2(3)	7848.0(5)
Z	2	2	2	4
d_{calc} (g cm^{-3})	1.266	1.347	1.360	1.360
μ (Mo-Kα) (mm^{-1})	0.485	1.936	4.28	4.73
T (K)	150	150	100	160
Total reflections	53944	59874	40663	67424
Unique reflections (R_{int})	14934 (0.085)	19015 (0.052)	21387 (0.0185)	18032 (0.0372)
wR_2 (F^2) (all data)	0.1132	0.0777	0.1057	0.1111
λ (Å)	0.71073	0.71073	0.71073	0.71073
R_1 (F)	0.0447	0.0329	0.0375	0.0421
F(000)	1692	1756	1828	3368

$R_{int} = \sum [|F_o^2 - F_o^2(\text{mean})|] / \sum [F_o^2]$; $wR(F^2) = [\sum [w(F_o^2 - F_c^2)^2] / \sum [w(F_o^2)^2]]^{1/2}$; $R(F) = \sum (||F_o| - |F_c||) / \sum |F_o|$

Table 5.11: *Selected crystallographic data for ligand **9** and complexes **16-18**.*

	9	**16**	**17**	**18**
Formula	$C_{104}H_{156}O_{16}P_2Si_8$	$C_{104}H_{156}Cl_2O_{16}P_2Si_8Pd$ ·2.52·CH_2Cl_2 1.96·CH_3CN	$C_{108}H_{156}MoO_{20}P_2Si_8$ ·2·CH_2Cl_2	$C_{106}H_{156}Cl_2O_{18}P_2Rh_2Si_8$
FW (g·mol^{-1})	1948.95	2420.86	2326.86	2281.70
Crystal size (mm)	0.24×0.36×0.66	0.09×0.27×0.52	0.52×0.44×0.27	0.05×0.10×0.30
Crystal system	Triclinic	Monoclinic	Monoclinic	Orthorhombic
Space group	$P\bar{1}$ (no. 2)	$P2_1/c$ (no. 14)	$P2_1/a$ (no. 14)	$P2_12_12_1$ (no. 19)
a (Å)	13.5395(1)	13.7930(1)	24.605(1)	14.2366(10)
b (Å)	14.2578(1)	32.0407(3)	18.882(1)	27.516(3)
c (Å)	29.4554(2)	31.6221(3)	25.723(1)	33.591(3)
α (°)	85.7071(3)			
β (°)	88.9721(3)	114.4920(10)	90.162(5)	
γ (°)	87.7415(3)			
V (Å^3)	5665.17(7)	12717.5(2)	11950.6(9)	13159(2)
Z	2	4	4	4
d_{calc} (g cm^{-3})	1.143	1.265	1.279	1.1517
μ (Mo-Kα) (mm^{-1})	0.181	0.452	0.326	0.442
T (K)	150	150	100	150
Total reflections	93379	75341	108533[a]	331952
Unique reflections (R_{int})	22295 (0.061)	22387 (0.054)	29433 (0.057)	30194 (0.062)
wR_2 (F^2) (all data)	0.1471	0.1441	0.2312	0.110
λ (Å)	0.71073	0.71073	0.71073	0.71073
R_1 (F)	0.0533	0.0564	0.0808	0.041
F(000)	2100	5116	4916	4808

$R_{int} = \sum [|F_o^2 - F_o^2(\text{mean})|] / \sum [F_o^2]$; $wR(F^2) = [\sum [w(F_o^2 - F_c^2)^2] / \sum [w(F_o^2)^2]]^{1/2}$; $R(F) = \sum (||F_o| - |F_c||) / \sum |F_o|$

[a] $F_o \geq 4.0\,\sigma(F_o)$ and 1453 parameters.

5.7 Notes and References

Parts of the work described in this chapter have been published:
J.I. van der Vlugt, M.M.P. Grutters, J. Ackerstaff, R.W.J.M.Hanssen, H.C.L. Abbenhuis and D. Vogt, *Tetrahedron Lett.*, accepted.
J.I. van der Vlugt, M. Fioroni, J. Ackerstaff, R. W.J.M. Hanssen, A.M. Mills, A.L. Spek, A. Meetsma, H.C.L. Abbenhuis and D. Vogt, *Organometallics*, accepted.
J.I. van der Vlugt, J. Ackerstaff, M.M.P. Grutters, T.W. Dijkstra, R.W.J.M. Hanssen, A.M. Mills, H. Kooijman, A.L. Spek, A. Meetsma, H.C.L. Abbenhuis and D. Vogt, *.J. Chem. Soc., Dalton Trans.*, submitted.
J.I. van der Vlugt, G. Ionescu, T.W. Dijkstra, H. Kooijman, A.L. Spek, R. Duchateau, H.C.L. Abbenhuis and D. Vogt, *manuscript in preparation.*
M. Fioroni, J.I. van der Vlugt and Dieter Vogt, *manuscript in preparation.*
A.L. Spek, A.M. Mills, J.I. van der Vlugt, J. Ackerstaff and D. Vogt, *Acta Cryst. E*, submitted.

1 J.F. Brown and L.H. Vogt, *J. Am. Chem. Soc.*, **1965**, *87*, 4313.
2 F.J. Feher, R. Terroba and J.W. Ziller, *Chem. Commun.*, **1999**, 2309.
3 a) F.J. Feher, D.A. Newman and J.F. Walzer, *J. Am. Chem. Soc.*, **1989**, *111*, 1741; b) F.T. Edelmann, *Angew. Chem., Int. Ed. Engl.*, **1992**, *31*, 586; c) F.J. Feher and T.A. Budzichowski, *Polyhedron*, **1995**, *14*, 3239.
4 N. Maxim, P.C.M.M. Magusin, P.J. Kooyman, J.H.M.C. van Wolput, R.A. van Santen and H.C.L. Abbenhuis, *Chem. Mat.*, **2001**, *13*, 2958.
5 J. Choi, J. Harcup, A.F. Yee, Q. Zhu and R.M. Laine, *J. Am. Chem. Soc.*, **2001**, 123, 11420.
6 F.J. Feher, R. Terroba, R.Z. Jin, K.D. Wyndham, S. Lucke, R. Brutchey and F. Nguyen, *PMSE*, **2000**, *82*, 301.
7 R. Duchateau, *Chem. Rev.*, **2002**, *102*, 3525.
8 a) R.W.J.M. Hanssen, A. Meetsma, R.A. van Santen and H.C.L. Abbenhuis, *Inorg. Chem.*, **2001**, *40*, 4049; b) H.C.L. Abbenhuis, *Chem. Eur. J.*, **2000**, *6*, 25; c) V. Lorenz, A. Fischer, S. Gießmann, J.W. Gilje, Y. Gun'ko, K. Jacob and F.T. Edelmann, *Coord. Chem. Rev.*, **2000**, *206/207*, 321.
9 a) L. Ropartz, D.F. Foster, R.E. Morris, A.M.Z. Slawin and D.J. Cole-Hamilton, *J. Chem. Soc., Dalton Trans.*, **2002**, 1997; b) L. Ropartz, D.F. Foster, R.E. Morris, A.M.Z. Slawin and D.J. Cole-Hamilton, *J. Chem. Soc., Dalton Trans.*, **2002**, 361; c) L. Ropartz, R.E. Morris, D.F. Foster and D.J. Cole-Hamilton, *J. Mol. Cat. A: Chem.*, **2002**, *182-183*, 99.
10 K. Wada, D. Izuhara, M. Shiotsuki, T. Kondo and T. Mitsudo, *Chem. Lett.*, **2001**, *31*, 734.
11 a) F.J. Feher, J.J. Schwab, S.H. Philips, A. Eklund and E. Martinez, *Organometallics*, **1995**, *14*, 4452-4453; b) B. Hong, P.S. Toms, H.J. Murfee and M.J. Lebrun, *Inorg. Chem.*, **1997**, *36*, 6146; c) S. Lücke, K. Stoppek-Langner, J. Kuchinke and B. Krebs, *J. Organomet. Chem.*, **1999**, *584*, 11; d) F.J. Feher, K.D. Wyndham, D. Soulivong and F. Nguyen, *J. Chem. Soc., Dalton Trans.*, **1999**, 1491.
12 B.J. Hendan and H.C. Marsmann, *Appl. Organomet. Chem.*, **1999**, *13*, 287.
13 a) F.J. Feher and T.L. Tajima, *J. Am. Chem. Soc.*, **1991**, *113*, 3618; b) F.J. Feher, J.F. Walzer and R.L. Blanski, *J. Am. Chem. Soc.*, **1991**, *113*, 3618; c) F.J. Feher and T.A. Budzichowski, *J. Organomet. Chem.*, **1989**, *379*, 33.
14 a) P.W.N.M. van Leeuwen and C.F. Roobeek (to Shell), Brit. Pat. 2068377, **1980** [*Chem. Abstr.*, **1984,** *101*, 191142]; b) P.W.N.M. van Leeuwen and C.F. Roobeek, *J. Organomet. Chem.*, **1983**, *258*, 343.
15 R.L. Pruett and J.A. Smith, *J. Org. Chem.*, **1969**, *34*, 327; b) R.L. Pruett and J.A. Smith (to Union Carbide) S. African Pat. 6,804,937, **1968** [*Chem. Abstr.*, **1969**, *71*, 90819].
16 A.K. Bhattacharya and G. Thyagarajan, *Chem. Rev.*, **1981**, *81*, 415-430.
17 T. Jongsma, G. Challa and P.W.N.M. van Leeuwen, *J. Organomet. Chem.*, **1991**, *421*, 121.
18 A. van Rooy, E.N. Orij, P.C.J. Kamer and P.W.N.M. van Leeuwen, *Organometallics*, **1995**, *14*, 34.
19 T. Omatsu (to Kururay) Eur. Pat. 303,060, **1989** [*Chem. Abstr.*, **1989**, *111*, 38870].
20 E. Billig, A.G. Abatjoglou and D.R. Bryant (to Union Carbide) U.S. Pat. 4,769,498, **1988** [*Chem. Abstr.*, **1988**, *111*, 117287].
21 E. Billig, A.G. Abatjoglou and D.R. Bryant (to Union Carbide) U.S. Pat. 4,668,651, **1987** [*Chem. Abstr.*, **1987**, *107*, 7392].
22 P.M. Burke, J.M. Garner, W. Tam, K.A. Kreutzer and A.J.J.M. Teunissen (to DSM/Du Pont) WO 97/33854, **1997** [*Chem. Abstr.*, **1997**, *127*, 294939].
23 K. Sato, Y. Karawagi, M. Takai and T. Ookoshi (to Mitsubishi) U.S. Pat. 5,235,113, **1993** [*Chem. Abstr.*, **1993**, *118*, 191183].

24 F.J. Feher and T.A. Budzichowski, *Organometallics*, **1991,** *10*, 812.
25 F.J. Feher, T.A. Budzichowski, R.L Blanski, K.J. Weller and J.W. Ziller, *Organometallics*, **1991,** *10*, 2526.
26 a) M.D. Sworonska-Ptasinska, R. Duchateau, R.A. van Santen and G.P.A. Yap, *Eur. J. Inorg. Chem.*, **2001**, 133; b) M.D. Sworonska-Ptasinska, R. Duchateau, R.A. van Santen and G.P.A. Yap, *Organometallics*, **2001**, *20*, 3519.
27 M. Sekine, K. Okimoto, K. Yamada and T. Hata, *J. Org. Chem.*, **1981**, *46*, 2097.
28 R. Duchateau, H.C.L. Abbenhuis, R.A. van Santen, S.K.H. Thiele and M.F.H. van Tol, *Organometallics*, **1998**, *17*, 5222.
29 Modified procedure from: F.J. Feher, K. Rahimian, T.A. Budzichowski and J.W. Ziller, *Organometallics*, **1995**, *14*, 3920; a) R. Duchateau, U. Cremer, R.J. Harmsen, S.I. Mohamud, H.C.L. Abbenhuis, R.A. van Santen, A. Meetsma, S.K.-H. Thiele, M.F.H. van Tol and M. Kranenburg, *Organometallics*, **1999**, *18*, 5447; b) J.R. Severn, R. Duchateau, R.A. van Santen, D.D. Ellis, A.L. Spek and G.P.A. Yap, *J. Chem. Soc., Dalton Trans.*, **2003**, 2293; c) J.R. Severn, R. Duchateau, R.A. van Santen, D.D. Ellis and A.L. Spek, *Organometallics*, **2002**, *21*, 4.
30 Z. Fei, R. Schmutzler and F.T. Edelmann, *Z. Anorg. Allg. Chem.*, **2003**, *629*, 353.
31 F.J. Feher, R. Terroba and J.W. Ziller, *Chem. Commun.*, **1999**, 2153.
32 M.S. Balakrishna, R. Panda and J.T. Mague, *J. Chem. Soc., Dalton Trans.*, **2002**, 4617.
33 D.W. Allen and B.F. Taylor, *J. Chem. Soc., Dalton Trans.*, **1982**, 51.
34 A. Suárez, M.A. Méndez-Rojas and A. Pizzano, *Organometallics*, **2002**, *21*, 4611. Actually this paper describes the conversion of a phosphine-phosphite into the corresponding diselenide. The corresponding coupling constants for the phosphine-selenide and the phosphite-selenide mark the outer limits for the value of $J_{Se\text{-}P}$.
35 R.S. Mulliken, *J. Chem. Phys.*, **1955**, *23*, 1833.
36 C.J. Cobley and P.G. Pringle, *Inorg. Chim. Acta*, **1997**, *265*, 107.
37 P.S. Pregosin and S.N. Sze, *Helv. Chim. Acta*, **1978**, *61*, 1848.
38 S. Steyer, C. Jeunesse, D. Matt, R. Welter and M. Wesolek, *J. Chem. Soc., Dalton Trans.*, **2002**, 4264.
39 a) S. Cserépi-Szűcs, G. Huttner, L. Zsolnai and J. Bakos, *J. Organomet. Chem.*, **1999**, *586*, 70; b) E.E. Nifantyev, E.N. Rasadkina, L.K. Vasyanina, V.K. Belsky and A.I. Stash, *J. Organomet. Chem.*, **1997**, *529*, 171.
40 a) M.S. Balakrishna, P. Chandrasekaran and P.P. George, *Coord. Chem. Rev.*, **2003**, *241*, 87; b) J.K. Hogg, S.L. James, A.G. Orpen and P.G. Pringle, *J. Organomet. Chem*., **1994**, *480*, c1.
41 G.M. Gray, F.P. Fish, D.K. Srivastava, A. Varshney, M.J. van der Woerd and S.E. Ealick, *J. Organomet. Chem.*, **1990**, *385*, 49.
42 H. Voelker, S. Freitag, U. Pieper and H.W. Roesky, *Z. Anorg. Allg. Chem.*, **1995**, *621*, 694.
43 P. Faidherbe, C. Wieser, D. Matt, A. Harriman, A. De Cian and J. Fischer, *Eur. J. Inorg. Chem.*, **1998**, 451.
44 P. Berdagué, J .Courtieu, H. Adams, N.A. Bailey and P.M. Maitlis, *J. Chem. Soc., Chem. Commun.*, **1994**, 1589.
45 D.R. Evans, M. Huang, J.C. Fettinger and T.L. Williams, *Inorg. Chem.*, **2002**, *41*, 5986.
46 M. Stolmar, C. Floriani, A. Chiesi-Villa and C. Rizzoli, *Inorg. Chem.*, **1997**, *36*, 1694.
47 G. Gerritsen, R. Duchateau, R.A. van Santen and G.P.A. Yap, *Organometallics*, **2003**, *22*, 100.
48 H.C.L. Abbenhuis, A.D. Burrows, H. Kooijman, M. Lutz, M.T. Palmer, R.A. van Santen and A.L. Spek, *Chem. Commun.*, **1998**, 2627.
49 T. Nishimata, K. Yamaguchi and M. Mori, *Tetrahedron Lett.*, **1999**, *40*, 5713.
50 C.G. Arena, D. Drommi, F. Faraone, C. Graiff and A. Tiripicchio, *Eur. J. Inorg. Chem.*, **2001**, 247.
51 Z. Csók, G. Szalontai, G. Czira and L. Kollár, *J. Organomet. Chem.*, **1998**, *570*, 23.
52 W. Xu, J.P. Rourke, J.J. Vittal and R.J. Puddephatt, *Inorg. Chem.*, **1995**, *34*, 323.
53 T.J. Bartczak, W.J. Youngs and J.A. Ibers, *Acta Cryst.*, **1984**, *C40*, 1564.
54 S.K. Armstrong, R.J. Cross, L.J. Farrugia, D.A. Nichols and A. Perry, *Eur. J. Inorg. Chem.*, **2002**, 141.
55 a) M. Hariharasarma, C.H. Lake, C.L. Watkins and G.M. Gray, *Organometallics*, **1999**, *18*, 2593; b) M. Hariharasarma, C.H. Lake, C.L. Watkins and G.M. Gray, *J. Organomet. Chem.*, **1999**, *580*, 328; c) G.M. Gray and K.A. Redmill, *J. Organomet. Chem.*, **1985**, *280*, 105.
56 J. Powell, A. Lough and F. Wang, *Organometallics*, **1992**, *11*, 2289.
57 C.M. Haar, J. Huang, S.P. Nolan and J.L. Petersen, *Organometallics*, **1998**, *17*, 5018.
58 A.D. Burrows, M.F. Mahon, M.T. Palmer and M. Varrone, *Inorg. Chem.*, **2002**, *41*, 1695.
59 K.G. Moloy and J.L. Petersen, *J. Am. Chem. Soc.*, **1995**, *117*, 7696.

60 a) S.C. van der Slot, J. Duran, J. Luten, P.C.J. Kamer and P.W.N.M. van Leeuwen, *Organometallics*, **2002**, *21*, 3873; b) S.C. van der Slot, P.C.J. Kamer, P.W.N.M. van Leeuwen, J. Fraanje, K. Goubitz, M. Lutz and A.L. Spek, *Organometallics*, **2000**, *19*, 2504.

61 S. Vastag, B. Heil and L. Markó, *J. Mol. Cat.*, **1979**, *5*, 189.

62 V.F. Kuznetsov, G.A. Facey, G.P.A. Yap and H. Alper, *Organometallics*, **1999**, *18*, 4706.

63 a) R. Kempe, M. Schwarze and R. Selke, *Z. Kristallogr.*, **1995**, *210*, 555; b) R. Kempe, A. Spannenberg and D. Heller, *Z. Kristallogr.*, **1998**, *213*, 631; c) R. Kempe, A. Spannenberg, D. Heller, R. Kadyrov and V. Fehring, *Z. Kristallogr.*, **2001**, *216*, 157.

64 a) T.V. RajanBabu, T.A. Ayers, G.A. Halliday, K.K. You and J.C. Calabrese, *J. Org. Chem.*, **1997**, *62*, 6012; b) T.V. RajanBabu, B. Radetich, K.K. You, T.A. Ayers, A.L. Casalnuovo and J.C. Calabrese, *J. Org. Chem.*, **1999**, *64*, 3429.

65 F.J. Parlevliet, M.A. Zuideveld, C. Kiener, H. Kooijman, A.L. Spek, P.C.J. Kamer and P.W.N.M. van Leeuwen, *Organometallics*, **1999**, *18*, 3394.

66 S.J. Sabounchei, A. Nagipour and J.F. Bickley, *Acta Cryst.*, **2000**, *C56*, e280.

67 T. Gebauer, G. Frenzen and K. Dehnicke, *Z. Naturforsch. B*, **1993**, *48*, 1661.

68 a) V. Sum, M.T. Patel, T.P. Kee and M. Thornton-Pett, *Polyhedron*, **1992**, *11*, 1743; b) V. Sum, T.P. Kee and M. Thornton-Pett, *J. Organomet. Chem.*, **1992**, *438*, 89; c) N. Greene, H. Taylor, T.P. Kee and M. Thornton-Pett, *J. Chem. Soc., Dalton Trans.*, **1993**, 821.

69 E.C. Alyea, G. Ferguson and M. Zwikker, *Acta Cryst.*, **1994**, *C50*, 676.

70 a) A. Maisonnat, P. Kalck and R. Poilblanc, *Inorg. Chem.*, **1974**, *13*, 661; b) J.J. Bonnet, Y. Jeannin, P. Kalck, A. Maisonnat and R. Poilblanc, *Inorg. Chem.*, **1975**, *14*, 743.

71 E. Fernández, A. Ruiz, C. Claver, S. Castillón, A. Polo, J.F. Piniella and A. Alvarez-Larena, *Organometallics*, **1998**, *17*, 2857.

72 a) C.J. Cobley, D.D. Ellis, A. G. Orpen and P.G. Pringle, *J. Chem. Soc., Dalton Trans.*, **2000**, 1109; b) C.J. Cobley, D.D. Ellis, A. G. Orpen and P.G. Pringle, *J. Chem. Soc., Dalton Trans.*, **2000**, 1101; c) S.D. Pastor and S.P. Shum, *Tetrahedron: Asymmetry*, **1998**, *9*, 543; d) S.P. Shum, S.D. Pastor, A.D. DeBellis, P.A. Odorisio, L. Burke, F.H. Clarke, G. Rihs, B. Piatek and R.K. Rodebaugh, *Inorg. Chem.*, **2003**, *42*, 5097.

73 K.N. Gavrilov, A.T. Teleshev, A.R. Bekker, N.N. Nevskii and E.E. Nifant'ev, *Zh. Obsch. Khim.*, **1993**, *63*, 2791.

74 S. Ini, A.G. Oliver, T.D. Tilley and R.G. Bergman, *Organometallics*, **2001**, *20*, 3839.

75 W.J. Grigsby and B.K. Nicholson, *Acta Cryst.*, **1992**, *C48*, 362.

76 D.A. Albisson, R.B. Bedford, S.E. Lawrence and P.N. Scully, *Chem. Commun.*, **1998**, 2095.

77 V.I. Sokolov, L.A. Bulygina, O.Y. Borbulevych and O.V. Shishkin, *J. Organomet. Chem.*, **1999**, *582*, 246.

78 A.M. Trzeciak, Z. Ciunik and J.J. Ziółkowski, *Organometallics*, **2002**, *21*, 132.

79 M.B. Dinger and M.J. Scott, *Inorg. Chem.*, **2001**, *40*, 856.

80 M.D.K. Boele, *PhD Thesis*, University of Amsterdam, **2002**, 89.

81 H.P. Chen, Y.H. Liu, S.M. Peng and S.T. Liu, *J. Chem. Soc., Dalton Trans.*, **2003**, 1419.

82 S.D. Pastor, S.P. Shum, R.K. Rodebaugh, A.D. Debellis and F.H. Clarke, *Helv. Chim. Acta*, **1993**, *76*, 900.

83 D.R. Drew and J.R. Doyle, *Inorg. Synth.*, **1990**, *28*, 346.

84 F.T. Ladipo and G.K. Anderson, *Organometallics*, **1994**, *13*, 303.

85 H.C. Clark and L.E. Manzer, *J. Organomet. Chem.*, **1973**, *59*, 411.

86 D.J. Darensbourg and R.L. Kump, *Inorg. Chem.*, **1978**, *17*, 2680.

87 M.J. Frisch, G.W. Trucks, H.B. Schlegel, G.E. Scuseria, M.A. Robb, J.R. Cheeseman, V.G. Zakrzewski, J.A. Montgomery Jr., R.E. Stratmann, J.C. Burant, S. Dapprich, J.M. Millam, A.D. Daniels, K.N. Kudin, M.C. Strain, O. Farkas, J. Tomasi, V. Barone, M. Cossi, R. Cammi, B. Mennucci, C. Pomelli, C. Adamo, S. Clifford, J. Ochterski, G.A. Petersson, P.Y. Ayala, Q. Cui, K. Morokuma, D.K. Malick, A.D. Rabuck, K. Raghavachari, J.B. Foresman, J. Cioslowski, J.V. Ortiz, B.B. Stefanov, G. Liu, A. Liashenko, P. Piskorz, I. Komaromi, R. Gomperts, R.L. Martin, D.J. Fox, T. Keith, M.A. Al-Laham, C.Y. Peng, A. Nanayakkara, C. Gonzalez, M. Challacombe, P.M.W. Gill, B. Johnson, W. Chen, M.W. Wong, J.L. Andres, C. Gonzalez, M. Head-Gordon, E.S. Replogle and J.A. Pople, *Gaussian 98, Revision A.3* (by Gaussian, Inc.), **1998**, Pittsburgh.

88 R.G. Parr and W. Yang in *Density Functional Theory of Atoms and Molecules*, Parr, R. G. and Yang, W. Ed.; Oxford Science Publications, **1989**, Oxford.

89 A.D. Becke, *J. Chem. Phys.*, **1993**, *95*, 5648.

90 C. Lee, W. Yang and R.G. Parr, *Phys. Rev. B*, **1988**, *37*, 785.
91 W.J. Hehre, R. Ditchfield and J.A. Pople, *J. Chem. Phys.*, **1972**, *56*, 2257.
92 M.J. Frisch, J.A. Pople and J.S. Binkley, *J. Chem. Phys.*, **1984**, *80*, 3265.
93 R. Krishnan, J.S. Binkley, R. Seeger and J.A. Pople, *J. Chem. Phys.*, **1980**, *72*, 650.
94 a) G.M. Sheldrick, SHELXS97; University of Göttingen, Germany, **1997**; b) A. Altomare, M.C. Burla, M. Camalli, G.L. Cascarano, C. Giacovazzo, A. Guagliardi, A.G.G. Moliterni, G. Polidori and R. Spagna, *J. Appl. Cryst.*, **1999**, *32*, 115; c) P.T. Beurskens, G. Beurskens, R. de Gelder, S. García-Granda, R.O. Gould, R. Israël and J.M.M. Smits, The *DIRDIF*-99 program system; University of Nijmegen, The Netherlands, **1999**.
95 G.M. Sheldrick, SHELXL97; University of Göttingen, Germany, **1997**.
96 a) P. van der Sluis and A.L. Spek, *Acta Cryst.*, **1990**, *A46*, 194; b) A.L. Spek, PLATON, A Multipurpose Crystallographic Tool; Utrecht University, The Netherlands, **2002**.

List of Publications

Jarl Ivar van der Vlugt, Christian Müller and Dieter Vogt, "New Developments in the Design of P-Containing Ligands for Rhodium Catalyzed Hydroformylation – Coordination Chemistry of Phosphinites and Phosphonites", *manuscript in preparation.*(Chapter 1)

Jarl Ivar van der Vlugt, Rafaël Sablong, Pieter C.M.M. Magusin and Dieter Vogt, "Sterically Constrained Diphosphonites in the Rhodium Catalyzed Hydroformylation of Terminal and Internal Alkenes", *Angew. Chem. Int. Ed.*, **2003**, *submitted.* (Chapter 2)

Jarl Ivar van der Vlugt, Rafaël Sablong, Allison M. Mills, Huub Kooijman, Anthony L. Spek and Dieter Vogt, "Coordination Chemistry and X-ray Studies with Novel Sterically Constrained Diphosphonites", *J. Chem. Soc., Dalton Trans.*, **2003**, *submitted.* (Chapter 2)

Jarl Ivar van der Vlugt, Allison C. Hewat, Samuel Neto, Rafaël Sablong, Allison M. Mills, Martin Lutz, Anthony L. Spek and Dieter Vogt, "Synthesis of Novel Sterically Constrained Diphosphonites – Nickel Catalyzed Isomerization of Unsaturated Nitriles", *to be submitted.* (Chapter 2)

Jarl Ivar van der Vlugt, Jos M.J. Paulusse, Jason A. Tijmensen, Allison M. Mills, Anthony L. Spek, Carmen Claver and Dieter Vogt, "Coordination Chemistry and Asymmetric Catalysis with A Chiral Diphosphonite", *manuscript in preparation.* (Chapter 3)

Ruben van Duren, Jarl Ivar van der Vlugt, Jeroen P.J. Huijbers, Allison M. Mills, Anthony L. Spek and Dieter Vogt, "Platinum Catalyzed Asymmetric Hydroformylation with a Chiral Diphosphonite", *Tetrahedron: Asymmetry*, **2003**, *submitted.* (Chapter 3)

Jarl Ivar van der Vlugt, Josep M. Bonet, Allison M. Mills, Anthony L. Spek and Dieter Vogt, "Modular Diphosphine Ligands Based on Bisphenol A Backbones", *Tetrahedron Lett.*, **2003**, *44*, 4389-4392. (Chapter 4)

Jarl Ivar van der Vlugt, Michiel M.P. Grutters, Allison M. Mills, Huub Kooijman, Anthony L. Spek and Dieter Vogt, "New Diphosphane Ligands Based on Bisphenol A Backbones – Synthesis and Coordination Chemistry", *Eur. J. Inorg. Chem.*, **2003**, *accepted*. (Chapter 4)

Michiel M.P. Grutters, Jarl Ivar van der Vlugt, Huub Kooijman, Anthony L. Spek and Dieter Vogt, "Highly Selective Cobalt Catalyzed Hydrovinylation of Styrene", *manuscript in preparation*. (Chapter 4)

Jarl Ivar van der Vlugt, Ruben van Duren, Auke Meetsma and Dieter Vogt, "Novel Terphenyl Derived Phosphorus Ligands for the Platinum Catalyzed Hydroformylation", *manuscript in preparation.* (Chapter 4)

Ruben van Duren, Jarl Ivar van der Vlugt, Jeroen Meeuwissen, Huub Kooijman, Anthony L. Spek and Dieter Vogt, "New Mechanistic Insights in the Platinum Catalyzed Hydroformylation", *manuscript in preparation.* (Chapter 4)

Jarl Ivar van der Vlugt, Michiel M.P. Grutters, Jens Ackerstaff, Rob W.J.M. Hanssen, Hendrikus C.L. Abbenhuis and Dieter Vogt, "POSSphites – Monophosphites Derived from Incompletely Condensed Silsesquioxanes", *Tetrahedron Lett.*, **2003**, *accepted*. (Chapter 5)

Jarl Ivar van der Vlugt, Marco Fioroni, Jens Ackerstaff, Rob W.J.M. Hanssen, Allison M. Mills, Anthony L. Spek, Auke Meetsma, Hendrikus C.L. Abbenhuis and Dieter Vogt, "The First Silsesquioxane Based Diphosphinite Ligand – Synthesis, DFT Study and Coordination Chemistry", *Orgnaometallics*, **2003**, *accepted*. (Chapter 5)

Jarl Ivar van der Vlugt, Jens Ackerstaff, Michiel M.P. Grutters, Tessa W. Dijkstra, Rob W.J.M. Hanssen, Allison M. Mills, Huub Kooijman, Anthony L. Spek, Auke Meetsma, Hendrikus C.L. Abbenhuis and Dieter Vogt, "Phosphite Ligands Based on Silsesquioxane Backbones", *J. Chem. Soc., Dalton Trans.*, **2003**, *submitted*. (Chapter 5)

Jarl Ivar van der Vlugt, Gabriela Ionescu, Tessa W. Dijkstra, Huub Kooijman, Anthony L. Spek, Robbert Duchateau, Hendrikus C.L. Abbenhuis and Dieter Vogt, "The First Completely Condensed Silsesquioxanes Functionalized with Phosphorus Moieties", *manuscript in preparation.* (Chapter 5)

Marco Fioroni, Jarl Ivar van der Vlugt and Dieter Vogt, "Density Functional Studies on Pd, Pt and Rh Complexes of a Silsesquioxane Based Diphosphinite Ligand", *manuscript in preparation*. (Chapter 5)

Anthony L. Spek, Allison M. Mills, Jarl Ivar van der Vlugt and Dieter Vogt, "Unprecedented Dimeric Rhodium Structure", *Acta Crystallographica E*, **2003**, *submitted.* (Chapter 5)

Curriculum Vitae

Jarl Ivar van der Vlugt is op 7 juni 1975 geboren te Schiedam. In 1993 is aangevangen met de studie Scheikundige Technologie aan de Technische Universiteit Eindhoven. De ingenieursstudie is gecombineerd met diverse activiteiten binnen de Technologische Studie Vereniging 'Jan Pieter Minckelers', zoals een bijdrage aan de Symposiumcommissie 1996, de taak van commissaris externe betrekkingen in *het* Bestuur 96-97 en deelname aan de studiereis naar Zuid-Afrika in 1997. Na een verblijf in Singapore voor het uitvoeren van een bedrijfsstage bij Shell (Pulau Bukom), het voltooien van het afstudeerproject binnen de vakgroep Polymeerchemie onder leiding van prof.dr. A.L. German en dr.ir. Grègory Chambard in 1998 en een tweede bedrijfsstage bij DSM Research te Geleen is eind februari 1999 de studie tot ingenieur in de chemische technologie afgerond. Daaropvolgend is half april 1999 gestart met het promotie-onderzoek binnen de capaciteitsgroep Katalyse en Anorganische Chemie, en specifieker binnen de leerstoel Homogene Katalyse geleid door prof.dr. D. Vogt, met financiële steun vanuit de onderzoeksschool NRSC-Catalysis. De belangrijkste resultaten van dit onderzoek staan beschreven in dit proefschrift.

Jarl Ivar van der Vlugt is born in Schiedam, the Netherlands, on the 7th of June 1975. In 1993 he started studying Chemical Engineering and Chemistry at the Eindhoven University of Technology. The following years, studying was combined with various activities and tasks for the Study Association 'Jan Pieter Minckelers', such as the co-organisation of a scientific one-day conference in 1996, the role of external affairs coordinator within *the* Board 96-97 on behalf of the association and participation in the study tour to South Africa in 1997. After a stay in Singapore as part of an internship at Shell (Pulau Bukom), his graduation project in 1998 in the group Polymer Chemistry led by prof.dr. A.L. German and under supervision of dr.ir. Grègory Chambard and a second internship at DSM Research in Geleen, the Netherlands, he became a chemical engineer at the end of February 1999. Subsequently, a position as PhD-student was accepted within the Catalysis and Inorganic Chemistry group, more specifically the laboratory of Homogeneous Catalysis, led by prof.dr. D. Vogt and supported by the research school NRSC-Catalysis. The most important results obtained during the versatile investigations are described in this thesis.

Dankwoord

'Iets is alleen maar leuk omdat het een keer ophoudt, want als iets leuk is en het houdt niet meer op, is het op een gegeven moment niet meer leuk'

Deze uitspraak, van de, door mij in het dagelijkse (laboratorium)leven veelvuldig geciteerde, cabaretier Youp van 't Hek, dient als inleiding voor dit laatste kapittel van mijn proeve van en queeste naar wetenschappelijke wasdom, omdat volgens mij de diepere gedachte achter deze twee regels de kern raakt van het uitvoeren en beleven van een promotie-onderzoek, alhoewel ik hiermee geenszins wil suggereren dat ik onverdeeld blij ben dat deze passionele tijd nu zo goed als afgelopen is.

"Sometimes you just have to go for it, although it is exactly a million-to-one chance'

Als eerste promovendus van mijn eerste promotor Herr Professor Dieter Vogt kan ik terugkijken op een samenwerking van vier-en-een-beetje jaar die in ieder geval voor mij zeer de moeite waard is geweest, niet alleen wat betreft het wetenschappelijke aspect maar ook vanuit een psychologisch en research-management oogpunt. Ook onze congres-reizen samen naar Frankfurt, Stockholm, Tarragona en Zürich waren enerverend en leerzaam. Erik 'de Ab' Abbenhuis heeft met zijn onorthodoxe aanpak van problemen, publicaties en promoties hier en daar een snaar geraakt. Hij is betrokken geraakt bij het laatste deel van het beschreven onderzoek en het (terechte) enthousiasme zijnerzijds werkte louterend. Ik wil ook graag Herr Christian Müller noemen vanwege zijn zeer snelle correctie van manuscripten, ook al stond zijn naam niet eens bij de lijst van auteurs vermeld! Danke schön. Voor een promotie zijn externe deskundigen onontbeerlijk. I would like to express my deepest gratitude to prof. David Cole-Hamilton for his kind acceptance to be my 2nd Promotor. Thank you very much for your efforts, kind criticism and your trip to Eindhoven. Verder verdient prof. Piet van Leeuwen mijn dank. Piet, je scherpe commentaren op het manuscript en feitenkennis hebben zeker geholpen. Ook prof. Cees Elsevier heeft zich ingespannen om mijn schrijfwerk van (scherp)zinnige kritiek te voorzien. Hartelijk dank voor uw interesse en medewerking als lid van de leescommissie. Verder ben ik de leden van mijn promotie-commissie, prof. Bart Hessen, prof. Bert Hulshof, dr.Hab. Stefan Mecking en dr. Rob Duchateau erkentelijk voor hun interesse en bereidheid als opponent te fungeren. Stefan, wir haben uns schon am Anfang meines Projektes getroffen, aber, so wie es manchmal geht, haben sich unsere chemischen Wegen etwas geteilt. Trotzdem finde ich es sehr nett und ganz reizend von dir, daß du bereit bist, nach Eindhoven zu kommen. Rob, leuk dat onze afspraak in Oostende stand heeft gehouden. Hartelijk dank aan de kristallografen Allison Mills, Huub Kooijman, Ton Spek en Auke Meetsma voor de vele onmisbare metingen en gedetailleerde uitwerkingen.

'Als je geluk hebt, zijn collega's de beste mensen om mee (samen) te werken'

Binnen de vakgroep SKA en nog meer binnen Dieters Homkat-club (de Homo's) heb ik vooral met diegenen die zich niet beperkten tot de pakweg 15 m^2 van hun kantoor veel plezier gehad op borrels, diverse activiteiten in en rond Eindhoven, SKI dagen, persoonlijkheidscursussen, barbeques en andere etentjes, NIOK voetbaltoernooien en op het forum. Oud-collega's Paul (alleen malts, **geen** blend!), Marco, Leon, Suzanne, Ralf, Roelant, Erik, Robin, Sam, Natalia, Wouter, Velitchka, Christophe H. (2 keer!), Peter, Arnoud, Nicu, Danka, Luis, Frank, Pieter, Emiel, Darek, en Danny de anti-sprinter: hartelijk dank voor een aantal prettige jaren. Dankzij de eigenzinnige Mark (V.B.E.) kwam ik voor het eerst in aanraking met SKA en de silsesquioxaan chemie. Tessa (laat me uitpraten!) was jarenlang een zeer aangename buurvrouw. Met de ervaren Eva en Alison heb ik min of meer lab STW 4.81 aangekleed. De rekken staan en hangen nog steeds zeer solide in het lab! Verder was met name post-doc en fosfor goeroe Rafaël uit Elzas van groot belang voor een goede start, een zachte landing en veel verhalen in de tussentijd. Raf, danke beaucoup (is this alsacian enough for you?). Wat de technische ondersteuning beteft, verdienen Ton Staring (de pietje-precies met allerhande kolommen), Wout van Herpen (wees gerust als hij het in elkaar klust) en de mannen van de glasblazerij, Sjaak, Henri en Frans, alle lof. De laatste drie hebben gezorgd voor de nodige kunstwerkjes en afwisseling. Goede secretaresses zijn onontbeerlijk, ook voor AiO's, dus wil ik Ingrid en Joyce bedanken voor de nuttige en leuke gesprekken op het secretariaat en hun onzichtbare maar immer aanwezige ondersteunende handen. De huidige (jonge) SKA groep is prettig divers, dankzij met name mensen als Chrétien (leuk(e) lachende limburger), Joost met zijn quotes, Davy (dankzij hem ben ik SKAsparov 2003 geworden), Thijs, Bouke, Eero, Zhu, Emiel, Gijs, Maria en Marco (thanks for the DFT-silsesquioxanes cooperation: Forza Roma!). Tourpool-Tiny, het was me elk jaar een genoegen om je met één puntje de dagzeges af te snoepen! Sander, bedankt voor je diversiteit en de oprechte belangstelling in de persoon. Met Niek heb ik menig congres, concert en café bezocht en het was altijd een ervaring. De sportgekke Ruben heeft een aantal van mijn ligand-systemen bereidwillig getest met zijn geliefde platina/num, waarvoor dank. Ook het werkcollege Anorganische Chemie en het tweedejaars-derde-trimester-prakticum waren leuk en leerzaam. De oude Vincent was vaak goed voor een grapje, goedbedoeld advies en een opbeurend woordje (dank, Kaas) en met Marije heb ik veel gelachen en gestoeid en nog meer cd's uitgewisseld. Jos heeft een aantal lekkere maaltijden geserveerd in een zeer onopgeruimde kamer. Gabriela was immer hoorbaar aanwezig maar gelukkig niet meer in mantelpakje, zoals op haar allereerste dag. Met mijn charmante colombiaanse collega en roomie Mabel (no yet!) heb ik veel basketbalpartijtjes afgewerkt en gesprekken van zeer uiteenlopend aard en niveau gehad. Volgens mij heb jij een goed beeld gekregen van de nederlandse man, zijn humor en zijn gebruiken. Ik vond het mede dankzij jou heel plezierig in STW 4.40! Muchas Gracias!

'De Jongens met een J'

Ik prijs me gelukkig dat ik vier studenten heb mogen begeleiden. Na de spaanse Josep (tsja) nam de eveneens in Spaans (sprekende dames) geïnteresseerde Jos het stokje over. Ik heb je in totaal maar 6 van de 12 maanden echt 'bij me' gehad vanwege je avonturen in Tarragona, maar het was een speciale tijd, onder meer door je aparte, droge humor en je gedrevenheid om het XantBino fenomeen te willen begrijpen. Bedankt voor je inzet en veel succes met je eigen promotie! Daarna kwam Jason die met zijn brede grijns en vlotte voorkomen zeer snel inburgerde en zijn weg als research-stagiair makkelijk vond. De syntheses gingen niet altijd even soepeltjes maar uiteindelijk hebben we toch een leuk resultaat behaald. Und dann war da jetzt der Jens. Wegen seiner deutschen Gründlichkeit und Begeisterung hat es sehr gut zwischen uns beiden geklappt. Nicht nur im persönlichen Bereich, aber auch die Arbeit mit den supertollen Silsesquioxanen hat sehr viel spaß gemacht. Verder wil ik de overige (ex-)studenten van onze groep en de tweedejaars praktikanten Michel, Christian, Sanne en Mariska bedanken voor hun inbreng en enthousiasme. Ik vond het erg plezierig en leerzaam.

'Vrienden, mag ik u wat zeggen? Wordt niet boos,want wie een proefschrift schrijft, is een beetje gek'

Academische vorming is allemaal leuk en aardig, maar er moet natuurlijk ook wel gelachen kunnen worden. Met behulp van de vrienden en vriendinnen van *het* bestuur '96-'97 van Japie is dit meer dan goed gekomen. Het is belangrijk om regelmatig, ook al is dat maar af en toe, gezamenlijke herinneringen op te kunnen halen, elkaars wel en wee te delen en de diverse toekomstplannen te bespreken. Jan en Hester, bedankt voor jullie gastvrijheid in Emmen en de getoonde interesse in de persoon achter de promotie. Een telefoongesprek met Jan is verrassend genoeg nog nooit kort geweest, maar dat vind ik helemaal niet erg. Jeroen en Tanja, dank voor de gastvrijheid in Eindhoven, jullie interesse en het gebruik van jullie achterbank! Jeroen, discussiëren met jou is een verzoeking, maar zeker wel de moeite waard, ondanks onze verschillen. Yvonne en Bastiaan, bedankt voor de gastvrijheid in Maastricht en incidentele peptalk! Mayk, bedankt voor je gastvrijheid in Utrecht, je heldere kijk op het leven en de bijbehorende levensinstelling, alsmede ook voor de gesprekken over van alles en nog wat. Martine, ik heb je de afgelopen zes en een beetje jaar steeds beter leren kennen en dat is zeer plezierig gebleken. Ook Bart was en is gelukkig weer vaak van de partij als ex-Japist.
Met mijn introbroertje Justin (Ennuh?) en jaargenoot Ralf (ook Ennuh!) heb ik menig kaartspelletje gespeeld in collegebanken, zuid-afrikaanse stenen hutjes zonder licht en studentenhuisvestings-huiskamers, veel gemenseerd en zeer infrequent een drankje genuttigd in met name café van Mol. Dank voor de volhardendheid en de gezelligheid. Dit geldt ook voor Ernst (drukdrukdruk).
Doktorin Maren, ich danke dir für deine Freundschaft und unseren speziellen Kontakt.

Sportieve ontspanning (door fanatieke inspanning) en wetenschap gaan zeer goed samen. Dit heb ik al hockeyend ondervonden bij E.S.H.V. 'Don Quishoot' maar vooral bij E.S.S.V. 'Isis'. De schaatstrainingen werden steeds leuker en sneller. Heel plezierig waren ook de contacten tijdens en dankzij fietstochten met enkelen van deze Isisianen, waaronder Niels, Joep, Alex, Janne, Maartje, Jeroen en Jacco. In het bijzonder een woord van dank aan de volgende 'bikkels': Wouter, je prettige omgangsvormen, rare ranzige humor en onze dito gesprekken heb ik zeer op prijs gesteld. 'It's a beautiful day!' Peter was en is het weekdier van ons pelotonnetje, met een geheel eigen stijl en humor. We hebben samen vele leuke momenten in en uit het zadel gehad. Erwin, ook al schaats me tien keer voorbij op de 10 km, die luxemburgse bolletjestrui zit stevig om mijn schouders.
Rob, je bent uitgegroeid tot meer dan een collega naar wie ik toeging als mijn computer of silsesquioxaan reactie het niet deed, onder andere door je oprechte interesse in mij(n chemie), de mensa/AOR avonden, je sociale inborst en vanwege het feit dat jij wel Kolonisten van Catan hebt. Veel plezier in de USA… Joyce, ik beloof je dat ik voortaan in Gent met alle liefde schapen wil ruilen. Bedankt voor de etentjes, rare dvd- en plaza-films en de diverse keren dat ik je mocht laten schrikken. Kamergenoot, bijna-buurman en eerste pinguïn Michiel wil ik bedanken voor onze chemische overpeinzingen, de vele voet-, basket- en trefbalsessies, je merentijds vrolijke en stabiele karakter, de vrollegiale gesprekken over kleine en grote zaken en je hulp met allerlei dingen. Eri*c*, mijn 'derde kamergenoot' en tweede pinguïn, was altijd in voor een (actieve) avondbesteding, of dat nu de mensa gecombineerd met de AOR Onderdruk betekende, Effenaren, een vage film, poolen, een culturele ontdekking tijdens een concert of voorstelling of het tot op de komma nauwkeurig corrigeren van een manuscript. Ik dank je voor de vele leuke momenten binnen en buiten het lab.

'Van je familie moet je het hebben'

In dat verband prijs ik me gelukkig met grootouders als Oma en Opa Bezemer, (de oude Beesjes) die me via de telefoon of middels op rijm gezette kattebelletjes vanuit Schiedam voortdurend hebben gesteund. Ook de warme interesse van naaste familieleden zoals Olga en Hans was altijd zeer welkom. Alle andere mensen, dichtbij en veraf, die zich wel eens afvroegen hoe het in Eindhoven ging, wil ik langs deze weg bedanken. Het gaat goed.
Pa en Ma, jullie hebben mij altijd gemotiveerd als het even iets minder soepeltjes ging of de frustratie iets te veel werd. Maar veel belangrijker was het geruststellende vertrouwen dat het allemaal wel in orde zou komen. Zoals zo vaak hebben jullie gelijk gekregen.

Jarl Ivar

'Ach ja, weet alles maar eens achteraf'

Stellingen

behorende bij het proefschrift

Versatile Phosphorus Ligands

Synthesis, Coordination Chemistry and Catalysis

door

Jarl Ivar van der Vlugt

1. Persoonlijke voorkeuren betreffende de geschikte reactie-condities waaronder de rhodium gekatalyseerde hydroformylering wordt uitgevoerd, verhinderen een goed vergelijk tussen verschillende ligand-systemen en substraten.

2. Het gebruik van citaties in een wetenschappelijk artikel is bedoeld om de lezer, indien gewenst, meer inzicht te geven in het onderzoek dat voorafging aan het werk dat beschreven wordt en niet om diezelfde lezer op een verkeerd been te zetten. Indien dus gerapporteerd wordt over 'phosphinite ligands', doet een verwijzing naar een overzichtsartikel dat louter betrekking heeft op 'phosphine' gerelateerde chemie meer schade dan dat het hulp biedt.

A.A. Nazarov, C.G. Hartinger, V.B. Arion, G. Giester and B.K. Keppler, *Tetrahedron*, **2002**, *58*, 8489.

Ook het eenduidig benoemen van fosfor-gefunctionaliseerde verbindingen verhoogt de overzichtelijkheid. Begrip van de auteurs van een wetenschappelijk artikel aangaande de gebruikte chemicaliën is daarvoor noodzakelijk. Zo classificeert men in het algemeen een molecuul met daarin een R_2POR fragment (R = een koolstof-gebrugde groep) als een 'phosphinite' en niet, tot vervelens toe, als een 'phosphite'.

S. Sjövall, C. Anderson and O.F. Wendt, *Inorg. Chim. Acta*, **2000**, *325*, 182.

3. De toepassing van silsesquioxanen als fundament voor de constructie van fosfor-gefunctionaliseerde liganden biedt diverse nieuwe mogelijkheden voor deze moleculen met nanometer-afmetingen.

Dit proefschrift, hoofdstuk 5.

Hieronder vallen naast de studie naar de coordinatiechemie van dergelijke verbindingen en de inzet van deze liganden in batchgewijze katalyse ook het gebruik in continue katalyse of in twee-fase katalyse.

4. Non-metallische (asymmetrische) katalyse, ook wel 'organokatalyse' genoemd, is een interessante en relatief nieuwe ontwikkeling. Als de reactie echter uitgevoerd moet worden over een periode van 7 dagen, met 15 mol-% katalysator en een tienvoudige overmaat van één substraat, dienen, ondanks de verkregen controle over de stereochemie van het product, vraagtekens gezet te worden bij het gebruik van de term 'catalytic'.

O. Andrey, A. Alexis and G. Bernardinelli, *Org. Lett.*, **2003**, *5*, 2559.

5. Het overmatig gebruik van nietszeggende woorden als 'molecular clocks', 'molecular mousetraps', 'molecular world cups' of zelfs 'technomimetic (..) molecular wheelbarrows' in (titels van) wetenschappelijke artikelen in de hoop dat dit de status van het gepresenteerde automatisch verhoogd, terwijl het feitelijke werk hier geen directe aanleiding toe geeft, dient door de redacties van alom gerespecteerde tijdschriften te worden ontmoedigd in plaats van, zoals heden ten dage het gebruik schijnt te zijn geworden, te worden beloond met een publicatie.

A.G. Martínez, J.O. Barcina, M. del Rosario Colorado Heras, A. de Fresno Cerezo and M. del Rosario Torres Salvador, *Chem. Eur. J.*, **2003**, *9*, 1157.
R.R. Julian, J.A. May, B.M. Stolz and J.L. Beauchamp, *Angew. Chem. Int. Ed.*, **2003**, *42*, 1012.
G. Jimenez-Bueno and G. Rapenne, *Tetrahedron Lett*., **2003**, *44*, 6261.
A. Soi and A. Hirsch, *New. J. Chem.*, **1998**, *22*, 1337.

6. Een theoretisch model voor het juist voorspellen van kristalstructuren zal bij een experimenteel chemicus veel van de mystiek van en euforie over een nieuwe kristalstructuur wegnemen.

J. Dunitz, *Chem. Commun*. **2003**, 545.

7. De uitspraak "You miss 100% of the shots you never take", van ijshockey-legende Wayne Gretzky, mist doel doordat er geen kwalitatief oordeel geveld wordt over de gevolgen en alternatieven van de keuze. Sommige kansen zijn de moeite van het aangrijpen niet waard.

8. Er is een fundamenteel verschil tussen het niveau van de academische opleiding tot chemisch technoloog anno 2003 in vergelijking met tien jaar terug. Het is echter stuitend dat ook de capaciteiten van de gemiddelde student een dergelijke ontwikkeling hebben ondergaan, maar dan in negatieve zin. Dit wordt nog eens versterkt door de verscholing van het wetenschappelijk onderwijs.

9. Het gegeven dat het boek 'No Logo' van Naomi Klein miljoenen malen over de toonbank is gegaan, zou, naast de constatering dat de idealistische inhoud heel veel mensen van 'all over the globe' aanspreekt, ook opgevat kunnen worden als een bevestiging van de succesvolle lancering van het merk 'anti'.

10. De meeste AiO's denken bij aanvang niet na over het echte doel van een promotie-onderzoek, waardoor ze geconfronteerd zullen worden met allerlei onverwachte tegenslagen en ze dientengevolge de belangrijke leermomenten en toegevoegde waarden van vier jaren niet inzien.

11. Never follow your own advice: there is a good reason for you to give it to others.

12. Oude liefde oxideert noch reduceert.

13. De fiets is de ideale schaats als er geen ijs ligt.

14. Promoveren dient een passie te zijn die niet wordt begrensd door stricte werktijden, niet een manier om gedurende vier jaar een dun belegde boterham en een karige verlenging van de 'studententijd' te bekostigen.

15. De wildgroei onder de huidige generatie cabaretiers gaat ten koste van de kwaliteit van het gebodene. Dientengevolge verdwijnt het louterende schok-effect dat na afloop van een voorstelling nog dagenlang dient na te ijlen. De noodzaak van een periodiek voorgeschotelde confrontatie met de waanzinnige realiteit van alledag neemt echter hand over hand toe.

16. De diersoort mens zal, juist gezien zijn huidige expansiedrift, op relatief korte termijn uitsterven. Dit zal de biodiversiteit zeer ten goede komen.

17. Sociale dienstplicht is een zeer efficiente manier om de algehele normvervaging in de hedendaagse maatschappij enerzijds en de acute problemen in onontbeerlijke, 'softe' sectoren als zorg, onderwijs en maatschappelijk welzijn anderzijds op te lossen.

18. Silsesquioxaan-kooitjes zijn net als vrouwen; ze reageren lang niet altijd zoals je zou willen.

19. One is better off feeling happy than satisfied. The first emotion brings joy, the second one merely lazyness.

20. Je kunt niet gelukkig worden, je kunt slechts gelukkig zijn.

21. Het leven is vurrukkulluk, alleen duurt het meestal zo lang voor je daar achter komt.